THE UNIVERSITY OF HULL

Self-Sterilising Surfaces to combat Healthcare Associated Infections

Being a Thesis submitted for the Degree of Doctor of Philosophy (PhD)

By

Lauren Clare Turner, MChem (Hons)

February 2017

Abstract

The immobilisation of photosensitisers on polymeric supports for use in photodynamic antimicrobial chemotherapy has become increasingly popular. The immobilisation of photosensitisers on polymeric supports has been attempted previously by covalent attachment between the photosensitiser and the support, and by entrapping the photosensitiser in a polymeric matrix. Even though porphyrins have been attached to polymeric supports there have been relatively few biological experiments carried out following immobilisation. There have also been few attempts at measuring the reusability of a surface incorporating a photosensitiser for bacterial inactivation. The work presented herein will focus on two main goals; the first is the formation of a self-sterilising surface which will activate under irradiation with visible light, allowing normal lighting conditions to be used, the second goal that will be targeted is the formation of a porphyrin immobilised on a polymeric surface which exhibits minimal leaching, and shows good anti-bacterial activity.

Synthesis of a range of conjugatable porphyrins and viologens bearing complementary peripheral functionalities has been carried out, followed by conjugation to solid supports using both microwave heating and normal heating.

Entrapment of polyviologens and porphyrins in two different polymeric matrices, silica and polyacrylamide, has been attempted. The entrapment was carried out using different solvent systems, and although it was found to be successful, both porphyrin and polyviologen were found to leach from the polymeric support upon washing. An alternative strategy was attempted *via* the formation of a water-soluble porphyrin containing a vinyl functionality for use in free radical polymerisation reactions.

The synthesis of a library of water-soluble porphyrins bearing vinyl groups was carried out. The library allowed for comparison of a non-metallated porphyrin, acting as a positive control, a copper porphyrin which acted as a negative control and a palladium porphyrin, which was found to produce the highest degree of inactivation of the Gram-negative bacteria *E.coli*.

Acknowledgements

I would firstly like to thank my supervisor Professor Ross Boyle for all of his help and support throughout this project, without which this project would not have been possible. I would also like to thank my second supervisor Dr Grazia Francesconi for her support throughout this project. Thanks also go to the University of Hull for my scholarship and funding for the project. I would like to give a massive thanks to Dr Francesca Bryden who has been the best friend I could have possibly asked for throughout this project, your proof reading skills are second to none and I really appreciate all of the time and effort you put in and I do not know how I will ever repay you for all of the help and guidance you gave me but maybe one day when I open up my bakery you can have unlimited cake. I would also like to thank my partner Joshua Smith who has put up with me and the ups and downs of my PhD for three years, and who also helped with the proof reading of my thesis, without your emotional support this project would not have been possible. It would not be right if I didn't thank my cat Princess, who has kept me company through high and low times with a cuddle and a one-way conversation.

I would also like to thank my friends who have been there for me throughout my whole PhD and who have always been at the end of the phone or a message; Dr Rachel Smith, Dr Kati Nicholson, Dr Louis Allott, Dr Christopher Randles, Martin Taylor, Kayleigh Marshall, Matthew Bennett, Shaun Johnston & Chris Jay. I would also like to thank Simon Fellows and Matthew Bennett for their help using the pXRD. I would like to thank Carol Kennedy for running my CHN samples, and Tony Sinclair for running my SEM samples. I would also like to thank Huguette Savoie for allowing me to use her facilities and providing excellent cake to help keep me motivated.

Thanks also go to our collaborators at Liverpool John Moores University, Dr Francesca Giuntini who allowed me to work in her lab for two weeks, your help was really appreciated. I would also like to thank Alessandro Pozzoli for putting up with me in his lab for two weeks constantly asking him where things were, thanks for helping me. I would also like to thank Professor John Greenman at the University of the West of England, Bristol for allowing me to carry out biological testing of my materials, and providing assistance and knowledge of the bacterial testing. I am also very grateful to Dr Cinzia Spagnul for her assistance in the biological testing, and for all the help she gave me throughout my project. I would also like to thank the people from lab C120 who have kept me company throughout my PhD; Steven Yap, Miffy Cheng, Guy Entract and Jordon Sandland, you will all go far just stick at it and don't give up.

Finally I would like to thank my family who have been there to support me through my PhD, even though they never understood how long it would take. I would also like to thank Ann-Marie and Graham Smith who have been there throughout my PhD and provided support.

Abbreviations

^{0}Ps – Ground state photosensitiser

^{0}PS* – Ground excited state photosensitiser

^{1}H-NMR – Proton nuclear magnetic resonance

^{13}C-NMR – Carbon nuclear magnetic resonance

AAHC – Azide alkyne Huisgen Cycloaddition

ABDA – 9,10-Anthracenediyl-bis (methylene)dimalonic acid

ABR – Antibacterial resistance

AFM – Atomic force microscopy

AHFP – Ammonium hexafluorophosphate

Am – Acrylamide

AMMSS – Anionic monodisperse mesoporous silica spheres

aPDT – Antimicrobial photodynamic therapy

APS – Ammonium persulfate

ASAP – Assisted solid atmospheric probe

ATR-FTIR – Attenuated total reflectance fourier transform infra-red

B. cereus – Bacillus cereus

BF_3 – Boron trifluoride

Boc_2O – Di-tert-butyl dicarbonate

CDI – 1,1'-carbonyldiimidazole

CdTPPS – [5,10,15,20-tetra(4-sodiumsulphonatophenyl)porphyrinato]cadmium(II)

CNC – Nanocrystalline cellulose

CPS – Cross-linked polystyrene

CuI – Copper iodide

$CuOTf.C_6H_6$ – Copper triflate benzene

DCC – Dicyclohexylcarbodiimide

DCM – Dichloromethane

DDQ – 2,3-Dichloro-5,6-dicyano-1,4-benzoquinone

DMAP – 4-Dimethylaminopyridine

DMF – *N*,*N*'-Dimethylformamide

$DNPV^{2+}$ – Dinitropolyviologen

DPiBF – 1,3-Diphenylisobenzofuran

E.coli – Escherichia coli

EDC – (N-ethyl-N'-(3-dimethylaminopropyl) carbodiimide

EDTA – Ethylenediaminetetraaceticacid

ESBLs – Extended spectrum beta-lactamases

GPC – Gel-permeation chromatography

HAIs – Healthcare associated infections

HCl – Hydrochloric acid

HOBt – Hydroxybenzotriazole

HPLC – High performance liquid chromatography

HRMS – High resolution mass spectrometry

Hz – Hertz

KOH – Potassium hydroxide

LAAAs – Light-activated antimicrobial agents

LBL – Layer-by-layer

$LiAlH_4$ – Lithium aluminium hydride

$LiAlO_2$ – Lithium aluminate

MALDI – Matrix-assisted laser desorption ionisation

MB – Methylene blue

MDRAB – Multi-drug resistant *A.baumanni*

MRSA – Methicillin- resistant Staphyccolus aureus

M.Smegmatis – Mycobacterium smegmatis

MV^{2+} – Methylviologen

MW – Microwave

NHS – National Health Service

NMR – Nuclear magnetic resonance

NaN_3 – Sodium azide

$NaNO_2$ – Sodium nitrite

$NaNO_3$ – Sodium nitrate

NHS ester – *N*-hydroxysuccinimide ester

NMP – *N*-methyl-2-pyrrolidone

PACT – Photodynamic antimicrobial chemotherapy

P.aeruginosa – Pseudomonas aeruginosa

PBS – Phosphate buffer solution

PBr_3 – Phosphorous tribromide

PDT – Photodynamic therapy

Pd $Cl_2(PPh_3)_2$ – Bis(triphenylphosphine)palladium(II) dichloride

$PdCl_2$(dppf) – [1,1'-Bis(diphenylphosphino)ferrocene palladium (II) dichloride

Pd $(PPh_3)_4$ – Tetrakis(triphenylphosphine) palladium (0)

$Pd(OAc)_2$ – Palladium (II) acetate

PEG – Poly(ethyleneglycol)

PET – Photoinduced electron transfer

P.gingivalis – Porphyromonas gingivalis

poly (HEMA) – poly (hydroxyethylmethmethacrylate)

PPIX – Protoporphyrin IX

p-TAPP – 5,10,15,20-tetra(4-aminophenyl)porphyrin

p-THPP – 5,10,15,20-tetra(4-hydroxyphenyl)porphyrin

p-TAPP – 5,10,15,20-tetra(4-aminophenyl)porphyrin

PUR – Polyurethane

pXRD – Powder x-ray diffraction

Rf – Retention factor

RNO – *N*,*N*-Dimethyl-4-nitrosoaniline

ROS – Reactive oxygen species

RT – Room temperature

S.aureus – Staphyccolus aureus

SDS – Sodium dodecyl sulfate

SEM – Scanning electron microscopy

SHE – Standard hydrogen electrode

S.mutans – Streptopcoccus mutans

SOSG – Singlet oxygen sensor green

TBAC – Tetrabutylammoniumchloride

TBO – Toluidine blue O

TCA – Trichloroacetic acid

TEM – Transmission electron microscopy

TEMED – *N*,*N*,*N*',*N*' - tetramethylethylenediamine

TEOS – Tetraethylorthosilicate

TFA – Trifluoroacetic acid

THES – Tetrakis (2-hydroxyethoxy)silane

THF – Tetrahydrofuran

TiO_2 – Titanium dioxide

TLC – Thin layer chromatography

$TMePyP^{4+}$ – 5,10,15,20-Tetra(4-*N*-methylpyridyl)porphyrin

TMOS – Tetramethoxyorthosilane

TMPyP – 5,10,15,20-Tetra- [4-methylpyridinium] porphyrin

TNS – Titania nanosheets

TPP – 5,10,15,20-Tetraphenylporphyrin

TPPS – 5,10,15,20-Tetra(4-sodiumsulphonatophenyl)porphyrin

TPP-NH_2 – 5-(4-Aminophenyl)-10,15,20-triphenylporphyrin

TPPS-NH_2 – 5-(4-Aminophenyl)-10,15,20-tri(4-sulphonatophenyl)porphyrin

tR – Retention time

TSP – 5,10,15,20-Tetra(4-vinylphenyl)porphyrin

TTP – 5,10,15,20-Tetra(4-methylphenyl)porphyrin

WHO – World Health Organisation

ZnTPPS - [5,10,15,20-tetra(4-sodiumsulphonatophenyl)porphyrinato]zinc(II)

COSHH statement

All experiments were carried out according to the University of Hull health and safety regulations, and carried out with COSHH statements numbering from LT01-LT052.

Tables of Contents

Table of Figures, Tables and Schemes

i. Figures

ii. Tables

iii. Schemes

1 Literature review

1.1 Healthcare associated infections

Healthcare associated infections (HAIs) have been defined by the Department of Health in the United Kingdom as "any infection caused by an infectious agent acquired as a consequence of a patient's treatment by the National Health Service (NHS)".[1] In 2014 the World Health Organisation (WHO) investigated the consequences of antibacterial resistance.[2] Antibacterial resistance (ABR) involves bacteria for which the treatment has become difficult or in some cases impossible, this can include bacteria that cause many common and life threatening infections acquired in hospitals and in the community. Antibacterial resistance within a wide range of infectious agents is a growing public health problem, which is a phenomenal threat to countries and multiple sectors. ABR is a complex and multifunctional problem, it involves a range of resistance mechanisms that affect an ever-widening range of bacteria. ABR is a global problem that will not have a single, simple solution, and will remain a challenge amongst scientists, who will have to delve deeper into the core of the problem and provide multiple solutions. Patients who have infections that are caused by bacteria that are resistant to a specific antibacterial drug generally have an increased risk of death and worse clinical outcomes, this is especially true of patients who may be immuno-compromised. In addition, since infected patients remain in hospital on average 2.5 times longer than uninfected patients the economic cost derived from the increased length of stay for infected patients is considerable.[1,3] In 2004 the Department of Health in the United Kingdom confirmed that the estimated number of healthcare associated infections each year was 300,000, which has an annual cost of over £1 billion a year.[4–6] Data gathered by the WHO in 2014,[2] reported a yearly cost to the US healthcare system of between $21-34 billion a year and 8 million additional hospital days. Antibiotic resistant bacteria causes 25,000 deaths in Europe each year and costs €1.5 billion.

It has been suggested that the main focus to help reduce HAIs should be on prevention of spread of infections. Reduction can be achieved by improving hygiene, improving sanitation and in third world countries improved access to clean water. As well as improving hygiene, efforts need to be made on the discovery of new antibacterial drugs and investigation into alternative methods to help prevent the spread of infections.

The last new class of antibacterial drugs was introduced in the 1980s, and it is essential to preserve the efficacy of existing drugs through measures to minimise the development and spread of resistance, whilst also attempting to provide alternative solutions.[7] For more

than 60 years antibacterial drugs have been regarded as the miracle cure for infections, the main problem is the overuse of antibacterial drugs, and they are still widely prescribed when they are not necessary. Alexander Fleming stated that "overuse could cause the bacteria to become resistant to antibiotics".[2] These wise words were right, and there is now a crucial need for the development of new antibacterial drugs. The pipeline for the development of new antibacterial drugs is virtually empty, particularly for use against Gram-negative strain bacteria, which are harder to kill.[8] Research treatments to replace antibacterial drugs are still in the early stages, but there is still hope for this area. Research into affordable replacements for antibiotics is vital, as the new products will need to be cheap, easy to make and affordable.

In 2016 it was thought that there was not enough public awareness of antimicrobial resistance,[8] and it is therefore important to raise awareness of this as part of any plan to tackle ABR. The WHO organised a world antibiotic week from 16th until 22nd November 2016 to help raise awareness of the problem. The main aim being to increase awareness of antibiotic resistance, and to encourage good practices such as good personal and food hygiene to help solve this problem. The WHO has worked hard to publicise this campaign to members of the public and those working in the healthcare sector.

1.2 Classification of bacteria

It was impossible to identity and classify bacteria until 1884 when Hans Christian Gram developed a staining method which allows the differentiation between Gram-positive and Gram-negative bacteria.[9] The dyes that were commonly used in staining were acidic dyes such as safranin, crystal violet and methylene blue shown in **Figure 1.** The dyes stained the nucleous and they also attached to the bacteria and cellulose. The majority of the dyes were *ortho*-chromatic, so when they were used the action was direct and predictable with the colour observed being the same as the colour of the dye used.

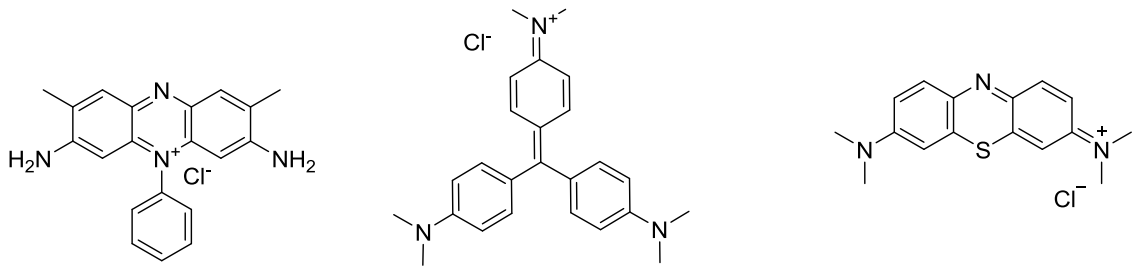

Safranin **Crystal violet** **Methylene blue**

Figure 1 – Structure of three dyes commonly used for bacterial staining.

To distinguish between Gram-positive and Gram-negative bacteria, Hans Christian Gram classified bacteria depending on whether they lost or retained a colour. The dye investigated for the classification of bacteria was crystal violet. The Gram stain test works based on the ability of the bacteria cell wall to retain the crystal violet dye during solvent treatment. The differences in cell wall structures of the Gram-positive and Gram-negative bacteria has allowed differentiation to be carried out by the differences in amounts of peptidoglycan and lipid content, as Gram-positive bacteria are known to have a higher content of peptidoglycan compared to Gram-negative bacteria. To carry out the test the bacteria are stained by adding crystal violet, followed by iodine solution, the bacteria are then washed with acetone and ethanol which dissolves the lipid layer causing thinning of the cell walls, and in the case of the Gram-negative cell wall it causes the cell wall to break and the dye to leach out. A counter stain, usually Safranin is added to give the decolourised bacteria (Gram-negative) a pink colour. **Figure 2** shows the differences in cell wall structure between Gram-positive and Gram-negative bacteria. Gram-positive bacteria have a simple cell wall structure with just three components; the plasma membrane, periplasmic space and an outer peptidoglycan, whereas the Gram-negative cell wall is more complex. The Gram-negative cell wall contains the same inner structure as the Gram-positive bacteria, but also contains another periplasmic space and an outer membrane. The complex structure of Gram-negative bacteria makes it more challenging to break through the cell wall.

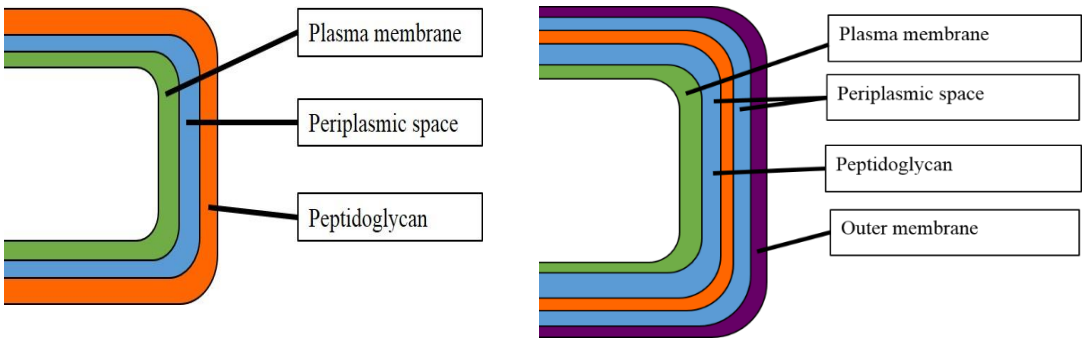

Gram-positive bacteria cell wall **Gram-negative cell wall**

Figure 2 – Comparison of Gram-positive and Gram-negative cell wall.

When comparing both Gram-positive and Gram-negative bacteria it can be seen that Gram-negative are more challenging to kill than Gram-positive bacteria, which is why the focus of this project is the killing of Gram-negative bacteria. From the WHO report it was seen that *Escherichia coli* is one of the most common and threatening Gram-negative

bacteria due to increased resistance, which indicates that development needs to be focused on a new approach for antibacterial resistance.[2]

1.2.1 Escherichia coli (*E.coli*)

Escherichia coli is a Gram-negative bacteria, which is part of the normal flora in the intestine in both humans and animals. *E.coli* is the most frequent cause of community and hospital acquired infections. It is also the most common cause of blood stream infections.[10] *E.coli* typically colonises the gastrointestinal tract of a human within a few hours of birth, it is also associated with intra-abdominal infections such as peritonitis and with skin and soft tissue infections. *E.coli* is also one of the leading causes of foodborne diseases.[8]

E.coli is resistant to third generation cephalosporins including resistance conferred by extended spectrum beta-lactamases and fluoroquinolones.[10] The infections that occur from *E.coli* usually originate from the person that is affected (auto-infection), but there are strains that have a particular resistance that can be transmitted from animals through the food chain or between individuals. Resistance to *E.coli* readily develops in humans through mutations. The resistance to third generation cephalosporins is mainly caused by enzymes known as extended spectrum beta-lactamases (ESBLs), these are enzymes that destroy many beta-lactam based antibacterial drugs, and they are transmissible between bacterial species. There are *E.coli* strains that have ESBL that are also generally resistant to several other bacterial drugs, which means that the only option remaining is the carbapenems, which are a group of parenterally administered bactericidal beta-lactam antibiotics that have an extremely broad spectrum; these antibiotics are extremely effective but they are also expensive. Although the use of carbapenems are available to help reduce the number of healthcare associated infections they should not be seen as a long term solution to this on-going problem.

1.3 Investigation into a possible solution involving antibacterial surfaces

In order to reduce the number of infections and the number of deaths extensive research has been carried out into the use of antimicrobial surfaces,[11,12,13] more specifically research on the use of titanium dioxide and the modification of titanium dioxide,[6,14] the use of light activating polymers,[15,16] and also the use of free radical producing photosensitisers.[15,16]

The main limitation to the use of titanium dioxide is the wavelength at which it absorbs, as the most intense absorption band is in the UV region, which makes it impractical for hospital applications as large UV lamps would be required to activate the surface. Many attempts have been made to modify titanium dioxide so that it absorbs visible light, which would make it more practical. To this end, attempts have been made by modifying the surface of titanium dioxide with amines, sulphurs and many others including the modification done by Sato in 1986 which involved the addition of NH_4OH to a titania sol followed by a calcination, this was found to give a material that exhibits a visible light response.[19,20,21]

Titanium dioxide exists predominantly in three forms: anatase, rutile and brookite.[22,23] Anatase is the most common form of titanium dioxide that is used in catalysis and photocatalysis as it has the highest surface area. Rutile is the higher temperature form of anatase, which forms at 500 °C. Titanium dioxide has band gaps of 3.2, 3.02 and 2.96 eV for the anatase, rutile and brookite forms, respectively.[24] The oxide vacancies created in titanium dioxide lead to the partial reduction of Ti^{4+} to Ti^{3+}. There is then an electron in the valence band that is available to be promoted into the conduction band. The electron created in the conduction band reacts with oxygen to form an effective oxygenation agent, superoxide, in a rate-limiting step which also scavenges excess photo-excited electrons. The process is thought to occur by initial dynamic trapping of the conduction-band electron in shallow traps at surface titanol groups to form TiOH groups, which then react with oxygen to re-oxidize the titanol groups.

Titanium dioxide has many different applications in photocatalysis and solar energy conversion.[20–22,25] The unique properties of titanium dioxide such as high thermal stability, high efficiency, high chemical stability and lack of toxicity makes titanium dioxide useful as a material for different applications that include self-cleaning surfaces, antibacterial agents and UV protection agents in sunscreen. Photocatalytic applications using titanium dioxide that are driven by solar light are limited due to the wide band gap,

3.2 eV for titanium dioxide.[26] A large band gap means that less than 5% of the available photons of the solar spectrum are absorbed.

Although the modification of titanium dioxide allows it to be used in the visible region of the spectrum there are limitations associated with titanium dioxide nanoparticles. Some limitations of titanium dioxide nanoparticles include; low solubility in water – this is true for most nanoparticles as they are held mostly in suspension due to their small particle size. Another limitation is that they are not easy to modify, and also that they absorb only in the UV region of the spectra.

Titanium dioxide has been investigated numerous times for different applications, and this research area is crowded when investigating the modification of titanium dioxide for use in visible light applications, suggesting that an alternative needs to be found.

A favourable alternative to titanium dioxide are organic photosensitisers, as these photosensitisers have improved solubility and the wavelength of absorption can be easily optimised. Organic photosensitisers generally have larger absorption spectral windows compared to titanium dioxide and other inorganic species. An organic photosensitiser also has more opportunities for modification. For example, the coordination of a metal into the core of porphyrins, and other modifications can be carried out on different positions on the chromophoric core. Photosensitisers can also be solubilised with ease, when compared to titanium dioxide.

1.4 The use of photosensitisers against healthcare associated infections

The use of photosensitisers against healthcare associated infections is known as antimicrobial photodynamic therapy (aPDT) or photodynamic antimicrobial chemotherapy (PACT).[27–32]

Antimicrobial photodynamic therapy uses a non-toxic photosensitiser and light to generate singlet oxygen and free radicals that are able to kill microbial cells.[27,29,31,33–36] Upon absorption of light, the photosensitiser follows a photochemical pathway, which is outlined in the Jablonski diagram shown in **Figure 3**. Photosensitisers have a stable electron configuration. Before light is absorbed they are in a singlet state, ^{0}PS, where they contain no unpaired electrons. When the photosensitiser absorbs light of a specific wavelength an electron is promoted to an excited state, ^{0}PS*, which is also a singlet state and has a short lifetime (10^{-6}–10^{-9} s). The photosensitiser can return to the ground state by the emission of a photon as light energy (fluorescence) or loss of energy as heat (internal conversion). The molecule can alternatively convert to the triplet state *via* a process called intersystem crossing: this involves a change in the spin of one electron. The triplet state has lower energy than the singlet state but it has a longer lifetime, due to the spin forbidden nature of the T (Triplet State) to S (Ground State) transition. The singlet state photosensitiser can react with molecules *via* a type I reaction. The excited triplet state photosensitiser can also react with surrounding molecules *via* a type I reaction, but can also transfer energy to molecular oxygen in a type II process. Type I reactions are characterised by electron transfer, while type II reactions are associated with energy transfer, usually to ground state (triplet) oxygen.[37,38] In a type II reaction the excited photosensitiser can transfer its energy directly to the molecular oxygen resulting in the production of reactive oxygen species (ROS), which are able to kill microbial cells and viruses.[38]

Both Gram-positive and Gram-negative bacteria are susceptible to the photosensitising action of a variety of photosensitisers under appropriate conditions. There are many examples showing photodynamic inactivation of a variety of both Gram-positive and Gram-negative bacteria, such as *E. coli*,[39] *S. aureus* [39], *S. mutans*,[40] *P. gingivalis*,[41] and *P. aeruginosa*.[42] Various studies have shown that there is a fundamental difference in susceptibility to photodynamic antimicrobial chemotherapy (PACT) between Gram-positive and Gram-negative bacteria, due to structural differences between the two strains.[9]

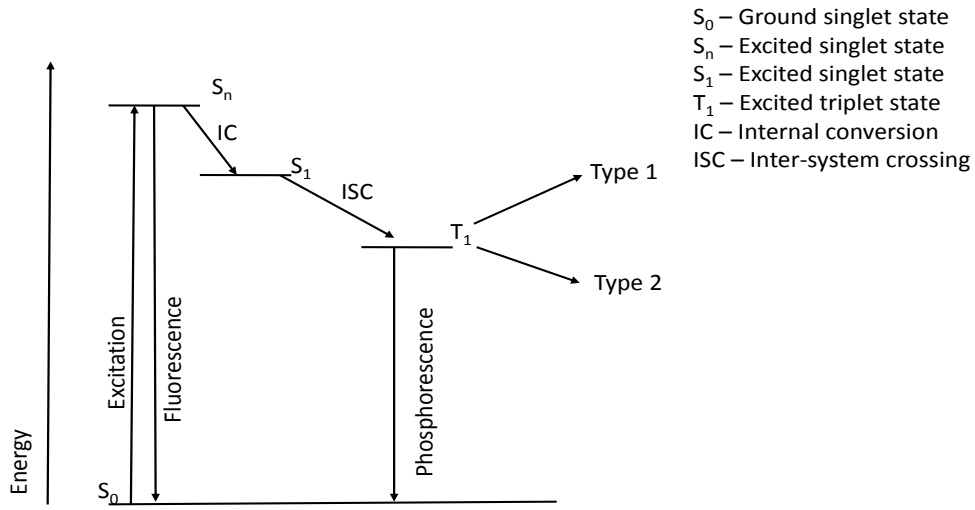

Figure 3 – Simplified Jablonski diagram.

Singlet molecular oxygen is known to react with unsaturated systems by attacking the double bond to form either peroxides or hydroperoxides, some typical reactions are shown in **Figure 4**.

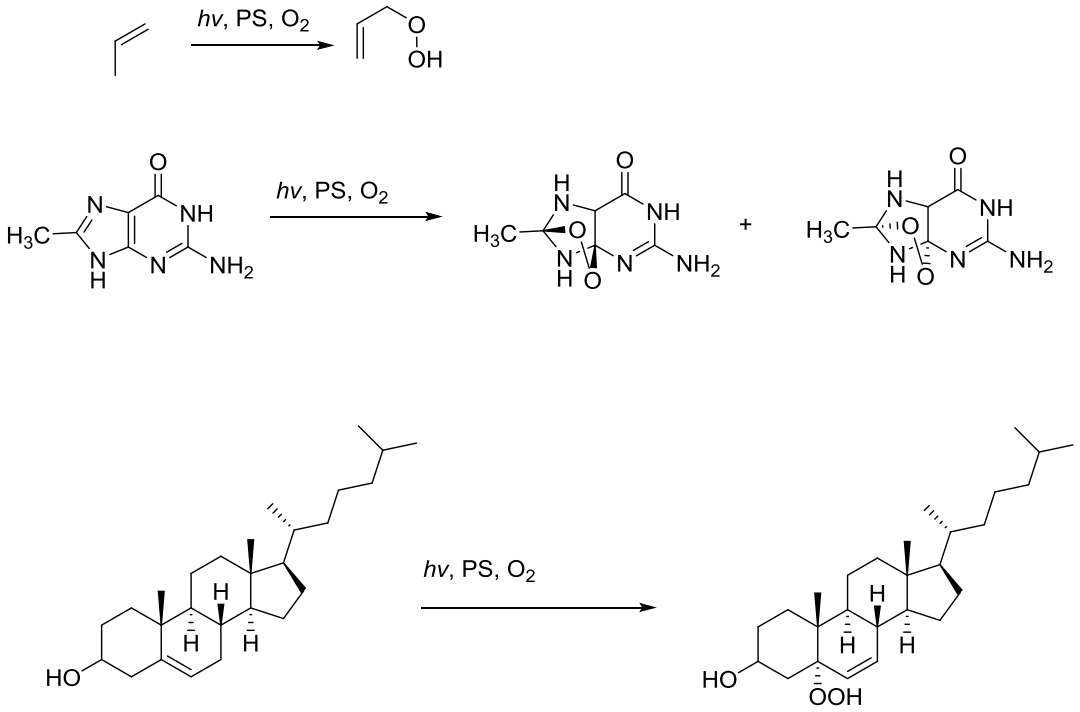

Figure 4 – Typical singlet oxygen reactions.

The use of singlet oxygen traps allows the detection of singlet oxygen spectroscopically, and various reagents are commercially available. The most common singlet oxygen traps

are singlet oxygen sensor green (SOSG), which detects singlet oxygen by fluorescence, and 9,10-anthracenediyl-bis (methylene)dimalonic acid (ABDA) which can be monitored spectrophotometrically by the decrease in the absorption band at 280-300 nm (**Figure 5**).

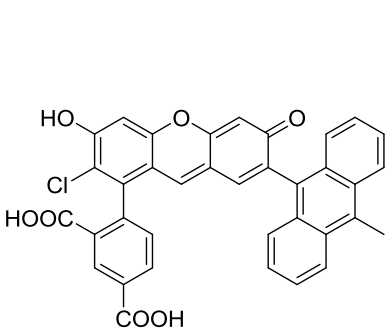

Singlet oxygen sensor green (SOSG)

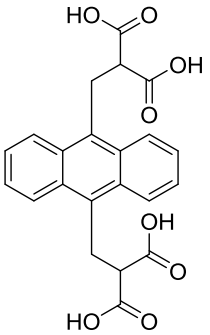

9,10-anthracenediyl-bis (methylene)dimalonic acid (ABDA)

Figure 5 - Structure of singlet oxygen sensor green and 9,10-anthracenediyl-bis(methylene)dimalonic acid.

For a molecule to be an efficient photosensitiser it must absorb light and form an excited triplet state suitable for electron or energy transfer reactions.[27] Molecules that are used as photosensitisers are typically rigid planar structures with a high degree of conjugation, these include porphyrins, phthalocyanines and the phenothiaziniums shown in **Figure 6**.

Porphyrins are heterocyclic molecules that are formed from four pyrrole subunits joined together by a methine bridge.[28,30] Phthalocyanine molecules are isoindole subunits connected *via* aza nitrogens as opposed to the methine bridges in the porphyrin molecules, and have additional conjugation from benzenoid rings fused to the pyrrolic positions. Phenothiazine molecules are usually three six-membered aromatic rings fused together with a nitrogen and sulphur moiety in the central ring.

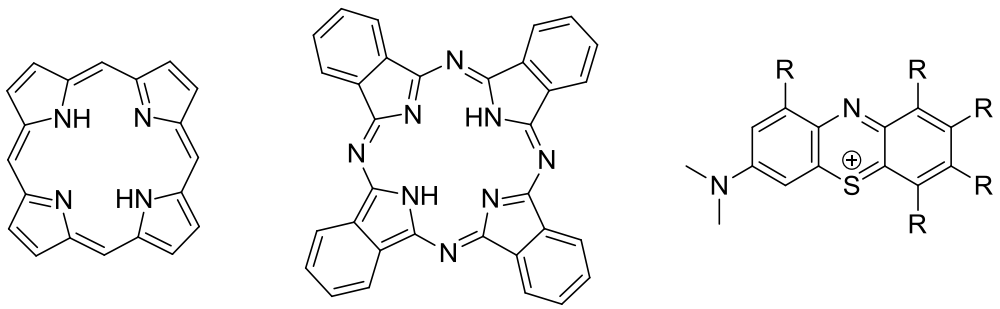

Figure 6 – Photosensitiser molecules; porphyrin, phthalocyanine and phenothiazinium.

Methylene blue (MB) and toluidine blue (TBO) are the most widely used phenothiazinium compounds for aPDT; they absorb at 656 nm and 625 nm respectively.[27] There has been research into the use of MB as an antimalarial drug,[43] in blood cell staining,[43,44] and also clinical potential against local infection due to high cytotoxicity against both Gram-positive and Gram-negative bacteria. Porphyrins, phthalocyanines and phenothiazines can be modified to be either positively or negatively charged to help aid water-solubility.

When comparing both anionic and cationic photosensitisers, cationic photosensitisers are known to be more efficient at killing bacterial cells compared to neutral or anionic photosensitisers.[35,45,46,47]Cationic photosensitisers have been proven to be more efficient due to their greater activity against Gram-negative bacteria which have an outer membrane, which is negatively charged and forms a barrier between the cell and the environment. In 1996 Merchant *et al.* carried out a study comparing the activity of two cationic porphyrins and an anionic porphyrin against both Gram-positive and Gram-negative bacteria.[47] The study found that all the porphyrins were able to inactivate the Gram-positive bacteria, but only the cationic porphyrins were able to inactivate the Gram-negative bacteria. This study was confirmed by Minnock *et al.* who carried out a similar study, but instead of using porphyrins as the photosensitisers they used phthalocyanines and similar results were found.[46] Cationic photosensitisers such as methylene blue bind to the bacterial cell *via* an ionic interaction to carboxylate or sulphonate residues in the various strata of the bacterial cell wall. The cations that are not bound enter the cell wall *via* the tiny channels known as porins, but there is a size limit.[48] Another mechanism that photosensitising molecules can use to penetrate into the cell is *via* self-promoted uptake. This approach allows the displacement of divalent cations from the binding site of the bacteria leading to a higher affinity of photosensitiser inside the cell.[49] The self-promoted approach for the uptake of photosensitiser molecules into bacterial cells can be summarised in a stepwise mechanism; binding of the cationic photosensitiser with the negatively charged groups on the outer wall of the cell, dark or photo-induced alteration of the outer wall permeability, translocation of the photosensitiser to the inner plasma membrane, visible light excitation of the photosensitiser and thus generation of reactive cytotoxic species, photooxidation of multiple targets in the photosensitiser subcellular microenvironment, impairment of cell functions and metabolism, and then inhibition of cell growth and cell death.

1.5 Porphyrin synthesis

Porphyrins have numerous characteristics that fit the requirements for the particular application of a sterilising surface. Porphyrins are versatile materials that have a large absorption spectral range. They are also synthetically versatile and different moieties can be introduced onto the molecule with ease, which can cause changes in the electronic properties of the porphyrin macrocycle. The tetrapyrrolic nature of a porphyrin allows for modification in numerous positions as shown in **Figure 7**.

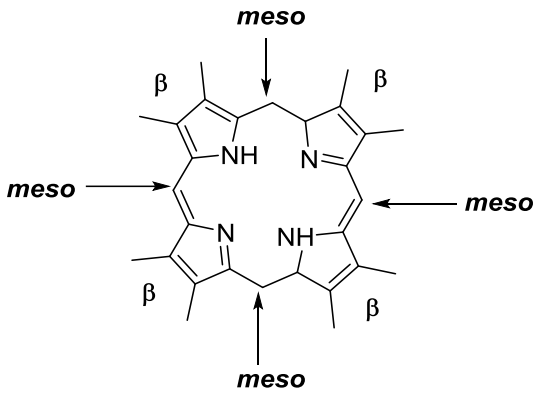

Figure 7 – Naming of the peripheral positions on a porphyrin, showing possible substitutions at the four meso positions and the eight beta positions.

Porphyrin research began with Rothemund in 1936,[50] and from that research it has been re-visited and optimised by Adler-Longo and MacDonald followed by Lindsey.[51,52,53] The anti-fungal properties of porphyrins have been investigated since the early 1980s. When porphyrin molecules are irradiated they are able to kill yeast cells, but they are not taken up by yeast cells. The phototoxic activity of porphyrins in yeast cells is due to the presence of the photosensitiser molecule in the aqueous medium. Water-soluble porphyrins have been found to be more effective in the killing of yeast cells. In contrast phenothiazinium molecules such as MB and TBO are known to localise in the plasma membrane of yeast cells leading to cellular structure damage upon illumination. This leads to increased permeability resulting in cell death.[28]

There has been progressive research into photo-antimicrobial agents and their uses. The main use of photo-antimicrobial agents is on surfaces.[48] The photo-antimicrobial agents can act as a disinfecting surface, the photosensitising agent may be placed on the surface or it may come as part of an integrated surface, for example as part of a surface coating or impregnated onto a catheter.

1.6 Immobilisation of photosensitisers on polymeric supports

Since currently available materials suffer a loss of antimicrobial activity by leaching of the biocide with the potential risk of releasing hazardous agents into the media, the PACT community should invest in the development of new supports, and, most importantly, in the development of new ways to immobilise photosensitisers onto solid supports to create new photo-killing materials with the potential capability of rapid, efficient and low-cost sterilisation of a wide range of bacteria.

A stable and uniform surface coating would allow a high availability of the dye at the surface and the most favourable conditions for the interaction with bacteria and with the oxygen naturally present in the environment. Nevertheless, this approach might be problematic due to the fact that sometimes it is difficult to have a uniform coating of the surface, leading to reproducibility problems. Embedding the dye in a porous support might be a promising alternative, since oxygen must be able to interact with both sensitizer and bacteria. The leaching of the photosensitiser is a general problem that has emerged frequently.[54,55] Thus the development of new ways to immobilize photosensitisers on solid supports seems to be a key challenge towards the practical application of solid-supported PACT devices.

The choice of the photosensitiser (cationic/anionic), besides being a key factor for activity against different bacterial strains, needs to be considered alongside other desirable characteristics, such as an economic viability and ease of synthesis.

Immobilisation of photosensitisers on polymeric supports allows for increased potential applications. The immobilisation allows for re-usability of the material, which is favourable when using in a community or hospital-based application. The use of a polymeric support can also aid in decreasing the toxicity of the photosensitiser. Immobilisation of the photosensitiser usually means that the amount of leaching of the photosensitiser in the aqueous medium or onto the surface is decreased and in most cases negligible.[54,56–59] The polymeric support that is used must have particular characteristics including: low toxicity; porous structure to allow for the permeation of oxygen; cheap, re-useable; and withstand the conditions required to kill bacteria. Two types of polymeric supports that can be used are natural and synthetic polymers. There are both strengths and weaknesses for the use of both natural and synthetic polymers outlined in **Table 1**.

Natural polymers	Synthetic polymers
- **Easily accessible**	- **Versatile**
- **Cost-effective**	- **Not always cost effective**
- **Not easily modified**	- **Easily modified**
- **Generally non-toxic or low toxicity**	- **Toxicity is sometimes unknown**

Table 1 – Comparison of natural and synthetic polymers for use as a polymeric support for the immobilisation of photosensitisers.

1.6.1 Natural polymers

Natural polymers such as chitosan, cellulose and cotton have been used for the immobilisation of photosensitisers.[58–71] The main advantage of using a natural polymer is that they are generally cheap and readily available. The main disadvantage is that natural polymers are not easily modified, which can cause problems when attempting to covalently attach a photosensitiser to the surface. Due to difficulties in covalent attachment, research has been carried out where the photosensitiser is not covalently bound to the support, which has meant that leaching of the photosensitiser from the polymeric support has been seen.

1.6.1.1 Immobilisation of porphyrins on natural polymers

The immobilisation of porphyrins to natural polymers has been a flourishing area of research. It has been shown that when immobilised on natural polymers porphyrins maintain their antimicrobial properties, this has been seen for immobilisation to natural supports such as chitosan, cellulose or dextran. Numerous natural polymeric supports have been investigated for the immobilisation of porphyrins including: cellotriose moieties,[60,61] iron oxide nanoparticles,[62] sulfonated C60,[63] cellulose,[64–68] dextran, cellulose diacetate, cellulose esters,[65–67] cotton,[58,64] paper[69], nanocrystalline cellulose (CNC)[59,68] and chitosan.[70,71] The immobilisation of porphyrins on natural polymers has been carried out using commercially available porphyrins such as protoporphyrin IX (PPIX) and non-commercially available synthetic porphyrins.

1.6.1.1.1 Immobilisation of porphyrins on cellulose and modified cellulose

The immobilisation of porphyrin on cellotriose was carried out by Sakakibara *et al.*[60] whereby a carboxylic acid functionalised porphyrin was bound to cellotriose for use in optoelectronic measurements with C60, which allowed the receptor ability of the synthesised compound to be analysed by studying the absorption spectrum changes in the decrease of the soret band and increase in a new band for the C60. Krouit *et al.* studied the effect of immobilising commercially available PPIX to cellulose *via* a one-pot two-step reaction.[65] The first step involved the esterification of cellulose with PPIX and then the next step involved the washing of the material to remove any unreacted starting materials. The material that was formed was tested against both Gram-positive (*S.aureus*) and Gram-negative (*E.coli*) bacteria and the results showed that a minimum amount of porphyrin immobilised (0.52% grafting) was required to kill *E.coli*, but that *S.aureus* did

not require such a high amount of porphyrin and results were seen for 0.19% porphyrin grafted on the surface.

Continuing on their interest in this research area, Krouit *et al.* investigated the use of synthetic porphyrins 5,10,15-tri(4-methylphenyl)-20-(4-*N*-methylpyridyl)porphyrin and porphyrins with spacer arms comprising 4- or 11-carbons such as 5-[4-(3-carboxypropyloxy)phenyl]-10,15,20-tri(4-methylphenyl) porphyrin) and 5-[4-(10-carboxydecanoxy)phenyl]-10,15,20-tri(4-methylphenyl) porphyrin immobilised on cellulose *via* the same one-pot two-step reaction as before, and evaluated against Gram-positive (*S.aureus*) and Gram-negative (*E.coli*) bacteria (**Figure 8**).[67]

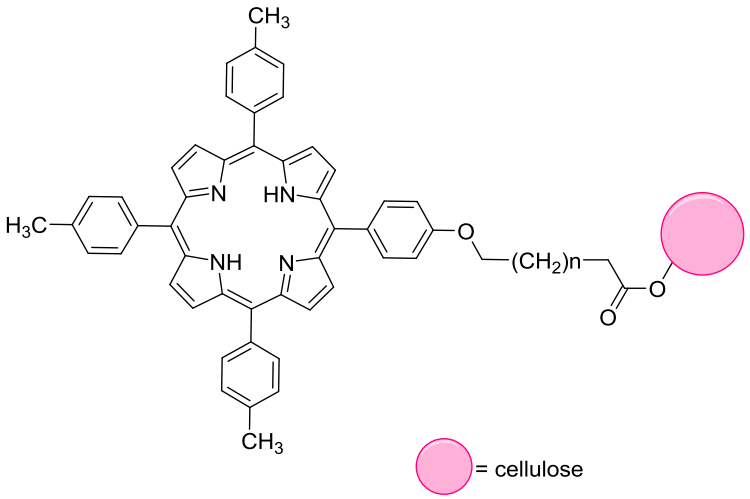

Figure 8 - Structure of porphyrins investigated by Krouit *et al.*[67]

The synthetic porphyrins had different chain lengths to see if the length of the alkyl chain had an effect on bacterial killing. The photobacterial materials were tested for singlet oxygen production using ergosterol acetate trapping and they were all found to produce singlet oxygen. The bacterial testing was successful and the minimum amount of porphyrin immobilised to kill both Gram-positive and Gram-negative bacteria was found to be 0.18%.

In 2012 Carpenter *et al*. investigated a different approach and investigated the use of nanocrystalline cellulose (CNC) nanocrystals and an alkyne-functionalised water soluble porphyrin. Carpenter *et al.*[59,68] and Feese *et al.* both used CNC as the support for a photobactericidal material formed from the covalent attachment of a [5,10,15-tri(4-*N*-methylpyridyl)-20-(4-alkylphenyl)porphyrinato]zinc(II) to the surface of an azide-modified cellulose nanocrystals through a "click" reaction. Nanocrystalline cellulose (CNC) is obtained from cotton fibre through the acid hydrolytic disruption of the amorphous domains of cellulose and the consequent conversion of native cellulose fibers into a colloidal dispersion.

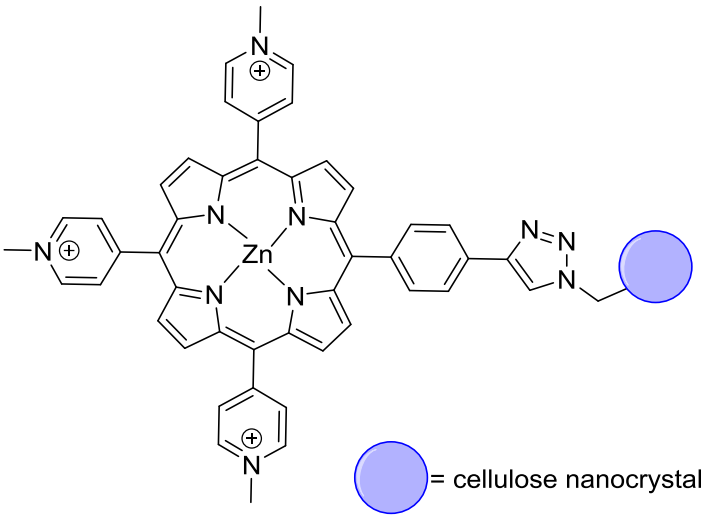

Figure 9 - Structure of clicked porphyrin used by Carpenter *et al*.[68]

Due to its favourable properties such as large surface area, good mechanical strength and biodegradability, as well as availability and biodegradability, it is currently being investigated as a component of transparent flexible films. The photobactericidal activity of porphyrin–cellulose nanocrystals films was investigated against a wide variety of bacteria, such as *A. baumannii*, multidrug-resistant *A. baumannii* (*MDRAB*), methicillin-resistant *S. aureus* (*MRSA*), *P. aeruginosa*, *E. coli*, *S. aureus* and *M. smegmatis* (mycobacterium smegmatis).[68]

1.6.1.1.2 Immobilisation of porphyrins on cotton

Ringot *et al.* studied the immobilisation of porphyrins on cotton.[58] The paper investigates the use of 5-(4-aminophenyl)-10,15,20-triphenylporphyrin (TPP-NH_2), anionic 5-(4-aminophenyl)-10,15,20-tri(4-sulphonatophenyl)porphyrin (TPPS-NH_2) and cationic 5-(4-methylpyridyl)-10,20-di(2,4,6-trimethylphenyl)-15-(4-aminophenyl)porphyrin(*trans*-MePy-NH_2) for attachment *via* the amine groups (**Figure 10**).

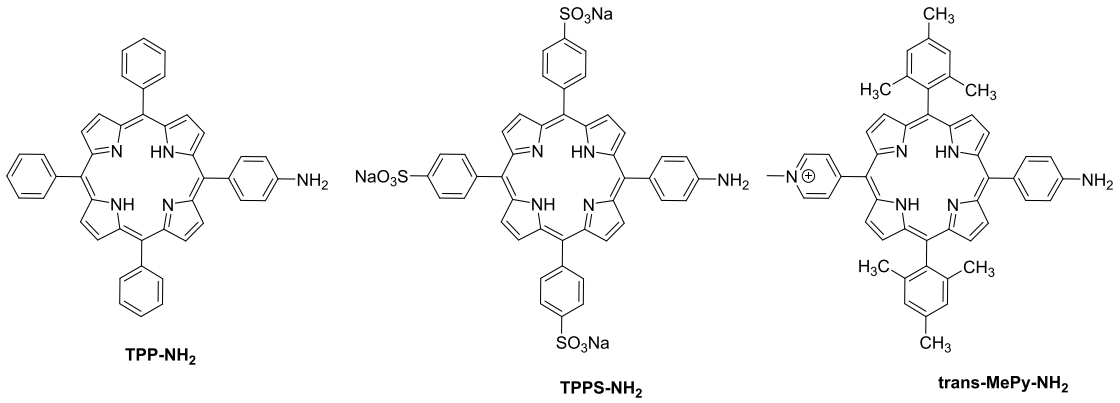

Figure 10 - Structure of three porphyrins used for immobilisation on cotton by Ringot *et al*.[64]

The attachment of the porphyrin to the cotton was made *via* a triazine linkage, which was carried out using cyanuric chloride which allows substitution of the chloride for the porphyrin with the amino functionality. The modified fabric was non-toxic towards either bacterial species in the dark. After 24 h exposure to white light irradiation, all modified surfaces caused a photobactericidal effect in Gram-positive bacteria *S. aureus*. Cationic cotton gave the best result in terms of bacterial growth inhibition, followed by neutral cotton and anionic cotton. Percentages of bacterial growth inhibition were 100% for cationic cotton, 94% for neutral cotton and 37% for anionic cotton, respectively. The most successful, in terms of bacterial killing against both Gram-positive (*S.aureus*) and Gram-negative (*E.coli*) was the cationic porphyrin, then the neutral porphyrin. The anionic porphyrin was the least effective.

1.6.1.1.3 Immobilisation of porphyrins on modified nanoparticles

Commercially available protoporphyrin IX (PPIX) was successfully attached to nanoparticles composed of an iron oxide core coated with dextran by an esterification reaction using 1,1'-carbonyldiimidazole (CDI: 2 eq./porphyrin) as the electrophilic activator.[62] These particles were incorporated into cultured cancer cell lines showing a potential application in PDT.

1.6.1.1.4 Immobilisation of porphyrins on chitosan

Organised, multilayer organic–inorganic films of sulfonated C60, 5,10,15,20-tetra(4-*N*-methylpyridyl)porphyrin ($TMePyP^{4+}$) and chitosan were formed using electrostatic layer-by-layer (LBL) assembly technology, which has proved to be a facile method for generating a wide range of organized and stable thin films.[63] Porphyrin-based photobactericidal materials have been developed by grafting porphyrin-based compounds

onto natural polymers, such as chitosan.[70,71] Porphyrins have been incorporated into reinforced nylon chitosan membranes by adsorption using 5,10,15,20-tetra(4-hydroxyphenyl)porphyrin, (*p*-THPP), or by dissolution and casting with 5,10,15,20-tetra(4-aminophenyl)porphyrin, (p-TAPP), and used in a circulating water photoreactor system as a model for a large-scale water-flow system.[70] The concentration of the adsorbed porphyrin was estimated to be about 5.7 μg cm^{-2} while the concentration of the porphyrin immobilised by casting was found to be 7.5 μg cm^{-2} based on solution molar absorbances or on the weight of porphyrin added, respectively. When tested on *E. coli*, both *p*-THPP/chitosan and *p*-TAPP/chitosan membranes displayed a photokilling ability after 40 mins of white light irradiation.

It has been shown that porphyrins maintain their antimicrobial properties when grafted to natural polymers such as chitosan, cellulose or dextran.[58,59,65,66,68–70,70,72,73] These modified polymers have been cast into photobactericidal membranes or films that have potential eco-friendly uses as antimicrobial coatings. The problem is that although the photosensitisers show activity against bacteria, an increase in activity is needed in order to fight Gram negative bacteria, as they are more difficult to kill.

An alternative approach that has been investigated is the use of synthetic polymers instead of natural polymers to allow more versatility of the material for the immobilisation of the photosensitiser.

1.6.2 Synthetic polymers

The use of synthetic polymers for the immobilisation of photosensitisers has been seen to be a more elegant approach. Synthetic polymers are generally more expensive to use. Their use is also more time consuming as the polymer also needs to be synthesised, along with any specific monomers that are required to generate a specific conjugatable handle to be used later in the synthesis. Synthetic polymers are more versatile than natural polymers as they can be synthesised with the appropriate synthetic handle that is required for the covalent attachment of the photosensitiser. Many synthetic polymers have been used for real-life applications. The most popular synthetic polymer that has been used for biomedical applications is poly (HEMA) which has been used for contact lenses,[74,75] and also poly(acrylamide) as it can be synthesised easily and is also a very versatile support.[76,77] Significant research has been carried out into the use of synthetic polymers for the immobilisation of porphyrins. The supports that have been investigated include: anionic Dowex resin,[76] Merrifield polymer,[72] per-fluorinated ion exchange membranes,[73] poly(methylmethacrylate)s, anionic polythiophene,[78] doped polysilsesquioxane,[79] various different modified polystyrenes,[54,56,57,80–84] polyurethane (PUR)[85] and silica.[70]

1.6.2.1 Porphyrins immobilised on anionic dowex resin

Water-soluble, [5,10,15,20-tetra(4-sulphophenyl)porphyrinato]iron(III) was immobilised into anionic Dowex resin for catalytic purposes.[76] The immobilisation was monitored by colour change occurring on the surface, and the amount of green colour present on the surface. The formation of the surface was carried out by having a suspension of the Dowex resin in distilled water with 4 mg of the iron(III) porphyrin, and stirring for 2-3 hours at room temperature. This system was stable. In fact, even after filtration and washing with distilled water, the solid was found to completely retain the adsorbed iron porphyrin, and this material was easily recovered after the reaction and reused without loss of activity.

1.6.2.2 Porphyrins immobilised on modified resins

Ribeiro *et al.* studied the photocatalytic behavior of porphyrins covalently linked to a Merrifield polymer previously modified with an excess of α,ω-diamines to obtain amino alkylated polymers suitable for reaction with chlorosulfonated porphyrins.[72] The authors also reacted the chlorosulfonyl porphyrin with commercially available aminomethylated polystyrene divinylbenzene co-polymer to obtain a porphyrin covalently linked to the polymer but close in proximity to the polymer backbone due to the absence of a spacer molecule. All of the supported photosensitisers were able to generate singlet oxygen with

an efficiency dependent on the structure of the spacer between porphyrin and polymer. The catalyst was filtered, washed and dried and could be recycled with a new substrate batch, with one of the catalysts being reused for three catalytic cycles.

Water-soluble Pd(II), Pt(II) and Rh(III) complexes with 5,10,15,20-tetra(4-*N*-methylpyridyl) porphyrin ($TMPyP^{4+}$) and 5,10,15,20-tetra-(4-*N*,*N*,*N*-trimethylaminophenyl)porphyrin were immobilised in per-fluorinated ion-exchange membranes (e.g. Nafion®) after boiling in concentrated nitric acid for 30 mins and in double distilled water for 30 mins to clean them, and to make them optically transparent above 240 nm.[73] The membranes revealed a good photostability and high oxygen permeability.

1.6.2.3 Porphyrins immobilised on polystyrene and modified polystyrene

Polystyrene has been shown to be a versatile support that can be used either modified or unmodified for the immobilisation of porphyrins and other photosensitisers.

Gao *et al.* investigated the use of cross-linked polystyrene (CPS) microspheres (0.32 - 0.45 mm in diameter), with a cross-linking degree of 4% for the direct synthesis of a porphyrin-polystyrene conjugate through modification of the polystyrene microspheres themselves.[80]

CPS microspheres are readily available, cheap, mechanically robust and chemically inert, and they can undergo facile functionalisation. The main application that Gao *et al.* studied was for use in phase transfer catalysis. The modified CPS microspheres were formed *via* multiple steps which involved the modification of the CPS microspheres themselves firstly with an aldehyde and then through the formation of the porphyrin on the surface *via* the standard Adler–Longo method using propionic acid as the catalyst and the selected aldehyde with pyrrole. Analysis of the porphyrin that had been immobilised using solid UV-Vis and AT-FTIR, and they revealed that the amount of porphyrin immobilised was found to be 0.2 mmol g^{-1}.

Griesbeck *et al.* recently reported polymer-bound sensitizer systems using TPP or 5,10,15,20-tetra(4-methylphenyl)porphyrin (TTP).[81,82] Commercially available polystyrene beads (approx. 60 μm) cross-linked with divinylbenzene were utilized as the polymeric support. The polystyrene beads were loaded with the sensitising molecule by swelling with a solution of catalytic amounts of TPP and TTP in ethyl acetate followed by evaporation of excess solvent from the solution. Following this, photooxidation of α-pinene and ethyl tiglate was used to quantify photoactivity of the porphyrin loaded beads.

The authors were able to show that singlet oxygen is produced in a solvent-free photooxygenation process.

Griesbeck *et al.* also designed a solventless reaction which has been the subject of considerable interest as an eco-friendly synthetic approach, reducing the amount of environmentally problematic and expensive solvents and retarding the production of side-products as a result of the enhanced selectivity.[82] Commercially available PPIX and 5,10,15,20-tetra(4-vinylphenyl)porphyrin (TSP) were attached to polystyrene beads cross-linked with divinylbenzene (**Figure 11**).

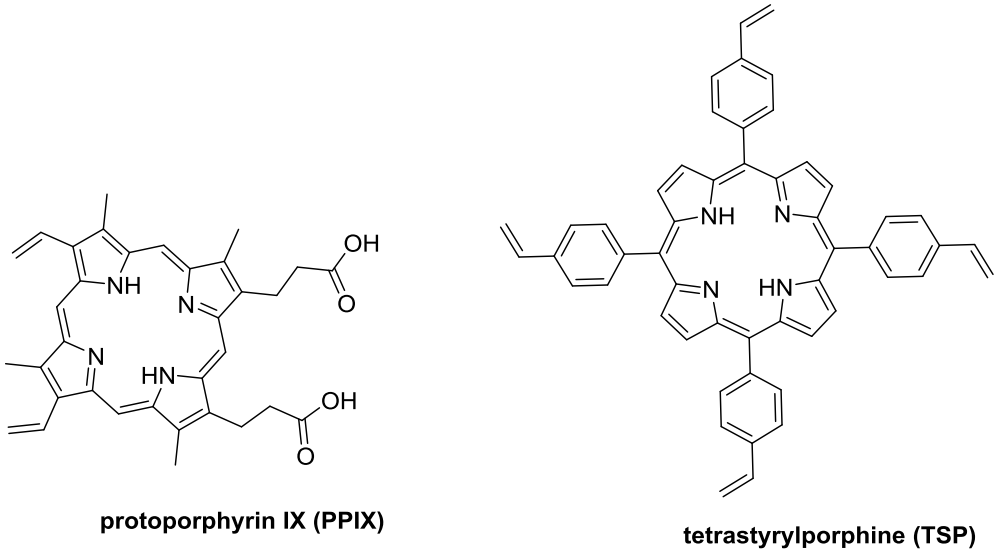

Figure 11 - Structure of two porphyrins used by Griesbeck *et al.*

The process was carried out using emulsifier-free polymerization of styrene with divinyl benzene for the formation of nanosized polystyrene-divinylbenzene particles. The method was a one-pot synthetic method with the porphyrin embedded in the backbone of the polymer. This technique allowed the syntheses of the translucent particles in a simple and reproducible way. In particular, the production of singlet oxygen under irradiation conditions was of interest from the viewpoint of PACT.

In 2003 Inbaraj *et al.* reported the functionalization of cationic *N*-alkylpyridinium polystyrene supports with 5,10,15,20-tetra(4-sodiumsulphonatophenyl)porphyrin (TPPS) and its metallo complexes [5,10,15,20-tetra(4-sodiumsulphonatophenyl)porphyrinato]cadmium(II) (CdTPPS) and [5,10,15,20-tetra(4-sodiumsulphonatophenyl)porphyrinato]zinc(II) (ZnTPPS). The polymeric support used was 2% cross-linked divinylbenzene with styrene. The porphyrin was attached *via* ionic interactions from a positive charge on the pyridine to the sulfonate group on the porphyrin. The researchers investigated the production of singlet oxygen of the

synthesised materials using *N,N*-dimethyl-4-nitrosoaniline (RNO) as an indicator for photo-induced singlet oxygen with imidazole as a chemical trap for singlet oxygen. Quantum yields were reported as 0.29, 0.27, and 0.16 for PS–H_2TPPS, PS–ZnTPPS, and PS–CdTPPS, respectively, whilst the unbound porphyrins had singlet oxygen quantum yields of 0.62 and 0.81 for H_2TPPS and ZnTPPS, respectively, which are significantly higher than those obtained when the porphyrin was immobilised. Inbaraj *et al.* found that the binding of the porphyrin to the polymer decreased the singlet oxygen quantum yield, which they speculated that it is due to the structural deformation of the appended porphyrins on the spherical shape of polymer bead surface, and the resulting decrease in exposure to light. The use of these materials against bacteria was not investigated, they simply reported the production of singlet oxygen.

1.6.2.4 Porphyrins immobilised on silica

Magaraggia *et al.* investigated the use of silica as a support for the immobilisation of meso-tri(*N*-methylpyridyl)mono(*N*-tetradecyl-pyridyl)porphyrin.[57] The porphyrin chosen was thought to have good antibacterial properties which is why it was chosen for this study. The material was synthesised by the modification of silica microparticles which were formed by the addition of the porphyrin to a binary mixture containing methanol and an ammonium solution with tetraethylorthosilicate (TEOS). Following the addition of the TEOS, the mixture was left for 6 h to produce a brown solid. The porphyrin loading was found to be 3.47 x10^{-5} M, with an encapsulation efficiency of 18%. Once produced the solid was tested for the production of singlet oxygen, comparing the singlet oxygen production both when the porphyrin had been encapsulated in the silica solid and when the porphyrin was in solution. The authors found that when the porphyrin was encapsulated in the silica microparticles the amount of singlet oxygen produced in the solid was less than that of the porphyrin in solution. They carried out testing against both Gram-positive (*MRSA*) and Gram-negative (*E.coli*) bacteria and they found that there was a 4 log decrease after 20 mins for *MRSA* and a 4 log decrease after 30 mins for *E.coli* when the porphyrin was encapsulated in the silica microparticles. When the effectiveness of the encapsulated porphyrin to the free porphyrin, the free porphyrin was found to have a 5 log decrease for *MRSA* and a 6 log decrease for *E.coli*.

Carvalho *et al.* investigated the use of magnetic nanoparticles for photodynamic inactivation of bacteria.[54] Alves *et al.* continued to perform research in this flourishing area and investigated the use of silica-coated iron oxide nanoparticles for water disinfection applications.[56] The production of the nanomagnet-porphyrin hybrid was

carried out using a cationic porphyrin, [5-(pentafluorophenyl)-10, 15, 20-tris (1-methylpyridnium-4-yl) porphyrin tri iodide, and Fe_3O_4 nanoparticles. The researchers studied the use of iron oxide nanoparticles for their magnetic properties as it allowed for easy removal using magnets when the material needs to be re-used against a fresh colony of bacteria. The re-usability of the material was studied and the reduction in viability was found to be a 4.8 log decrease for *E.coli*.

Rychtarikova *et al.* also investigated the use of silica supports for the immobilisation of porphyrins against both Gram positive and Gram negative bacteria. This report considers two different types of silica source, comparing tetrakis (2-hydroxyethoxy)silane (THES) and tetramethoxyorthosilane (TMOS) and compares the use of them against bacteria, as they have different compositions when the solid support is formed. The porphyrin used was a cationic porphyrin, 5,10,15,20-tetrakis(1-methyl-4-pyridino)porphyrin (TMPyP), which was entrapped inside the two different silica matrices using the sol-gel method. The solid materials that were synthesized were tested for the production of singlet oxygen through using the iodometric method using a halogen lamp. The material itself, without the incorporation of the porphyrin, was found to not produce singlet oxygen. There was no visible leaching of the porphyrin from the solid matrix when investigated by absorption spectroscopy: only leaching of the contra-ion *p*-toluene sulfonic acid was seen at 220 nm. The solid supports were also tested against bacteria, using genetically modified *E.coli* (BL21 (DE3)), and the one incorporating THES was found to give better bacterial killing than TMOS.

1.6.2.5 Porphyrins immobilised on poly (urethane)

Mosinger *et al.* investigated the use of poly (urethane) as a solid support for the immobilisation of ZnTPP against genetically modified Gram-negative bacteria (*E.coli*, DH5α containing plasmid pGEM11Z).[85] The materials were prepared using the electrospinning method, and the loading of the porphyrin was 0.1%. The material was found to be active against the Gram-negative bacteria with no bacteria growing on the support with the porphyrin present after overnight incubation. The control without the porphyrin present showed bacterial growth, which indicates that the porphyrin is causing bacterial cell death.

1.6.2.6 Conclusion of porphyrins immobilised on synthetic supports

The immobilisation of porphyrins on synthetic supports is a flourishing area of research, with numerous different types of supports being investigated including; polystyrene, silica, nanoparticles and commercially available resins. Synthetic supports have shown

promising results for the formation of an antibacterial surface, as they show minimal leaching of the porphyrin from the support which is important for real-life applications, as the toxicity needs to be low. The synthetic support allows more modifications than the natural support which has meant that the use of different porphyrins to help improve bacterial killing has been investigated, by optimising the properties of the porphyrin be it the substitution pattern, or the metal inside the central cavity the bacterial killing can be increased giving a better antibacterial surface. The use of synthetic supports also allows for more control over the structure of the polymeric support, including the size of the support and the also the texture of the support.

1.7 Self-sterilising revolution – Light activated antimicrobial agents

One method for disinfecting a surface is by using a coating that produces reactive radical species. These species will have no target within a microbe and are completely non-selective.[12] There are two coatings that have been popular in this research area that are able to produce reactive oxygen species and therefore act as antimicrobial surfaces; one which has a photosensitiser immobilised in a coating, and one that is formed from titanium dioxide acting as a photocatalyst. Both of these are known as light-activated antimicrobial agents (LAAAs), as they are activated by light. Photosensitisers are used as antimicrobial agents in a similar way to those used for photodynamic therapy (PDT): the photosensitiser is irradiated with light and forms an excited state which can then produce reactive oxygen species (ROS).

A significant amount of research has been carried out into the formation of materials and surfaces that can be used against bacteria, but another major problem is the reusability of the material and the cost of the material. In order for the material to be viable to be used in real life applications it needs to be reusable, cheap and affordable. An example of a commercially available antimicrobial coating is Microban® which contains triclosan.[12] The main problem with triclosan is that under UV light triclosan can produce dioxins, which are extremely hazardous to humans.

1.7.1 The use of photosensitisers for light-activated antimicrobial agents

The photosensitisation of micro-organisms was first reported at the start of the 20th century, when Oskar Raab observed the phototoxicity of acridine hydrochloride against *Paramecia caudatum*.[86] It was initially thought that the bacterial death could be due to heat, but further investigations by his supervisor Herman von Tappeiner confirmed that the effect seen was not heat induced, but rather it was a light-activated effect, a photodynamic reaction.

Due to the current rise in antibacterial drug resistance there has been research into the development of alternative anti-infective strategies.[45] Surfaces in hospitals have been found to be bacterial reservoirs encouraging the spread of infections. Whilst the transfer of *MRSA via* person-person contact may not be serious in the community, it is a serious problem in a healthcare setting as patients may be immunocompromised and therefore are more likely to catch the infection. The transfer can be more widespread in a healthcare setting and this can be attributed to poor hygiene in hospitals,[86] improved hygiene will not solve the problem completely, so an alternative approach is the development of antimicrobial surfaces or coatings.

Some of the strategies that have been investigated include the use of photosensitisers on polymeric surfaces and the use of titanium dioxide and doped titanium dioxide on hard surfaces.

The use of photosensitisers for the development of light activated surfaces is a possible solution to the problem. The main advantage of using a photosensitiser is that they have a multi-site mode of action against micro-organisms. There has already been research into the use of porphyrins grafted to nylon and alkylated cellulose for the photosensitisation of pathogenic micro-organisms.[59–61,64–68] Porphyrins have been grafted onto both natural and synthetic polymers for inactivation of bacteria. The main disadvantage of using a photosensitiser immobilised in a polymeric support is that when the ROS are produced by the photosensitiser over time it may cause the polymeric support to degrade, so studies should be carried out to check the polymeric support for possible degradation.

1.7.2 The use of titanium dioxide as a light activated antimicrobial agent

An alternative to the use of an organic photosensitiser is the use of semiconductor light activated antimicrobial surfaces such as titanium dioxide.[12] TiO_2 has been used previously for the sterilisation of drinking water and for self-cleaning windows.[87] The main problem with using titanium dioxide is that it is a UV-driven photocatalyst due to the large band gap. Although using titanium dioxide is possible, the amount of UV light present in hospitals is low and therefore, if used, specific UV light sources would need to be installed in hospitals for this to be able to work effectively. The method of bacterial cell death using titanium dioxide was investigated by Lu *et al.*, who studied the effect of photocatalysis on both Gram-positive and Gram-negative bacteria cell walls.[88] They concluded, using atomic force microscopy (AFM), that titanium dioxide when illuminated with light of appropriate wavelength breaks down the cell wall of the bacteria, and the intracellular species leak out of the cell interior.

The modification of titanium dioxide can allow visible light to be used. Doping titanium dioxide with either metals or non-metals can allow for normal lighting conditions to be used.[19] Metal ions can be doped into the structure of titanium dioxide, replacing the Ti^{4+} ions. The first row transition metals have been found to be effective. Other metals that can be used for doping of TiO_2 include the lanthanides, and other metals that have antimicrobial properties such as silver and copper, which are well known for their antimicrobial effects. Research into the use of silver nanoparticle doped titania films has been carried out by Page *et al.* and Dunnill *et al*. for use in antimicrobial coatings.[89,90] The main focus of this research area is the shift of the band onset from the UV region into the visible region.

The shift into the visible region is crucial if the system is to be used in hospital environments. Page *et al.* prepared their coating using glass slides and the sol-gel method, followed by the dipping method for the attachment of silver ions.[89] The film is produced firstly by forming the film of titanium dioxide, which is usually applied as a paste, then this is followed by impregnation with a solution that contains silver, such as silver nitrate. The film produced is then reduced by photolysis to form silver nanoparticles on the surface, which was confirmed by transmission electron microscopy (TEM). The paper reports the bacterial properties of the material against both Gram-positive (*S. aureus* and *B. cereus*) and Gram-negative bacteria (*E.coli*). When comparing the results the film was found to perform better against Gram-positive bacteria than Gram-negative bacteria, and it was speculated that the effectiveness of titanium dioxide as a photocatalyst is partly dependent on the rate of production of hydroxyl radicals at the surface of the semiconductor. The effectiveness is also dependent on the energy of the light used to illuminate the surface, and the competition between electron hole recombination and the redox processes occurring on the surface. Dunnill *et al.* carried out similar research into the use of silver doped titanium dioxide for antimicrobial films.[90] They prepared antimicrobial films that contained a film of titania and silver nanoparticles modified on the surface, which was done by dipping the film into a solution of silver nitrate. The mechanism of action by which the semiconductor thin film acts as an antimicrobial coating follows that of self-cleaning films.

1.7.3 Alternative light-activated antimicrobial agents

Alternative research into this area has been carried out by Pappas *et al.* in 2015,[91] who studied the formation of a surface that is formed of two polymeric networks for use in the prevention of hospital acquired infections. The two active materials are poly(*p*-phenyleneethynylene) and poly(*N*-isopropylacrylamide). Poly(*p*-phenyleneethynylene) is known to be able to inactivate a wide range of microbes and pathogens, and poly(*N*-isopropylacrylamide) is able to switch between being in a hydrophobic "capture" state and a hydrophilic "release" state, which allows a switch on / switch off strategy approach. The combination of the two polymers together creates a material with a surface that can both bind microbes in a suitable way and kill surface bound microbes efficiently. This surface was synthesised by utilising a layer-by-layer approach for the formation of layers of poly(*p*-phenyleneethynylene). Surface initiated atom transfer radical polymerisation was then carried out for the attachment of poly (*N*-isopropylacrylamide) between the layers. The surface was tested against both Gram-positive and Gram-negative bacteria. Following exposure to light of 420 nm for an hour 65% of the Gram-positive *S. aureus* were killed and 70% of the Gram-negative *E.coli* were killed.

1.7.4 Alternative self-sterilising techniques to photosensitisers

Although a sterilising surface is a step forward in terms of research for use against bacteria in hospital settings, the next step would be the production of a self-sterilising surface. A self-sterilising surface is one that sterilises itself when activated by visible light and maintains activity when no visible light is present. The main advantage of the production of a self-sterilising surface is that it can be re-used multiple times and even when the lights are not on the surface will maintain activity.

The ideal surface could contain an electron transfer agent and an electron acceptor molecule, which would change colour when the surface is no longer active. There has been large volumes of research into the use of viologens as electron transfer agents. The viologens show a distinctive colour change when they undergo electron transfer, which would make them ideal for use in this particular project.

1.8 Viologens

The viologens are organic dye compounds that are the parent compound of the paraquat family.[92] Paraquat was first synthesised in 1881, and contains a dimethylated dipyridyl derivative and chloride counter-ions as shown in **Figure 12**.

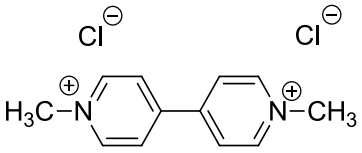

Figure 12 – Chemical structure of paraquat.

Paraquat is widely used as a commercially available weed killer. It is highly toxic so can cause death to animals and humans. A dosage as small as one teaspoon can be enough to be fatal to both humans and animals.

The viologens are more formally known as 1,1' – disubstituted 4,4'- bipyridinium ions, they have a structure similar to that of a substituted derivative of bipyridine as shown in **Figure 13**, where R is a substituent such as an alkyl chain.[93]

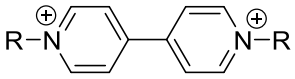

R = alkyl chain or aryl group

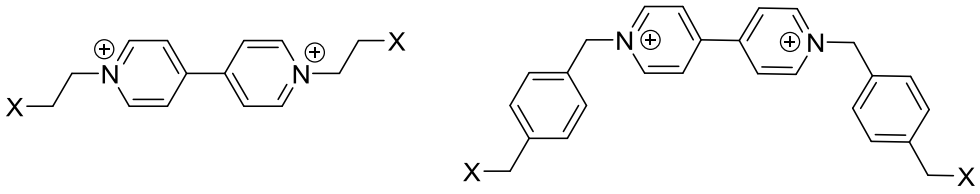

X = halide group, tosyl group or mesyl group.

Figure 13 – General structure of viologen (top), example of aryl spacer (right) example of alkyl spacer group (left).

The repeating group forming the monomer for the polyviologen also contains a xylene group, which can be in either the *ortho, meta* or *para* substituted positions. The anions can be any simple anions, for example; halides, nitrates, sulphates, carbonates or phosphates. The most commonly used anions are the halides and tosylates.[94] In the case of the structure and the properties of the viologens, the 4,4' substituted bipyridine monomer is favoured, relative to the alternative 3,3' or 2,2'isomers, as it allows for a less

sterically hindered, linear polymer to be produced, with the different monomer structures shown in **Figure 14**.

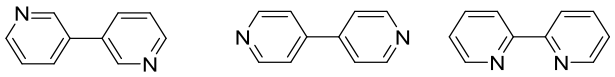

Figure 14 – Structures of 4,4' bipyridine, 3,3’ and 2,2' bipyridine.

The viologens were first investigated for their uses as redox indicators; they have low redox potentials, compared to the standard hydrogen electrode (SHE). The redox values vary with temperature and pH. The potential for methylviologen at 30 °C against the SHE was found to be -0.446 volts.[95] The viologens, unlike most indicators, have a coloured reduced form and colourless oxidised form. The low reduction potential allows for easier electron reduction reactions, thus making the compound better for electron transfer.

From the dication state the viologen undergoes reductive electron transfer to form the radical cation, which is intensely coloured.[93,96,97] The viologens generally have highly anodic redox potentials, but those with cathodic reduction potentials are also known. For example methyl viologen has a redox potential of -0.466 volts compared to benzyl viologen which has a redox potential of -0.359 volts.[95]

1.8.1 Polyviologens

Polyviologens are formed by condensation polymerisation of 4,4’ bipyridine and an alkyl dihalide or ditosylate.[98] The general synthesis involves reacting equimolar amounts of 4,4’ bipyridine with the dihalo or ditosylate derivative in acetonitrile for 18 hours under nitrogen. The product is usually isolated using suction filtration and then dried *in vacuo* at 40 °C overnight. Non-symmetrical viologens can be synthesised by using a non-polar reaction solvent that results in the precipitation of the single substituted mono-cation intermediate, which is then reacted in a more polar solvent with a second electrophile in order to form the fully distributed non-symmetric viologen compound.[92]

The properties of the viologen are maintained when the viologen is polymerised. The polymers are similar to the viologens in that they are colourless in the oxidised form and coloured in the reduced form. Only a small fraction of the polyviologen needs to be reduced in order to obtain the coloured reduced form, but the higher the fraction that is reduced the more intense the colour change. The polymerisation reaction is favoured for good leaving groups such as halides and tosylates.

The polyviologens can be classified as ionene type polymers, which are cationic polymer where the active centre is positively charged, which in this case is the nitrogen on the 4,4’

bipyridine ring system.[99] The polymerisation will proceed with monomers that have substituent groups that can form good leaving groups to help stabilise the active centre of the polymer. Viologens can form polyviologens in two main ways, by having the bipyridine as the backbone for the polymer chain, or by having the bipyridine as the centre and form a star-type polymer.[100] If the viologen is used as the backbone for the polymer it can undergo graft-polymerisation, in which molecules are attached to the side of the main chain of the polymer.[92] This results in highly branched polymers with high molecular weights.

Polyviologens have fascinating properties that make them suitable for use as electron transfer agents, such as the alteration in colour when changing from the dicationic species to the monocationic species and the di-reduced species. Polyviologens also have interesting electrochemical properties including low reduction potential which allows for ease of electron transfer, and they have been used previously for this purpose for example in the splitting of water.[101–104]

1.9 Conjugation methodologies

Conjugation methodologies are a key part of organic synthesis, allowing the joining together of two simple molecules to form a new molecule. There are numerous conjugation methodologies including; peptide couplings, palladium catalyst cross-couplings and, more recently, click chemistry.

1.9.1 Peptide coupling reactions

Peptide coupling can be loosely described as the formation of a peptide bond between a molecule containing a carboxylic acid functionality and an amine functionality with the loss of water.

The most traditional peptide coupling reaction is a carbodiimide-mediated reaction.[105] The reaction proceeds by the use of a carbodiimide reagent, most commonly dicyclohexylcarbodiimide (DCC), which contains two nitrogens that are weakly alkaline allowing for the reaction between an acid to produce an *o*-acylisourea intermediate which rapidly reacts with an amine to form a peptide bond as shown in **Scheme 1**.

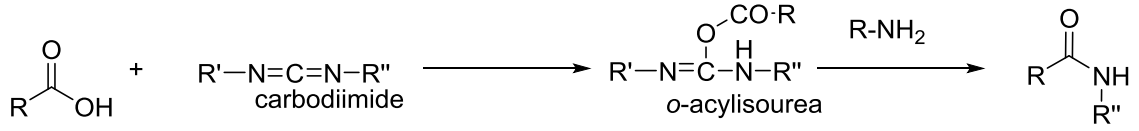

Scheme 1 – Peptide bond formation using carbodiimide coupling reagents.

The main problem when using DCC is that it produces by-products that cannot be removed by column chromatography, which is why alternative diimide reagents have been investigated such as (N-ethyl-N'-(3-dimethylaminopropyl) carbodiimide (EDC).

1.9.2 Palladium catalysed cross coupling reactions

The two palladium cross coupling reactions that are going to be discussed are the Suzuki coupling reaction and the Sonagashira coupling reaction.

1.9.2.1 Suzuki coupling reaction

The Suzuki cross-coupling reaction was first investigated by Suzuki *et al*. [105-107,] who utilised an aromatic halide with an aromatic boronic acid to form a new aryl-aryl bond, shown in **Scheme 2**.

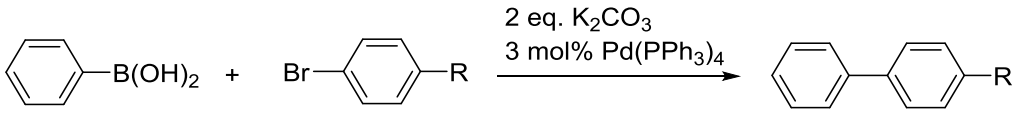

Scheme 2 – Suzuki coupling schematic between an aryl boronic acid and a halogenated aryl derivative.

Palladium-catalysed cross-coupling reactions between organoboron compounds and organohalides or triflates provide a powerful and general methodology for the formation of carbon-carbon bonds.[106] Generally, the aryl halides used in the Suzuki coupling reaction are bromides and iodides, as aryl chlorides do not always react in the coupling reaction except when they are substituted with electron withdrawing groups. A possible alternative is the use of aryltriflates, but they are base-sensitive and thermally labile and therefore require milder conditions when they are coupled with boronic acids, along with the selection of more efficient catalysts such as $PdCl_2$(dppf) and a weak base that is suspended in solution with a polar solvent such as THF.

The general catalytic cycle is shown in **Figure 15**, the sequence involves three main steps; oxidative addition, transmetallation and reductive elimination.[107]

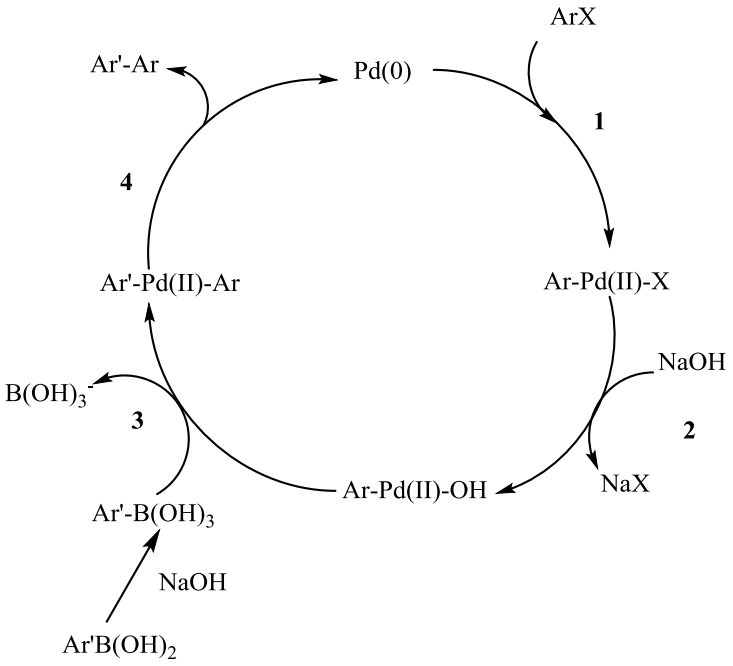

Figure 15 – Catalytic cycle of Suzuki coupling.

The first step in the catalytic cycle is the oxidative addition, which is the rate-determining step. Oxidative addition of 1-alkenyl, 1-alkynyl, allyl, benzyl and aryl halides to the palladium (0) complex gives a stable *trans* palladium (II) complex. The relative reactivity of the halides is I> OTf > Br> Cl. Transmetallation then occurs where the complex reacts with a base such as sodium hydroxide to displace the halide and form instead a hydroxy group. In step 3 the hydroxyl ligand reacts with the boronic acid to form the aryl-palladium-aryl bond. Reductive-elimination then reforms the palladium (0) complex and creates an aryl-aryl bond.

The main catalyst used for Suzuki coupling reactions is $Pd(PPh_3)_4$. These phosphine ligands are known to be stable under prolonged heating which is advantageous.[106] Alternative catalysts include $PdCl_2(PPh_3)_2$ and $Pd(OAc)_2$: the presence of the triphenyl phosphine makes the catalyst favourable as they are stable to air, yet readily reduce to form the palladium (0) complex.

The main advantages of the Suzuki coupling reaction include versatility due to readily available starting materials and mild reaction conditions.

The Suzuki coupling is a promising approach for the formation of porphyrin-viologen conjugates due to the versatility of the reaction.

1.9.2.2 Sonogashira coupling

An alternative reaction to the Suzuki coupling reaction which also utilises palladium as the catalyst is the Sonagashira coupling reaction.[108–111] The Sonagashira coupling reaction is different to the Suzuki coupling reaction in that it uses an alkyne instead of a boronic acid, and produces a molecule which contains an alkyne linker between the two coupling partners as shown in **Scheme 3.**

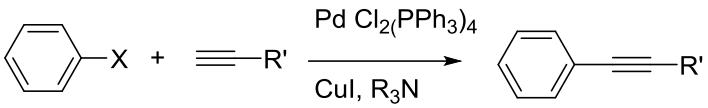

Scheme 3 – Sonogashira coupling reaction schematic.

The use of the Sonogashira reaction was first reported in 1975 when Sonogashira, [111] Tohda and Hagihara reported that an acetylinic hydrogen can be easily substituted by iodoarenes, bromoalkenes or bromopyridines in the presence of catalytic amounts of $PdCl_2(PPh_3)_2$ and copper iodide in diethylamine. The reaction was carried out under mild conditions, typically stirring at 25°C for 3-6 hours to give the desired product. The mechanism for the coupling reaction was not fully understood, but it was speculated that the first step involves substitution through a Pd(II) complex followed by reductive elimination and then subsequent oxidative addition and alkynylation to give the product.

The Sonogashira reaction is categorised as a palladium-catalysed cross-coupling reaction between an sp^2 carbon and an sp carbon.[108–110] The original reaction utilised a copper co-catalyst which was thought to increase the rate of reaction. There are disadvantages to using a copper co-catalyst, (the copper salt is not environmentally friendly)[110] and when used it makes it difficult to recover any unreacted starting materials from the reaction mixture. Another problem with using a copper co-catalyst is that the *in situ* generation of copper acetylides generates homo coupling of the terminal alkyne, which is a by-product.

The catalytic mechanisms for Sonogashira coupling is still not well known.[108] The main reason behind the catalytic cycle not being fully understood is the difficulty in analysing the combined action of two metal catalysts, even though speculations have been made that the reaction takes place in two different cycles. A simplified catalytic cycle is shown in **Figure 16**: the role of palladium in the catalytic cycle is very similar to that observed in the Suzuki coupling reaction. The first step in the catalytic cycle is initiated by oxidative addition of the aryl or vinyl halide to the palladium complex, this step is believed to be the rate-limiting step as it is thought to proceed *via* an end-on ligation of the halogen to the palladium *via* an electron donation. The subsequent steps involve a

transmetallation where a copper acetylide is formed. This palladium complex then undergoes a reductive elimination after cis/trans isomerisation to the final alkyne and regeneration of the catalyst.

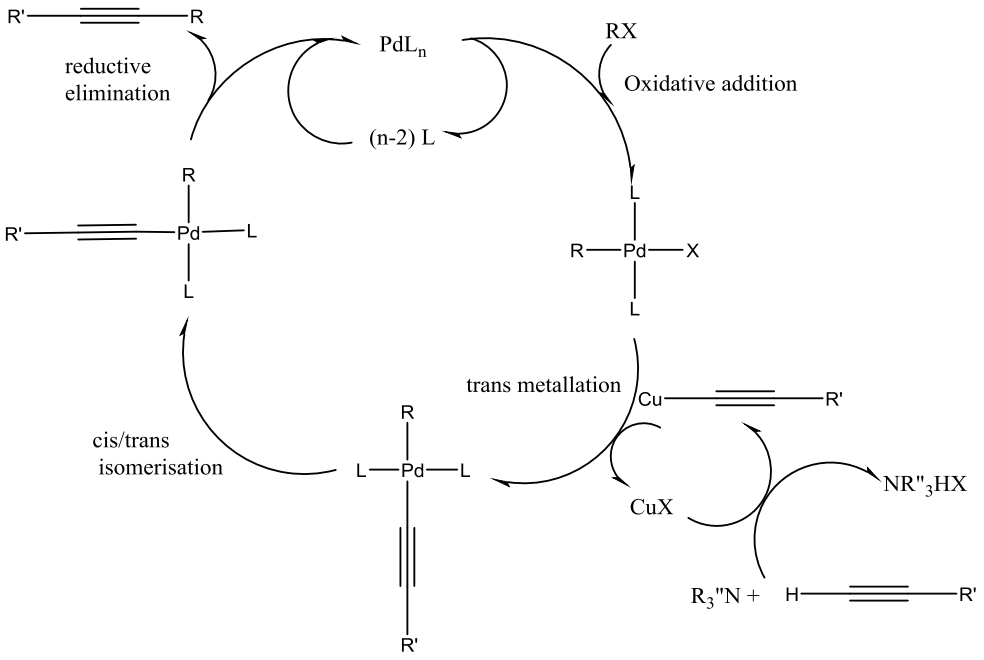

Figure 16 – Catalytic cycle for the Sonagashira coupling reaction.

The Sonogashira reaction is a very popular choice for the coupling of terminal alkynes, and it was originally used with a copper co-catalyst but recent research has been focussed on the use of alternative catalysts to minimise the use of the copper co-catalyst.

Palladium cross-coupling reactions are versatile and allow the use of readily available starting materials. An alternative to using palladium cross coupling reactions is the use of click chemistry.

1.9.2.3 Click chemistry

Click chemistry was first coined by Sharpless *et al.* in 2001.[112–115] The main aim was to generate substances by the joining together of small units and heteroatom linkers. There is strict criteria that a process must meet in order to be used in click chemistry; the reaction must be modular, have a wide scope, give high yields, and generate by-products that can be easily removed. The reaction must be a simple synthetic procedure,[116] it must be insensitive to oxygen and water and only use readily available reagents, and the workup of the reaction must be simple with as little purification by column chromatography as possible. Click reactions are known to be highly specific reactions that have a high thermodynamic driving force, which is usually greater than 20 kcal mol^{-1}.

There are two types of click reactions that have influenced drug discovery; the nucleophilic opening of strained ring systems and 1,3-dipolar cycloadditions.[117] The Huisgen [3 + 2] cycloaddition is a reaction between a terminal alkyne and an azide to generate substituted 1,2,3- triazoles.

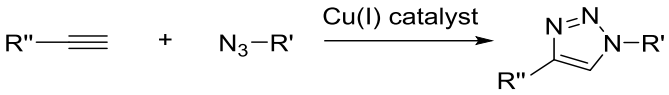

Figure 17 – Schematic for the click reaction - formation of the 1,4-triazole product.

The Huisgen 1,3-dipolar cycloaddition between a terminal alkyne and an azide has become the most popular click reaction to date.[116] The reaction generates a mixture of 1,4- and 1,5- disubstituted triazoles but attempts have been made to control the regioselectivity, this was not successful until 2002, when it was discovered that copper(I) catalysed the exclusive production of the 1,4-disubstituted 1,2,3- triazole.[112–116] The copper (I) catalyst can be copper salts such as CuI or CuOTf.C_6H_6, and the reactions must be run with acetonitrile as the co-solvent. The azide used in the reaction can be primary, secondary, tertiary or aromatic. The copper-catalysed reaction is thought to proceed in a step-wise manner starting with the generation of copper (I) acetylide. The reaction follows the cycle shown below:

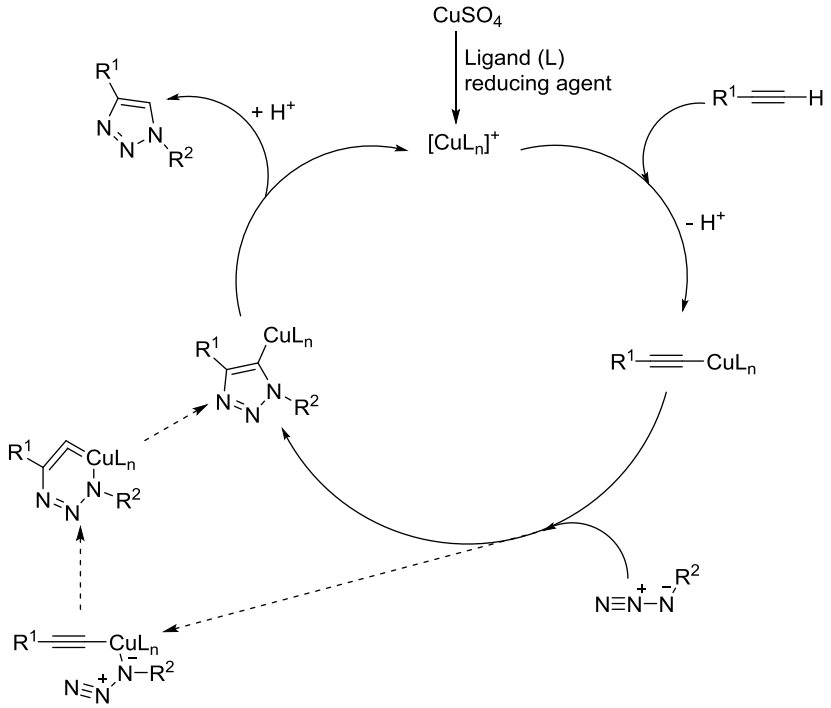

Figure 18 – Catalytic cycle for the click reaction.

In the absence of an appropriate catalyst this reaction is usually quite slow as alkynes are poor 1,3-dipole acceptors.[115] In the presence of copper, which can bind to terminal alkynes, cycloaddition reactions are dramatically accelerated, regioselective and highly efficient (yields are often above 95%).

1.10 Research Outlook and project aims

Healthcare associated infections have been shown to be a growing problem, and the development of antibiotics and alternatives to inactivate bacteria are needed. This project focuses on the development of an alternative technique for the inactivation of bacteria: the development of a self-sterilising surface. The self-sterilising surface will utilise a photosensitiser immobilised on a polymeric surface, which will allow for control and modification of characteristics for potential applications. The project will also look at the synthesis of a self-sterilising surface which will utilise polyviologen molecules attached to an electron transfer agent, which in case of this project will be a porphyrin. This will allow the surface to remain active for a period of time, even after removal of the light source. An advantage of this system is that it self-indicates its activity, and will change colour when the sterilisation period has expired.

The main aim of this project is the synthesis of a library of polyviologen compounds for comparison of electron transfer properties. Another aim of the project is the synthesis of a library of porphyrins with varying substituents to test for electron transfer to the polyviologens. A further aim is the production of a sterilising surface prototype which contains a porphyrin immobilised on a synthetic polymer support, and to test this material against bacteria to thus study the inactivation of the bacteria using this material.

2 Synthesis of polyviologens and conjugatable viologens

2.1 Introduction

2.1.1 History of polyviologens

The viologens were first prepared in 1881 by A.W. Hoffman who prepared dipyridylium iodide, although the yields obtained by this method were found to be very low.[95] The method involved the preparation of a quaternary base of pyridine, followed by the condensation of two molecules with a dipyridyl, compound and the subsequent treatment with sodium amalgam to give the polyviologen product. In order to test for the formation of the dipyridyl compound a small amount of the product can be dissolved in 50% acetic acid and chromous chloride: if a violet colour is formed, which disappears when shaking it exposed to air then a bipyridyl compound has been formed. The dipyridine can react with two molecules of an alkyl-halide to form a bi-quaternary base as shown in **Figure 19**. The reaction is known as the Menshutkin reaction and proceeds *via* an S_N2 mechanism.

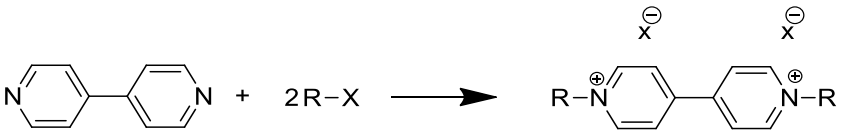

Figure 19 – Formation of a bi-quaternary base.

The obvious site for substitution of 4,4'-bipyridine is at the *N*-substituent position, but a less obvious place is on the ring itself. Substitution of cyano groups at the 2- and 2'-positions has been carried out by Fielden and Summers.[118] They found that substitution at these positions led to a shift in the reduction potential due to the electron withdrawing effect of the cyano groups which further stabilises the radical formed.

The viologens were originally investigated for their use as redox indicators in biological studies.[93,119] The viologens exist in three main oxidation states; V^{2+}, $V^{+\cdot}$ and V^0.[93]

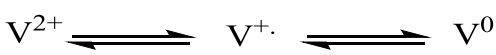

Figure 20 – The three oxidation states of the viologens.

The first reduction step is highly reversible from the $V^{+\cdot}$ to the V^{2+}, and this can be cycled many times without any significant side reactions taking place. The further reduction to the fully reduced species V^0 is less reversible, as the product is frequently an insoluble species in the neutral form.[93,95]

The viologens are chemically stable. However, when placed in alkaline solution the alkyl group can be lost to form an alcohol, which can act as a reducing agent and lead to the formation of the monocation species.[93]

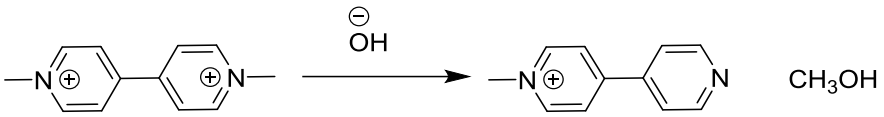

Figure 21 – Reaction of 4, 4' bipyridine in alkaline solution.

2.1.2 Herbicidal activity and toxicity of viologens

The herbicidal activity of the viologens was discovered in 1958 by R. C. Brian, and were reviewed by Calderbank in 1968.[120,121] The most popular example of the viologens is paraquat, most commonly found in weed killers.[122] The combination of paraquat with oxygen leads to the production of superoxide radicals.

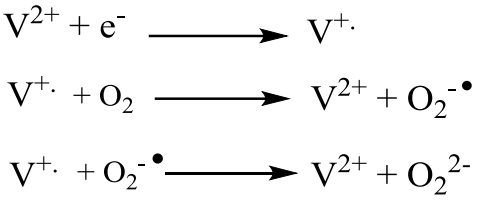

Equation 1 – Formation of superoxide radicals by viologen.

Once formed the superoxide radicals are able to kill cells non-selectively which is a reason why the viologens have been investigated for use in antibacterial surfaces.

2.1.3 Polyviologens

The viologens may also be incorporated into polymers, with the resulting materials retaining the chemical and electrochemical properties of the viologens. The polyviologens were first investigated in 1972 by Simon *et al.*[123]

Polyviologens can be produced in two different ways. Firstly, the polymer can be incorporated into the backbone of the polymer giving the polymer a charge, also known as ionene polymers. Ionene polymers can be produced by a condensation reaction of 4,4,'-bipyridine with either a dihaloalkane or dihaloaryl molecule. An alternative strategy for the formation of ionene type polymers is *via* a condensation reaction of a bifunctional acid chloride, whereby the monomer is produced by the Menshutkin reaction and then the polymerisation reaction can occur *via* a Schotten-Baumann reaction with the bifunctional acid chloride to form the polyamide. An alternative is the formation of pendant

polyviologens *via* a vinyl polymerisation reaction. This allows the viologen to be grafted onto a polymeric support for use in antimicrobial surfaces for example.[124]

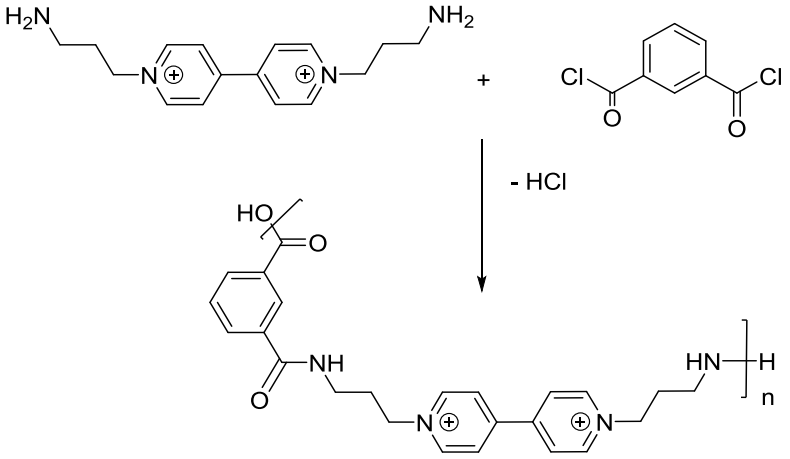

Scheme 4 – Schotten Baumann reaction to produce the polymer from viologen *via* the an acid chloride.[125]

2.1.4 The use of polyviologens as electron transfer agents with titanium dioxide

Investigations into the use of titanium dioxide as a sacrificial donor for electron transfer has been carried out.[89,94,127] The use of titanium dioxide and polyviologen molecules has been investigated for use in oxygen sensing in food packaging.[98,126] A similar concept would be utilised; whereby the titanium dioxide undergoes an electron transfer to the polyviologen molecule, which would change colour with the change in oxidation state.

The main problem found using titanium dioxide is the absorption maxima for TiO_2, which is in the ultra-violet region. Modifications of titanium dioxide can be carried out, but as discussed previously they are not always favourable, and so an alternative may be required.

2.1.5 Shifting the wavelength - Porphyrin-viologen systems in the literature

Research into the use of porphyrin-viologen hybrid molecules for various applications including natural light harvesting,[127] photoinduced hydrogen evolution,[128,129,130] water reduction for the production of hydrogen and water splitting.[101,102,103,104] Also for the studies regarding electron transfer between a porphyrin and viologen have been carried out.[127,128,131–135]

Harriman *et al.* investigated the production of hydrogen by the reduction of water using viologens as early as 1980.[101,102,104] In 1981 Harriman, Porter and Richoux investigated

the reduction of water to hydrogen using water soluble zinc porphyrins and methylviologen.[136] The main finding confirmed that a positively charged water soluble zinc porphyrin photosensitises the reduction of water to hydrogen with high efficiency. This system consists of three components and has since then been known as the three component system. The components are; porphyrin as the photosensitiser, methyl viologen (MV^{2+}) as the electron transfer agent and sodium ethylenediaminetetraaceticacid (EDTA) as the sacrificial electron donor. They found that the reaction mechanism involves reduction of MV^{2+} by the triplet excited state of the porphyrin and the resulting porphyrin π- radical cation is then in turn reduced by EDTA. This research idea has gained a lot of interest primarily for applications in fuel storage. Water solubilisation of the porphyrin using a methylated pyridyl group gave a positive charge on the nitrogen atom. The positive charge was found to localise on the nitrogen atom and not delocalise on the pyridyl ring like it had been speculated.[136]

A similar study was carried out by Harriman *et al.*[101] who utilised sulphonated phthalocyanines instead of porphyrins as the photosensitiser. Phthalocyanines have a distinct advantage over metalloporphyrins in that they have a wider spectral range in the visible. This research has a key requirement in that the photosensitiser must act as an electron donor to the MV^{2+}, which requires a high triplet yield. It has been known that metalloporphyrins and sulphonated phthalocyanines will readily undergo net electron transfer to an acceptor molecule forming the separated radical ions, but in this case the sulphonated phthalocyanine was found to be less effective when compared to the metalloporphyrins.

Continuing their interest in this research area Harriman *et al.* investigated further the use of zinc porphyrin and viologens for electron transfer *via* fluorescence quenching.[137] In previous research Harriman *et al.* investigated the use of porphyrins and viologens for electron transfer. In this study, they investigated the effect of separation distance on electron transfer. They found that longer alkyl chains favour more efficient fluorescence quenching, and that the behaviour observed when the system was enclosed in a polymeric matrix was different to that observed in solution. In rigid media the longer chains gave shorter separations, indicating that the molecules reside mainly within the cavities, which favour a folded conformation, whereas in solution the molecule seems to be extended and not confined to a particular space. The chain length is a particularly important factor that needs to be investigated further.

Following on from this research, Aono *et al*. carried out research using tritoyl porphyrin,[129] which was then alkylated using dibromoalkane in toluene, followed by the addition of the viologen and then zinc using zinc chloride in ethanol. Research was carried out varying the chain length between the porphyrin and the viologen, the chain lengths investigated had between 2-6 methylene chains separating the porphyrin and viologen as shown in **Figure 22**.

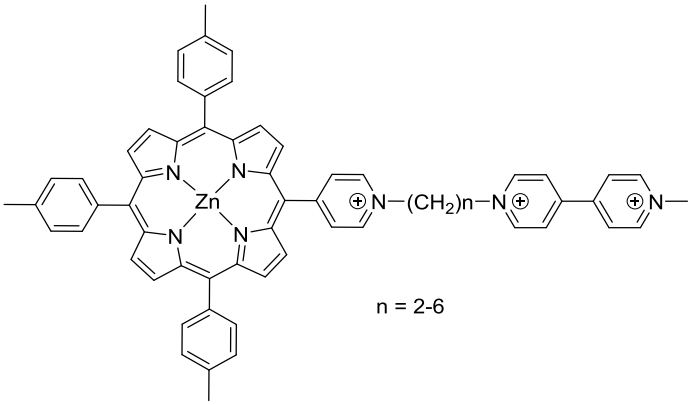

Figure 22 – Structure of porphyrin-viologen hybrids synthesised by Aono *et al*.[129]

It was found that shorter chains are more effective for electron transfer than longer chains. Chain lengths between n = 3-6 were found to be inefficient for electron transfer. This gives vital information about what factors are required for electron transfer; the use of shorter chain lengths and carrying out the electrochemistry measurements in methanol, gave the best results in terms of electron transfer and stability of the radical formed for detection.

Batteas *et al*. took a different approach and investigated the development of a model that utilises a chromophore covalently linked to an electron donor or acceptor *via* a flexible or rigid spacer group.[127] The chromophore used in this model was a porphyrin and the electron acceptor a viologen molecule. They showed that the attachment of two viologen molecules to one single porphyrin was more efficient in fluorescence quenching of the porphyrin, and that longer spacer groups between the porphyrin and the viologen favoured slower charge separation. The charge separation was found to arise from the excited triplet state of the porphyrin and, in theory, increasing the number of viologens attached to the porphyrin should result in extremely efficient quenching. The fluorescence quantum yield for the conjugated complex was only 15% of that measured for the porphyrin, and it has been speculated that the terminal viologen groups function as efficient quenchers for the porphyrin excited singlet state.

There has also been research into the use of porphyrin-viologen molecules in the evolution of hydrogen.[128,129] Hosono *et al*. studied the use of a model which comprised: a photosensitiser (porphyrin), an electron carrier (methyl viologen), a sacrificial electron donor (sodium EDTA) and a catalyst (colloidal platinum). The model was placed onto a film which consisted of the platinised viologen-linked porphyrin. The monolayer of the film was prepared by spreading a benzene-methanol solution onto a distilled water sub-phase, it was prepared by a layer-by-layer (LBL) technique. The evolution of hydrogen was analysed using gas chromatography.

Amao *et al*.[130] also investigated the use of a porphyrin-viologen hybrid system for the production of hydrogen. Photoinduced hydrogen evolution systems containing an electron donor, a photosensitiser and an electron carrier and a catalyst have been used extensively for the conversion of solar energy into chemical energy. Amao *et al.* utilised a series of water soluble viologen linked cationic porphyrins and anionic porphyrins that were synthesised using the Adler Longo method and analysed for their electron transfer properties. Noda *et al.* investigated the use of porphyrin-viologen molecules for electron transfer,[131] in particular they looked at varying the methylene spacer group whereby n = 4-7 as shown in **Figure 23**.

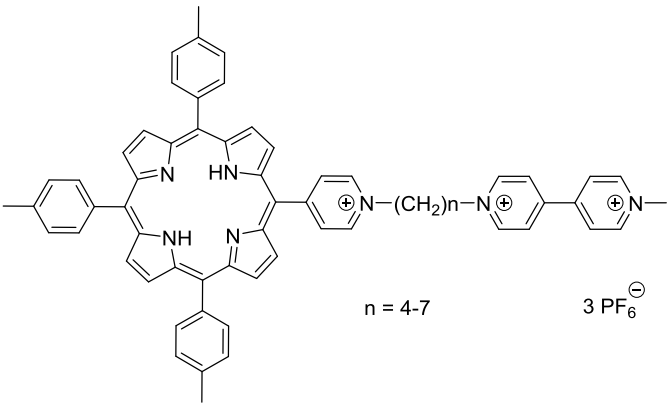

Figure 23 – Structure of porphyrin-viologen hybrids investigated by Noda *et al*.[131]

The key finding from this investigation was that the intramolecular electron transfer process from the porphyrin to the bonded viologen becomes less effective when the methylene chain length increases. There was also speculation that there were two possible conformations of the porphyrin-viologen molecule, the first being the complexed conformer where the viologen lies closed and wraps around the porphyrin, and the other being the extended conformer where the viologen is extended away from the porphyrin ring: this is, in turn, affected the efficiency of electron transfer.

More recently there has been research into the use of porphyrin-viologen hybridised in a matrix.[133,138] Yui *et al*. reported on the preparation of hybrid films adsorbed separately by methyl viologen (MV^{2+}) and H_2TCPP^{4-} in titania nanosheets (TNS) and anionic monodisperse mesoporous silica spheres (AMMSS), respectively. It was thought that dye molecules incorporated into the structure should be isolated from each other to avoid the loss in excitation energy resulting from concentration quenching of the aggregated dye molecules. The porphyrin molecules were found to electrostatically bind with the ammonium groups on the surface *via* the carboxylic functionality on the porphyrin. The amount of electrostatic binding between the carboxylic group on the porphyrin and the ammonium group on the surface was found to be 40% binding between the carboxylic group and the porphyrin, with the remainder of the porphyrin not electrostatically bound. The average occupied area as found to be 10.5 nm^2 and the distance between the porphyrin molecules was found to be 3.4 nm. When the porphyrin was used in the AMMSS hybrid material a shift in the Soret band was observed when analysed by UV-Vis spectroscopy from 414 nm to 426 nm, this could be due to aggregation or due to the incorporation into a solid matrix. The MV^{2+} ions were reduced to $MV^{+\cdot}$ within the TNS due to the free electrons in the conduction band, the porphyrin was also oxidised by the holes that were left in the conduction band. The reduction/ oxidation of the viologen and porphyrin can be coupled and this process can cause electrons and/or holes to migrate through the TNS AMMSS surface.

Konno *et al*. utilised a different approach for their matrix.[138] These researchers investigated the use of clay as the surface for photoinduced electron transfer (PET) using a porphyrin-viologen hybrid system. Previous to this research it was believed that electron transfer within a clay matrix is inefficient due to the aggregation and segregation behaviour of the dyes on the clay surface, the photosensitiser used for this study was Ru(II) $(bipy)_3$ and it was found to be inefficient. Instead Konno *et al*. utilised a porphyrin as the photosensitiser for electron transfer with $DNPV^{2+}$ as the electron transfer agent. The fluorescence quenching behaviour due to electron transfer was investigated. They found that the size matching of distances between the charged sites on the porphyrin and corresponding distances on the clay were important, and the cationic porphyrin synthesised was found to be the perfect fit for the size found. The structures are shown in **Figure 24**.

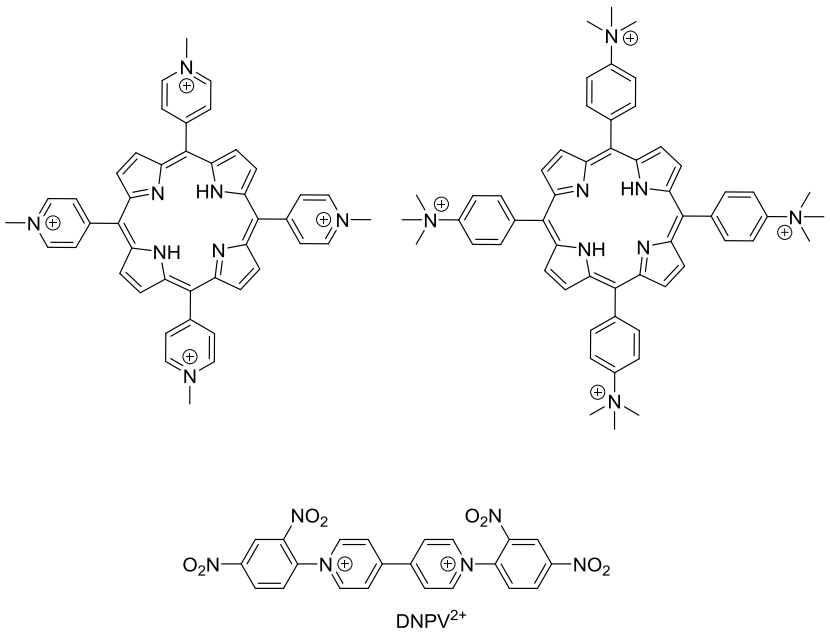

Figure 24 – Structure of porphyrins and $DNPV^{2+}$ investigated by Konno *et al.*[138]

Konno *et al*. found that there was significant fluorescence quenching due to electron transfer for the porphyrin $DNPV^{2+}$ system, and that the porphyrins form an island structure on the clay which is dependent on the molecular structure of the porphyrin.[138]

Research into the use of porphyrins and viologens attached to a polymeric backbone has been carried out by Nosaka *et al.* in 1986.[139] These researchers studied the effect of an ionic polymer environment on the photoinduced electron transfer from zinc porphyrin to the viologen. There was no covalent attachment between the porphyrin and the viologen modified on the polymer.

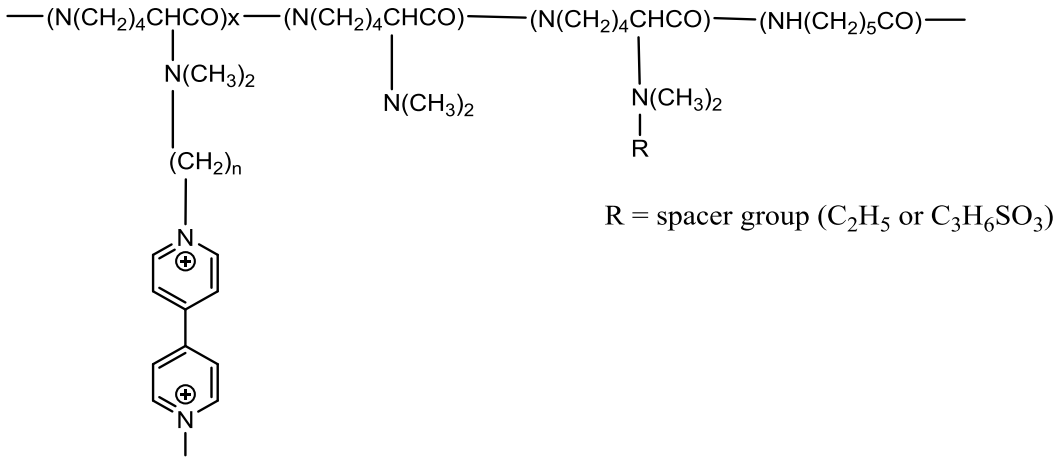

Figure 25 – Structure of viologen attached to polymeric backbone by Nosaka *et al.*[139]

In this study a water soluble metalloporphyrin was used due to the longer lifetime of the excited state. The researchers studied the change in the charge on the porphyrin and how this would affect the formation of the viologen cationic radical. The range that was studied was from a +4 charge to a -4 charge. The researchers found that porphyrins having a neutral or negative charge are less efficient for photoinduced electron transfer. The researchers also found that the addition of a cationic polymer increases the electron transfer quantum yield.

In conclusion, there has been a large amount of research into the use of porphyrin-viologen hybrid materials for electron transfer applications. There have also been in-depth investigations into the different spacer group chain length between the porphyrin and the viologen, as well as the effect of the different substituents on the porphyrin as the photosensitiser. There has also been research into the incorporation of a porphyrin-viologen hybrid material into a solid material matrix and what effect this has on fluorescence quenching and electron transfer processes.

2.2 Aims

The primary aim of this work was the synthesis of polyviologen molecules with different spacer groups, comparing alkyl and aryl groups and different counter-ions. The polyviologen molecules have been entrapped into different polymeric supports and also combined with titanium dioxide and porphyrins for the study of electron transfer in either the UV region of the spectrum or in the visible region of the spectrum, respectively.

An alternative strategy was the use of conjugatable viologen molecules for attachment to porphyrin molecules, allowing a shift into the visible region. The viologen molecules were synthesised with a range of conjugatable moieties.

The synthesised molecules were analysed using UV-Vis spectroscopy for their electron transfer properties and their ability to be reduced and oxidised respectively.

The main aim of this project was to obtain the most favourable orientation of photosensitiser and viologen as close in proximity as possible, thereby enhancing the efficiency of electron transfer. A distinct advantage of the system proposed in this work is that it can be assembled in a modular fashion, with parallel synthesis of the photosensitiser, viologen and polymeric supports, followed by convergence of these components into an optimised antimicrobial material. With this strategy in mind the synthesis of suitable viologens was investigated.

This current chapter investigates the use of polyviologen and viologen molecules for their use in electron transfer. The chapter will focus on the synthesis of selected polyviologens and modified viologen molecules that can be used in different coupling reactions in order to form a covalent bond to the chosen electron donor. The first electron donor investigated was titanium dioxide for its ease of use and its known photocatalytic properties. [19,140,141,142] The second electron donor investigated enabled a shift to the visible region to be carried out by the use of a porphyrin, which has been previously investigated for use in electron transfer with viologen molecules.

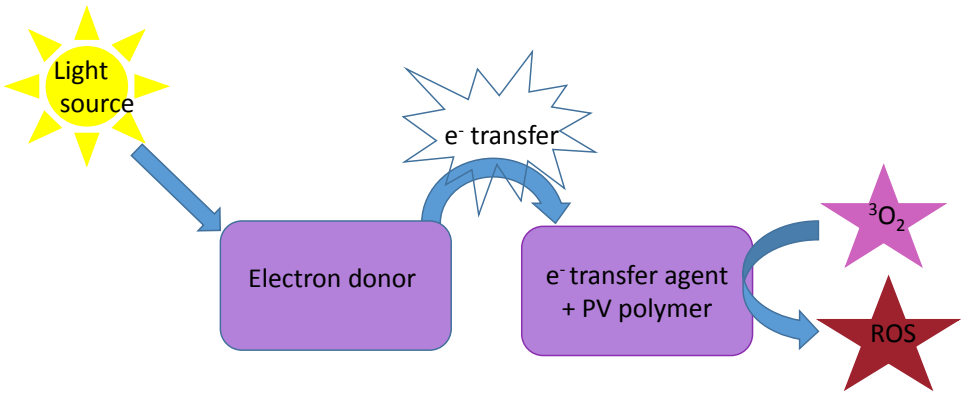

Figure 26 – Schematic of electrochemistry occurring at the surface.

Figure 26 shows a simple schematic of the photochemistry occurring at the surface, and indicates the purpose of each of the elements and how they fit together. The electron donor loses an electron to the electron acceptor, which in turn reacts with ground state molecular oxygen to produce reactive oxygen species.

2.3 Synthesis of polyviologens

The use of different spacer groups, aromatic and alkyl, and the role of counter-ions, was investigated to determine their effects on electron transfer and solubility.

2.3.1 Synthesis of precursors for use in formation of polyviologens

Prior to the synthesis of the polyviologen molecules it was essential to carry out the synthesis of a number of precursors for use in polymerisation reactions.

Investigations into the use of tosylate counter-ions were carried out as a tosylate is known to be a good leaving group and thus could work well in polymerisation reactions. The first spacer group investigated was the alkyl spacer group, as it has been known that methylene spacer groups promote electron transfer, and they have been successfully used previously.[127,129,136,137]

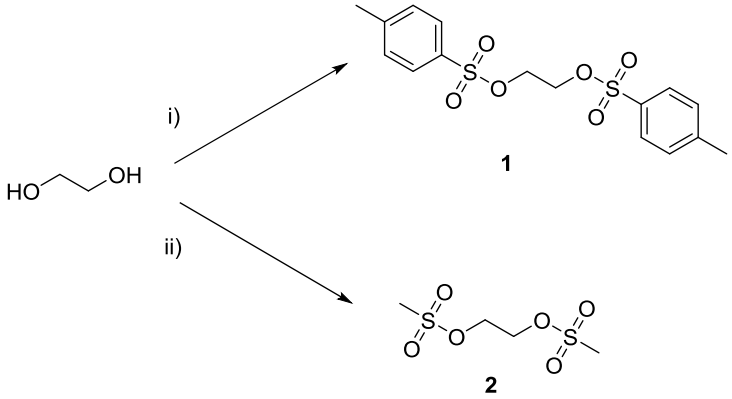

Scheme 5 – Synthesis of compounds 1 and 2. Reaction conditions: i) pyridine, dichloroethane, 0 °C, *p*-toluenesulphonylchloride, ii) triethylamine, dry dichloromethane, 0 °C, methanesulphonylchloride.

The synthesis of **1** was carried out using standard base-catalysed S_N2 reaction conditions. The reaction was carried out by converting the hydroxyl group into a tosylate group. The reaction yielded the product as a white solid in a yield of 68%. The structure of the compound was confirmed using ^{1}H-NMR, ^{13}C-NMR and mass spectrometry. The proton NMR showed two peaks in the upfield region for the alkyl functionalities. The peak representing the two methyl groups was seen at 2.46 ppm as a broad singlet with an integration of six. The peak for the two CH_2 groups was seen at 4.18 ppm as a broad singlet. The aromatic protons appeared in the downfield region. The splitting pattern gave two doublet peaks exhibiting the typical rooftop effect seen for 1,4 disubstituted phenyl rings. The peaks appeared at 7.34 ppm and 7.73 ppm. respectively, and both had J values of 8.0 Hz. Carbon NMR and mass spectrometry also confirmed the structure of **1**. CHN

analysis was carried out on compound **1**, but the values differed slightly from the expected values C, 51.88; H, 4.90; N, 0.00; S, 17.31 found: C, 51.77; H, 4.82; N, 0.00, S, 17.31. The differences were attributed to the presence of small amounts of solvent present in the compound.

The synthesis of **2** was carried out according to a literature procedure, whereby ethylene glycol was reacted with methanesulphonylchloride in dry solvent to convert the hydroxyl group into a mesylate group.[143] Challenging purification using column chromatography gave the product as a colourless oil in 75% yield, compared to a literature yield of 96%. The lower yield is thought to be due to the challenging purification, and the product adhering to the silica. The ^{1}H-NMR showed the presence of two alkyl region peaks. The peak for the CH_2-CH_2 has been shifted downfield compared to those in compound **1**, and the peak was seen as a singlet at 4.46 ppm. The peak for the methyl groups was seen as a singlet at 3.02 ppm, which aided in the confirmation of the structure.

Following investigations into the use of alkyl groups a number of different aryl groups were synthesised with varying substituents for use in polymerisation reactions.

The different counter-ions investigated included; bromides, chlorides, tosylates and mesylates. The aryl group with bromide and chloride leaving groups were commercially available, so did not require synthesis, but synthesis was required for the formation of those containing tosylates and mesylates.

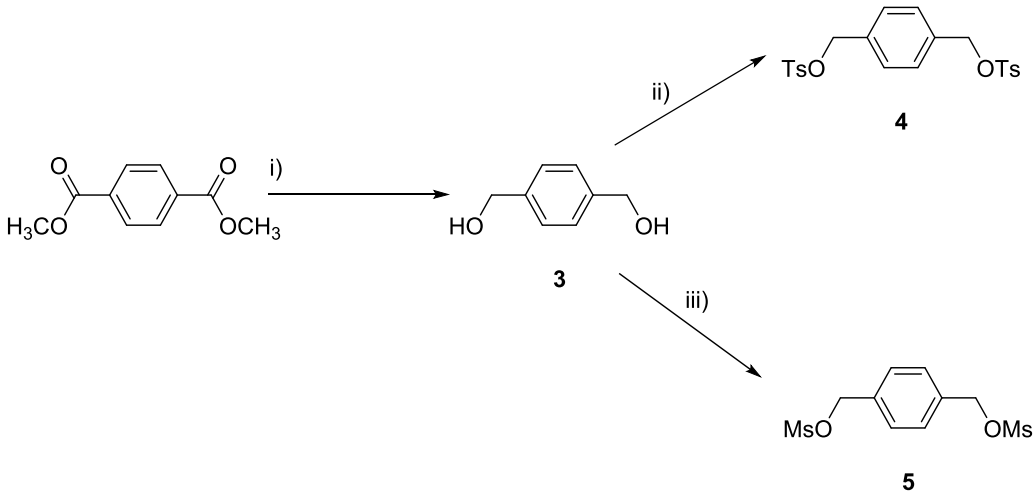

Scheme 6 – Synthesis of compounds 3, 4, and 5 for use in polymerisation reactions. Conditions used; i) dry THF, $LiAlH_4$ 0°C, ii) pyridine, *p*-toluenesulphonylchloride, 0°C, iii) triethylamine, methanesulphonylchloride, 0°C.

Compound **3** was synthesised from the commercially available compound dimethylterephthalate. The ester was reduced to an alcohol using $LiAlH_4$ in dry THF. The reaction gave the product as a white solid following an aqueous extraction in a yield of 58%, compared to a literature yield of 60%.[144] The compound was confirmed by ^{1}H-NMR, ^{13}C-NMR and mass spectrometry. Due to the symmetry in the molecule the ^{1}H-NMR showed only two peaks, one in the downfield region representing the aromatic protons of the phenyl ring at 7.33 ppm which appeared as a singlet where a 1,4-disubstituted rooftop effect was expected. The upfield region contains a singlet representing the peak for the 2 x CH_2, the peak appears as a singlet with an integration of four protons.

The diol was converted to either tosylate groups (**4**) or mesylate groups (**5**). These reactions were carried out *via* nucleophillic substitution reactions. The synthesis of compound **4** was not successful. It was speculated that this could be due to steric hindrance from the two tosylate groups when attached to the phenyl ring. The synthesis of compound **5** was also not successful *via* the simple S_N2 type reaction that was attempted, this could be due to the strength of the base being used. An alternative speculation of the lack of success of the synthesis of **5** was thought to be due to the decomposition of the mesylate groups on silica as purification was necessary due to the presence of starting material and the mono substituted product.

With the appropriate precursors in hand shown in **Figure 27**, the polymerisation reactions were carried out.

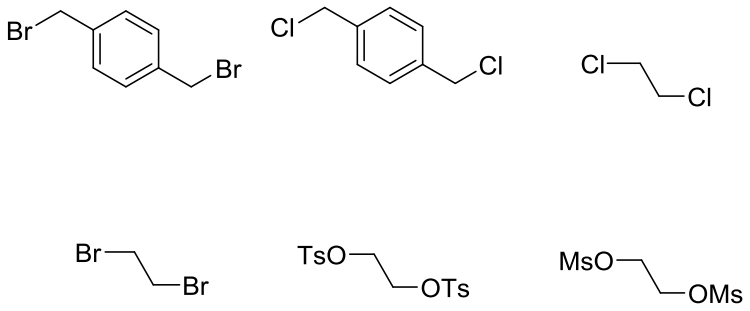

Figure 27 – Structure of precursors for polyviologen synthesis.

2.3.2 Synthesis of polyviologen compounds

Polymerisation reactions were carried out involving different leaving groups for S_N2 type reactions, and spacer groups to determine what effect they had on the properties of the resulting polymer. Different leaving groups were investigated, including bromides, chlorides, tosylates and mesylates. Two different spacer groups were also investigated

representing a relatively rigid aromatic unit versus a short chain aliphatic, linker with greater flexibility.

The polymerisation method involved reacting 4,4'-bipyridine with the spacers in dry acetonitrile. Those with benzylic spacer groups required only stirring, but those with alkyl chain spacer groups were heated at reflux temperature (**Figure 28**).

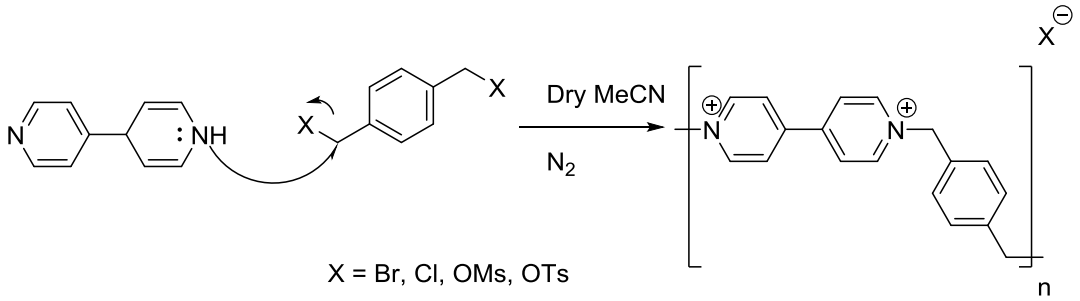

Figure 28 – General procedure for polymerisation of 4,4'-bipyridine with the chosen spacer group.

The synthesis of the polyviologens used a modified literature method.[95] The method involved the use of 4,4'-bipyridine and the desired aryl spacer group stirred at rt for 30 mins and then the solution was left to polymerise for 24 h. The product then precipitated out of solution and was then isolated *via* filtration. The literature method for the synthesis of alkyl spacer group polyviologens reported the mixture heating at reflux temperature for 21 h instead of stirring and leaving at rt, as per the method used herein.

Compound **6** was synthesised according to the literature method, whereby 4,4'-bipyridine and dibromo-*p*-xylene were dissolved in acetonitrile and the mixture then stirred at rt for 24 h. Following this the product precipitated from solution. Analysis of the compound was carried out using ^{1}H-NMR and mass spectrometry. ^{1}H-NMR was used to estimate the number of repeating units in the polymer itself, these polymers are known to only polymerise to a small number of repeating units. Roberts *et al.*[98] and Adeogun *et al.*[145] found that the polymer would generally form no more than 5 repeating units. From mass spectrometry it was found that this polymer contained 2-3 repeating units. Due to the charge on the polymer it was not possible to obtain gel permeation chromatography (GPC) analysis because once a base was added to the solution the product started to form a precipitate, which made it unsuitable for analysis by GPC.

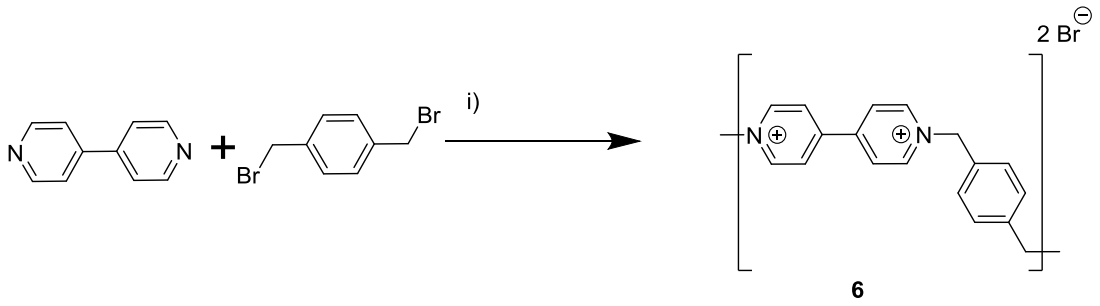

Scheme 7 – Synthesis of compound 6. Reaction conditions used; i) acetonitrile, 24 h, rt.

Compounds **7** and **8** were synthesised using similar methods, whereby the chloro alkyl spacer group was heated under reflux with 4,4'bipyridine for 21 h. Analysis of the compounds was carried out in the same way as for compound **6**, using NMR and mass spectrometry. Analysis indicated that the reaction gave 2-3 repeating units for both compound **7** and compound **8** (**Figure 29**).

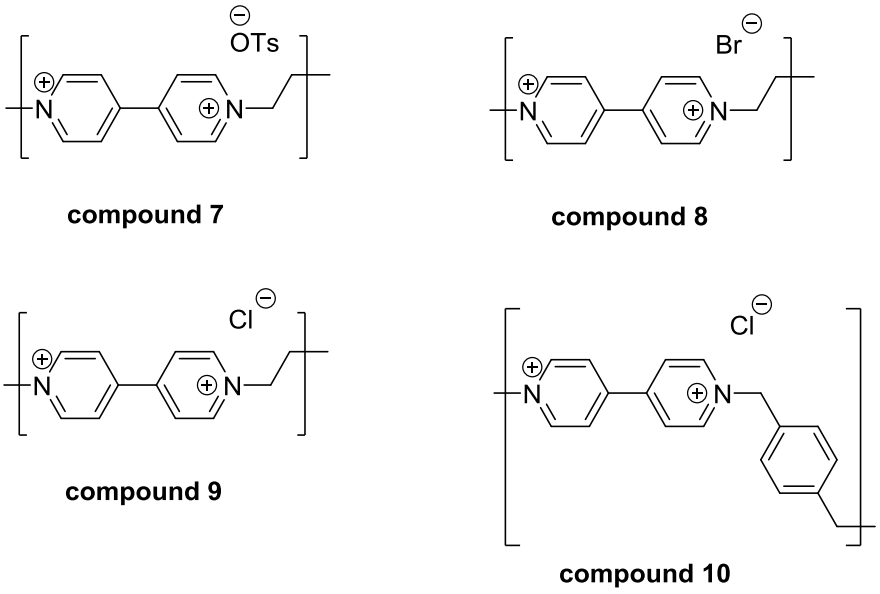

Figure 29 - Structures of compounds 7-10.

The synthesis of compounds **9** and **10** was not successful using the same methods as for **6**-**8**, this could be due to the chloride not being a good enough leaving group to aid the polymerisation (**Figure 29**).

An alternative strategy to the formation of a polyviologen backbone is the polymerisation of a viologen molecule into the backbone of a polymer using a vinyl polymerisation reaction, similar to that carried out by Nosaka *et al*.[139]

2.4 Synthesis of alternative monomers for use in co-polymerisation reactions with styrene

The use of vinyl polymerisation reactions allows versatility in the formation of monomers for use in polymerisation. Research carried out by Griesbeck *et al.* looked at the use of copolymerisation reactions for the immobilisation of PPIX with styrene and divinylbenzene.[81,82] With this concept in mind it was thought that a polymerisable group could be attached to viologen to carry out vinyl polymerisation reactions. Vinyl polymerisation reactions require the use of an initiator which aids in the formation of radical species that can react with vinyl groups to form a new product *via* the formation of a new bond. The polymerisation process is terminated by the coupling of any radical species to form a stable product.

2.4.1 Synthesis of monomers

The specification for radical polymerisation reactions, required the viologen to have an alkenyl group which will be used in free radical polymerisation reactions. In order to introduce an alkenyl group onto the viologen backbone the reaction shown in **Scheme 8** was used.

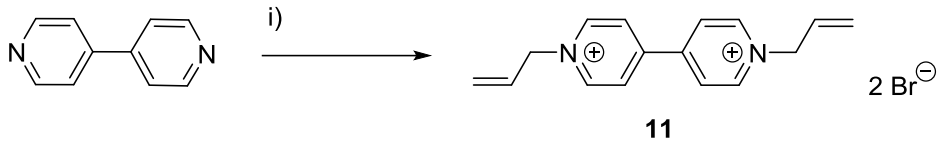

11

Scheme 8 – Formation of compound 11. Conditions used i) allyl bromide, dry acetonitrile, reflux 4h.

Compound **11** was formed *via* a simple S_N2 type reaction using allyl bromide to give the alkenyl group required for use in polymerisation reactions.[146] The structure was confirmed using ^{1}H-NMR, ^{13}C-NMR and mass spectrometry. The ^{1}H-NMR showed three peaks in the upfield alkyl region, corresponding to CH=C*H*, C*H*-CH_2 and CH_2-CH. A doublet at 5.40 ppm representing the CH_2 peak with a *J* value of 8 Hz. A multiplet at 5.60-5.66 ppm represents the *cis* and *trans* isomers of the CH_2-CH peak. The CH peak appears as a complex multiplet at 6.17-6.32 ppm, the complexity being due to coupling between the CH_2 and the alkenyl protons. The downfield region shows a pair of doublets corresponding to the aromatic protons on the pyridyl rings. The ^{13}C-NMR showed six representative peaks for compound **11** at 63.5 ppm, 122.9 ppm, 127.1 ppm, 130.1 ppm, 145.7 ppm and 150.33 ppm. Mass spectrometry also confirmed the structure of the compound with an $[M-H]^+$ of 237.1386.

Alternative monomers were required for the polymerisation reaction, the monomers must have the polymerisable group and mimic those used by Griesbeck *et al.*[82]

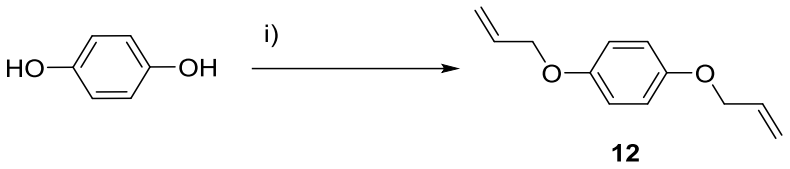

Scheme 9 – Synthesis of 12. Conditions used; i) allyl bromide, potassium carbonate, dry acetone, reflux.

Compound **12** was synthesised to mimic the use of divinylbenzene in the study by Griesbeck *et al.*[82]

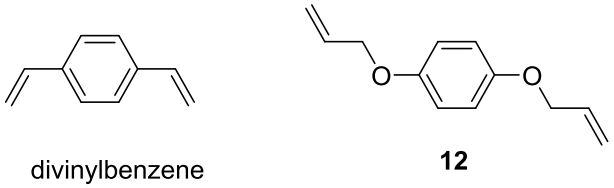

Figure 30 – Comparison of compound 12 and divinylbenzene.

The synthesis of **12** was carried out according to a modified literature procedure.[147] The reaction procedure involved a nucleophilic substitution reaction on the hydroxyl group for the insertion of the vinyl group. Purity of the compound was confirmed using ^{1}H-NMR, ^{13}C-NMR and mass spectrometry. The ^{1}H-NMR showed the distinctive multiplet peak present for the CH peak as a multiplet at 5.99-6.12 ppm, which integrated to 2H. The aromatic region showed the peak for the 1,4-disubstituted phenyl ring was seen as a broad singlet at 6.85 ppm, due to the symmetry of the molecule. The mass spectrometry data collected supported the structure with an $[M+H]^+$ at 191.1066

Following the synthesis of **11** and **12** compound **13** was synthesised, which was a mimic for styrene.

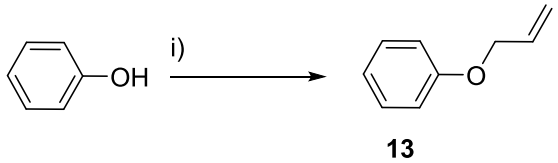

Scheme 10 – Synthesis of compound 13. Reaction conditions; i) allyl bromide, potassium carbonate, acetone, reflux.

Compound **13** was synthesised using the same method as **12**, whereby phenol was dissolved in acetone and allyl bromide and potassium carbonate were added.[148] The

method followed a literature precedent and gave the desired compound as a colourless oil in a 53% yield, which compared to a 57% yield obtained in the literature. The purity of compound **13** was confirmed using ^{1}H-NMR, ^{13}C-NMR and mass spectrometry.

The ^{1}H-NMR showed the typical multiplet in the upfield region for the vinyl group at 6.01-6.17 ppm. The upfield region also contained peaks for the CH_2-CH peak which appeared as two multiplets. The downfield region had two peaks for the phenyl ring, with an integration of 3H and 2H observed. The mass spectrometry data supported the structure with an $[M+H]^+$ at 135.0802.

2.4.2 Polymerisation reactions carried out using synthesised monomers with vinyl handles to incorporate viologens into the backbone of a polymer.

With appropriate precursors with vinyl moieties in hand, vinyl polymerisation reactions were carried out using a modified literature method from Griesbeck *et al.*[81,82]

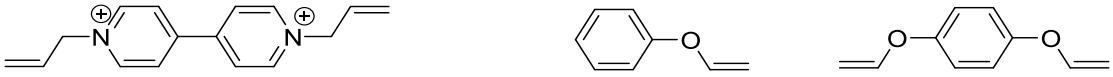

Figure 31 – Structure of monomers 11, 12 and 13 for the formation of compound 14 via a free radical polymerisation method.

Compound **14** was synthesised using monomers **11, 12** and **13** (**Figure 25**), which were added to water that had been previously acidified using sulphuric acid (pH = 2.0), and the solution was heated to 70 °C. Once heated, the monomers were added to the solution and potassium peroxydisulfate was added as the radical initiator. The mixture was heated overnight and quenched with methanol to stop the polymerisation process. Purification of the compound was performed using a cut-off membrane to remove any products with a molecular weight of less than 10 kDa, unfortunately after this procedure there was no product formed with a molecular weight above 10 kDa.

Compound **15** was synthesised according to a known literature procedure, which involved the use of commercially available PPIX, which was chosen due to its vinyl groups which can be used in vinyl polymerisation reactions. The free radical imitator used was potassium peroxydisulfate. A similar method, described above, for compound **14** was used for this reaction. The pH used for this reaction was pH = 2.3. The monomers used are shown in **Figure 32**.

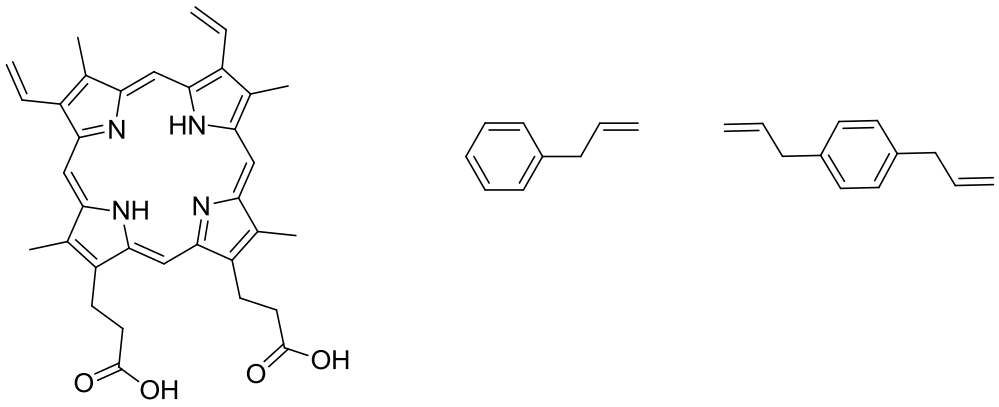

Figure 32 – Structure of monomers used for polymerisation reaction and formation of compound 15.

The reaction mixture was filtered using a cut-off membrane as before but no polymerised product with a molecular weight above 10 kDa was observed, which is the molecular weight of the expected polymer in the literature.[81]

Compound **16** was formed *via* a vinyl polymerisation reaction using compound **11** with styrene and divinylbenzene, utilising the same method as **14** and **15**. As before the method was not successful in the formation of compound **16**, and due to the insolubility of the sample it could not be analysed further.

2.5 Polyviologens with titanium dioxide

The use of titanium dioxide for light activated antimicrobial agents has proven a popular choice for the formation of a solid surface.[14,19,25,140,142,149,150] The use of titanium dioxide for this application would mean that UV light sources would have to be present for the system to be activated, as titanium dioxide absorbs in the UV region of the spectrum, unless it has been modified.

2.5.1 Synthesis of titanium dioxide

A method from the literature was used for the production of titanium dioxide using titanium (IV) isopropoxide *via* hydrolysis.[151]

$$Ti(OCH(CH_3)_2)_4 + H_2O \xrightarrow[24\ h]{Air,\ 100°C} Ti(OCH(CH_3)_2)_{4-x}(OH)_x + HOCH(CH_3)_2$$

$$Ti(OCH(CH_3)_2)_{4-x}(OH)_x \xrightarrow[5\ h]{Air\ 400°C} TiO_2 \text{ (anastase)}$$

Figure 33 – Synthesis of titanium dioxide, pure anatase.

The method involved the drop-wise addition of 5.00 mL of distilled water to 20.0 mL of titanium isopropoxide whilst stirring. Once complete the white solid was placed in the oven to remove any impurities at 100 °C for 24 h. Following this the solid was heated at 400 °C for 5h. The solid was not heated higher than this temperature as the desired form for titanium dioxide is anatase, and at temperatures above this the form of titanium dioxide will change from anatase to rutile.[140]

Once synthesised, titanium dioxide was analysed using powder X-ray diffraction (pXRD) to confirm the phase of titanium dioxide formed against a database of patterns. The synthesised titanium dioxide was confirmed to be pure anatase, which is the favourable form as it has a larger surface area available for photocatalysis.

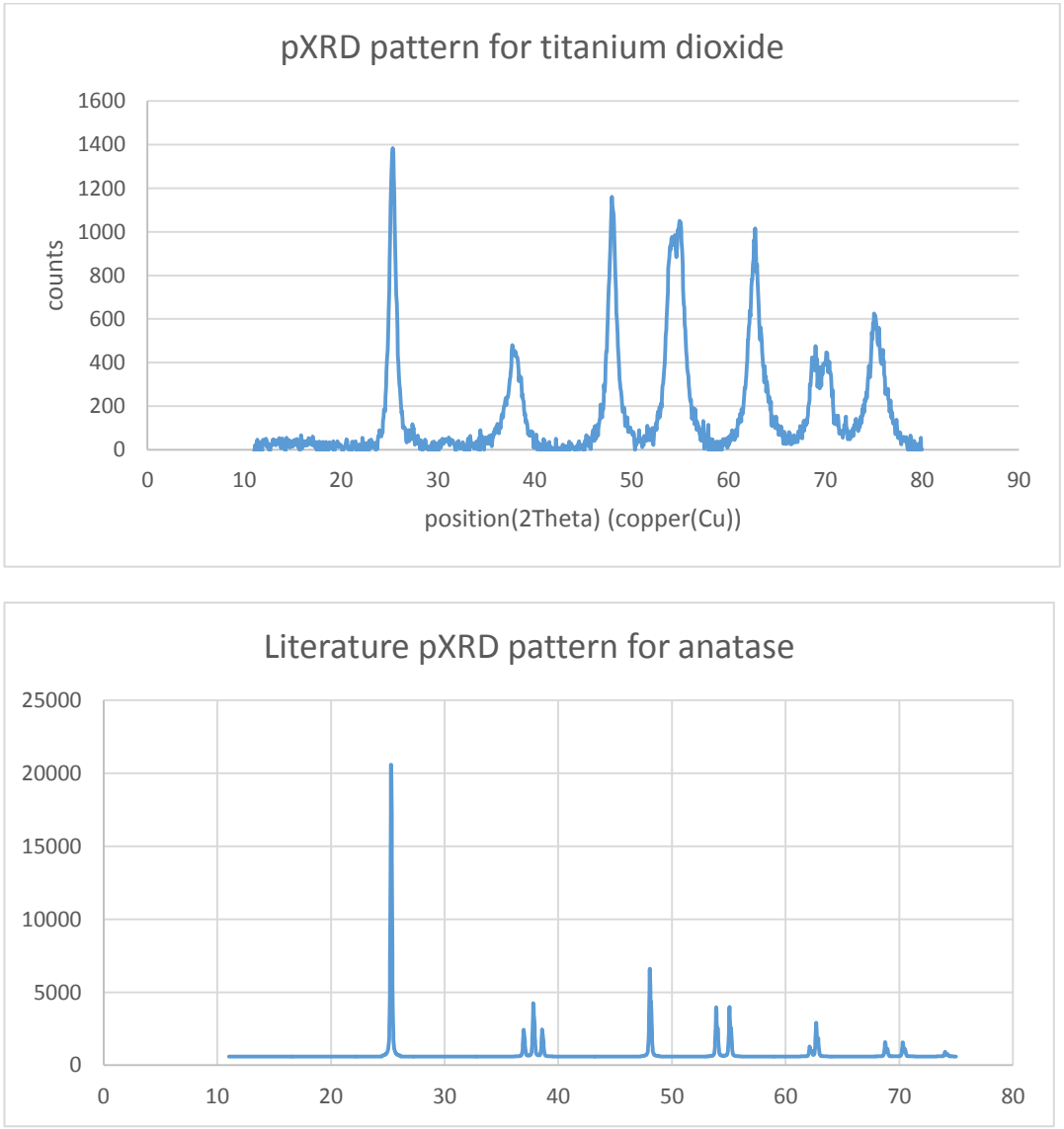

Figure 34 – Powder X-ray diffraction pattern collected for the synthesised titanium dioxide (top), compared to the literature pattern of titanium dioxide (anatase) (bottom).

The patterns shown in **Figure 34** compare the synthesised titanium dioxide to the reference pattern of anatase, which confirmed that the polymorph of titanium dioxide that has been formed is pure anatase.[152]

Analysis was also carried out by scanning electron microscopy (SEM) to study the homogeneity of the nanopowder produced. **Figure 35** shows that the titanium dioxide formed is a homogenous powder, as expected.

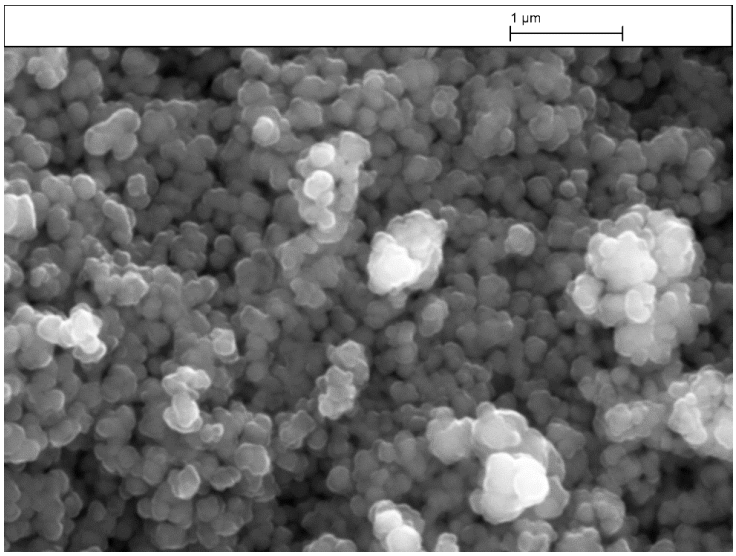

Figure 35 – SEM image of titanium dioxide.

Successful synthesis of titanium dioxide meant that it could be used for testing electron transfer between titanium dioxide and polyviologen. Following testing it was found that the synthesised titanium dioxide did not remain in suspension for long enough to allow for in-depth analysis using UV-Vis spectrometry. Another concern in using titanium dioxide is that it only absorbs in the UV region of the spectrum so using it without modification would mean that it would not be applicable for real world applications.

In order to shift the wavelength to the visible region modifications, possible modifications can be carried out on the surface by the introduction of amines, which also allows for conjugation. Attempts were therefore made to introduce amines on the surface of titanium dioxide, replacing the Ti-OH with Ti-NH_2.

2.5.2 Attaching amine groups to the surface of TiO_2

The surface of titanium dioxide contains hydroxyl groups, which are not efficient when trying to attach molecules to the surface of titanium dioxide. However, the titanium dioxide nanoparticles can be surface modified, to allow for different methods of conjugation to the surface to be investigated. To this end the following method was

carried out: titanium dioxide was placed in a furnace at 200 °C and the system was then flushed with nitrogen for 10 minutes, before then switching to flush with ammonium gas for 1 hr. The sample was left to cool and analysed using pXRD, where the results were compared to the starting material which contained pure anatase. This was found to be have been unsuccessful, after to bubbling through ammonia gas for 1 hr, 2 hrs and 3 hrs, then testing with fluorescamine,[153] no free amines could be detected.

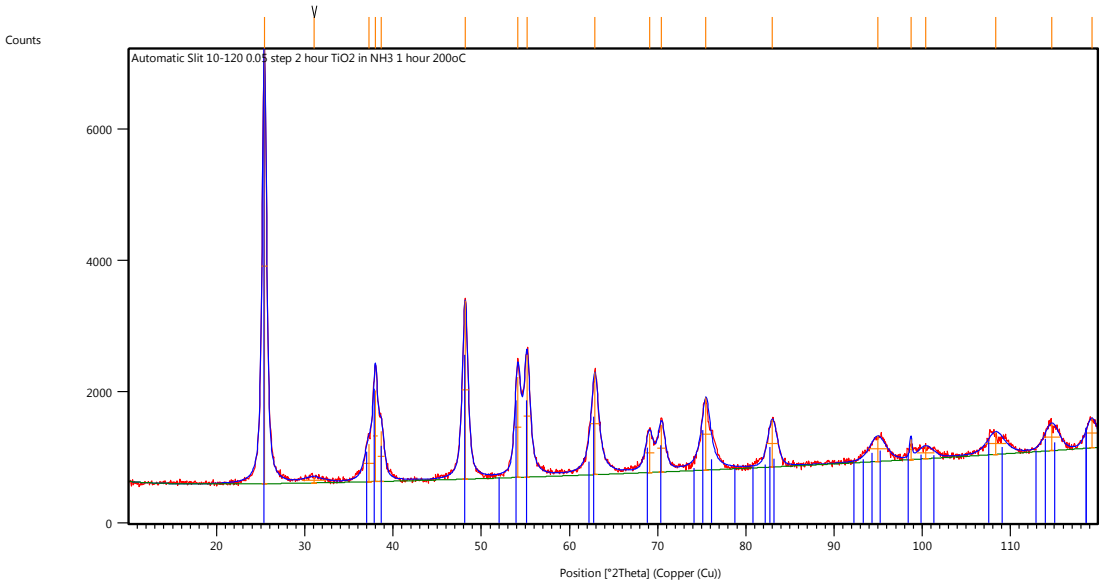

Figure 36 – Powder X-ray diffraction pattern for attempted ammonia modified titanium dioxide.

2.6 Shifting the wavelength to the visible region with the use of a photosensitiser

Due to the limitations of using titanium dioxide for this application it was decided that instead of using titanium dioxide a porphyrin would be used instead, as it already absorbs in the visible region and can be synthesised according to the functional groups that are required.

2.6.1 Synthesis of conjugatable viologen molecules

A small library of conjugatable viologen type molecules have been synthesised in this project for use in coupling reactions with porphyrins. The different moieties investigated were boronic acids, for palladium catalysed cross-coupling reactions, and alkyne-functionalised viologens, for use in click chemistry, more specifically in the azide-alkyne Huisgen cycloaddition (AAHC), and also for use in Sonogashira coupling reactions.

2.6.1.1 Synthesis of viologens for use in palladium catalysed cross-coupling reactions

The obvious site for modification of 4,4'-bipyridine with a boronic acid is at the nitrogen position. Substitution at the nitrogen position has been carried out utilising two different aromatic boronic acids to make the two different constructs in forming compounds compounds **17** and **18**, as shown in **Scheme 11**. The two different substitution patterns; *ortho* and *para* were both synthesised as this allowed a possible comparison between the two products, as it was thought that the *ortho* substituted may lead to steric problems, which could be overcome by a change in substitution pattern.

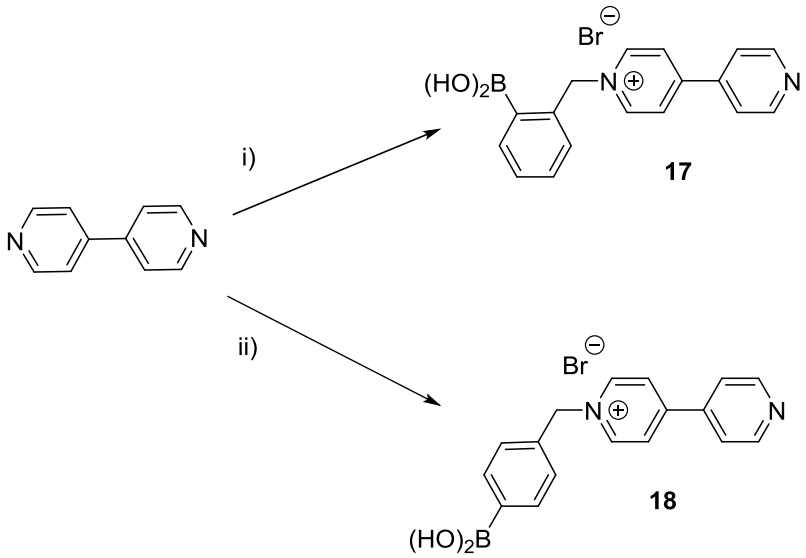

Scheme 11 – Synthesis of 17 and 18. Reaction conditions used; i) 2-bromomethylphenylboronic acid, acetone, reflux, 15 mins ii) 4-bromomethylphenylboronic acid, acetone, reflux 15 mins.

The synthesis of **17** and **18** was carried out according to a modified literature method,[154] with both methods being similar, the only difference between the two compounds was the substitution position of the boronic acid on the phenyl ring. The same method was used for both of the nucleophilic substitution reactions. The starting materials were heated under reflux in acetone for 15 mins. The products were precipitated using diethyl ether, to give **17** as a yellow solid in a yield of 24%, compared to a literature yield of 72%. The low yield may be due to difficulty in collection of product by precipitation. The synthesis of compound **17** was confirmed using ^{1}H-NMR, ^{13}C-NMR and mass spectrometry. The pyridyl protons appear in the downfield region as four doublets, and the phenyl protons appear as two multiplets with integrations of 3H and 1H. The ^{13}C-NMR shows six peaks, which correspond to the number of carbon environments in the compound. The mass

spectrometry was collected for the $[M+H]^+$ $C_{17}H_{16}O_2N_2B$: 290.1340 found 290.1336. Compound **18** was synthesised using the same method as **17** to give the *para* substituted boronic acid functionalised bipyridine molecule. The structure of **18** was confirmed by ^{1}H-NMR, ^{13}C-NMR and mass spectrometry. The ^{1}H-NMR showed a change in the downfield region compared to **17** due to the change in the symmetry pattern of the phenylboronic acid group. The downfield region showed peaks at 7.66-7.69 ppm and 7.84-7.88 ppm for the two pyridyl peaks, and the phenyl protons are shown at 8.41-8.45 ppm 8.64–8.67 ppm, and 8.78-8.82 ppm. In the upfield region the alkyl region contained a peak for the CH_2 as previously seen in **17**.

2.6.1.2 Synthesis of viologen molecules that can be used in the copper catalysed click reaction

An alternative strategy to using the palladium-catalysed cross-coupling reaction is the use of the Azide-Alkyne Huisgen cycloaddition which utilises an alkyne and an azide to form the 1,4-triazole. The viologen was modified to contain an alkyne functionality that can be used in the click reaction.

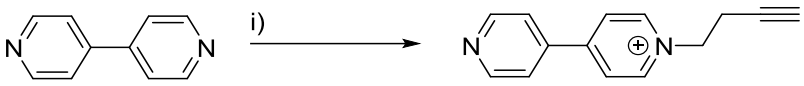

19

Scheme 12 – Synthesis of compound 19. Conditions used: i) 1-bromo-4-butyne, DMF, 80 °C, overnight.

Compound **19** was synthesised using a nucleophilic substitution reaction on the nitrogen of the pyridyl ring. The work-up proved challenging with the product precipitating using acetonitrile to give **19** as a brown solid in a 30% yield. The structure of **19** was confirmed using ^{1}H-NMR, ^{13}C-NMR and mass spectrometry. The ^{1}H-NMR spectrum showed a multiplet in the upfield region, 3.27-3.34 ppm corresponding to the alkyl chain and the alkyne peak. The downfield region showed four peaks corresponding to the four aromatic proton environments for the 4,4-bipyridyl portion. The ^{13}C-NMR showed the presence of ten carbon environments, which corresponds to the number present in **19**. The mass spectrometric analysis showed an $[M]^+$ ion peak and the HRMS calcd. for $C_{14}H_{13}N_2$: 209.1072 found 209.1073.

Following the successful synthesis of **19** it was speculated that there may be problems with steric hindrance between the alkyne on the viologen substituent and the azide on the

corresponding clickable porphyrin, so an alkyne with a poly (ethylene glycol) (PEG) spacer chain was synthesised to help solve this possible problem.

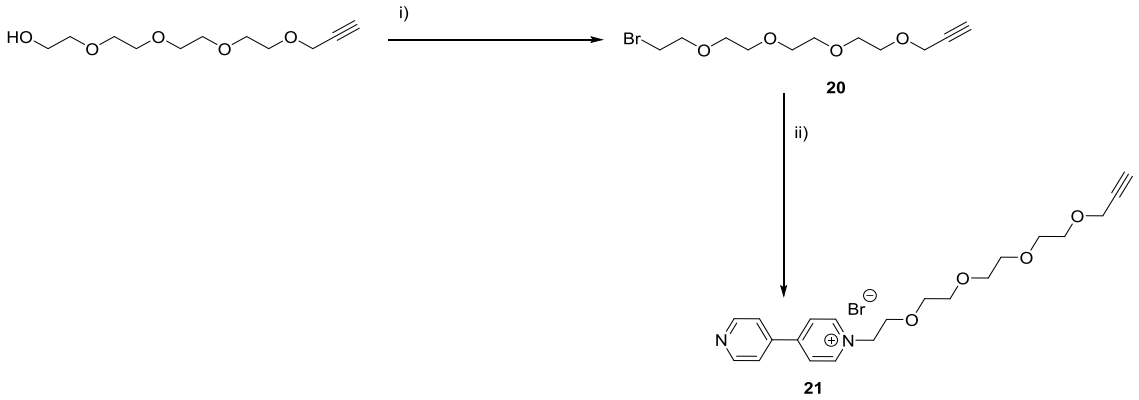

Scheme 13 – Synthesis of compound 21 *via* 20. Conditions used; i) dry DCM, PBr_3, rt, ii) 4,4'-bipyridine, DMF reflux.

Prior to the formation of the alkyne-PEG modified viologen **20** was synthesised *via* modification of a commercially available PEG chain bearing an alkyne and an alcohol functionality. The formation of **20** was carried out using PBr_3 in dry DCM to substitute the alcohol group for the bromide, as the bromide is a better leaving group for nucleophilic substitution reactions. The structure of **20** was confirmed using ^{1}H-NMR, ^{13}C-NMR and mass spectrometry. The ^{1}H-NMR showed four peaks in the upfield region corresponding to the CH_2 for the PEG chain and a typical peak for the terminal alkyne at 2.42-2.45 ppm. The ^{13}C-NMR showed six distinctive peaks for the six different carbon environments, and the mass spectrometry showed a molecular ion peak for the $[M+ NH_4]^+$ at 312.0805, HRMS calcd. for $C_{11}H_{23}BrO_4N$: 312.0805 found 312.0805.

With appropriate precursors in hand for use in both palladium cross coupling reactions and click reactions the viologens could be prepared for later conjugation to the porphyrin molecule.

2.7 Analysis of viologens

2.7.1 Photochemistry of the polyviologens investigated

Polyviologens are being utilised in this project for their ability to undergo electron transfer *via* the di-cationic species, to yield firstly the mono reduced species which is purple,[95] then followed by the doubly reduced species which is light brown or colourless. The main advantage of using the polyviologens is that they change colour when reduced and then revert to being colourless upon re-oxidation. This would be advantageous in a hospital setting, as the surface coatings could self-indicate their level of activity.

In order to investigate the reducibility of the synthesised polyviologens the UV-Vis spectra was collected for each of the polyviologens, in both oxidised and reduced forms.

The spectra were collected by preparing a fresh stock solution of sodium dithionite in water (500 mg, 50.0 mL), which was then sonicated until the solid was dissolved. Following this, the solution was degassed with argon for 15 mins. For each experiment a fresh solution of the chosen polyviologen molecule was dissolved in water, or a suitable solvent that the compound was soluble in. The solution was then degassed for 15 mins and a balloon of argon placed on each sample as the measurements were carried out under an inert atmosphere to allow for the distinctive peaks on the UV-Vis spectrometer to be seen. The polyviologen is expected to follow the redox behaviour shown in **Figure 37**.

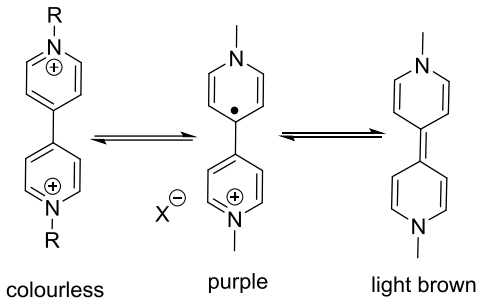

Figure 37 – Schematic of the different redox states of viologen.[95,145]

The oxidised form of viologens usually shows a broad absorbance peak between 260-270 nm, the extinction coefficient of which is relatively intense (approximately 10,000 – 16,000 cm^{-1} M^{-1}).

The spectrum of the viologen reduced species was obtained when a sodium dithionite solution (1 % mol solution) was added. A small amount of this solution (approximately 20 µL) was required to effect the spectral change. It has been speculated that the one electron reduction product could be associated with the peaks at approximately 310-320 nm, [93,155] and a broad peak of a lower absorbance that appears at approximately 520 nm.

The second peak for the mono cationic species at 520 nm was only seen when analysing compound **6**, which is a polyviologen with an aromatic spacer group and a bromide counter-ion. One explanation why only this compound shows a peak at 520 nm could be that it is the only one that forms a stable one electron reduced species with a slow back electron transfer between reduced and oxidised species. Similar reduced viologens have been reported to exhibit low stability and rapid electron transfer back to the oxidised species.[155,156]

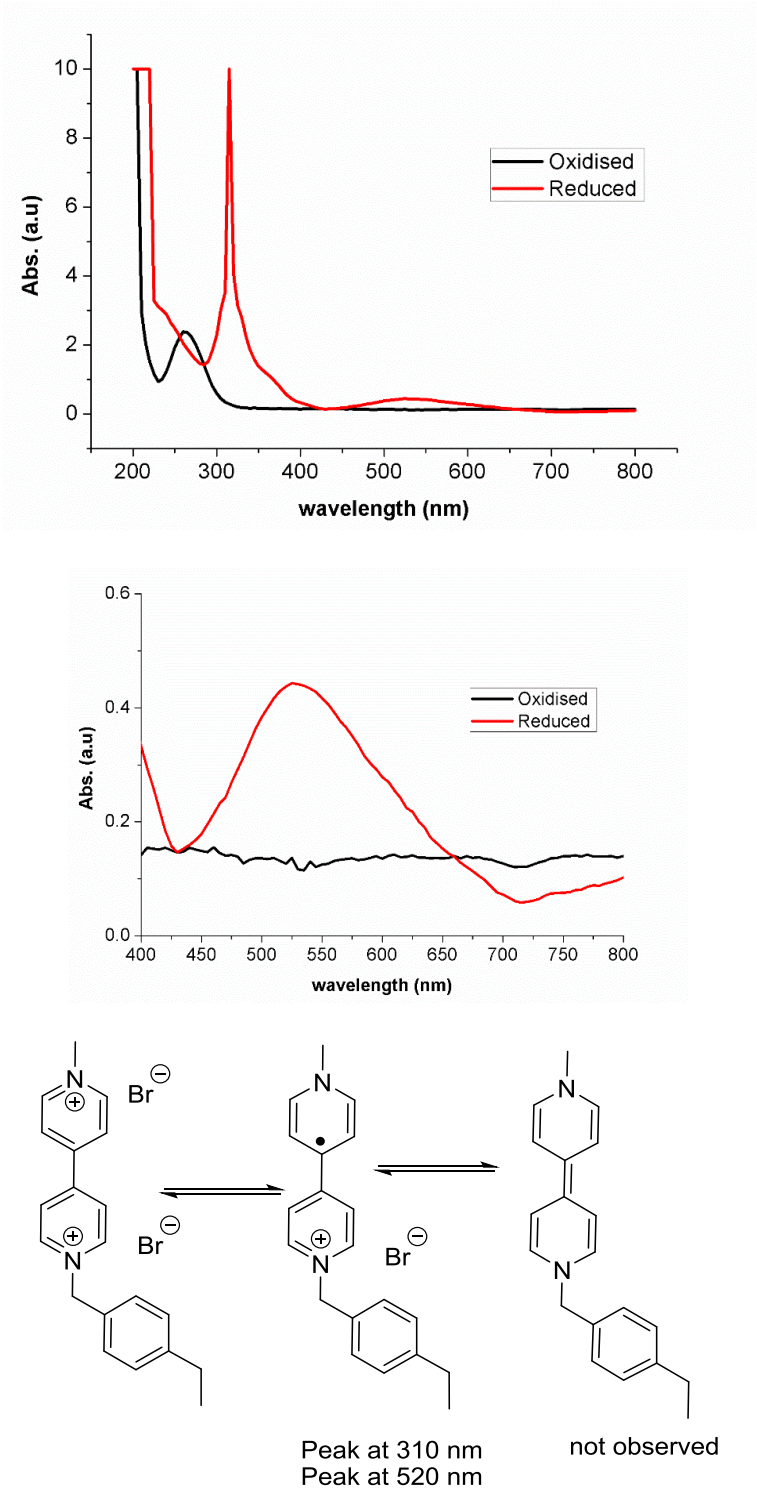

Figure 38 – Spectrum showing the oxidised and reduced species of compound 6, which shows two peaks in the reduced species (top), below shows an expanded spectrum of the second peak of reduced compound.

As well as investigating the formation of the mono-reduced species, the lifetime of this species was also investigated; this proved challenging because in normal aerobic conditions the species would be quenched by oxygen, generating reactive oxygen species,

and thus the peak at approximately 520 nm would not be seen. In fact this peak was only seen when the system was back filled with argon before the measurements were taken, or if the measurements were taken in a completely closed system. The lifetime of this species was found to be longer than expected, because literature values quoted for the lifetime of similar species are in the ms range.[93,102] When investigating compound **6** a lifetime of between 15-20 minutes was observed. After this time, the species returned slowly back to the fully oxidised form, as shown by the UV-Vis analysis.

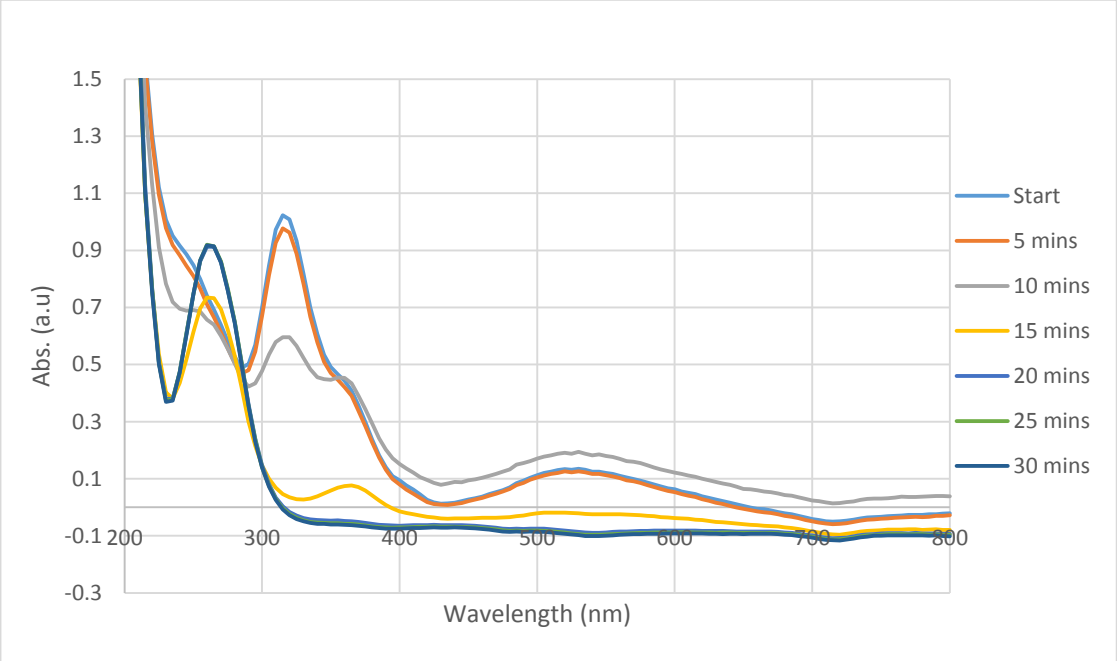

Figure 39 – UV-Visible spectrometry data showing redox states of compound 6 over 30 minutes.

From inspection of **Figure 39** it can be seen that the reduced species starts to return back to the fully oxidised form between 10-15 minutes, where three distinct peaks can be seen. By 20 minutes compound **6** has completely returned to the fully oxidised form with a single sharp peak present at 260 nm. A further study was carried out in order to investigate more accurately and precisely the time taken for this polyviologen molecule to transfer from the two electron reduced form to the fully oxidised form. This is shown in **Figure 40**. The results of this study showed that the time taken to carry out the electron transfer between the reduced species and the fully oxidised species under argon is approximately 17 minutes. These experiments would be expected to become increasingly difficult to follow, because the reduced species cannot be detected in the presence of oxygen. However, this does not necessarily mean that the di-reduced species is not being formed,

but could instead mean that reactive oxygen species are being produced under steady state conditions.

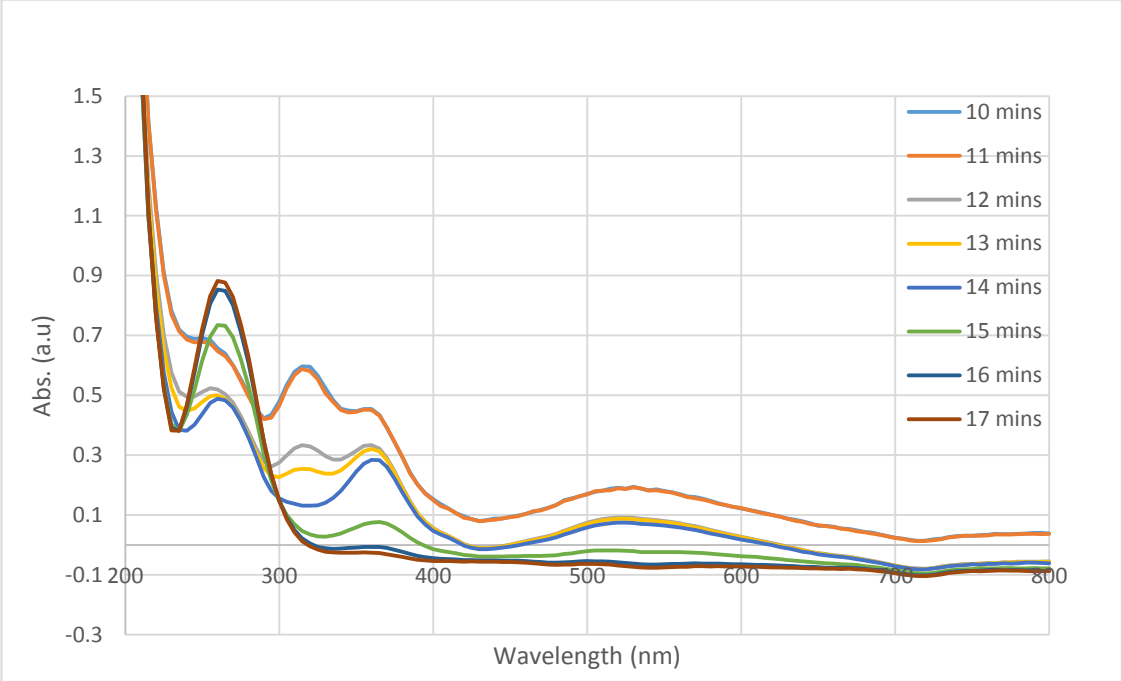

Figure 40 – UV-Vis spectra showing the electron transfer between 10-17 minutes to investigate the lifetime of the species formed.

Figure 40 shows a more detailed graph of the measurements taken between 10-17 minutes, and by 17 minutes the fully reduced form had gone completely back to the fully oxidised form, at 15 minutes the oxidised peak was dominant but a small peak at 320 nm was seen which is thought to represent the mono-reduced species.

Compound **7** was analysed in the same way as compound **6** with all the solutions being degassed before use and kept under inert atmosphere. The UV-Vis spectrum of **7** shown in **Figure 41** indicates the presence of a peak at 310 nm following the addition of sodium dithionite, but there was no indication of a peak at 520 nm. Following the addition of more sodium dithionite solution no further changes were seen.

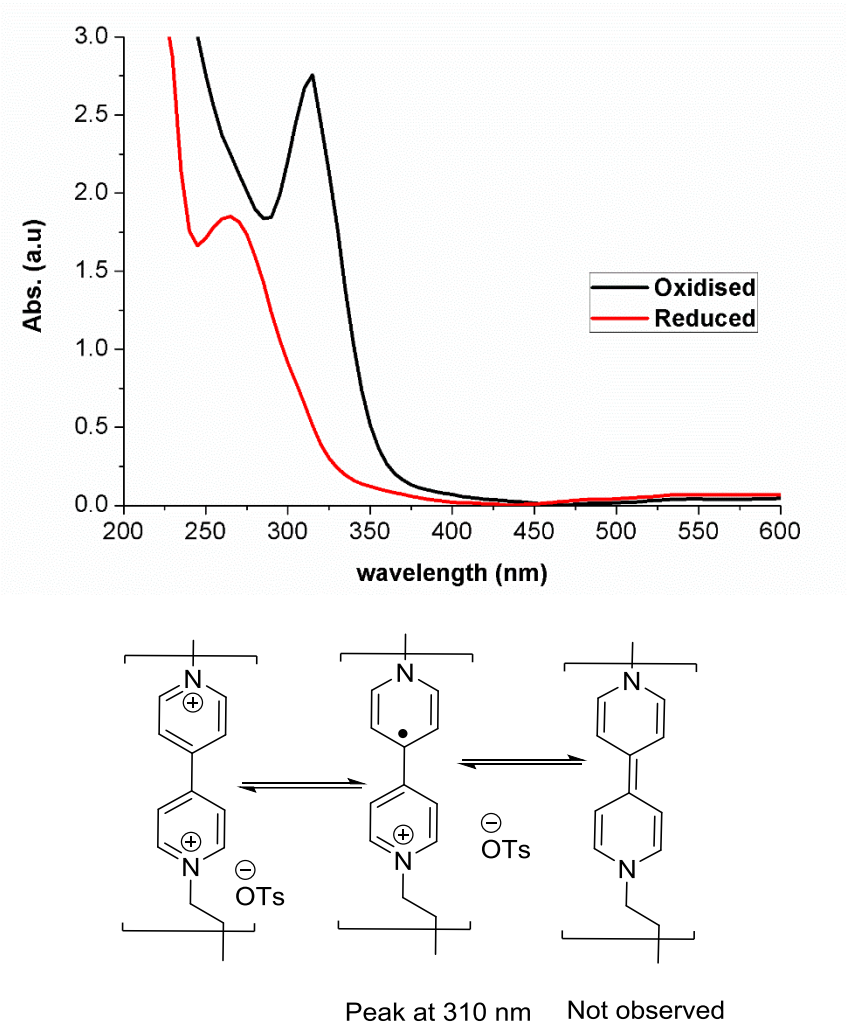

Figure 41 – UV-Vis spectra showing the oxidised and reduced forms of compound 7.

2.7.2 Photolysis measurements

In order to investigate the electron transfer using the proposed system of a porphyrin linked to, or in close proximity with, a polyviologen molecule photolysis measurements were carried out to study the electron transfer. The aim of the photolysis measurements was to investigate if electron transfer from the porphyrin to the viologen molecule could be detected, and if so what effect this has on the UV-Vis spectra observed. Before the measurements were carried out, control samples were tested using only the porphyrin and the polyviologen separately. The samples were irradiated with white light.

The main problem encountered during the measurements was from the extended exposure of the porphyrin-polyviologen solution to the white light. This meant that there was considerable photobleaching of the porphyrin and so the electron transfer between the porphyrin and the viologen was not detected. This could have been due to the short

lifetime of the species formed, or it could be due to the radical species not being stable enough to be detected spectrophotometrically, as it is so short-lived.

Further investigations would need to be carried out on electron transfer using a laser flash photolysis apparatus, and a specific singlet oxygen trap to study the electron transfer and ROS production occurring.

2.8 Conclusions

In conclusion, a library of polyviologen molecules has been synthesised as well as their precursors. The molecules have been analysed and studied using UV-Vis spectrometry for their electron transfer properties. The polyviologen molecules have been entrapped in polymeric matrices and tested for electron transfer using initially titanium dioxide, which proved challenging due to issues with solubility. The next idea was to shift the wavelength of excitation and look into the synthesis of a porphyrin that is able to undergo electron transfer with a polyviologen molecule.

An alternative to using polyviologen molecules is the use of viologen molecules that are conjugated to a porphyrin molecule. A number of conjugatable viologen molecules have been synthesised that can be used in either a click reaction with an azide-functionalised porphyrin, or in a palladium-catalysed cross-coupling reaction with a halogenated porphyrin.

The spectroscopic properties of the polyviologens show that these species are able to undergo an electron transfer process to result in the formation of radical species. This is promising as it shows that they are able undergo electron transfer to form radical species.

The next step moving forward would be the synthesis of conjugatable porphyrins and coupling reactions to study the electron transfer between the porphyrin and the viologen molecule before entrapping them in a polymeric matrix.

3 Porphyrins for conjugation and immobilisation on polymeric surfaces

3.1 Introduction

Porphyrins are the photosensitiser of choice for this project, as they have a large absorption range, with a Soret band around 400 nm and 2-4 Q-bands between 500-650 nm (for metallated and free-base porphyrins, respectively). This is highly advantageous as the wavelength used for the excitation of the photosensitiser can be anywhere within this range, although clearly the molar absorptivity will vary with wavelength. Another reason for using porphyrins is due to their ease of synthesis and versatility; porphyrins with a variety of substituents are easily synthesised in few steps. Porphyrins can also be easily modified *via* simple synthetic reactions and are easily conjugated to solid supports *via* a number of different coupling reactions.

Before devising a synthetic route for the formation of a porphyrin there are several factors to consider. Firstly, the nature of the substituents needs to be examined, as some groups can be introduced directly by electrophilic substitution such as halogens, nitro groups and sulphonic acids; while others, such as alkyl groups, *via* the Friedel Crafts reaction, cannot. The position of the substituents also needs to be considered, as porphyrins have four *meso* substituent positions and eight *beta*-substituent positions, as shown in **Figure 7**.[71,157] Multiple substituents at the *beta*-positions exhibit much larger steric hindrance compared to those in the *meso* positions,[157] and can cause distortion of the porphyrin, out of the plane.

The retro-synthetic approach is the most logical when designing the synthesis of a porphyrin. This approach involves deconstructing the molecule into smaller components and determining which starting materials can be used for the synthesis, as shown in **Figure 42**.

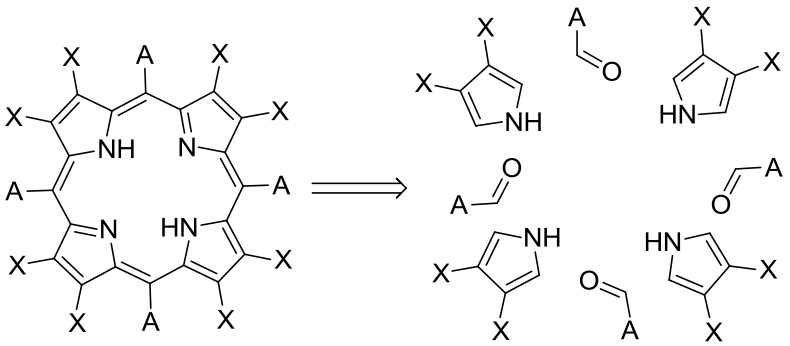

Figure 42 – Retrosynthetic analysis of a porphyrin, showing possible starting materials.

Through retrosynthetic analysis, the most obvious route to the synthesis of porphyrins is by using pyrrole and an aldehyde. This method was developed by Rothemund in 1936, who first reported the synthesis of a porphyrin using an aldehyde and pyrrole in a sealed container at 150°C for 24 hours,[50,51] with these relatively harsh conditions resulting in low yields.

In 1967 A. D. Adler and F. R. Longo carried out research into further optimisation of porphyrin synthesis, in particular the synthesis of 5,10,15,20-tetraphenylporphyrin (TPP).[52] It was found that both the yield and the condensation rate of pyrrole and benzaldehyde to give TPP, depend on many different factors; the acidity of the reaction mixture, the solvent, the temperature, the availability of atmospheric oxygen and the initial concentration of the reagents. The method proposed by Adler and Longo uses an acidic solvent, which also acts as a catalyst, and operates at atmospheric pressure.[52] Oxidation of porphrinogen to the porphyrin occurs due to the availability of ambient oxygen. The reaction time compared to the Rothemund method is much shorter (approximately 30 minutes) and the yields are higher (typically *ca.* 20%).[52] The mechanism for the Adler-Longo synthesis is shown in **Scheme 14**.[51] The primary steps involve the use of pyrrole and the chosen aldehyde to form a substituted pyrrolic intermediate, which then forms the corresponding porphyrinogen, which is in turn air oxidised to form the porphyrin; the oxidation can be carried out by opening the vessel to air, or chemical oxidants such as 2,3-dichloro-5,6-dicyano-1,4-benzoquinone (DDQ) or *p*-chloranil can be used.

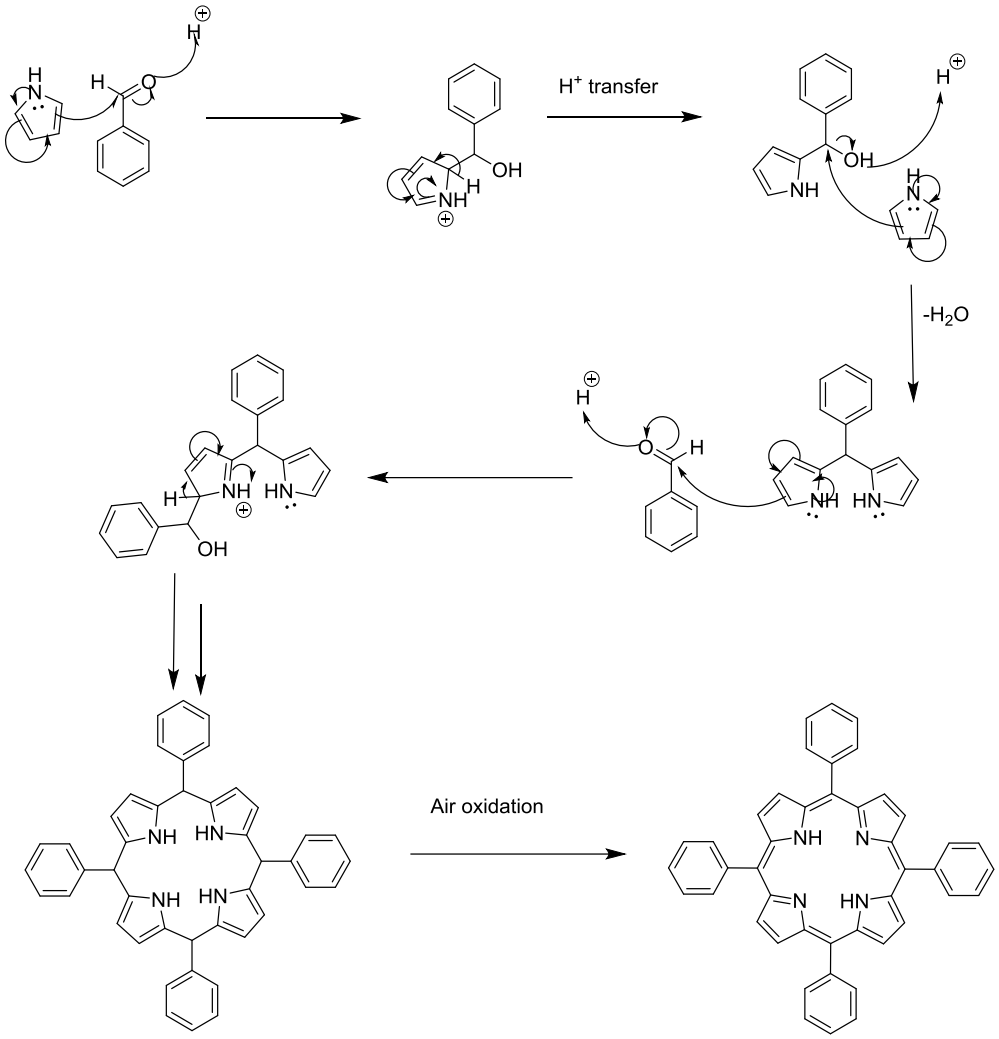

Scheme 14 – Mechanism for the formation of 5,10,15,20 – tetraphenylporphyrin *via* the Adler-Longo porphyrin synthesis.

While the Adler-Longo method is ideal for tetrasubstituted porphyrins such as tetraphenylporphyrin, this method can also be used to obtain unsymmetrically substituted porphyrins. The mixed aldehyde condensation method is slightly different to a normal Adler-Longo synthesis, as it involves the use of two different aldehydes and varying the molar ratio of those two aldehydes in order to obtain the desired product in the highest possible yield. An equimolar ratio of the two aldehydes in a mixed condensation allows the highest yield of the A_2B_2, *cis* and *trans* porphyrins to be obtained, and the different isomers can be separated and purified using column chromatography. This method is complicated by the number of porphyrins that require separation and purification; while this is time consuming, the simplicity of the reaction makes it appealing. **Figure 43** shows the six possible porphyrin products that may be obtained when carrying out a mixed aldehyde condensation reaction.

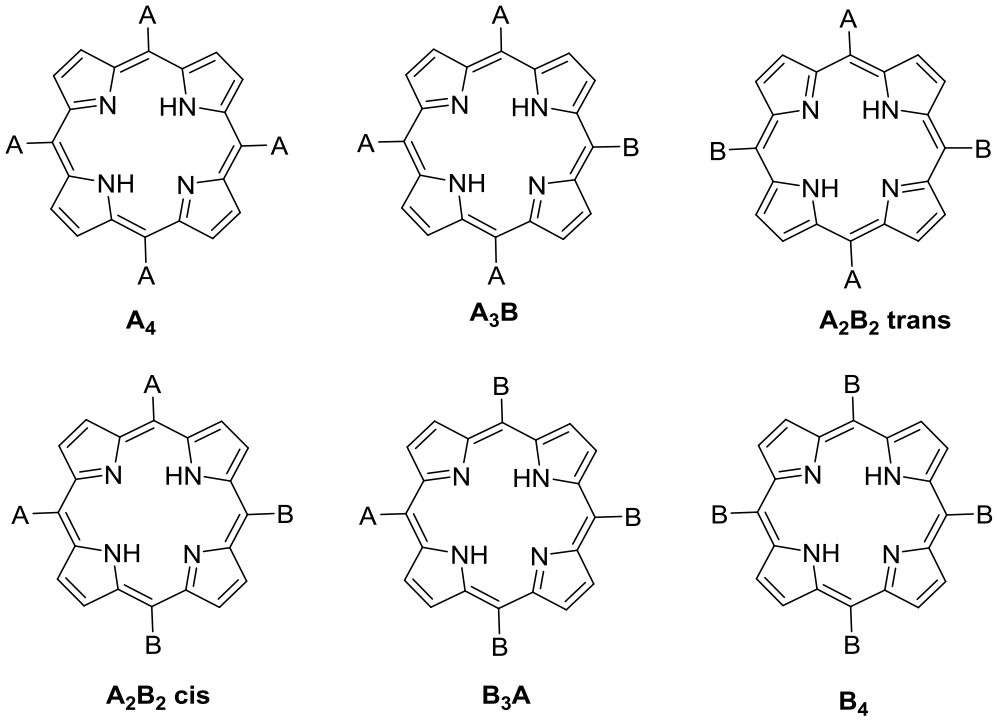

Figure 43 – Structure of possible products formed from an Adler-Longo mixed aldehyde condensation.

An alternative synthesis for the production of porphyrins was carried out by MacDonald in the 1960s.[52,158]

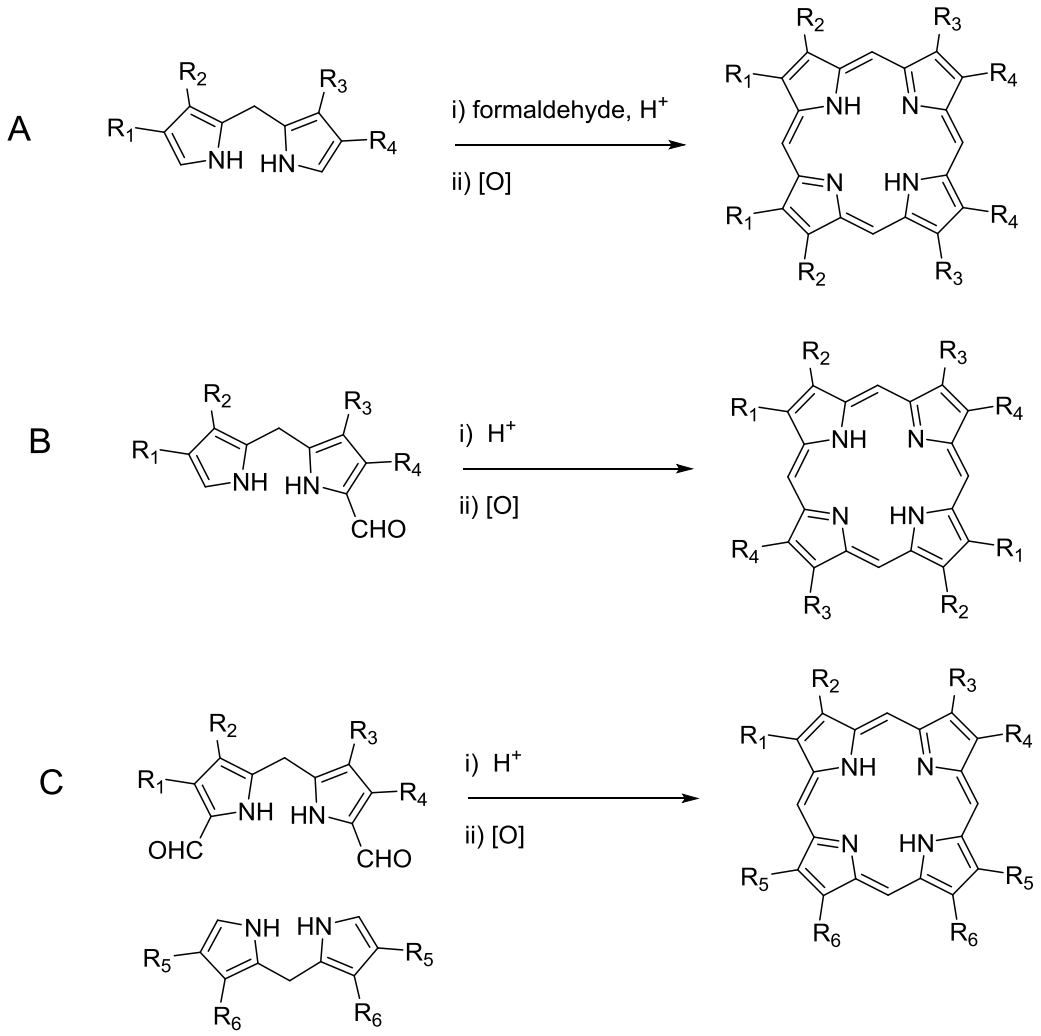

Figure 44 - Three possible routes using the MacDonald synthesis *via* dipyrromethanes to form A_2B_2 porphyrins.

The MacDonald porphyrin synthesis relies on the initial formation of dipyrromethanes, which is generally carried out at room temperature, and then a condensation reaction is performed in acetic acid containing 0.4% hydrogen iodide.[53] The synthesis of porphyrins is thus carried out *via* an acid-catalysed reaction between two dipyrromethanes, *via* one of three alternative methods (**Figure 44**); in the first method (**A**) an unsubstituted dipyrromethane undergoes a self-condensation reaction in the presence of a separate 1 carbon bridging unit (formaldehyde for example) to give the porphyrin. The second method (**B**) utilises a dipyrromethane that has a formyl group on the carbon atom neighbouring the pyrrolic nitrogen: this allows the use of four different substituents. The third method (**C**) involves the use of a dipyrromethane and a diformyl dipyrromethane.[158] This method has restrictions, chiefly that labile substituents had a large effect on the yield obtained, and "scrambling" can occur, resulting in mixtures of products.[159,160]

In 1987 Lindsey *et al*. developed a mild synthetic method that allowed expansion of the use of sensitive aldehydes in porphyrin synthesis.[51,160] The main aim was to eliminate acid-catalysed polypyrrolic rearrangement in the synthesis of *trans*-porphyrins.[160] The desired aldehyde and pyrrole react reversibly at room temperature under inert atmosphere with traces of a weak acid catalyst such as boron trifluoride (BF_3) and an oxidant such as 2,3-dichloro-5,6-dicyanobenzoquinone (DDQ) or *p*-chloranil to form the cyclic tetraphenylporphyrin. The porphyrin is obtained in higher yields using the Lindsey method (*ca.* 40%). The main problem with the Lindsey method is the scale at which the reaction is carried out; the nature of the cyclotetramerisation requires high dilution conditions, thus making it difficult to scale up. The three methods are compared in **Table 2**.

Synthetic Method	*Rothemund (1936)*	*Adler-Longo (1967)*	*MacDonald (1963)*	*Lindsey (1987)*
Conditions	150 °C, 24 h, High pressure.	141°C, 30 mins	Room temperature, 1h	Room temperature, 1 h, Inert atmosphere.
Solvent	Pyridine	Propionic/ acetic acid	Dichloromethane, TFA	Dichloromethane
Additives	-	-	DDQ	DDQ, BF_3
Yield	<10%	Approx. 20%	0.1 – 40%	Approx. 40%

Table 2 – Comparison of the main synthetic routes to porphyrins.[50,51]

3.1.1 Metalloporphyrins and their synthesis

Porphyrins are highly efficient metal chelators.[161,162] The insertion of metals can be carried out *via* conventional heating or *via* the use of microwave synthesis.[163–165]

The insertion of metals into the porphyrin cavity causes distortion of the porphyrin ring, with the amount of distortion being dependent on the metal utilised.[161] The most common distortion seen in porphyrins is tilting of opposite pyrrolic rings relative to each other, which gives a saddle conformation,[166] and the twisting of the plane of the pyrrole rings, giving carbon atoms above and below the plane. The presence and nature of the central metal ion strongly influences the photophysical properties of the photosensitiser.[167] The

chelation of paramagnetic metals appears to shorten the triplet lifetime of the photosensitiser, and this generates variations in the triplet quantum yield.[168,169] In addition, the triplet state lifetime can be increased through coordinating a heavy metal atom, such as Pt or Pd.[170]

3.1.2 Microwave heating

Since the 1980s there have been continual improvements made to the practicalities of using microwave heating in organic synthesis.[165] The slow initial uptake of microwave synthesis is attributed to lack of control, lack of reproducibility and safety issues, which have since been rectified. Microwave heating allows for some reactions to be carried out in minutes, whereas these same reactions would normally take hours on the bench. Microwave heating is also known to reduce side reactions, increase yields, and improve the reproducibility of reactions.[163,164,171] The main disadvantage of using a microwave reactor is the scale of the reaction, which is limited by the size of the microwave cavity. Microwave-enhanced chemistry is based on the efficient heating of materials by microwave dielectric heating effects. This is dependent on the ability of a material to absorb microwave energy and convert it to heat.

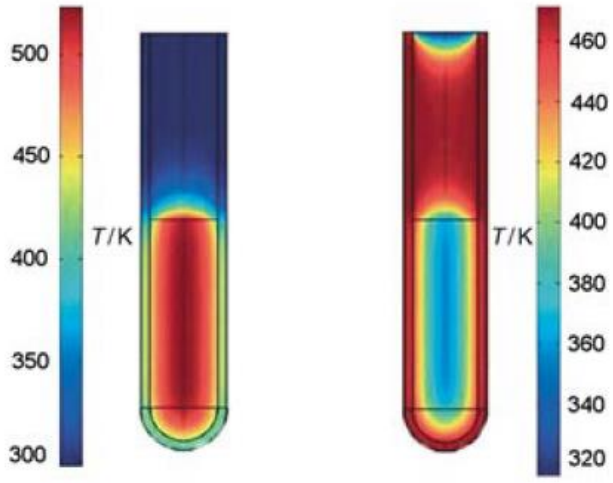

Figure 45 – Comparison of bench heating (right) and microwave heating (left).[163]

Figure 45 compares the heating effect on the bench and in the microwave. The heating in the microwave is more efficient, allowing reaction times to be reduced. The reaction vessels used in microwave reactors are typically made of microwave transparent materials. Microwave heating uses an inverted temperature gradient compared to typical conventional heating. Microwave irradiation produces efficient internal heating by direct coupling of microwave energy with the molecules that are present in the reaction mixture.

3.1.2.1 Microwave heating for metal insertion into porphyrins

Microwave heating for the insertion of metals into porphyrins has been utilised in several literature examples, and demonstrates advantages such as decreased reaction time and increased yield.[170,172,173]

Nascinmento *et al.* studied the use of a microwave reactor for the synthesis of porphyrins and their metal derivatives.[173] They found that the use of a microwave allows a more rapid and facile synthesis with fewer side products and higher yields.

Dean *et al.* investigated the use of microwave heating for the insertion of group 10 metals (Ni, Pd and Pt) into porphyrins and chlorins.[172] The main finding was that microwave heating allowed lower temperatures and shorter reaction times to be used, while still resulting in acceptable yields of product. Palladium insertion generally takes hours to days using conventional heating, in contrast to minutes *via* microwave irradiation, with less palladium metal by-product being produced.[170]

Giuntini *et al.* also investigated the use of microwave heating for the insertion of palladium and platinum into water-soluble porphyrins.[170] Conventional heating was attempted for metal insertion, but it was not found to be successful. In contrast, to the same reaction performed *via* microwave irradiation was successful.

Investigations into the use of microwave-assisted synthesis for metal insertion into porphyrins will be carried out in this project due to the many advantages over conventional heating.

3.1.3 Analysis of porphyrins

3.1.3.1 Spectroscopic properties of porphyrins

Porphyrins are composed of a highly conjugated system that absorbs strongly in the visible region of the electromagnetic spectrum. A typical porphyrin spectrum consists of five bands.[167] An intense peak at around 400 nm is known as the Soret band ($\varepsilon \approx 150{,}000$ cm^{-1} M^{-1}); the Soret band is due to the S_0 to S_2 electronic transition.[167,174] Four less intense peaks are seen at around 500-650 nm with an intensity of approximately 10,000 cm^{-1} M^{-1} :these are known as the Q-bands, which are due to the S_0 to S_1 transitions, a typical non-metallated porphyrin spectrum can be seen in **Figure 46**.

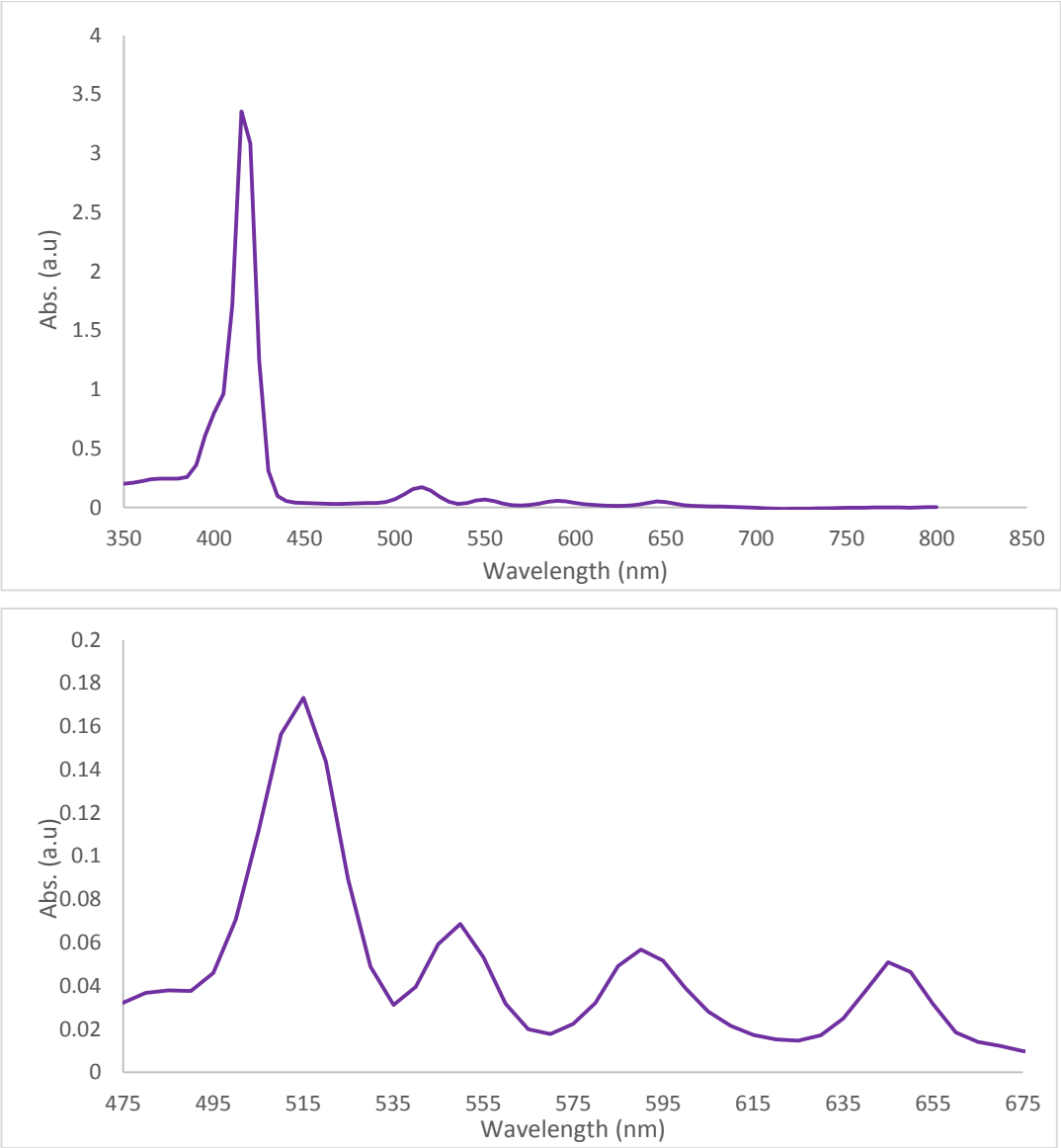

Figure 46 – Typical UV-Vis spectrum of a porphyrin showing an intense Soret band and four Q-bands.

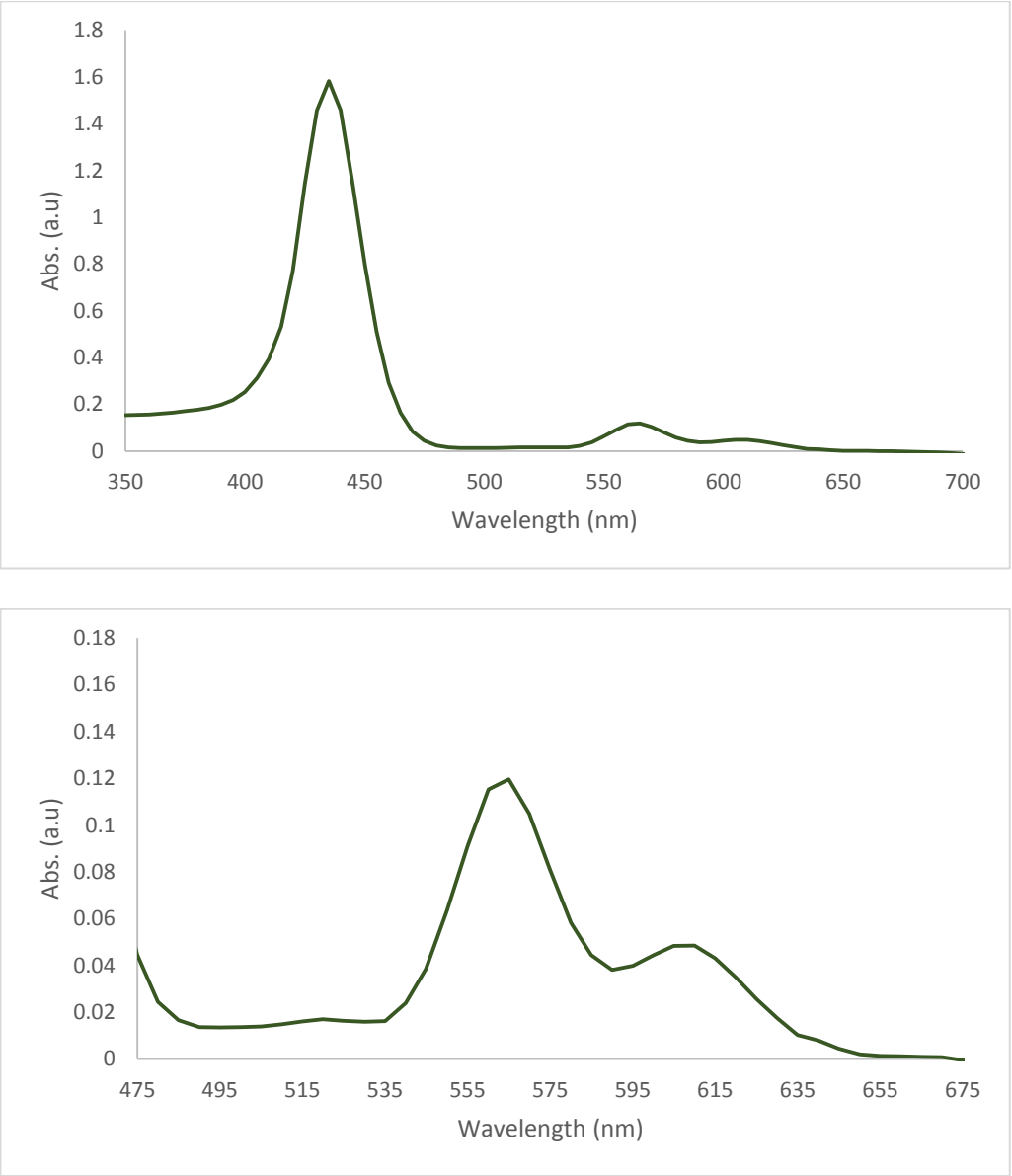

Figure 47 – UV-Vis spectrum of a metalloporphyrin showing an intense Soret band and two Q-bands.

A metalloporphyrin UV-Vis spectrum differs from that of a metal free porphyrin spectrum as shown in **Figure 47**; a metalloporphyrin has only two Q-bands compared to the four Q-bands seen in the spectrum of a porphyrin. The change in the absorption characteristic spectrum is due to an increase upon metal complexation, thus the porphyrin is in point group D_{4h}, and the metal complex is in C_{2v}.

3.1.4 Porphyrin synthesis outlook

The synthesis in this project will explore combinations of all of the most common porphyrin synthesis methods, with the aim of producing both A_2B_2 and A_3B type porphyrins.

The MacDonald method will be used to produce the dipyrromethane precursors for the synthesis of A_2B_2 porphyrins. The Lindsey method will also be explored for the synthesis of the A_2B_2 porphyrin molecules, as it is known to be higher yielding than the mixed condensation reaction. However, the aforementioned limits of scalability may be problematic in the generation of large quantities of porphyrins for immobilisation.

The Adler-Longo mixed aldehyde condensation method will also be used for the formation of a porphyrin that contains a singlet conjugatable moiety. This porphyrin will subsequently be used for conjugation to a viologen molecule, or may contain a vinyl group for use in free radical polymerisation reactions.

Requirements for the synthesised porphyrins include; conjugatability, ease of synthesis, electron donating / electron accepting properties, low light and dark toxicity, and good electron transfer possibilities.

3.2 Synthesis of porphyrins for conjugation to viologens

A number of porphyrins have been synthesised for conjugation to viologen molecules *via* the nitrogen atom on the viologen. The formation of porphyrins containing a reactive handle is aimed to replicate the reaction carried out when the viologens are polymerised, forming a monomer which could be polymerised to give a porphyrin-linked viologen in the backbone of the polymer.

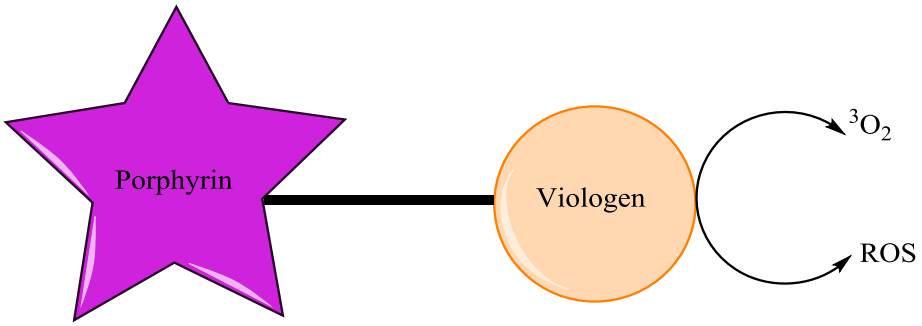

Figure 48 – Proposed schematic of porphyrin-viologen hybrid.

3.2.1.1 Synthesis of dipyrromethane precursors

Dipyrromethanes are key intermediates in the A_2B_2 strategy. The first dipyrromethane synthesised was the unsubstituted dipyrromethane (**22**), as shown in **Scheme 15**. While the method followed was a known literature method, the procedure was found to be extremely challenging,[175] as the compound decomposed rapidly upon purification *via* column chromatography. It is know that this class of compound is more likely to

decompose when there are no substituents on the methylene bridging positions, and that such derivatives are also prone to polymerisation, forming polypyrrole structures.

Scheme 15 – Synthesis of unsubstituted dipyrromethane (22), conditions used; i) dry DCM, TFA, 15 mins.[176]

An alternative to using the unsubstituted dipyrromethane is using a dipyrromethane with a bridging substituent, and subsequently using formaldehyde to form the desired porphyrin product. The synthesis of dipyrromethanes with either a pyridyl substituent or an ester substituted phenyl derivative on the bridging position was carried out (**Scheme 16**).

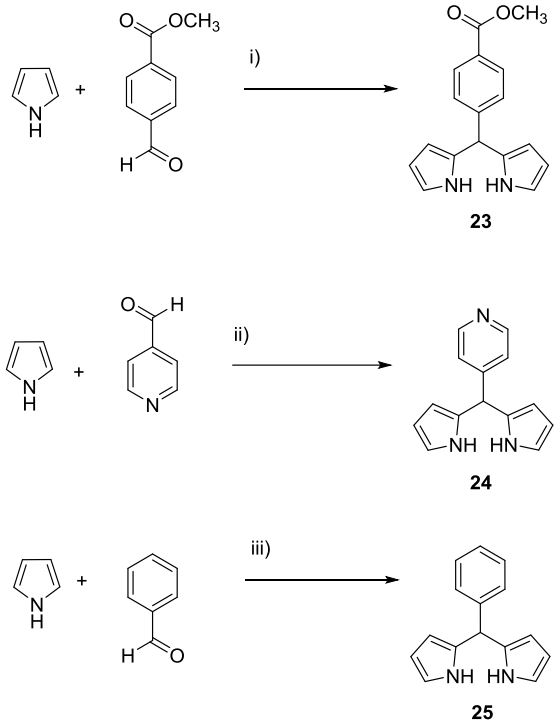

Scheme 16 – Synthesis of *meso*-substituted carboxyester phenyl, phenyl and pyridyl dipyrromethanes i) N_2, TFA, rt, 20 mins, ii) N_2, 85 °C, 15h, iii) N_2, TFA, rt, 40 mins.

The reaction to prepare pyridyl dipyrromethane required harsher conditions than that required for the preparation of **23** and **25**, with heating at reflux employed in comparison to the room temperature synthesis of the phenyl dipyrromethanes, due to resonance stabilisation of the pyridyl ring.[177,178] The purification of these compounds was carried

out *via* column chromatography using alumina, due to the strong adhesion of the compound on silica.

The synthesis of compound **23** was carried out according to a modified literature method,[178] using inert conditions and TFA, with stirring for just 20 mins instead of the 4 h used in the literature. The product was then purified using column chromatography on alumina to give the product as a white solid in a 55% yield, which compares favourably with a literature yield of 42%.[178] The structure was confirmed by ^{1}H-NMR, ^{13}C-NMR and mass spectrometry. The proton NMR showed the typical splitting for a 1,4 disubstituted phenyl ring with doublets at 7.29 ppm and 7.98 ppm, both having *J* coupling values of 8.0 Hz. In the upfield region there was a distinctive singlet representing the methyl group of the ester at 3.91 ppm, with an integration of 3H. A peak at 5.53 was seen as a singlet, representing the bridging proton. The protons representing the pyrrole were seen as multiplets at 6.15-6.18 and 6.71-6.74.

The synthesis of compound **24** was carried out using a literature method,[177] by heating 4-pyridinecarboxaldehyde with pyrrole at 85°C for 15 hours under nitrogen. The mixture was then purified using column chromatography to give a brown solid in a 41% yield, which is lower than the literature yield of 58%. The yield was probably lower than expected due to challenging purification using column chromatography. The structure was confirmed using ^{1}H-NMR, ^{13}C-NMR and mass spectrometry. The proton NMR showed the distinctive peaks for the 1,4-disubstituted pyridyl ring, but interestingly it also showed a broad singlet for the two NH peaks at 8.02 ppm which was not seen in compound **23**.

An alternative strategy is the formation of phenyl dipyrromethane for the formation of 5,15-diphenyl porphyrin which can then be substituted at the *meso* positions. Compound **25** was formed using a similar method to **23**. A literature method was used, whereby the pyrrole and benzaldehyde are degassed, followed by the addition of TFA.[179] The crude product was then purified using column chromatography to give a brown solid in a yield of 77%, compared to the literature yield of 54%. The structure of **25** was confirmed using ^{1}H-NMR, ^{13}C-NMR and mass spectrometry. The ^{1}H-NMR showed a distinctive multiplet for the 5 protons of the phenyl ring, and also showed 4 distinctive peaks representing the protons of the two pyrrole rings and the bridging proton, as seen previously for dipyrromethanes.

3.2.1.2 Synthesis of disubstituted porphyrins from dipyrromethane precursors

The synthesis of **26** was carried out using a typical Lindsey method. The reported synthesis involves a large dilution factor, using dry solvents and a long reaction time when compared to the Adler-Longo synthesis. Under these conditions either trifluoroacetic acid (TFA) or trichloroacetic acid (TCA) can be used, as the acid catalyst, with TFA being a stronger acid than TCA due to the inductive effect. For compound **26,** TFA was used as the acid catalyst to give the porphyrin. The crude product was purified using column chromatography to give **26** as a purple solid in less than 1% yield, which is very low compared to standard Lindsey yields of *ca*. 20%. The low yield of product from the reaction is due to the high dilution factors and challenging purification. The product was found to be insoluble in common NMR solvents, but mass spectrometry analysis gave a good match for [M+H] at 579.2027. The insolubility of the compound is thought to be due to aggregation of the molecule in solution.

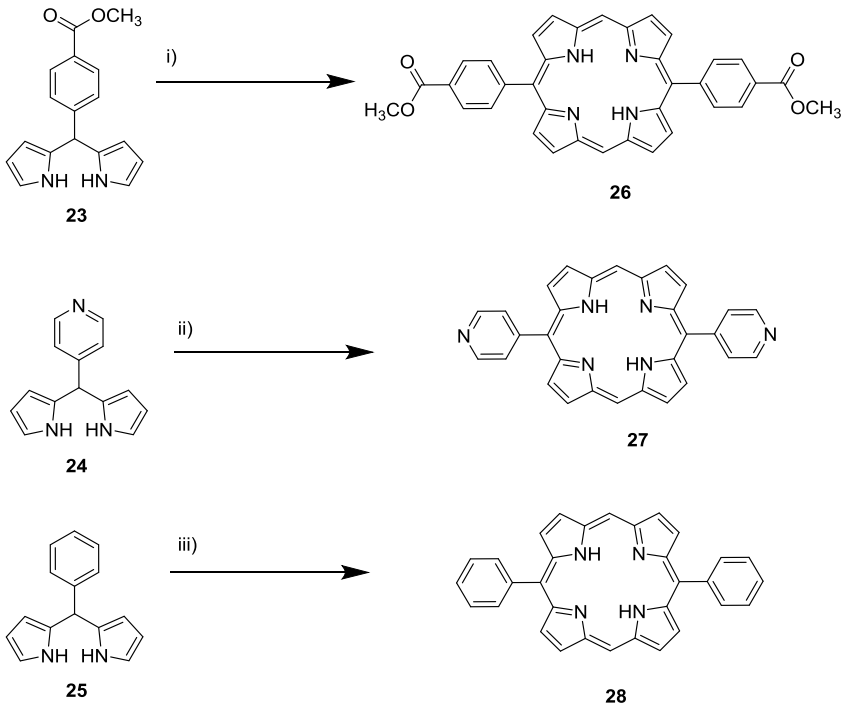

Figure 49 – Synthesis of disubstituted porphyrins from dipyrromethane precursors. Conditions used; i) trimethylorthoformate, dry DCM, TFA, 4 h, pyridine, rt, stir 17 h, ii) trimethylorthoformate, dry DCM, TCA, 4 h, pyridine, rt, stir 17 h, iii) trimethylorthoformate, dry DCM, TFA, 4 h, pyridine, rt, stir 17 h.

The synthesis of **27** was carried out using a similar method, the main difference being that for this synthesis TCA was used as the catalyst. The crude product was purified using column chromatography, which proved challenging as the pyridyl groups adhered to the

silica giving only 5.5 mg of product. The product was analysed by ^{1}H-NMR, ^{13}C-NMR and mass spectrometry, which confirmed the structure of the porphyrin. The proton NMR spectrum showed four distinctive peaks in the downfield region representing the four different proton environments in the molecule. The *meso* protons were shifted furthest downfield and were seen at 10.40 ppm as a singlet, the *beta* protons were seen as a double doublet at 9.08 ppm with *J* values of 4.0 Hz and 8.0 Hz. The protons representing the pyridyl rings were seen as doublets representing the 1,4-disubsituted pattern of the ring.

The synthesis of **28** was carried out using the same method as **27** using TCA as the acid catalyst. The purification of **28** was not as challenging as **27** because the substituent was a phenyl group which does not adhere to silica as much as the pyridyl substituent of **27**, and thus gave **28** in a 10% yield, comparable to standard literature yields, but still would need optimising to produce enough to be used in further synthesis.

The structure of **28** was confirmed using ^{1}H-NMR, ^{13}C-NMR and mass spectrometry. The proton NMR spectrum showed five distinctive environments in the downfield region. The *beta* protons were split into two doublets representing four protons each, and the phenyl substituents were split into two peaks with four and six protons respectively. The *meso* protons were seen furthest downfield at 10.32 ppm which could be due to the lack of shielding from the beta protons causing them to be shifted downfield.

Although the syntheses of **26**-**28** were successful from the dipyrromethane precursors, the main problem in all cases was the subsequent porphyrin condensation reactions, with the high dilution factors preventing synthesis of porphyrins on an appropriate scale. An alternative methodology to using the dipyrromethane precursors is the Adler-Longo method, with the mixed aldehyde condensation reactions conventionally giving lower yields, but also using significantly lower dilution factors compared to the Lindsey method. The lower dilution factors would mean that more product is formed on a smaller scale synthesis.

3.2.1.3 Synthesis of porphyrins *via* the Adler-Longo method for potential use in conjugation to viologen molecules

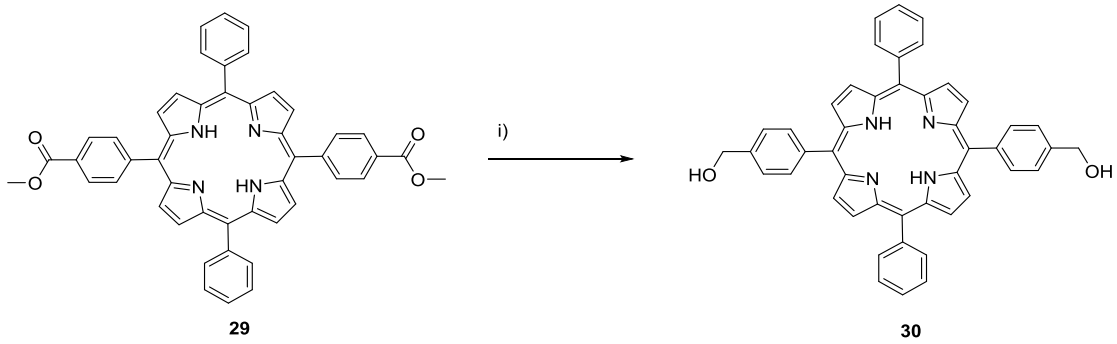

Figure 50 – Hydrolysis of 29 to form 30. Conditions used; i) dry THF, $LiAlH_4$, 0 °C-rt stir 5 h.

The synthesis of **29** was carried out using the Adler-Longo method, using the two aldehydes in a 1:1 ratio in order to give the highest amount of A_2B_2 product. The mixture was purified successfully using column chromatography to separate the six possible porphyrin products to give the desired product in a 0.58% yield, a good yield for this type of condensation. The structure was confirmed using ^{1}H-NMR, ^{13}C-NMR and mass spectrometry. The proton NMR showed a singlet in the downfield region at 4.02 ppm representing the six protons of the methyl ester, and also showed five distinctive peaks in the aromatic region, which showed the different environments of the porphyrin ring system and the phenyl substituents. The aromatic region showed a distinctive rooftop pattern representing the 1,4-disubstituted ring system and showed the *beta* protons as a pair of doublets.

Following successful synthesis of **29** the ester was converted into the alcohol (**30**) using a simple reduction reaction with $LiAlH_4$. The reaction was carried out under anhydrous conditions to prevent the $LiAlH_4$ being hydrolysed by water to $LiAlO_2$ and producing hydrogen gas. The work up was successful and the product was purified using column chromatography, but the yield was not high, giving the product in a 20% yield compared to a literature yield of 90%.[180] Analysis of the product using ^{1}H-NMR, ^{13}C-NMR and mass spectrometry confirmed the structure of the compound. The alkyl region contained a peak at 5.02 ppm representing the C*H*$_2$–OH peaks, and in the aromatic region there was three peaks, representing the phenyl ring system, and the *beta* protons and the phenyl ring substituted at the *para* position.

Following the reduction of the porphyrin to compound **30,** a number of reactions were attempted in order to produce a porphyrin that could be polymerised with the bipyridine molecule, as outlined in **Scheme 17**.

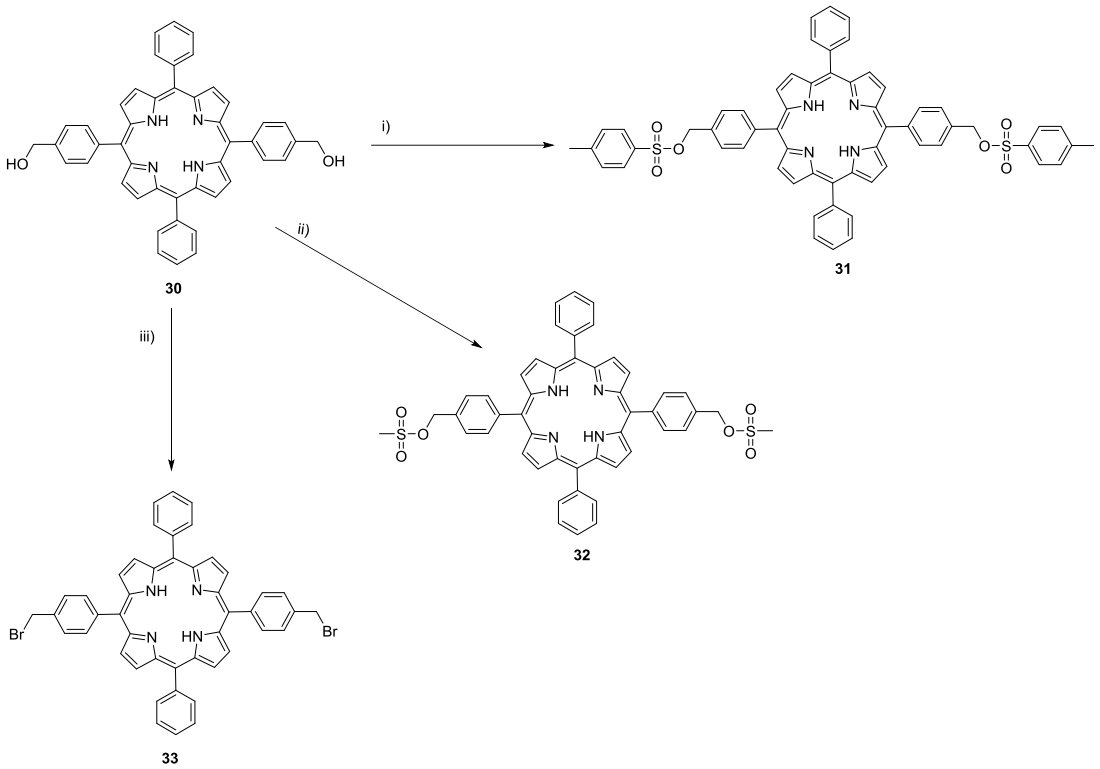

Scheme 17 – Formation of bromide, tosylate and mesylate leaving groups, i) CH_2Cl_2, triethylamine, *p*-toluenesulphonyl chloride, 0 °C-rt, N_2, 12 h, ii) methanesulphonyl chloride, 0°C-rt, N_2, 12 h, iii) PBr_3, Dry CH_2Cl_2 N_2, rt 12 h.

The synthesis of **31** was carried out using standard conditions to convert an alcohol to a tosylate group, a simple base-catalysed S_N2 reaction. Compound **30** was dissolved in dichloromethane with triethylamine, then *p*-toluenesulphonyl chloride was added. Following a simple aqueous work-up, it was found that the reaction did not reach completion, this was thought to be due to steric hindrance between the porphyrin and the two tosylate groups.

A less bulky alternative to the tosylate group is the mesylate group. However, their poorer stability means that rapid isolation is necessary. The formation of the mesylate group was carried out by cooling the mixture of the starting material and triethylamine to 0 °C, followed by the drop-wise addition of methanesulphonyl chloride. Following this a TLC of the mixture showed that product had been formed, but column chromatography proved challenging and the product was not isolated, with significant decomposition of the mesylate group on the silica observed.

An alternative to this was the addition of bromine groups, using phosphorous tribromide as the brominating agent. Following a simple aqueous extraction, the product was obtained in a good yield of 44% compared to a literature yield of 41%.[181] The product was confirmed using ^{1}H-NMR, ^{13}C-NMR and mass spectrometry. The proton NMR spectrum was slightly different to that of **30**, whereby the doublet seen for the CH_2 is now seen as a singlet. Mass spectrometry confirmed the presence of the bromine and gave an [M+H] of 799.1053 with the distinctive isotope pattern for two bromines present.

Due to the low yields obtained from the bromination reaction, and the challenging tosylation and mesylation reactions it was decided that instead of utilising the porphyrin directly, the porphyrin would firstly be attached to the spacer group and then polymerised with 4,4'-bipyridine.

3.2.1.4 Pyridyl porphyrins for spacer group attachment

The first porphyrin that was investigated was an A_2B_2 porphyrin with two pyridyl substituents and two phenyl substituents. The goal was to use the porphyrins for conjugation *via* an S_N2 reaction, to the spacer group, followed by polymerisation with 4,4-bipyridine to give the porphyrin and viologen molecule in the backbone of the polymer.

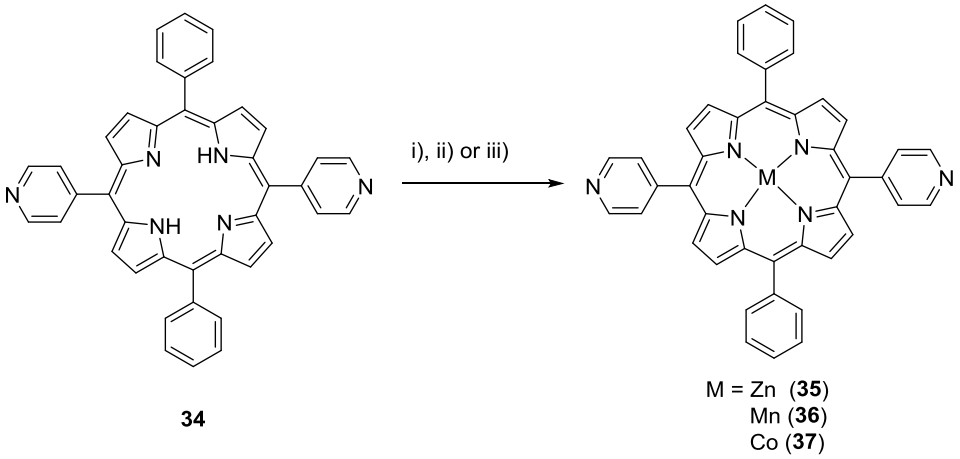

34

Figure 51 – Synthesis of 34-37 for conjugation with spacer groups for polymerisation. Conditions used: i) zinc acetate, CH_2Cl_2, rt 1 h, ii) manganese acetate, DMF, 165 °C MW, 30 mins iii) cobalt acetate, DMF, 165 °C MW, 30 mins.

The synthesis of **34** was carried out using a typical Lindsey method, utilising the pyridyl substituted dipyrromethane and benzaldehyde in dilute conditions to give the product in an excellent yield of 47% following purification of the product by column chromatography. The structure of **34** was confirmed using ^{1}H-NMR, ^{13}C-NMR and mass

spectrometry as well as UV-Vis spectrometry. The proton NMR showed five distinctive peaks in the aromatic region representing the five different environments in the molecule. A pair of doublets was seen, representing the 1,4-disubstituted pyridyl ring at 8.17 ppm and 9.02 ppm with *J* values of 8.0 Hz. The signal representing the *beta* protons was seen as a multiplet.

Following the successful synthesis of **34** on a large scale, metals were inserted into the central cavity, in order to study the effect that the metal has on the electron transfer properties of the system.[182] The system aims to mimic that of artificial photosynthesis, with the porphyrin as the electron donor and the viologen molecule as the electron acceptor.[183]

Zinc was inserted using zinc acetate and in a mixture of dichloromethane and methanol, producing **35** in a yield of 96%. The UV-Vis spectra of **35** showed the presence of only two Q-bands compared to four seen for the parent compound (**34**). The UV-Vis spectra showed the Soret band at 420 nm and the two Q-bands were seen at 559 nm and 606 nm, confirming successful metallation.

The insertion of manganese into the porphyrin proved more challenging than the insertion of zinc, but it was still achieved in a yield of 95%. Microwave heating was used to insert manganese into the porphyrin, with heating at 165 °C for 30 mins giving the manganese porphyrin, which was confirmed using UV-Vis and mass spectrometry. The UV-Vis spectra showed the presence of a shifted Soret band at 471 nm and two Q–bands at 593 and 622 nm.

Compound **37** was synthesised with the addition of cobalt using the same method as **36**, the cobalt was inserted in a 98% yield. The compound was analysed using UV-Vis spectrometry and showed the presence of the Soret band at 409 nm and two Q-bands at 530 and 662 nm.

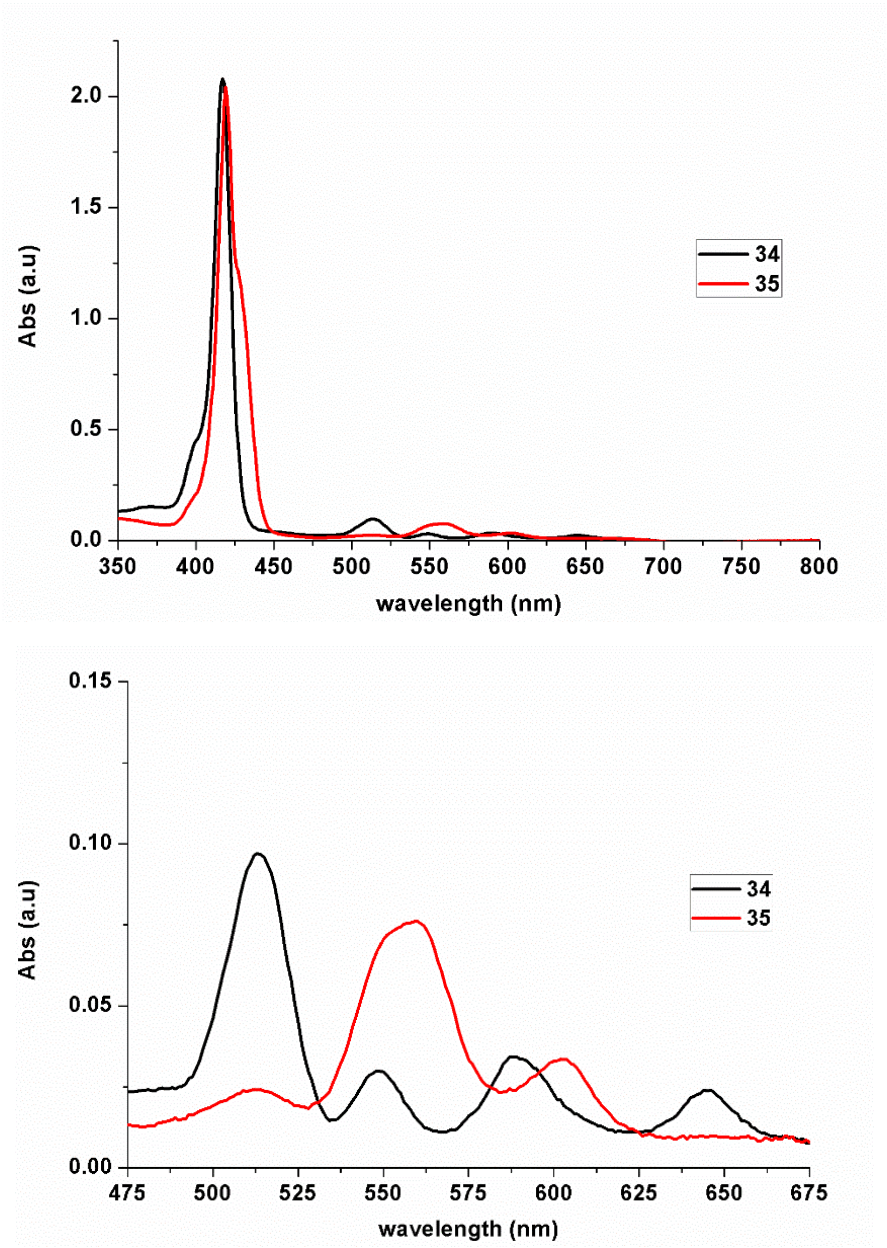

Figure 52 – UV-Vis spectrum comparing compound 34 with 35, comparison of non-metallated porphyrin (34) with a metallated porphyrin (35), showing the change in number of Q-bands.

3.2.1.5 Subsequent reactions utilising the pyridyl ring on the porphyrin

Following successful synthesis of **34**, reactions were attempted to produce a porphyrin with the appropriate spacer group that could be used for further polymerisation with 4,4'-bipyridine.

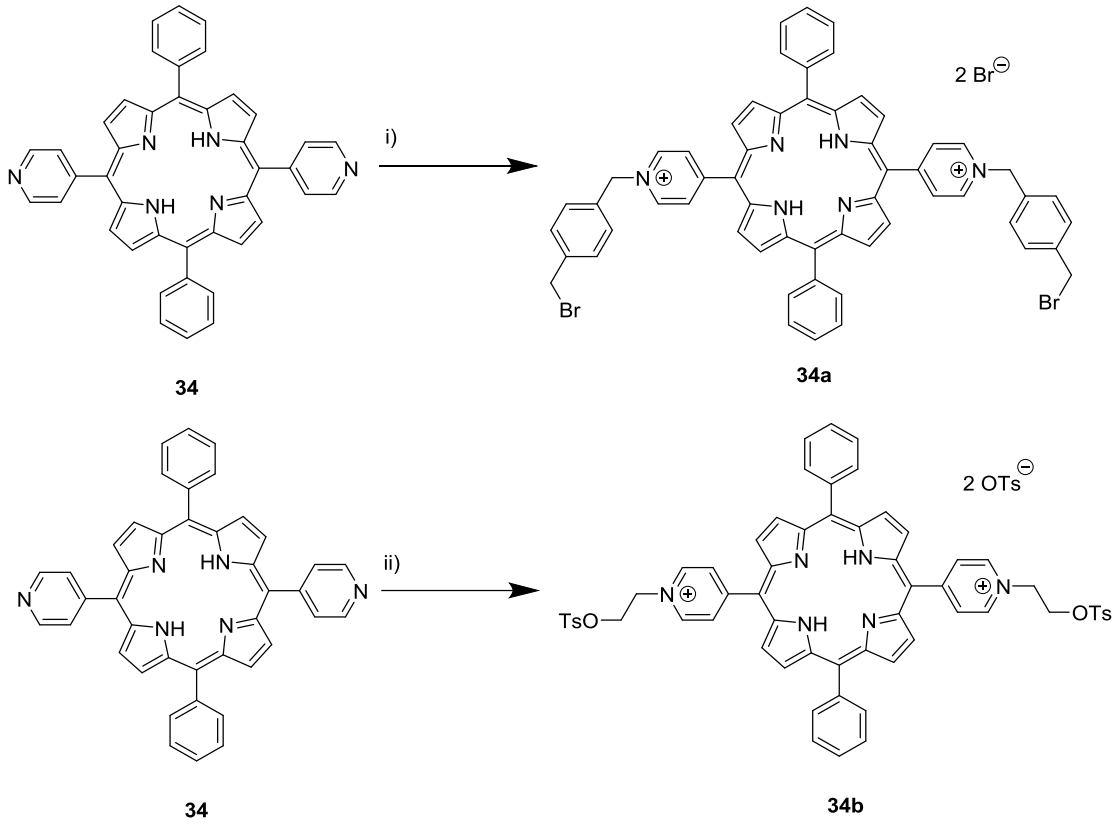

Scheme 18 – Synthesis of porphyrin linked spacer groups. Conditions used: i) 1,4-bis(bromomethyl)benzene, acetonitrile, rt, overnight, ii) ethane-1,2-diyl bis(4-methylbenzenesulfonate), acetonitrile, reflux overnight.

Scheme 18 shows the two reactions that were attempted utilising the nitrogen on the pyridyl ring of the porphyrin. The reactions were not successful: there was no product formation and only starting material was shown when analysing using TLC and NMR. This was attributed to both the modest leaving group ability of both the bromides and the tosylates, as well as the large steric hindrance effect between the porphyrin and the two tosylate groups.

As this method was shown to be unsuccessful, investigations into the coupling of porphyrin and viologens *via* both click and cross coupling reactions were carried out.

3.2.2 Porphyrin viologen hybrids *via* click chemistry

3.2.2.1 Synthesis of clickable porphyrins

Click chemistry involves the use of an azide and an alkyne functionality which are joined together to form a 1,2,3-triazole linker.[112,113,116] Click chemistry has been demonstrated as a successful methodology for conjugation of porphyrins to numerous structures, with both azide,[113,184–187,188,189] and alkyne[190] porphyrins synthesised previously in the literature. In this project the azide functionality was placed primarily on the porphyrin

molecule due to ease of synthesis and purification of both the porphyrin and the alkyne-functionalised viologen molecule. The azide was not placed on the viologen molecule as a viologen containing a short chain azide could be explosive.

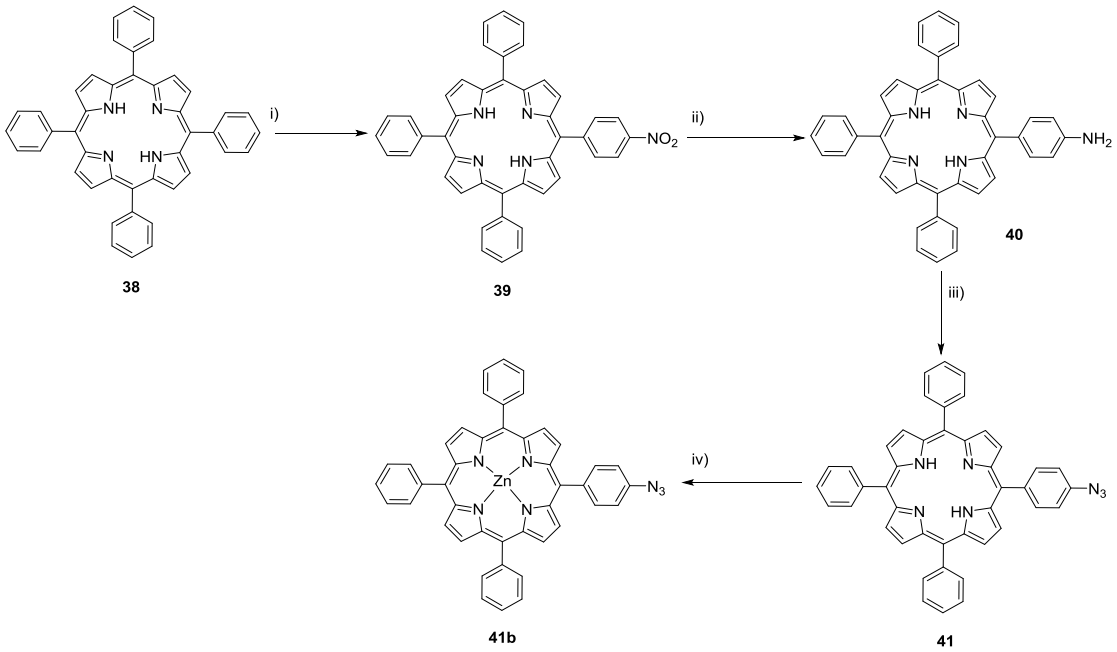

Scheme 19 – Synthesis of azide functionalised porphyrin for click chemistry. Conditions used; i) TFA, $NaNO_3$ 0 °C – rt 8 mins ii) tin(II)chloride, HCl 60 °C 1 h, iii) TFA $NaNO_2$, NaN_3, 0 °C- rt 15 mins then rt 1 h iv) zinc acetate, rt 12 h.

Synthesis of 5,10,15,20-tetraphenyl porphyrin (**38**) was carried out using the Adler-Longo synthesis with benzaldehyde and pyrrole in refluxing propionic acid. The yield of this reaction is high for a porphyrin synthesis, with the product achieved on a gram scale in a 25% yield. Confirmation of the formation of tetraphenylporphyrin (**38**) was carried out using NMR spectroscopy, whereby the distinctive pattern for a tetrasubstituted porphyrin can be seen. In this case, the ^{1}H-NMR spectrum showed an aromatic region with a multiplet at 7.71-7.82 ppm with an integration of 12H representing the *meta* and *para* phenyl ring substituents, and a multiplet at 8.18-8.26 ppm representing the *beta* protons and a peak at 8.85 ppm representing the *ortho* phenyl substituents with an integration of 8H.

Formation of 5-(4-nitrophenyl)-10,15,20-tri-phenyl porphyrin (**39**) was carried out using TFA and $NaNO_3$. Optimisation of this method was carried out to produce the highest yield of the mono-substituted nitro phenyl porphyrin possible, with variation of the

reaction time and reagent excess to produce an optimised yield of 80% compared to a literature yield of 75%.[191] The structure of **39** was confirmed using ^{1}H-NMR, ^{13}C-NMR and mass spectrometry. The ^{1}H-NMR shows a pair of doublets representing the 1,4-disubstitution of the phenyl ring at 8.39 ppm and 8.63 ppm with *J* values of 8.0 Hz. The proton NMR spectrum also shows a distinctive long range multiplet for the *beta* protons at 8.71-8.92 ppm, which is not expected as a double doublet is expected according to the symmetry of the molecule.

The reduction of the nitro-substituted porphyrin to the corresponding amine (**40**) was carried out in HCl using tin (II) chloride, with the product purified using an aqueous work-up only.[188] The reaction followed a literature procedure and gave the product in a yield of 98%, compared to the literature yield of 99%. The structure of **40** was confirmed using ^{1}H-NMR, ^{13}C-NMR and mass spectrometry. The ^{1}H-NMR shows an upfield shift of the protons representing the 1,4-disubstituted phenyl ring. The doublets appear at 7.06 ppm and 7.99 ppm, which is an upfield shift of 1.33 pm and 0.64 ppm compared to **39**.

Conversion of the amine to the azide (**41**) was carried out *via* diazotization, utilising sodium nitrite and sodium azide at 0 °C. The reaction was carried out at 0 °C due to the instability of the diazo salt. The product was purified using a simple chromatographic separation to give the pure product in a good yield of 92%. The structure of **41** was confirmed using ^{1}H-NMR, ^{13}C-NMR and mass spectrometry. The ^{1}H-NMR showed a doublet representing the 1,4-disubstituted phenyl ring at 7.42 ppm and another doublet representing 2H overlapped with the other *ortho* phenyl ring peaks at 8.17-8.21 ppm, which shows a downfield shift compared to compound **40**.

In order to utilise the synthesised azido porphyrin for click reactions, prior metallation is required in order to prevent metallation with the copper catalyst during reaction. To prevent insertion of copper, zinc was coordinated in the central cavity of the porphyrin, with zinc selected due to its ease of insertion and removal. This was achieved using zinc acetate in dichloromethane at room temperature overnight to give compound **41b** in a yield of 77%. The yield obtained was lower than usual metallation reactions which are nearer 100%, and could be due to poor solubility of the product in the methanol/ dichloromethane mixture, as the product is only sparingly soluble in methanol. Complete metallation was confirmed by UV-Vis spectroscopy, compound **41b** shows a Soret band at 422 nm with an extinction coefficient of 396,572 $M^{-1}cm^{-1}$ and two less intense Q-bands at 560 and 604 nm (**Figure 53**).

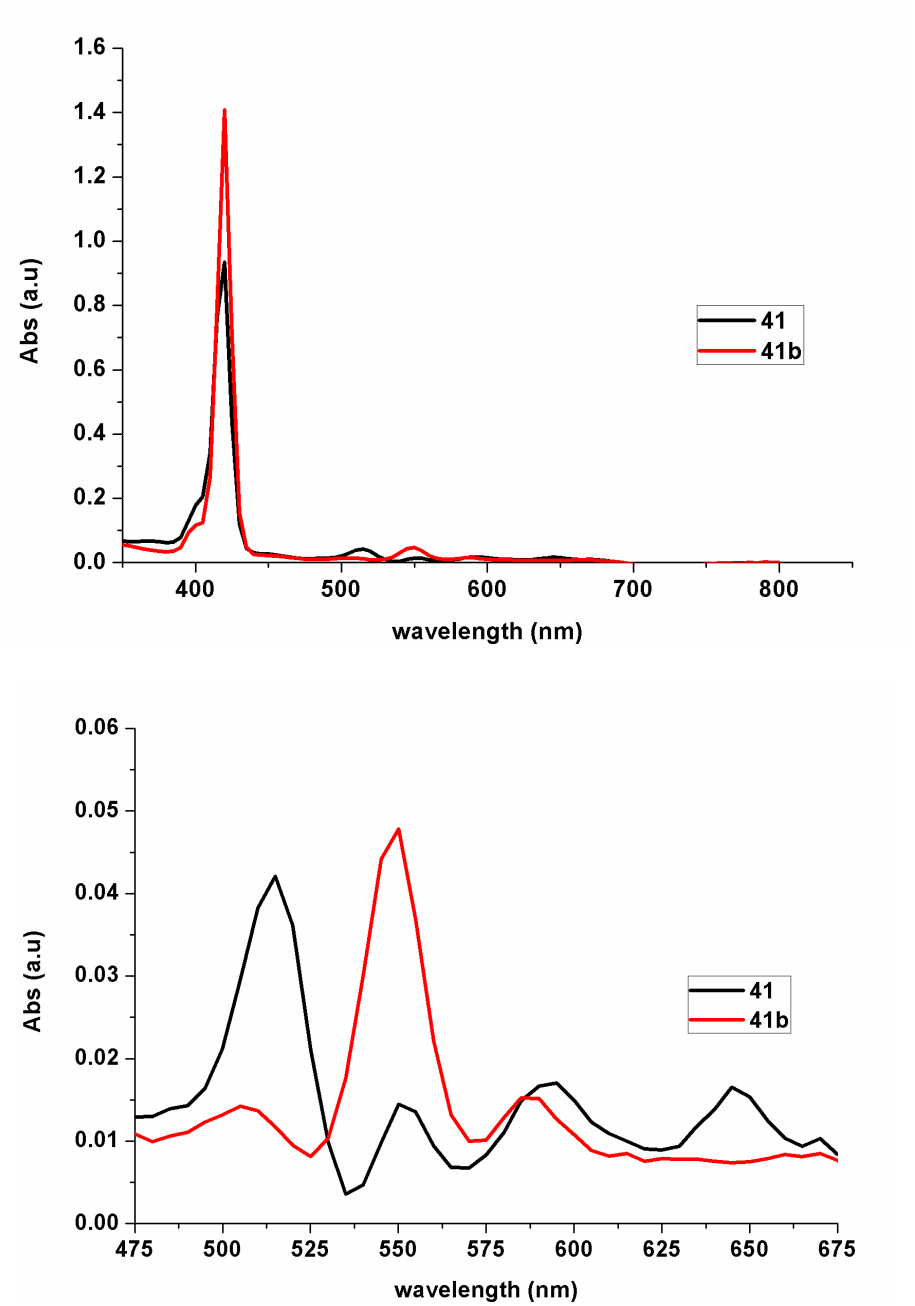

Figure 53 – UV-Vis overlay of compound 41 and compound 41b showing change in UV-Vis spectrum following metallation of the porphyrin.

The structure of **42** was also confirmed using mass spectrometry with an $[M+H]^+$ at 718.1692.

3.2.2.1.1 Subsequent click reactions utilising the azide functionalised porphyrin

Generally, the click reaction utilises a mixture of solvents, most commonly THF/water and a copper (II) catalyst, which is reduced to copper(I) *in situ*. However copper (I) catalysts such as CuI are also used instead due to a better solubility in organic solvents. In this particular project, the click reaction was carried out on two compounds that are

not water soluble, and this makes solvent choices more challenging. Optimisation of the click reaction was carried out using a large range of different solvents and solvent mixtures, as shown in **Table 3**. The most promising solvent mixture for the click reaction of the azide-functionalised tetraphenylporphyrin (**41b**) and the alkyne-functionalised viologen (**19**) was found to be a mixture of *t*-butanol and water in a ratio of 9:1.

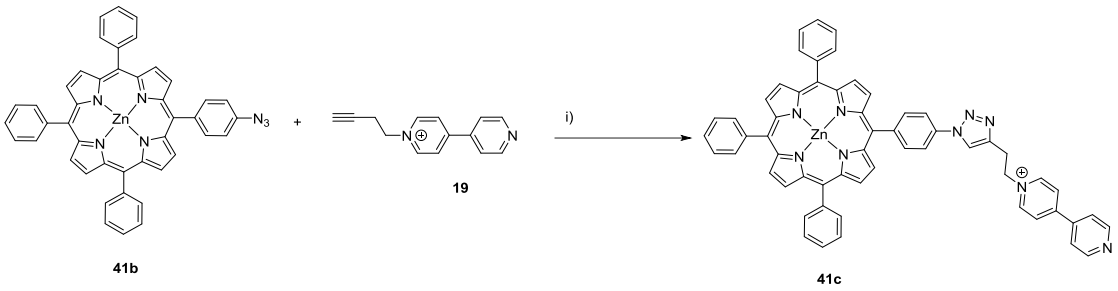

Figure 54 – Synthesis of porphyrin-viologen hybrid using the click reaction. Conditions used; i) copper sulphate, sodium ascorbate, *t*-butanol/water (9:1) 100 °C microwave 6 h.

Reaction number	Amount of porphyrin used	Amount of alkyne used	Solvent used	Amount of catalyst	Temperature	Time
1	10 mg	10 mg	THF/water (1:1)	Copper sulphate/sodium ascorbate 10 mg	80 °C	48 h on bench
2	10 mg	10 mg	THF/water (1:1)	Copper sulphate/sodium ascorbate 10 mg	50 °C	1 h in microwave followed by 1 h at 80°C in microwave
3	10 mg	10 mg	DMSO	Copper acetate 10 mg	RT, then heat to 80 °C for 48 h.	24 h
4	10 mg	10 mg	DMF	Copper iodide 15 mg	80 °C microwave	2 h.
5	10 mg	10 mg	*t*-butanol/water (9:1)	Copper sulphate/sodium ascorbate 10 mg	80 °C microwave	2 h
6	10 mg	10 mg	*t*-butanol/water (9:1)	Copper sulphate/sodium ascorbate 10 mg	80 °C microwave	4 h
7	10 mg	10 mg	*t*-butanol/water (9:1)	Copper sulphate/sodium ascorbate 10 mg	80 °C microwave	6 h
8	10 mg	10 mg	*t*-butanol/water (9:1)	Copper sulphate/sodium ascorbate 10 mg	90 °C microwave	2 h
9	10 mg	10 mg	*t*-butanol/water (9:1)	Copper sulphate/sodium ascorbate 10 mg	100 °C microwave	2 h

Table 3 – Different reagents used in attempting click reaction between porphyrin and viologen.

The main issue with using an azide porphyrin in the click reaction is that the azide starts to degrade at approximately 90 °C. This temperature of degradation was observed to be 85 °C when using microwave heating, with this degradation observed on TLC. However ideal reaction conditions were found to be temperatures above this. This is a problem as significant contamination of product with degraded azide porphyrin can result. A different solvent system that requires less heating would be more suitable for this reaction, as it would mean that less degradation of the azide porphyrin would take place.

An alternative to a different solvent system would be to minimise the steric hindrance between the porphyrin and the viologen. This problem can be overcome by the addition of a PEG chain spacer between the porphyrin and the viologen.

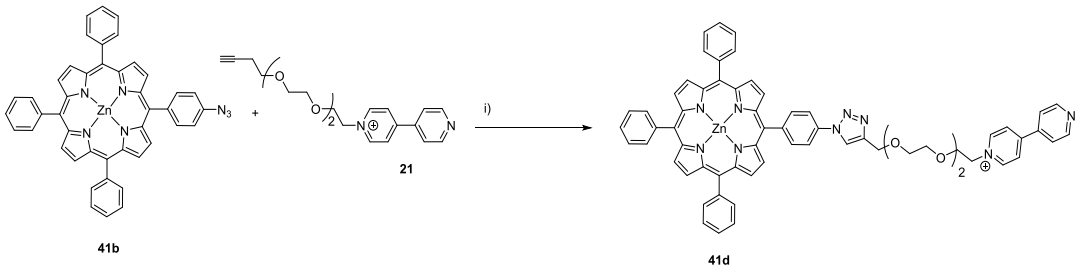

Scheme 20 – Synthesis of porphyrin viologen conjugate *via* click chemistry with a PEG spacer.

Unfortunately following multiple attempts the click reaction utilising the porphyrin and the alkyne functionalised PEG chain was not successful, as the high temperature conditions required meant that degradation products were being produced and isolation of the product was challenging.

In conclusion, the click reaction strategy showed some promise, but due to the low degradation temperature of the azide on the porphyrin and the high temperature required for the reaction this method was not viable, so attempts were made using different strategies.

3.2.3 Alternative strategy using palladium cross coupling porphyrins

A possible alternative to the click reaction is the use of reactions such as the Suzuki or Sonagashira coupling reactions. While both use palladium catalysts and a halogen precursor, the Suzuki reaction utilises a boronic acid moiety to form an aryl-aryl bond, while the Sonagashira reaction uses an alkyne moiety to form an alkyne bond.[192–194]

3.2.3.1 Synthesis of bromo-substituted porphyrins

The aim of this synthesis was to produce a library of bromo-substituted porphyrins for use in Suzuki coupling reactions, with the halogenated porphyrins selected instead of boronic acid substituted porphyrins, due to their comparative ease of synthesis (**Scheme 21**).

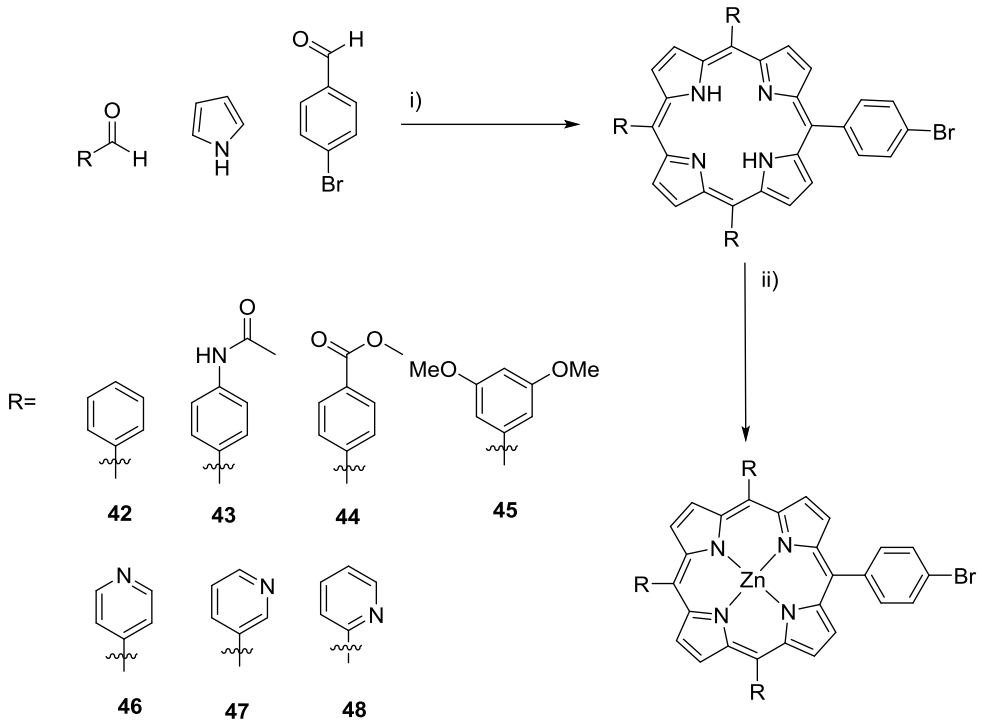

Scheme 21 – Synthesis of metalloporphyrins bearing different substituents. Conditions used: i) propionic acid, 170 °C 3 h ii) zinc acetate, DMF, 80 °C 12 h.

The synthesis of **42** was carried out using standard Alder-Longo conditions with refluxing propionic acid and the drop-wise addition of pyrrole. While the synthesis of **42** was carried out successfully, the Rf values of the simple tetraphenyl porphyrin and bromo substituted variants were virtually identical, making separation using column chromatography impossible.

As a result, porphyrins bearing alternative phenyl ring substitutions which allowed for facile separation was attempted. Compound **43** bearing acetamido functional groups was therefore synthesised using the Adler-Longo method, and the differences in polarity allowed good separation of the six porphyrin products using column chromatography to give the desired product in an excellent yield of nearly 6%, which is good for an A_3B type porphyrin. The structure of **43** was confirmed using ^{1}H-NMR spectroscopy, ^{13}C-NMR spectroscopy and mass spectrometry. The ^{1}H-NMR spectrum shows a singlet in the alkyl region at 2.24 ppm representing the 9H for the three CH_3 groups of the acetamido groups.

The aryl region shows a pair of doublets representing the 1,4-disubstituted pattern for the phenyl ring with the acetamido substituent. It also shows two peaks for the *ortho* and *meta* phenyl ring and the *beta* protons.

The synthesis of **44** bearing ester functionalities was also attempted was carried out using Adler-Longo conditions to give the crude product. However, again purification of **44** using column chromatography proved challenging due to the near identical Rf values, and so the ideal product was not isolated.

A possible alternative utilising the phenyl ring is the synthesis of a 3,5-dimethoxy group which can then be converted into the corresponding 3,5-dihydroxyl analogue, thus aiding water-solubilisation. The synthesis of **45** was carried out using normal Adler-Longo conditions followed by purification *via* column chromatography, which while challenging allowed the product to be isolated in a reasonable yield of 3%. The lower yield can be attributed to the challenging purification using column chromatography, as the six different porphyrin products had near identical Rf values. Confirmation of the structure of **45** was carried out using ^{1}H-NMR, ^{13}C-NMR and mass spectrometry. The ^{1}H-NMR spectrum contains a peak in the alkyl region at 3.96 ppm representing the 6 x CH_3 groups. The proton NMR spectrum also shows a different splitting pattern to the normal 1,4-disubtiuted pattern due to the 3,5 substituents on the phenyl ring. The aryl region shows a splitting of 6H and 3H for the *ortho* and *para* substituents respectively.

An alternative to the phenyl substituents are pyridyl substituents; as these groups are known to be more polar than phenyl substituents, they offer improved opportunities for separation by column chromatography, as they differed from the other substituents in Rf values.

Synthesis of **46**, **47** and **48** was carried out using normal Adler-Longo conditions. The purification of **46** was carried out using column chromatography, and separation of the six porphyrins was achieved. Confirmation of the structure was carried out using ^{1}H-NMR ^{13}C-NMR spectroscopy and mass spectrometry. The ^{1}H-NMR spectrum shows a distinctive pattern for the 1,4-disubtituted pattern of the pyridyl ring, with two doublets at 7.92 ppm and 8.07 ppm with *J* values of 8.0 Hz. The mass spectrometry data showed an $[M+H]^+$ peak at 696.1506. The synthesis of **47** was carried out using the Alder-Longo method, and following purification the product was isolated. The structure of **47** was confirmed using ^{1}H-NMR ^{13}C-NMR spectroscopy and mass spectrometry. The ^{1}H-NMR spectrum shows the pattern for the 1,4-disubstitution of the phenyl ring with the

phenylbromo substituents at 8.08 ppm and 8.53 ppm as a pair of doublets representing the roof top effect. The ^{1}H-NMR spectrum also shows a unique splitting pattern for the protons of the pyridyl rings of the porphyrin, splitting into three signals of 3H, as expected for this particular substitution pattern.

The synthesis of **48** was carried out using the Adler-Longo method, but column chromatography proved challenging and the desired product was not isolated.

Following the synthesis of a library of bromo substituted porphyrins, their subsequent zinc porphyrins were synthesised as shown in **Figure 55**, as metalloporphyrins have extremely rich electron transfer properties.[195] Examples using zinc porphyrins have been reported,[196] with low temperatures being preferable for electron transfer.

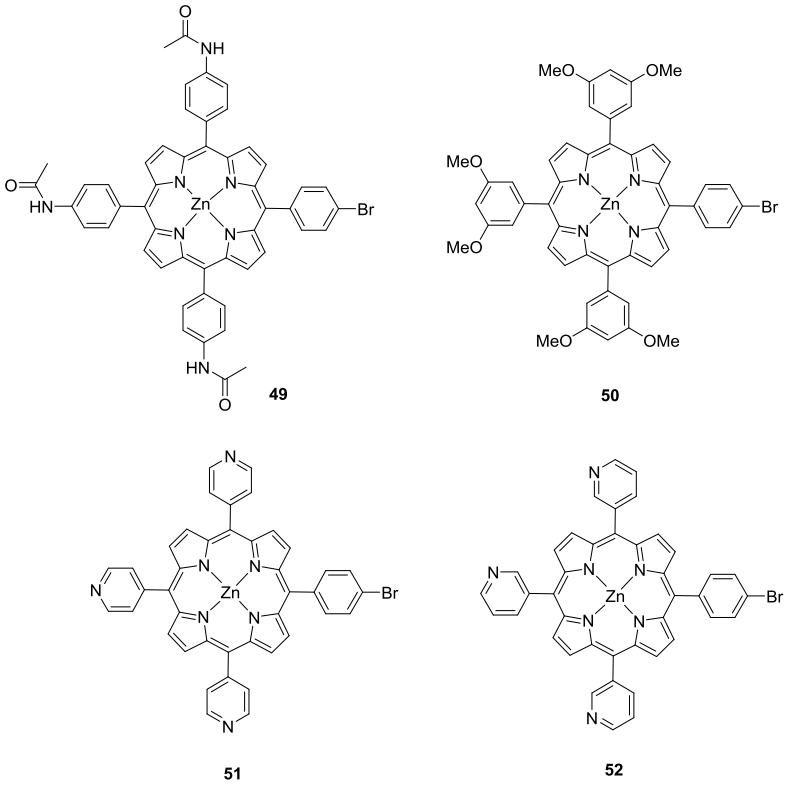

Figure 55 – Structure of zinc bromo substituted porphyrins.

3.2.3.2 Synthesis of zinc bromo-substituted porphyrins

Metal insertion into compounds **43**, **45**, **46** and **47** was carried out using zinc acetate to give the metallated products as shown in **Figure 55**.

Compound **49** was synthesised by inserting zinc into the parent compound (**43**). This was carried out by using zinc acetate in DMF, and heated to 40 °C overnight to give the product in a low yield of 56%. The yield is much lower than those reported in the literature for zinc metallation of porphyrin, which are nearer 100%. The identity of the product

confirmed using UV-Vis spectroscopy and mass spectrometry. The UV-Vis spectrum shows a distinctive change compared to the parent compound, as the four Q-bands collapse into two Q-bands due to an increase in the symmetry of the molecule following metal insertion. The Soret band is seen at 430 nm and two less intense Q-bands are seen at 562 and 602 nm. The mass spectrometry shows an $[M+H]^+$ peak at 926.1427 confirming the presence of the zinc and the bromine with distinctive patterns.

Compound **50** was synthesised using a similar method to that of **49**, whereby the porphyrin was dissolved in DMF and the solution was heated to 60 °C overnight. The product was then precipitated through the addition of water over DMF and gave the product in a respectable yield of 84%. Complete metallation of the porphyrin was seen using UV-Vis spectroscopy, where only two Q-bands were seen at 552 nm and 588 nm. Mass spectrometry also confirmed the structure of **50**, with an $[M + H]^+$ peak at 935.1417.

Compound **51** was synthesised from the parent compound **47**. Zinc was inserted into the central cavity using zinc acetate in a mixture of dichloromethane and methanol and heating the solution to 60 °C for 6 hours. Following this, the product was precipitated using water in an excellent yield of 98%. Complete metallation was observed using UV-Vis spectrometry, where only two Q-bands were seen at 558 and 598 nm.

Compound **52** was synthesised from the parent compound **46**. Zinc was inserted into the central cavity using zinc acetate in a mixture of dichloromethane and methanol and heating the solution to 60 °C for 6 hours. Complete metallation of the porphyrin was seen using UV-Vis spectrometry, where only two Q-bands were seen at 564 and 600 nm.

While the pyridyl substituents allow for improved separation using column chromatography they can also act as the fifth axial ligand for the zinc metallation. When the pyridyl substituent acts as the fifth axial ligand for the metal, the solubility of the compound decreases making it less useful for use in coupling reactions. Synthesis of porphyrins with 2-pyridyl, 3-pyridyl and 4-pyridyl substituents was carried out in an attempt to avoid this problem, allowing comparison of which position is best for hindering axial ligation of the metal. The purification of the 2-pyridyl was challenging compared to the 3-pyridyl and the 4-pyridyl: it was more polar and thus it stuck more to the silica making separation virtually impossible. The position of the nitrogen atom on the pyridyl ring plays an important role in the formation of a bond from the nitrogen to the metal inside the porphyrin. It is thought that if the nitrogen is free and readily available to bind to the metal it will wrap round and act as a ligand for the metal.

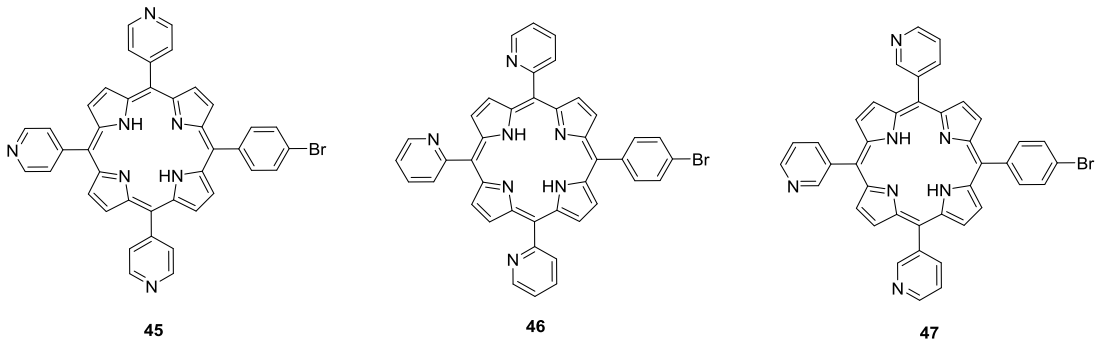

Figure 56 – Comparison of the different positions of the nitrogen on the pyridyl substituents.

An alternative to pyridyl substituents was required that does not form the fifth axial ligand with the metal in the porphyrin complex. Some possible alternatives that have been investigated are; acetamido substituents and methoxy substituents. The porphyrin with the methoxy substituents with the bromo substituents were found to be the most soluble when a metal was inserted into the cavity, which may prove useful when it comes to studying the electron transfer reaction between the porphyrin and the viologen.

3.2.3.2.1 Palladium-catalysed Suzuki coupling reactions between a bromo substituted porphyrin and a boronic acid functionalised viologen

Following the successful synthesis of metallated bromo-substituted porphyrins c **49**-**52**, these compounds were utilised in coupling reactions with boronic acid substituted viologen.

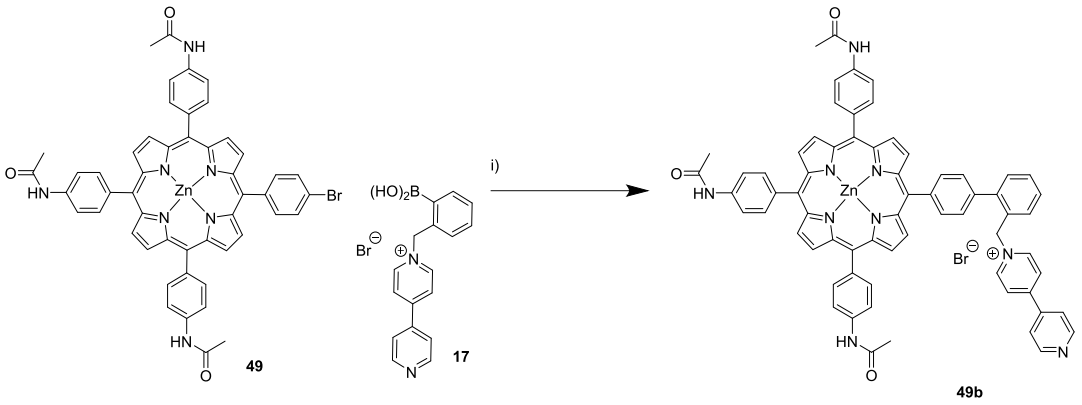

Scheme 22 – Synthesis of porphyrin-viologen hybrid using a Suzuki coupling reaction with 49 and 17. Reaction conditions used: i) DMF, potassium carbonate, Pd $(PPh_3)_4$, MW heating 90 °C 5 h.

Scheme 22 shows the reaction carried out between the porphyrin and boronic acid substituted viologen. The attempted reaction was carried out using different conditions as shown in **Table 4**. However changes in temperature and reaction time, using conventional heating did not drive the reaction forward. The most promising results were seen when the reaction was carried out in the microwave for 6 h with the formation of a new band observed *via* TLC, but when isolated it was found to not be the desired product.

Reaction number	Amount of porphyrin	Amount of viologen	Catalyst	Solvent	Temperature	Time
1	50 mg	25 mg	10 mg	DMF	60 °C	24 h
2	50 mg	25 mg	10 mg	DMF	100 °C	48 h
3	50 mg	50 mg	20 mg	DMF	90 °C	24 h
4	20 mg	20 mg	10 mg	DMF	100 °C	4 h MW
5	10 mg	10 mg	5 mg	DMF	100 °C	6 h MW

Table 4 – Suzuki coupling reactions attempted using porphyrin 49 and viologen 17.

Subsequent attempts utilising the analogous *para* substituted boronic acid were also found to be unsuccessful. It was concluded that the main reason for the lack of success of the Suzuki coupling reactions is the steric hindrance between the porphyrin and the viologen due to the sterically bulky boronic acid,[106] as well as the slow rate of reaction of the bromo substituent.

3.2.4 Synthesis of porphyrins with an iodo substituent for use in Sonogashira coupling reactions.

Following the successful synthesis of porphyrins bearing a bromo substituent, the synthesis of porphyrins bearing an iodo substituent were then carried out for comparison. These more reactive modalities allow versatility for coupling reactions, and could be reacted with an alkyne-functionalised viologen in the Sonogashira reaction.

The design of the porphyrins had to include a metal inside the cavity of the porphyrin. There are two main reasons for the insertion of the metal and these are; the metal aids in electron transfer and also to avoid metallation with the metal catalyst, especially when carrying out the click reaction with a copper catalyst.[112,195]

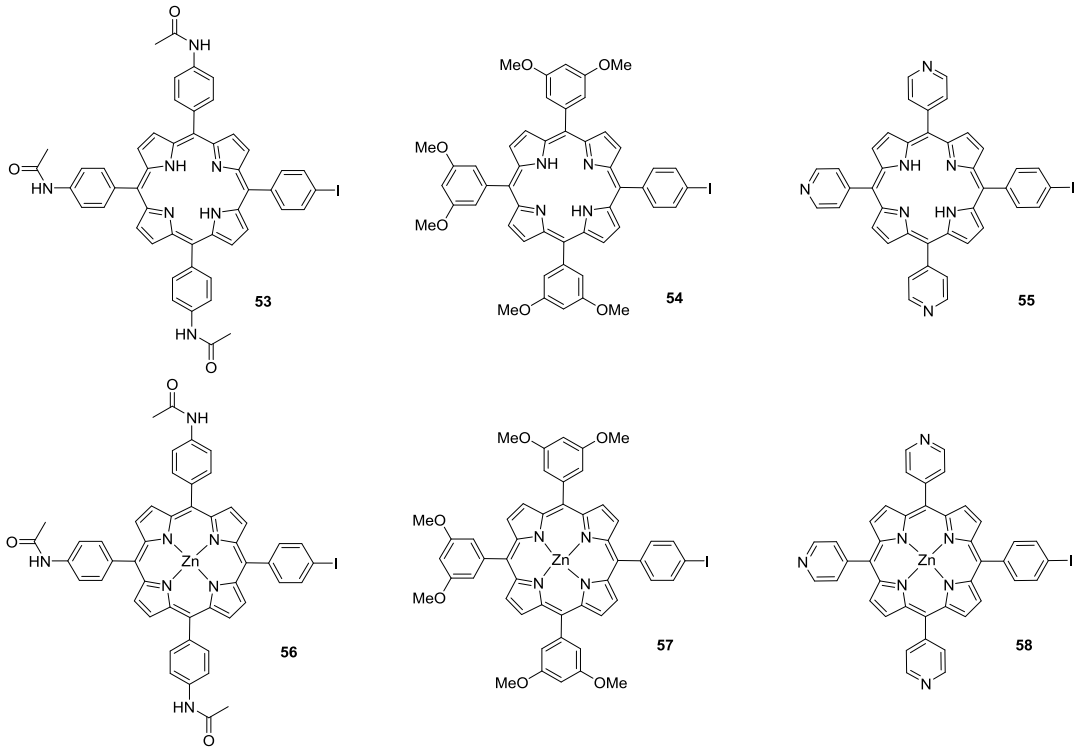

Figure 57 – Structure of iodo substituted porphyrins and their subsequent zinc derivatives.

The synthesis of a library of zinc porphyrins containing an iodo substituent was carried out *via* the Adler-Longo method to form the six different porphyrin products, whereupon the free base porphyrins were then purified using column chromatography.

Compound **53** was successfully synthesised and purified using column chromatography, to give the product as a purple solid in a 3% yield, which is lower than the expected yield of an A_3B porphyrin. The low yield could be accounted for due to challenging purification of the product *via* column chromatography. The structure of **53** was confirmed using ^{1}H-

NMR and ^{13}C-NMR spectroscopy and mass spectrometry. The ^{1}H-NMR spectrum shows a peak in the alkyl region at 3.17 ppm integrating as 9H to represent the 3 x CH_3 for the acetamido functionality. The aryl region contains two pairs of doublets for the two 1,4-disubstituted patterns present in the compound.

Compound **54** was successfully synthesised and purified using column chromatography, to give the product in a good yield of 5%, with the improved yield compared to that of **53** attributed to better separation *via* column chromatography. The structure of **54** was confirmed using ^{1}H-NMR and ^{13}C-NMR spectroscopy and mass spectrometry. The ^{1}H-NMR spectrum shows a peak in the alkyl region at 3.94 ppm integrating as 18H to represent the 6 x CH_3 for the dimethoxy functionality. The aryl region contains a pair of doublets for the two 1,4-disubstituted pattern present in the compound, and a 6H and 3H splitting representing the 3,5-dimethoxy phenyl rings.

Compound **55** was successfully synthesised and purified using column chromatography to give the product in an excellent yield of 7%. The excellent yield was due to good solvent selection for purification using column chromatography, with the solvent system at the beginning at 4% methanol and then steadily increasing to 4.5% and then 5% to give the optimised purification of product. A solvent gradient was essential to obtain the optimum yield of product. The structure of **55** was confirmed using ^{1}H-NMR and ^{13}C-NMR spectroscopy and mass spectrometry. The ^{1}H-NMR spectrum shows five peaks in the aryl region, a pair of doublets for the 1,4-disubstituted pattern present in the compound, two multiplets for the 6H peaks of the *ortho* and *meta* protons for the pyridyl ring substituents and a multiplet for the *beta* protons integrating to 8H.

3.2.4.1.1 Subsequent metallation reactions

Metallation of the corresponding iodo substituted porphyrins was carried out to form compounds **56**-**58** with zinc in the central cavity of the porphyrin.

Compound **56** was synthesised by dissolving the parent compound in DMF with zinc acetate and heating to 60 °C overnight. The product was precipitated through the addition of water to give a purple/blue solid in a yield of 60 %. Interestingly, metallation reactions are usually high yielding but in this case the low yield is thought to be due to the precipitation of the product not being successful, as the product was slightly soluble in methanol. Complete metallation of the porphyrin was seen using UV-Vis spectrometry, with the metallated porphyrin having only two Q-bands, the UV-visible spectrum showed

an intense Soret band at 425 nm and two less intense Q-bands at 560 and 600 nm. Mass spectrometry also confirmed the structure of **56**, with an $[M+H]^+$ peak at 974.1289.

Compound **57** was synthesised using the same method as **56**. The product was obtained in a 94% yield, which is excellent compared to that of **56** and similar to expected metallation reaction yields. Complete metallation was confirmed using UV-Vis spectrometry. The UV-visible spectrum showed the presence of an intense Soret band at 419 nm and a less intense Q-band at 545 nm. Mass spectrometry also confirmed the structure of **57**, with an [M+H] of 983.1279. Compound **58** was synthesised using the same method as **56** and **57**, with the high solubility of this particular product in many different solvents making precipitation extremely challenging to achieve. A number of different solvents were explored including; dichloromethane/methanol, dichloromethane/hexane and methanol/diethylether, with optimised conditions were found using water over methanol to give the product in a 94% yield. Complete metallation was seen using UV-Visible spectrometry with peaks at 425 nm and 559 nm observed. Mass spectrometry also confirmed the structure of **58** with an $[M + H]^+$ peak at 805.0429.

3.2.4.1.1.1 Subsequent iodo porphyrin coupling reactions

Following the successful synthesis of compounds **56**-**58,** subsequent Sonogashira coupling reactions with an alkyne functionalised viologen were carried out (**Scheme 23**).

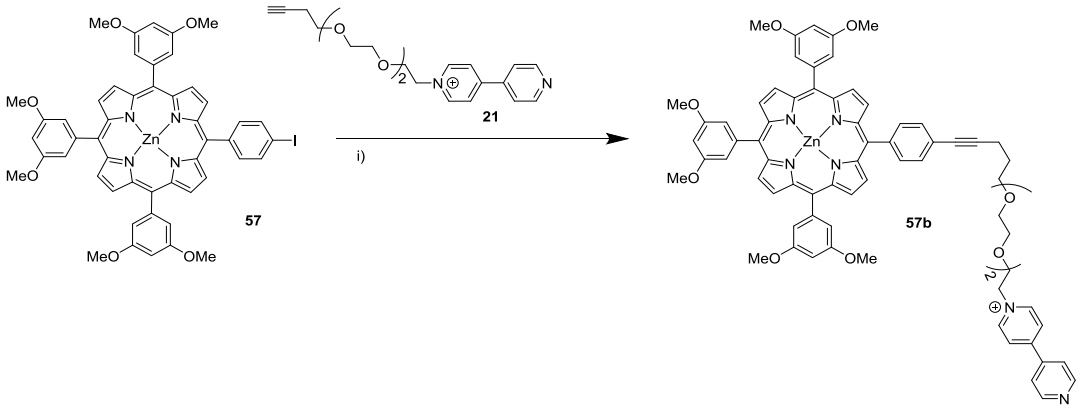

Scheme 23 – Formation of porphyrin-viologen hybrid via Sonogashira reaction. Conditions used; i) CH_2Cl_2, Pd $(PPh_3)_4$, CuI, triethylamine, 40 °C MW 3 h.

Scheme 23 shows the reaction carried out for the formation of porphyrin-viologen hybrid **57b**. Initially the reaction was carried out on the bench but did not show any product formation by TLC. Following lack of success using conventional heating for two days, microwave heating was used (**Table 5**). Microwave heating at different temperatures and for different lengths of time allowed for the formation of a new band after 4 hours, but

when the band was isolated it was found to not be the product, as determined given the lack of NMR signals due to the presence of the PEG chain. This lack of reactivity is attributed to the possibility of the viologen pyridyl ring co-ordinating with the zinc, or a possible interaction between the charge on the pyridyl ring and the oxygens of the methoxy substituents.

Experiment	Porphyrin	Viologen	Catalyst	Solvent used	Temp	Time
1	40 mg	20 mg	$Pd(PPh_3)_4$ – 20 mg CuI – 20 mg	DCM / TEA	40 °C	24 h
2	40 mg	20 mg	$Pd(PPh_3)_4$ – 20 mg CuI – 20 mg	DCM / TEA	40 °C	48 h
3	40 mg	20 mg	$Pd(PPh_3)_4$ – 20 mg CuI – 20 mg	DCM / TEA	40 °C	1 h MW
4	40 mg	20 mg	$Pd(PPh_3)_4$ – 20 mg CuI – 20 mg	DCM / TEA	40 °C	2 h MW
5	40 mg	20 mg	$Pd(PPh_3)_4$ – 20 mg CuI – 20 mg	DCM / TEA	60 °C	3 h MW

Table 5 – Sonogashira reactions attempted using porphyrin and viologen.

3.3 Synthesis of water-soluble porphyrin bearing an acrylamide functionality

Due to the lack of success of previous strategies, an alternative strategy was needed in order to obtain a porphyrin and viologen immobilised in a polymeric network for use in bacterial testing. Initially, the aim was to produce a porphyrin immobilised on a surface to test against bacteria, and then build upon this strategy to incorporate the viologen into this system.

The secondary aim is the formation of a porphyrin-acrylamide conjugate that can be used in the formation of a polyacrylamide hydrogel for testing against bacteria, this is shown in **Figure 58**.

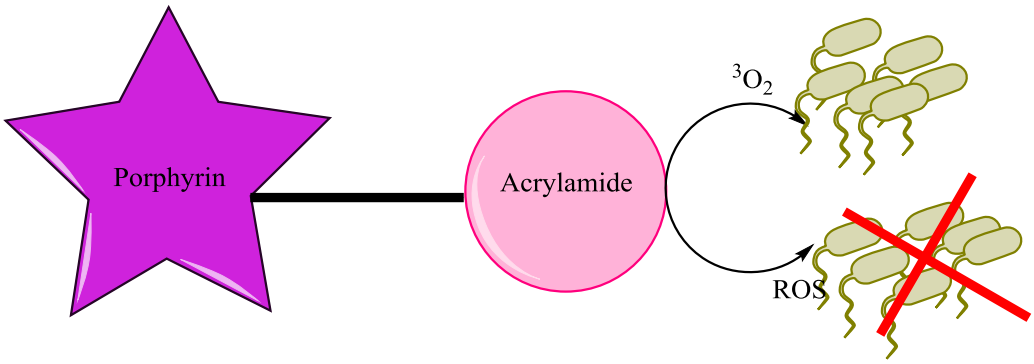

Figure 58 – Schematic showing porphyrin-acrylamide conjugate.

In order to successfully conjugate the porphyrin and the acrylamide for use in polymerisation a water-soluble porphyrin was used to ensure greater applicability for use in biological systems. Water-solubilisation of porphyrin macrocycles can be carried out using numerous methods: a neutral porphyrin containing several hydroxyl groups or PEG chains can be rendered water soluble;[197,198] an anionic porphyrin bearing sulphonate groups can be rendered water soluble;[199] or a cationic porphyrin bearing positive charges from a pyridyl ring or quaternary nitrogen atom can be made water soluble (**Figure 59**).[200]

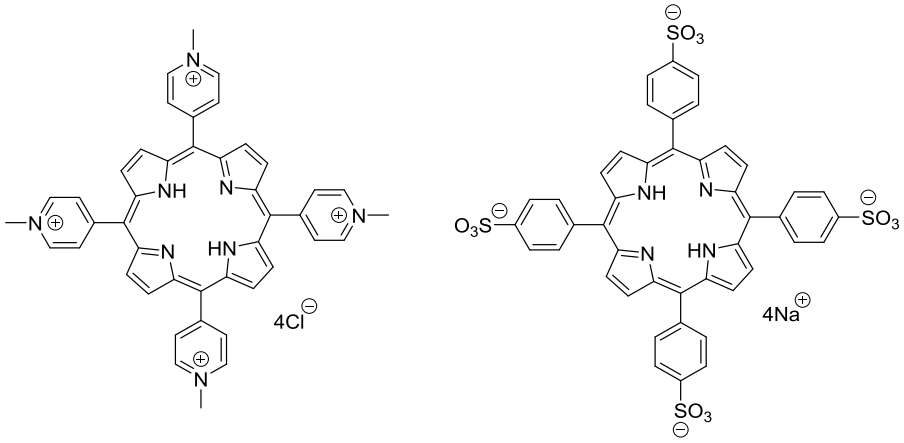

Figure 59 – Typical structure of cationic (left) and anionic (right) porphyrins.

The different counter-ions on charged porphyrins also affect the solubility of the molecule. For example, when carrying out the synthesis of a cationic porphyrin, counter-ion exchange is crucial for water-solubility, with the chloride counter-ions offering improved water solubility in comparison to the iodide counter-ions. The counter-ions can be directly changed from the iodide to the chloride *via* a resin, but this is not always favourable. An alternative technique is required following methylation of pyridyl rings, and this involves a driving force of precipitation. Direct counter-ion exchange from the iodide to the chloride would not be successful *via* precipitation because the rate at which the precipitation occurs would not favour the chloride product. An alternative route, *via*

a hexafluorophopshate counter-ion intermediate, was carried out (**Scheme 24**). Initially the iodide counter-ion is soluble in water, but following the addition of ammoniumhexafluorophosphate the porphyrin precipitates out of solution, as the hexafluorophosphate counter-ions are not water soluble. The exchange of the hexafluorophosphate ions to the chloride ions is carried out by dissolving the porphyrin in acetone and adding tetrabutylammoniumchloride. This causes the porphyrin to precipitate out of the solution because it is no longer soluble in acetone it is soluble in water due to the presence of the chloride counter-ions. The counter-ion exchange method *via* precipitation would not work directly from the iodide to the chloride as the solubility is the same.

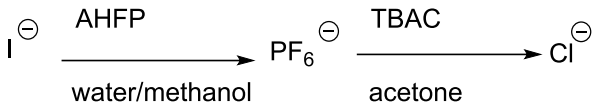

Scheme 24 – Counter-ion exchange schematic showing exchange from iodide counter-ions, as synthesised, to the chloride counter-ions *via* the hexafluorophosphate counter-ions that render water-solubility of the porphyrin.

The porphyrin must contain two key features; firstly, a vinyl handle for it to be used in a free radical polymerisation reaction in the formation of a polyacrylamide hydrogel matrix. The vinyl handle will ensure that the amount of leaching is minimised, due to the incorporation of the porphyrin into the conjugated network within the polymer. The second feature is a water-solubilising moiety. Water-solubility of the porphyrin can be challenging, in the case of this project it will be carried out using the formation of a cationic porphyrin with chloride counter-ions. The cationic porphyrin was chosen for this project because positively charged photosensitisers have been shown to be the most active against Gram-negative bacteria, which are more challenging compared to Gram-positive bacteria to kill.[32,47,49,201]

3.3.1 Synthesis of water-soluble porphyrins for conjugation to acrylamide chain

In order to achieve both desirable functionalities, peptide coupling reactions were carried out between an amine-functionalised PEG chain with a vinyl functionality and a cationic carboxylic acid or NHS ester functionalised porphyrin (**Figure 60**).

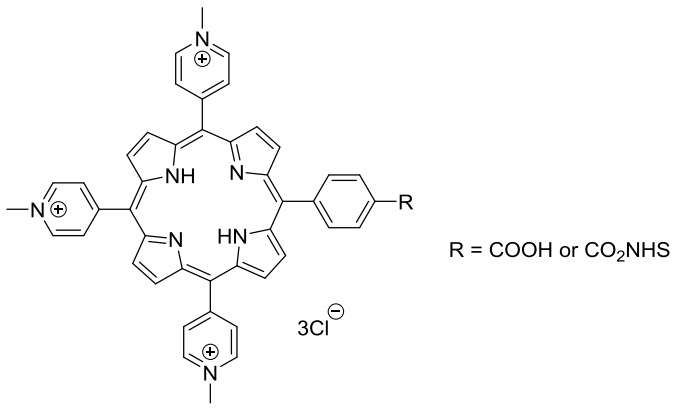

Figure 60 – Proposed structure of porphyrin containing a functional handle suitable for peptide coupling.

Firstly the synthesis of the water-soluble NHS-ester functionalised porphyrin was carried out (**Scheme 25**).

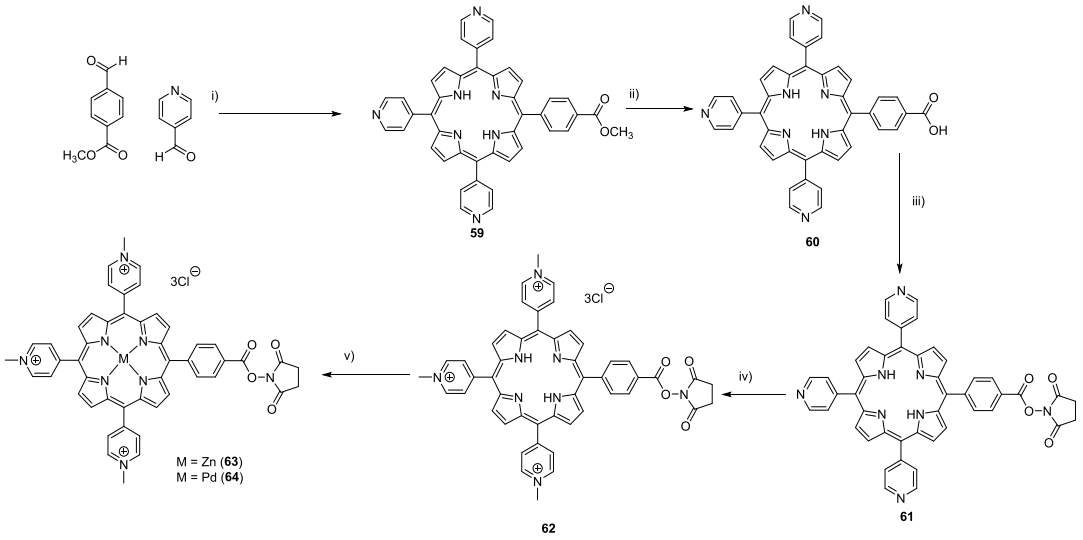

Scheme 25 – Synthesis of water-soluble porphyrin bearing an NHS ester group for conjugation. Reagents and conditions used; i) propionic acid, 170 °C, 1 h ii) KOH, DMF/water, rt 12 h iii) dry pyridine, thionyl chloride, *N*-hydroxysuccinimide, 50 °C 3 h, iv) CH_3I, 40 °C overnight.

Synthesis of the asymmetric A_3B porphyrin containing a methyl ester (**59**) was carried out using normal Adler-Longo method conditions.[202] The product was isolated using column chromatography in an excellent yield of 7 % compared to 5.9% achieved in the literature. Confirmation of the structure was carried out using ^{1}H-NMR and ^{13}C-NMR spectroscopy and mass spectrometry. The ^{1}H-NMR spectrum showed a peak for the alkyl

ester at 4.12 ppm which integrated to 3H, and another distinguishable peak was seen for the 1,4-disubstituted phenyl ring which appeared as two doublets representing the rooftop effect, the peaks are seen at 8.30 ppm and 8.46 ppm with *J* values of 8.0 Hz.

Following successful synthesis of the ester (**59**) a hydrolysis reaction was carried out to give the corresponding carboxylic acid functionalised porphyrin (**60**). The conversion was carried out using a literature method.[202] A simple basic hydrolysis gave the pure product without column chromatography in a 90% yield, which is excellent compared to the 84% achieved in the literature. Analysis of the compound using ^{1}H-NMR confirmed the structure of **60**, and the peak seen for **59** at 4.12 ppm was no longer present due to the conversion of the ester to the carboxylic acid.

The carboxylic acid was subsequently converted to the NHS ester *via* formation of the acyl chloride using thionyl chloride, with addition of *N*-hydroxsuccinimide, then leading to the formation of the NHS-ester. Following column chromatography, the NHS ester was isolated in reasonable yield (68% compared to literature values of 98%).[203] This reduced yield can be attributed to the use of column chromatography, as some degradation of the product on the silica was observed. However, this step is necessary to obtain a product of suitable purity for methylation. Confirmation of the formation of the NHS ester (**61**) was carried out using ^{1}H-NMR and ^{13}C-NMR spectroscopy and mass spectrometry. The ^{1}H-NMR shows a distinctive peak at 3.03 ppm, and a broad singlet which represents the 2 x CH_2 groups for the NHS ester.

Following the conversion of the ester to the NHS ester, *via* the carboxylic acid, the porphyrin was rendered water soluble with the use of methyl iodide to give compound **62**. The purification of **62** was carried out *via* a simple counter-ion exchange method to increase water solubility. The counter-ions were exchanged from iodides to chlorides *via* ammonium hexafluorophosphate anions, to give the product with the chloride ions in an excellent yield of 98% which is comparable to literature yields.[203] Confirmation of the structure of **62** was carried out using ^{1}H-NMR and ^{13}C-NMR spectroscopy and mass spectrometry. The ^{1}H-NMR spectrum shows a distinctive peak at 4.70 ppm representing the N-CH_3 protons, which integrates to 9H. It also still shows the distinctive broad singlet of the NHS ester at 3.18 ppm, representing the 2 x CH_2.

Following the successful synthesis of **62**, metals were inserted into the porphyrin cavity, in order to allow comparison of the effects of different metals against the killing of bacteria. Palladium and zinc were chosen for this particular study, zinc due to the ease of

insertion of the metal into the cavity, with no reported loss of singlet oxygen quantum yields, while palladium is known to induce the heavy atom effect, and increase the triplet state lifetime.[204] Zinc was inserted into the cavity using zinc acetate and stirring at room temperature for an hour. Following this, the counter-ions were exchanged to the chloride to give the product in an acceptable yield of 82%. This is slightly lower than expected, but this could be due to the loss of product when carrying out the counter-ion exchange.

The insertion of palladium proved more challenging, requiring microwave heating to high temperatures (100 °C) for an hour. The successful metallation was evaluated using UV-Vis spectroscopy, and showed a decrease in the amount of Q-bands from four to two. While initial yields were moderate (*ca*. 60%), optimisation was carried out by varying the amounts of solvent used in the counter-ion exchange method and also by using a mixture of methanol and water when changing from the iodide counter-ion to the hexafluorophosphate counter-ion, allowing eventual synthesis of the product in 92% yield.

The successful synthesis of the NHS ester functionalised water soluble porphyrin allowed for peptide coupling reactions to be carried out utilising this porphyrin.

Reaction number	Amount of porphyrin	Amount of chain	Solvent	Additives	Temp	Time
1	20 mg	10 mg	methanol	DIPEA (0.1 mL)	35°C	48 h
2	20 mg	15 mg	methanol	DIPEA (0.1 mL)	40°C, N_2	48 h
3	20 mg	15 mg	methanol	DIPEA (0.1 mL)	rt, N_2	24 h
4	20 mg	20 mg	methanol	DIPEA (0.1 mL)	rt, N_2	24 h
5	20 mg	20 mg	DMSO	DIPEA (0.1 mL)	40°C, N_2	24 h

Table 6 – Peptide coupling reactions attempted using NHS ester functionalised porphyrin.

Table 6 shows the different reactions carried out in attempts to couple the NHS ester porphyrin to the acrylamide functionalised chain. Increasing the excess of acrylamide chain and use of inert conditions in reaction number **2** led to formation of a new product on TLC, but the isolated product was found not to be the desired product. Similarly, a change in solvent for reaction **5** showed a different band forming by TLC, which was also found not to be the desired product. The main problem in these reactions was the formation of by-products, in combination with the highly water soluble porphyrin; this made small scale purification using preparative TLC extremely complex and time

consuming. A different approach was required that allowed for less challenging purification, that could be carried out on a reasonable scale.

3.3.2 Alternative porphyrins for use in peptide coupling

An alternative for the synthesis of a porphyrin attached to an acrylamide chain is to form the conjugate between porphyrin and an acrylamide functionalised chain prior to making the conjugate water soluble. This strategy allows for purification of a lipophilic product, and facile removal of by-products using column chromatography.

3.3.2.1 Synthesis of carboxylic acid porphyrin for use in peptide coupling

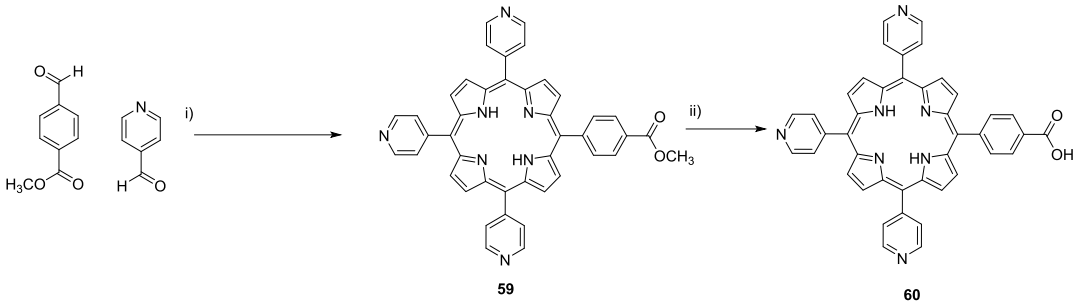

Scheme 26 – Synthesis of carboxylic acid functionalised porphyrin (60). Conditions used: i) propionic acid, reflux, pyrrole, 1 h, ii) KOH, DMF, rt overnight.

The synthesis of **60** was carried out as described above *via* the Adler-Longo method followed by hydrolysis. Following successful synthesis and purification of porphyrin **60** *via* column chromatography, an acrylamide PEG chain was then synthesised bearing a complementary amine functionality for use in peptide coupling reactions. Water-solubility could then be engendered following successful coupling between the porphyrin and the acrylamide PEG chain.

3.3.2.2 Synthesis of PEG chain bearing both an amine and an acrylamide functionality

A modified diamino functionalised triethyleneglycol PEG chain was used to synthesise the acrylamide chain, allowing decreased steric hindrance between the porphyrin and the vinyl functionality and increased water solubility due to the amphoteric nature of the PEG chain.

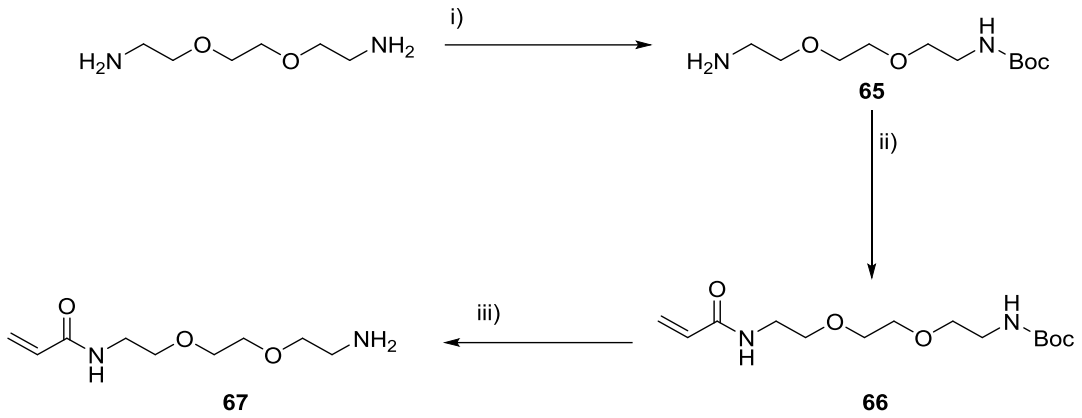

Scheme 27 – Synthesis of modified acrylamide chain bearing amine functional handle. Reagents and conditions: i) Boc_2O, MeOH, TEA, 24 h, 35 °C ii) DIPEA, acryloylchloride, dry CH_2Cl_2, rt, 5 h iii) HCl in dioxane, rt 1 h.

Scheme 27 shows the synthetic route to a modified acrylamide chain. The first step of the synthesis involved a mono-Boc protection of a diamino chain to give **65**, carried out using a modified literature procedure,[205] where an aqueous extraction was carried out to remove any PEG chain starting material. Following this the crude product was purified using column chromatography. This proved challenging as the product adheres strongly to silica. The yield obtained for this reaction was 96%, which compared to a literature value of 90%.[205] The structure of **65** was confirmed using ^{1}H-NMR and ^{13}C-NMR spectroscopy and mass spectrometry. The ^{1}H-NMR showed a distinctive singlet at 1.25 ppm, representing the Boc protecting group with an integration of 9H. The alkyl region also showed a triplet at 2.69 ppm representing CH_2-CH_2-NH_2 with *J* values of 12.0 Hz and 4.0 Hz. The structure was also confirmed by mass spectrometry, with an $[M+H]^+$ at 249.1809.

Acryloyl chloride was then used in the presence of a base to introduce the vinyl functionality on the amine and give compound **66**. Following aqueous work-up and column chromatography, the product was obtained in an excellent yield of 88% in comparison to the literature value of 70%.[205] Analysis of the product using NMR spectroscopy showed the distinctive pattern for the vinyl functionality of the chain, which confirms the presence of the product. The ^{1}H-NMR spectrum shows a series of double doublets representing the acrylamide functional group. At 5.64 ppm there is a double doublet with J_{cis} = 10.2 Hz and J_{gem} = 1.6 Hz which represent the $CH_2C\mathit{H}CO$. There is also a double doublet at 6.12 ppm where J_{trans} = 14.0 Hz and J_{gem} = 1.6 Hz the third peak representing the acrylamide functionality is seen at 6.27 ppm as a double doublet with a J_{trans} = 14.0 Hz and a J_{gem} = 2.0 Hz. Confirmation of the product was also seen from mass spectrometry, with an $[M+H]^+$ peak seen at 303.1913.

Following the addition of the vinyl functionality the Boc protecting group was removed to give the final compound (**67**). This was carried out using 4M HCl in dioxane, with simple diethyl ether washing giving the pure product in a 97% yield which is higher than that reported in the literature (92%).[205] The structure of the product was confirmed by ^{1}H-NMR, ^{13}C-NMR and mass spectrometry. The ^{1}H-NMR spectrum showed the absence of the distinctive peaks for the Boc protecting group which were seen at 1.43 ppm in compound **66** and **65**. The mass spectrometry data confirms the structure of **67**, with an $[M+H]^{+}$ peak at 203.1390.

Following successful synthesis of both the porphyrin bearing a carboxylic acid functionality and the acrylamide chain functionality, peptide coupling reactions were attempted before water solubilisation was carried out.

3.3.2.3 Peptide coupling reaction between carboxylic acid functionalised porphyrin and amine functionalised vinyl chain

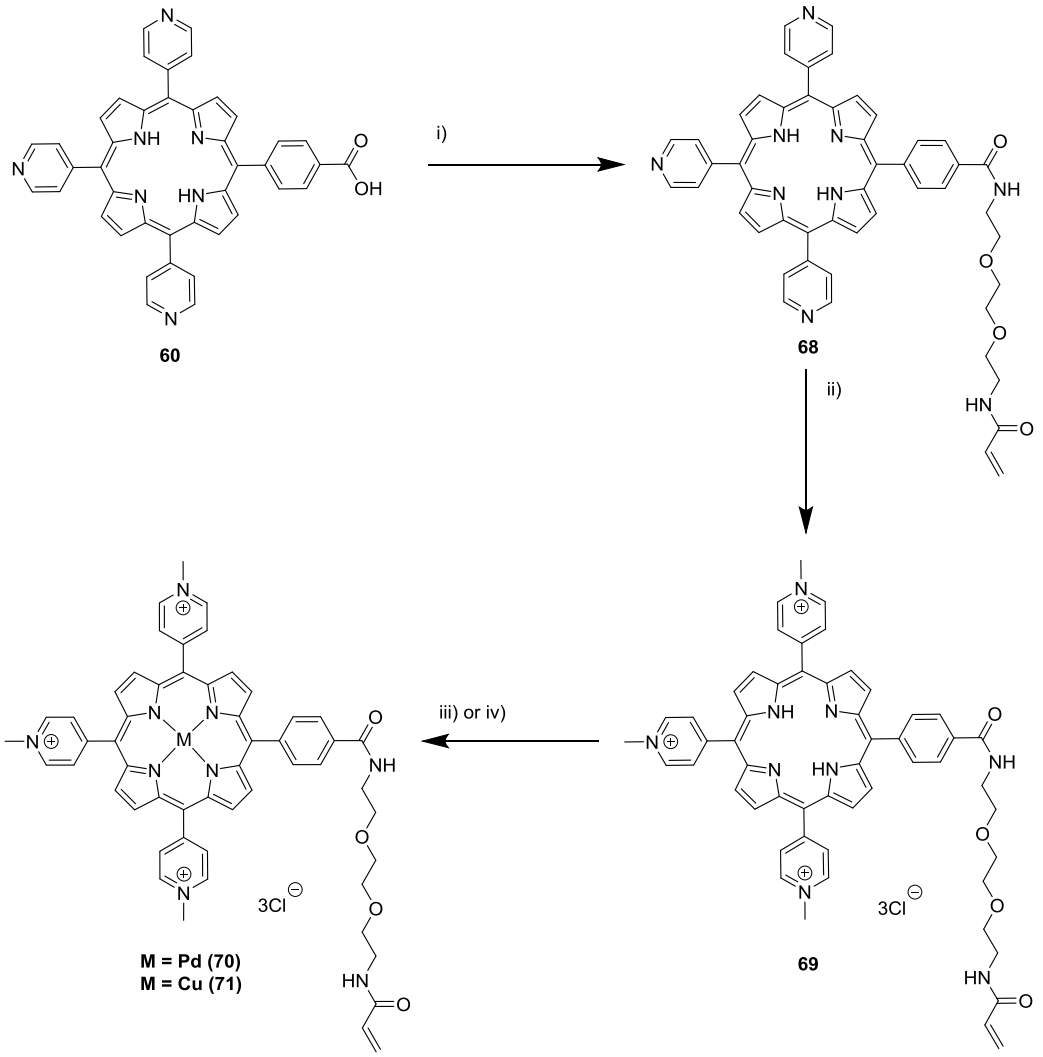

Scheme 28 – Synthesis of water-soluble porphyrin-acrylamide chain conjugate 69 and subsequent metalloporphyrins. Conditions used; i) EDCI, HOBt, DMAP, 66,

dry DMF, rt overnight, ii) CH_3I, 40 °C overnight iii) copper acetate pentahydrate, water, rt overnight, iv) palladium acetate, water/methanol (9:1), MW, 100 °C, 2 h.

The synthesis of conjugate **68** is shown in **Scheme 28**, following successful synthesis of **60** and **66**. Conjugation was carried out using a peptide coupling reaction to give compound **68**. The peptide coupling reactions proceeded by stirring the chain (**60**) with 4-dimethylaminopyridine (DMAP) in dry DMF for 45 minutes before being added to the porphyrin with hydroxybenzotriazole (HOBt) and 1-ethyl-3(3-dimethylaminopropyl) carbodiimide (EDCI). The reaction was monitored using TLC and column chromatography was carried out to isolate the product in a 42% yield. Despite optimisation of the reaction with varying amounts of DMAP and time showing no increase in this yield. Confirmation of the structure of **68** was carried out using ^{1}H-NMR and ^{13}C-NMR spectroscopy and mass spectrometry.

^{1}H NMR and ^{13}C NMR spectra clearly demonstrated that **68** is an asymmetric structure. The resonances of the two equivalent pyridyl rings trans to one another are indistinguishable from those of the third pyridyl ring; similarly, the eight pyrrole protons (βH) give a single unresolved multiplet (four doublets would be expected, based on the symmetry). In the downfield region, besides the two doublets for the pyridyl protons at 9.05 ppm (2,6 Py) and 8.27 ppm (3,5 Py) and the singlet for the *o,m* Ph protons at 8.31 ppm, the spectrum shows the triplet of the amide NH at 8.22 ppm partially overlapping with the doublet of the 3,5 Py protons. The ^{1}H NMR spectrum of **68** shows the characteristic resonances of the acryloyl group at 6.26 ppm (CH_2=C*H*CO), at 6.06 ppm for the C*H*$_2$=CHCO *trans* and at 5.55 ppm for the C*H*$_2$CH=CO *cis.* In the upfield region, the spectrum shows the multiplet of the alkylic chain (δ = 3.70–3.59) and the triplet at 3.51 ppm of the C*H*$_2$NHCOCH. The two internal NH pyrrole protons appear as a relatively sharp singlet at - 3.0 ppm.

Methylation using methyl iodide was carried out at 40 °C overnight in DMF to give **69**, with the product isolated by ion exchange precipitation as previously described. The product was analysed by NMR and mass spectrometry. The ^{1}H-NMR shows a distinguishable peak for the N-CH_3 protons at 4.70 ppm showing complete methylation of the product in a good yield of 92%.

3.3.3 Metal insertion into porphyrin-acrylamide conjugate

Following successful peptide coupling and methylation reactions, metallation reactions were carried out to insert palladium or copper into the porphyrin. Copper was chosen to be inserted into the porphyrin cavity because of its paramagnetic properties,[168,207,208]

which showed that there is no production of singlet oxygen, whereas palladium was chosen due to the heavy atom effect, and it was thought to increase the triplet state lifetime and thus increasing the amount of reactive oxygen species produced.

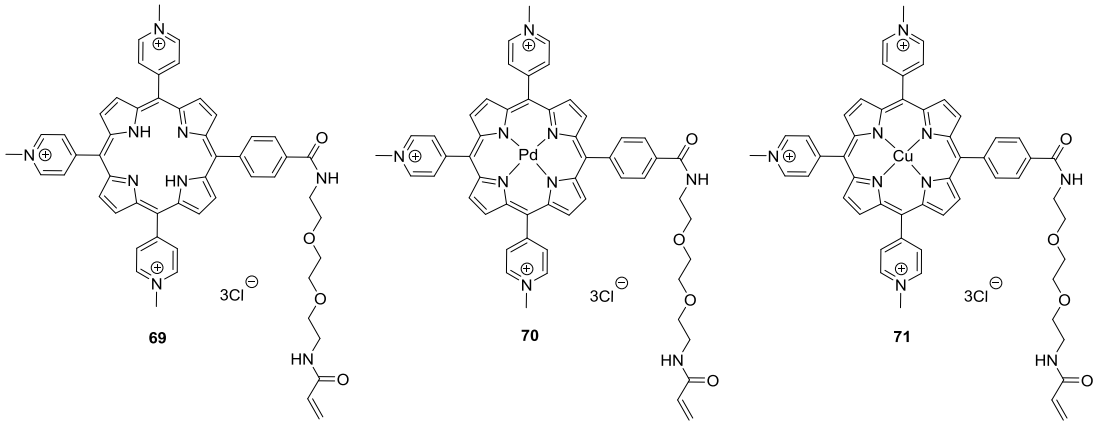

Figure 61 – Chemical structures of final compounds (69-71) that have been used for immobilisation on a polyacrylamide polymeric support.

The metal insertion into the free-base porphyrin was straightforward for copper. The conditions required the use of copper sulphate in water, stirred at room temperature overnight to give the metallated product in a 91% yield. Analysis of the compound was carried out using UV-Vis and mass spectrometry. The UV-Vis spectrum showed three distinctive bands at 425 nm for the Soret band, and at 550 nm and 575 nm for the two Q-bands. Analysis by mass spectrometry showed a $[M\text{-}3Cl]^{3+}$ peak at 317.1088.

The insertion of palladium into the free-base porphyrin proved more challenging, and was initially attempted using the method of Giuntini *et al*.[170] This literature method uses *N*-methyl-2-pyrrolidone (NMP) as the solvent and while it allows metallation of non-water soluble porphyrins, and higher temperatures to be used, the solvent cannot be easily removed. The product must therefore be precipitated from NMP during purification, with poor precipitation leading to product loss and subsequent lower yield.

As a result, an alternative methodology was developed, using water as the solvent instead of NMP, with the change in solvent allowing for removal of the precipitation step and improved yields. Despite this, yields of only approximately 70% were obtained as opposed to at least 80% for other metal complexations of porphyrins. This was attributed to the production of palladium (0) during the reaction, which appears as a black soot when carrying out the metal insertion using palladium (II) acetate. The removal of the palladium (0) was carried out by filtering through celite, with this added purification step compromising the yield.

Figure 62 shows comparative UV-Vis spectra for all three porphyrins that were synthesised**;** a non-metal porphyrin, a copper porphyrin and a palladium porphyrin. The non-metal porphyrin was used as the control in this case and gives the Soret band and the four distinctive Q-bands. The copper porphyrin was used as a "switch off" scenario, with the paramagnetic properties of the metal thought to quench the singlet oxygen production.[207] The palladium porphyrin represents an enhanced scenario, with the induction of the heavy atom effect known to increase the singlet oxygen quantum yield, by increasing the excited triplet state lifetime, leading to an enhanced bacterial killing effect.[204]

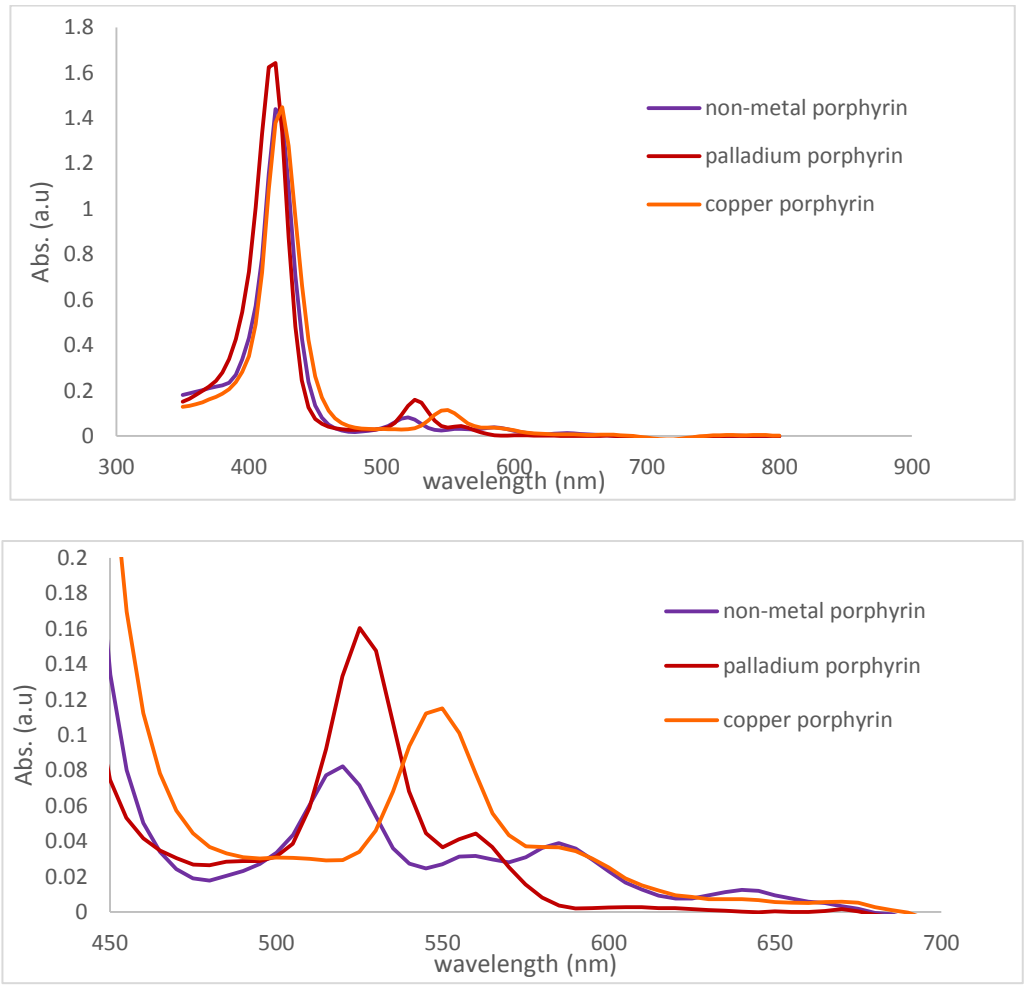

Figure 62 – UV-Vis spectrum comparing non-metallated porphyrin, copper and palladium porphyrin with a particular study into the Q-bands.

3.4 Water soluble porphyrins conclusion

In conclusion a library of water-soluble porphyrins with an acrylamide functionality have been successfully synthesised and characterised for use in the production of polyacrylamide hydrogels. The porphyrins synthesised allow for a comparative study to be carried out to study the effect that the metal has on the bacterial killing.

3.5 Future work

The finalised porphyrin structures bearing the acrylamide handle will be polymerised and used in the formation of polyacrylamide hydrogels with varying molarity to allow for comparison of porphyrin loading. The synthesised polyacrylamide hydrogels will be tested against bacteria to see how effective the system is at killing bacteria.

4 Immobilisation of photosensitisers on polymeric supports

4.1 Introduction

The immobilisation of photosensitisers on polymeric supports is a flourishing area of research and investigations into the use of both natural and synthetic supports have been carried out.[32] The immobilisation of photosensitisers allows for versatility in the applications of supports, and can also allow for reduced toxicity in comparison to the free photosensitiser in solution.

The use of synthetic polymers allows for increased flexibility in design, as modifications to the monomer can be made prior to the polymerisation. Two different polymeric supports have been investigated for the immobilisation of porphyrins in this work; polyacrylamide and silica. These supports were chosen due to their different properties; they are versatile, biocompatible and easy to synthesise.

4.1.1 Polyacrylamide

The structure of polyacrylamide allows for easy functionalization both prior to and post polymerisation; with the amino group being available for peptide couplings, among other reactions (**Figure 63**).

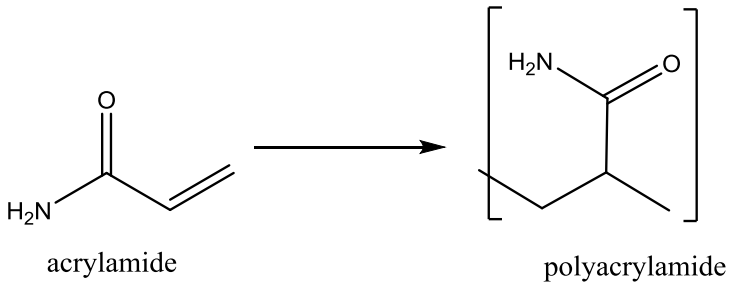

Figure 63 – Formation of polyacrylamide from acrylamide *via* a free radical polymerisation method.

Polyacrylamide has been used as a support for various applications including nanoparticles for sensing and drug delivery,[55] and nanodevices.[77] Investigations into the use of polyacrylamide as a solid support have, to date, focused on the formation of polyacrylamide nanoparticles *via* a reverse microemulsion method; although they offer many advantages as nanoparticles, the formation of a hydrogel is better suited to the applications envisaged here, since the hydrogel can be moulded to fit the required need.

Polyacrylamide-based hydrogels have been used for drug delivery,[209] and modifying the hydrophobicity of drugs,[210] while the hydrophilic surface of the polyacrylamide based nano-platform also makes them a suitable candidate for the development of therapeutic entities.[209] The flexible nature of polyacrylamide synthesis allows it to be co-polymerised with various different monomers and cross linkers bearing a vinyl functionality, permitting a range of novel derivatisations and synthetic applications for different polyacrylamide based materials.[205]

Polyacrylamide has been a popular support for photosensitisers in the form of nanoparticles and hydrogels.[55,77,205,211]

Josefsen *et al.* investigated the use of amine-functionalised polyacrylamide nanoparticles (PANPS) for conjugation to a porphyrin and calcium green for the sensing of reactive oxygen species.[211] This particular system responds to changes in calcium levels in cells using calcium green, calcium green was polymerised within the matrix after being anchored to dextran to minimise leaching. This system combines a ROS-generating photosensitiser and a luminescent probe within one system using polyacrylamide nanoparticles. Confirmation of the presence of both the photosensitiser and the calcium detector (calcium green) was seen from the emission spectra following the excitation of the porphyrin-nanosensor at 488 nm. The generation of ROS was investigated using a cholesterol assay, whereby the photosensitised oxidation of cholesterol to the corresponding hydroperoxide is measured, the reaction with cholesterol was monitored using TLC.

Recent research by Giuntini *et al.* describes the use of PANPs as cargo carriers for photosensitisers,[77] selected for their hydrophilic character and stable dispersions in water. Use of nanoparticles allows the cargo to be either loaded inside the nanoparticle *via* encapsulation or conjugated to the outside of the nanoparticle *via* a modification of the nanoparticle surface. Giuntini *et al*. modified the nanoparticle surface to contain both amine and alkyne functional groups, allowing bioorthogonal conjugation of two different photosensitisers for two different applications.

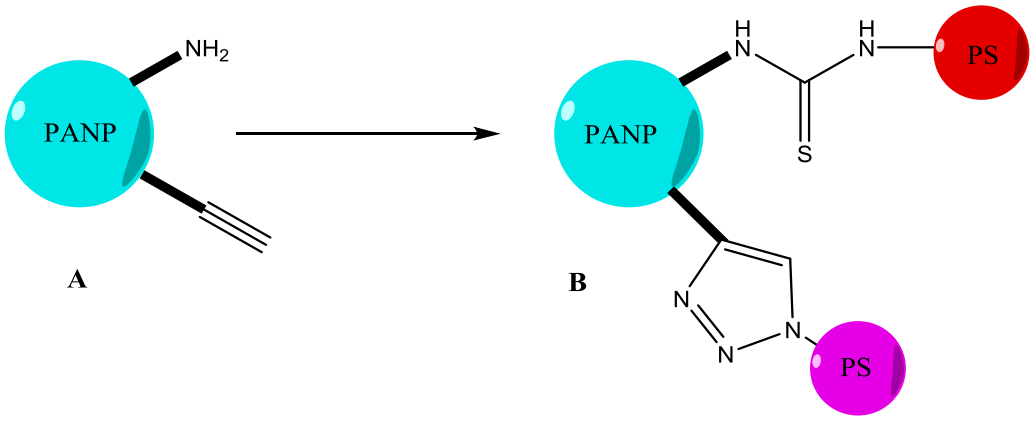

Figure 64 – Schematic of work carried out by Giuntini *et al.* A - functionalised nanoparticles with amine and alkyne groups on the surface, B – nanoparticles conjugated to photosensitiser.[77]

Kuruppuarachchi *et al.* investigated the use of polyacrylamide nanoparticles for the chemical entrapment of porphyrins for use in PDT.[55] The photosensitiser was conjugated to poly(lysine) to help prevent leaching of the photosensitiser from the polyacrylamide nanoparticles, as it has been previously reported that 45-50% of photosensitisers are leached from nanoparticles in 48 h if they are physically entrapped.[212]

An alternative support to nanoparticles is the use of hydrogels, which allow a more versatile approach.

4.1.2 Hydrogels

Hydrogels were the first biomaterial designed for clinical use.[74,213] They are water swollen polymeric materials that maintain a distinct 3D structure.[214,215] Hydrogels are generally prepared from hydrophilic polymers that absorb 10-20 thousand times their dry weight in water, and can be classified as natural or synthetic based upon the origin of this polymer.[215] They can also be classified as permanent or physical hydrogels, depending on whether the bonds holding together the hydrogel network are permanent or non-permanent in nature. Covalently-linked cross networks form permanent hydrogels while ionic bond supported networks are classified as physical hydrogels. The network of physical hydrogels can be easily broken by the collapse of the ionic bonding within the network.

Synthetic hydrogels are prepared using free radical polymerisation of water-soluble or hydrophilic monomers in the presence of either difunctional or multifunctional monomers. Neutral synthetic polymers can be generated from derivatives of polyhydroxyethylmethacrylate (HEMA), poly(ethylene glycol) (PEG) and poly(vinyl

alcohol) (PVA), for example. PEG derivatives are the most widely used polymers for biomedical applications, due to their non-toxic properties, with PEG being approved by the US Food and Drug Administration.[216] While potentially less biocompatible, conventional polyacrylamide hydrogels were found to not degrade in biological systems,[210] which also makes them a suitable candidate for use in immobilisation of photosensitisers.

Historically, the primary challenge faced during the design of materials for medical use was that the materials lacked the desired functional properties to interface with biological systems, and they were not designed to optimise performance.[216] The excellent biocompatibility of hydrogels originates from their high water content, allowing them to be used for numerous applications including medical applications, antibiotics and anticancer drugs, as part of a formulation.[74]

The first investigation into the use of hydrogels was carried out by Wichterle and Lim in 1960,[217] who investigated the use of polymeric materials for use in medical applications. The key findings of this work demonstrated the importance of hydrogel structural demands; the structure must permit the desired water content, the material must have inertness to normal biological processes and must be permeable to metabolites. The material must also have a 3D structure with at least enough cross linkages to prevent absorption.

Research into the use of hydrogels for biomedical applications has become increasingly popular.[75,218–220]

Lovell *et al.* investigated the immobilisation of tetra-[4-carboxyphenyl] porphyrin onto a PEG monomer for the formation of a photoactive hydrogel (**Figure 65**).[218] The decision to use PEG stemmed from its biocompatibility and its swelling capacity, making it suitable for the formation of a hydrogel. The porphyrin was attached to the amine functionalised PEG *via* the formation of an amide bond, which in turn created the polyamide 3D network, formed as a hydrogel. However, the use of the porphyrin as a crosslinker limited the length of PEG chain that could be used due to the bulky nature of the porphyrin and the gel-creating properties.

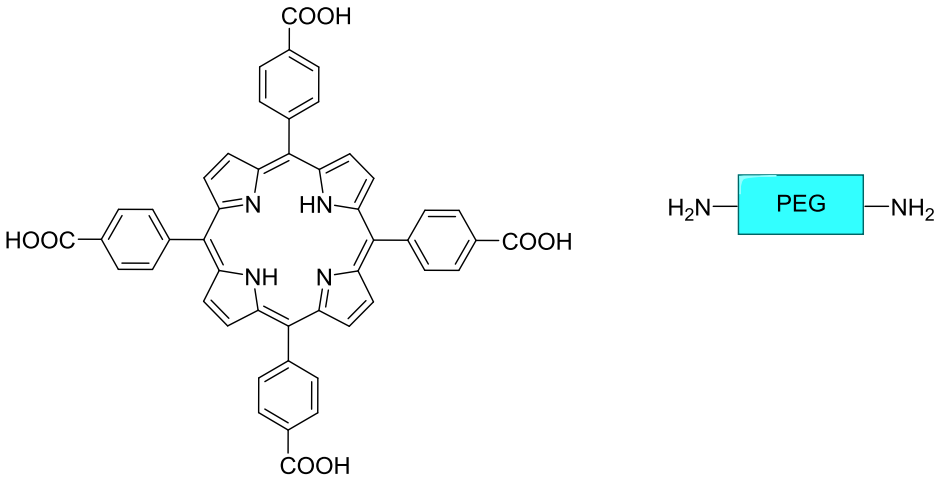

Figure 65 – Structure of 5,10,15,20-tetra-[4-carboxyphenyl]porphyrin and diamino PEG used by Lovell *et al.*[218]

Similarly, Unruh *et al.* examined the covalent attachment of an acrylate-functionalised palladium benzoporphyrin for polymerisation with poly(HEMA-*co*-acrylamide) for use in glucose sensors.[75] The covalent attachment is of key importance in this work, allowing reduction of the extent of photosensitiser leaching from the matrix.

In contrast to this, Brady *et al.* and Parsons *et al.* studied the use of non-covalent attachment of porphyrins to polyHEMA surfaces *via* ionic bonding.[219,220] Brady *et al.* investigated the use of hydrogels which have charged surface for an ionic attraction to either a cationic 5,10,15,20-tetra-[4-methylpyridinium] porphyrin (TMPyP) or an anionic porphyrin tetrakis (4-sulphanato) porphyrin (TPPS) (**Figure 66**).

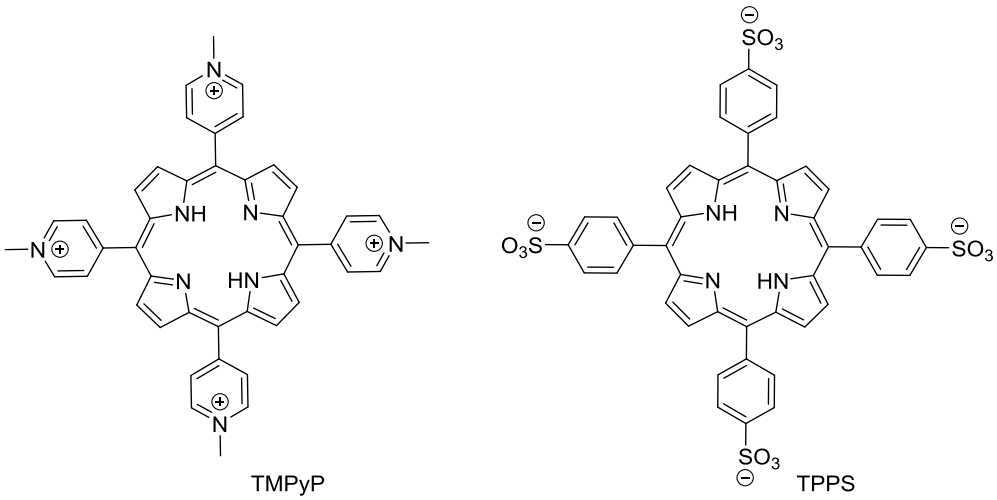

Figure 66 – Structure of two charged porphyrins (5,10,15,20 tetra-[4-methylpyridinium] porphyrin) and (5,10,15,20-tetra(4-sodiumsulphonatophenyl)porphyrin) used by Brady *et al*.[219]

The hydrogels used were formed from a co-polymerisation of HEMA with either methacrylic acid or diethylaminomethacrylate to form either positively charged surfaces (diethylaminomethacrylate) or negatively charged surfaces (methacrylic acid) which ionically bind with the relevant porphyrin (**Figure 67**).[219]

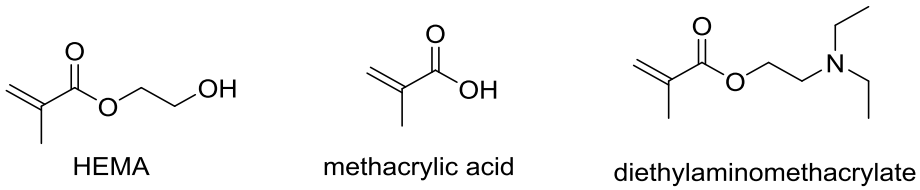

Figure 67 – Structure of monomers used by Brady *et al*. for formation of hydrogels.[219]

The hydrogels were formed *via* a free radical polymerisation method using benzyl peroxide as the free radical initiator and ethylene glycol dimethylacrylate (EGDMA) as the cross linking agent. Once the blank hydrogel had been formed, the porphyrin was incorporated by immersing the hydrogel into a porphyrin solution, with the porphyrin remaining immobilised in the polymer matrix even after washing.

Similarly, Parsons *et al*. investigated the use of negatively charged polymers using HEMA co-polymerised with methacrylic acid for ionically binding with TMPyP.[220] The same method as Brady *et al.* was used for the incorporation of the porphyrin and was found to be successful.[219] The photoactive materials were tested against *S. epidermidis* and *Proteus mirabilis* and were found to be successful in deactivating the bacteria.

Recently, the use of polyacrylamide hydrogels has been investigated for the immobilisation of methylene blue by Spagnul *et al*.[205] The methylene blue was modified to contain a vinyl group, which underwent a free radical polymerisation with acrylamide and *N*,*N*'-bis acrylamide to form an acrylamide hydrogel with methylene blue immobilised in the support. Unlike the work carried out by Brady *et al*.[219] and Parsons *et al*.[220] the investigations involved the covalent attachment of the photosensitiser to the polymeric support (**Figure 68**). The photoactive hydrogel was tested against both Gram-positive *S. aureus* and Gram-negative *E. coli* bacteria. When tested against Gram-positive bacteria the photoactive gel was found to give a 3.32 log decrease after 25 minutes, with a kill rate of 0.139 and a 1 log reduction seen after 7.2 minutes. When comparing the bacterial kill for the Gram-positive bacteria to the Gram-negative bacteria, the photoactive hydrogel caused a 2.30 log decrease after 25 minutes for the *E.coli*. The results obtained by Spagnul *et al.* show a promising system that can be adapted to include any photosensitiser attached *via* the vinyl group.

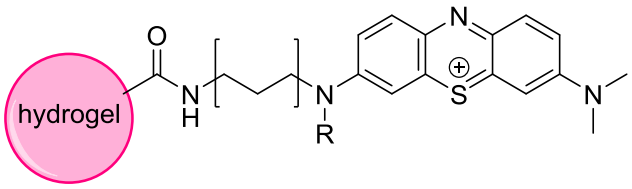

Figure 68 – Schematic of photoactive hydrogel system used by Spagnul *et al*.[205]

4.1.3 Silica as a support

Silica as a support has been used previously for the immobilisation of photosensitisers for various applications including photoinactivation of bacteria and as photoactive catalysts.[54,56,84,221–224] Silica supports are generally formed from one of three sources of silica, namely tetraethylorthosilicate (TEOS), tetramethylorthosilicate (TMOS) and tetrakis (2-hydroxyethoxy) silane (THES) (**Figure 69**).

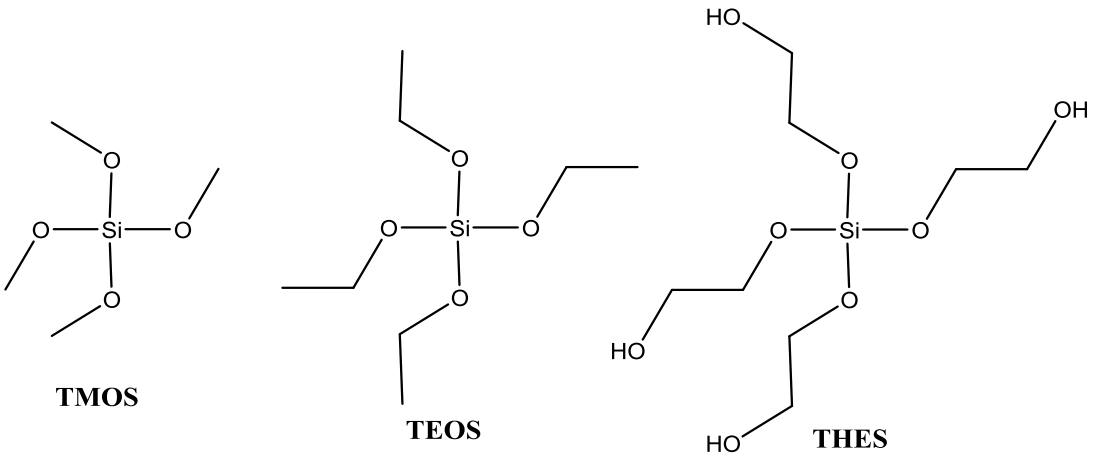

Figure 69 – Structure of typical silica sources for using in silica supports.

Guo *et al*. investigated the use of Rose Bengal-modified silica nanoparticles for inactivation of Gram-positive bacteria (**Figure 70**).[221]

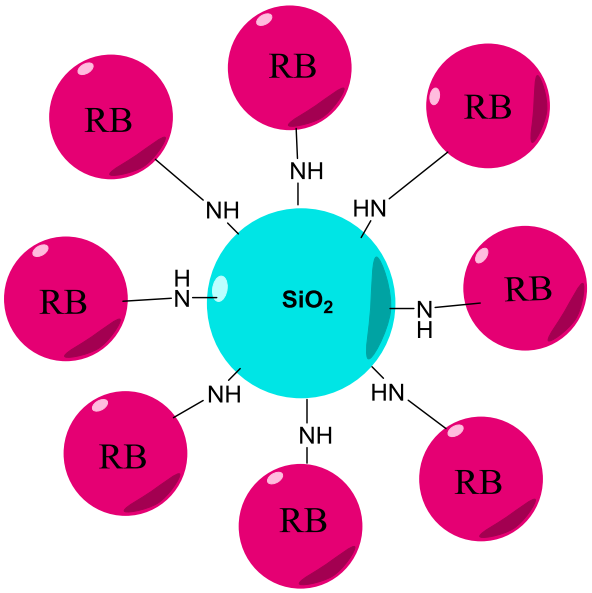

Figure 70 – Schematic of Rose Bengal (RB) modified silica by Guo *et al.*[221]

The silica nanoparticles were synthesised *via* a reverse microemulsion method using tetraethoxyorthosilicate (TEOS); the surface was then functionalised with amine groups which made them readily available for use in peptide coupling reactions with the commercially-available photosensitiser Rose Bengal. The functionalised material was characterised by IR and TEM and the production of singlet oxygen evaluated using 9, 10-anthracenedipropionic acid (ADPA) (**Figure 71**).

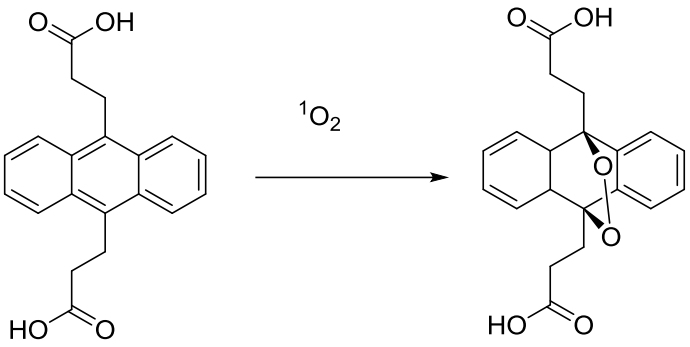

Figure 71 – Structure of ADPA and its reaction with $^1O_2$.

The silica nanoparticles were found to have many advantages including; water dispersibility, chemical and photochemical stability, and ease of modification. The Rose Bengal immobilised on silica nanoparticles was found to produce singlet oxygen with a singlet oxygen quantum yield of 0.6, compared to 0.75 when Rose Bengal is free in solution.

Benabbou *et al*. investigated the immobilisation of two different photosensitisers on silica powder;[222] 9,10-anthraquinone-4-carboxylic acid (ANT) and 9,14-dicyanobenzo[b]triphenylene-3-carboxylic acid (DBTP-COOH) (**Figure 72**).

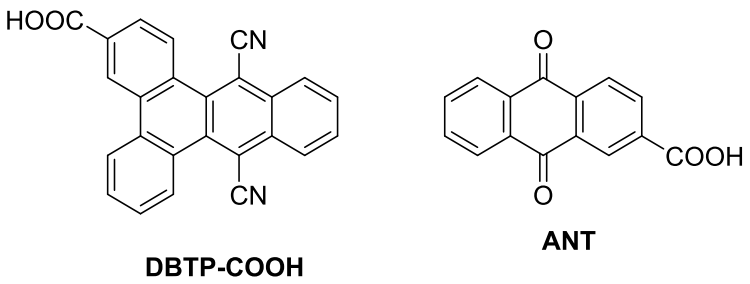

Figure 72 – Structure of photosensitisers used by Benabbou *et al.* immobilised on silica support.

DBTP was grafted onto amine-modified silica *via* a peptide bond, while ANT was converted to its triethoxysilyl derivative through condensation with (3-aminopropyl) triethoxysilane (APTES), and grafted onto commercially available silica beads. The photosensitiser content of both materials was evaluated using UV-Vis spectroscopy. Both photoactive materials were tested against Gram-negative bacteria, *E.coli* and found to deactivate the bacteria, with the bacterial kill rate constant *K*, being higher for SiO_2-ANT (K = 0.13 L g^{-1} min^{-1}) when compared to $SiNH_2$-DBT (K = 0.02 L g^{-1} min^{-1}).

Artarsky *et al*. investigated the use of zinc phthalocyanines non-covalently immobilised in silicate matrices for the inactivation of Gram-negative bacteria *E.coli*.[224] Two different phthalocyanines were investigated; tetrasulfonic acid and tetra tertiary butyl zinc phthalocyanines (**Figure 73**). The production of singlet oxygen by the two materials was monitored using the photobleaching of 1,3-diphenylisobenzofuran (DPBF) at 430 nm in DMF.

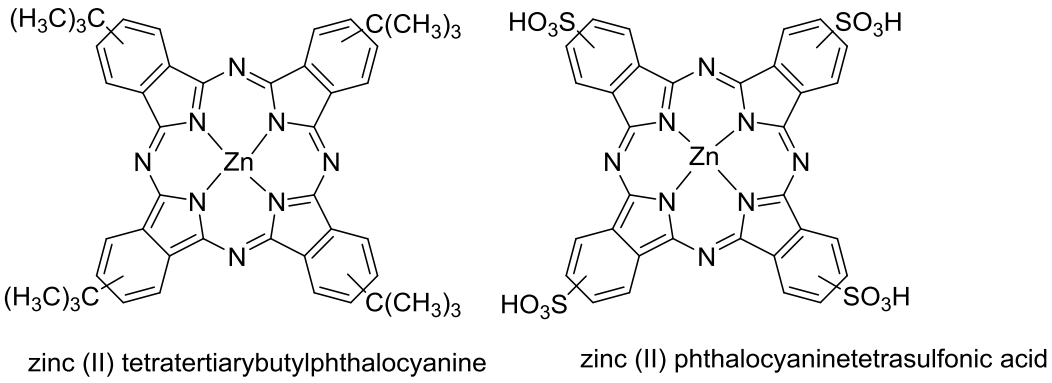

Figure 73 – Phthalocyanines investigated by Artarsky *et al*.[224]

The *t*-butyl phthalocyanine was found to be the most effective generator of singlet oxygen when free in solution, while the tetrasulfonic acid was found to be the most effective when immobilised in the silicate matrix, a fact which was attributed to the hydrophilic nature of the sulfonic acid groups. This results in the photosensitiser lying close to the surface when immobilised, whereas the hydrophobic character of the tertiary butyl group means it is more in the bulk of the matrix, and will therefore produce less singlet oxygen. The main problem with this support is the non-homogenous distribution of photosensitiser in the matrix.

The use of porphyrins immobilised on silica supports has also been investigated.[54,56,84,223] Carvalho *et al.* described the immobilisation of cationic porphyrins on silica supports for use in the photoinactivation of bacteria (**Figure 74**).[54]

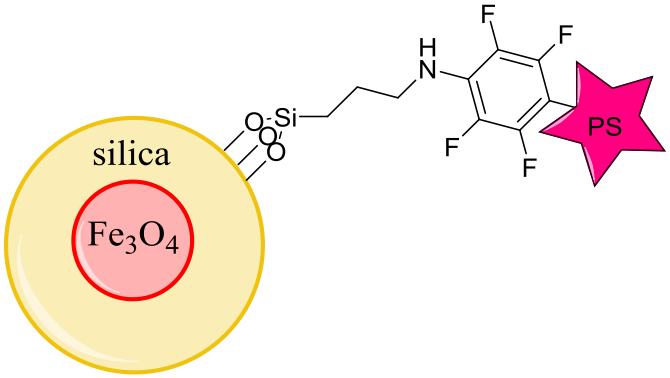

Figure 74 – Schematic of work carried out by Carvalho *et al.*[54]

Carvalho *et al.* used the presence of magnetic nanomaterials for the conjugation to a porphyrin *via* a pentafluorophenyl group. The magnetic nanoparticles were chosen as the support as they can be readily removed from a reaction mixture with the use of a magnet. The nanoparticles were formed using a magnetic core of iron oxide nanoparticles with an amine-functionalised silica shell, allowing conjugation to porphyrin photosensitisers *via* a pentafluorophenyl group. Leaching of the photosensitiser from the support was monitored using UV-Vis spectroscopy, with only 4-5% remaining on the support after washing. The porphyrin-nanomagnetic hybrid material was then tested against both Gram-positive *E.facelis* bacteria, and Gram-negative *E.coli* bacteria, with a cationic porphyrin found to be the most successful against both the Gram-positive and the Gram-negative bacteria. The positive charges on the photosensitiser were found to be essential to achieve significant photoinactivation of *E.coli*, as well as allowing stabilisation of the magnetic nanoparticle suspension, and a higher availability of the photosensitiser for the photodynamic process.

Following the work of Carvalho *et al*., Alves *et al.* investigated the use of analogous nanoparticles with both iron and cobalt cores for the inactivation of bacteria.[56] The reusability of the materials was investigated, and the materials were found to be active after three cycles of 4.5 hours. However, in the third cycle only a 3 log reduction of bacteria was seen after 4.5 hours. Biological evaluation of the material was carried out using a bioluminescent strain of *E.facelis*, and while the silica hybrid gave good results, the iron core without modification with cobalt at the core was found to demonstrate superior killing of bacteria.

Rychtarikova *et al.* investigated the use of 5,10,15,20 tetra-[4-methylpyridinium] porphyrin (TMPyP) entrapped in a microporous silica gel.[84] The silica gel was prepared by the sol-gel method from THES and TMOS, with successful incorporation of the porphyrin without covalent attachment to the silica support. As TMOS had been shown previously to suffer from low mechanical and chemical stability, THES was used as a comparison. The materials formed using TMOS had a glass like texture, whereas those prepared with THES had a more gel like texture. Both supports were found to produce ROS when monitored using iodometric methods.[225]

4.2 Immobilisation of photosensitisers on polymeric supports

4.2.1 Aims

The primary aim of this work was the immobilisation of a photosensitiser and a polyviologen on a synthetic support. Initially, a methodology involving the entrapment of both the photosensitiser and the polyviologen in a synthetic support was attempted, allowing for efficient electron transfer from the porphyrin to the polyviologen with minimal synthetic effort.

An alternative strategy was also explored and it involved the covalent attachment of the photosensitiser to the polymeric support; allowing for a more sophisticated, yet synthetically complex, approach. An advantage of this latter approach is that it would minimise leaching of the photosensitiser from the polymeric matrix.

4.2.2 Synthesis of silica support with porphyrin and polyviologen entrapped

Silica was initially selected as a support as it has previously been separately used for the entrapment of porphyrins,[54,56,84,224] and polyviologens.[226] Silica is easily modified and functionalised, and can be made into brittle or soft materials depending on the source of silica used.

A literature method by Adeogun and Hay was followed for the formation of a polyviologen entrapped in a silica matrix.[226] The method involved dissolving the chosen polyviologen in distilled water, with ethanol added, with agitation in order to aid dissolution of the poorly water-soluble polyviologen. Following this, glacial acetic acid was added to further help dissolve the polymer. Tetraethoxyorthosilicate (TEOS) was then added to the mixture, and upon addition the mixture turned turbid due to the slight acidic nature of the mixture.

Figure 75 – Photograph of polyviologen and porphyrin entrapped in silica matrix (left top), Photograph of polyviologen entrapped in silica matrix (left bottom). Photograph of porphyrin and polyviologen entrapped in silica matrix (right)

The sample was left at room temperature and covered with parafilm for two days with pierced holes to allow for slow evaporation of excess solvent from the material; following this, the solid was heated at 80 °C for 3 days, resulting in a glassy material. Subsequent UV-Vis spectroscopic analysis of water and ethanol washings showed no loss of excess polyviologen detected. This strong entrapment of the polyviologen into the silica matrix could be attributed to one of two interactions; the polyviologen could be forming a non-covalent bond between the OH groups of the siloxyl and the nitrogen of the pyridyl ring of the polymer which is holding it in the matrix, as reported by Hay and Adeogun (**Figure 76**).[226]

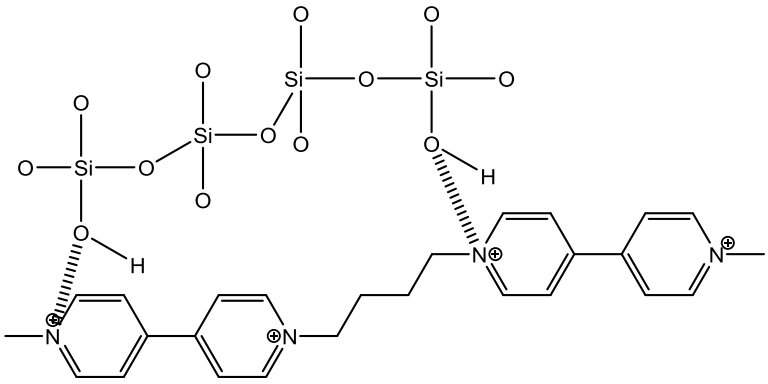

Figure 76 – Non-covalent bonding between SiOH and viologen molecule.

Alternatively, due to the cationic nature of the polymer, the silica support could form in a way similar to that reported by Rychtarikova *et al*. who observed binding of the porphyrin within the TMOS matrix.[84]

The entrapment of porphyrin and polyviologen into a single silica matrix was carried out using a similar method to that of Hay and Adeogun[226] and Rychtarikova *et al*.[84] The silica source was selected on the basis of the porphyrin solubility in order to prevent transesterification reactions between the silicate and the solvent from occurring. For ethanol-soluble porphyrins TEOS was used, while tetramethylorthosilicate (TMOS) was used for methanol soluble porphyrins. The porphyrin-polyviologen silica matrix was synthesised and then washed sequentially with water, ethanol and methanol. Subsequent analysis of these washings by UV-Vis spectroscopy demonstrated porphyrin leaching from the silica support in all solvents used to wash the support. This makes the structure less useful for potential applications, as the leaching of the photosensitiser could cause problems in real world applications.

4.2.3 Analysis of silica matrix using scanning electron microscopy (SEM)

Analysis of the glassy silica matrices was carried out using SEM in order to evaluate the structure of the pores. These pores are necessary to allow the penetration of oxygen into the solid support, allowing formation of the reactive oxygen species essential to function as anti-bacterial agents.

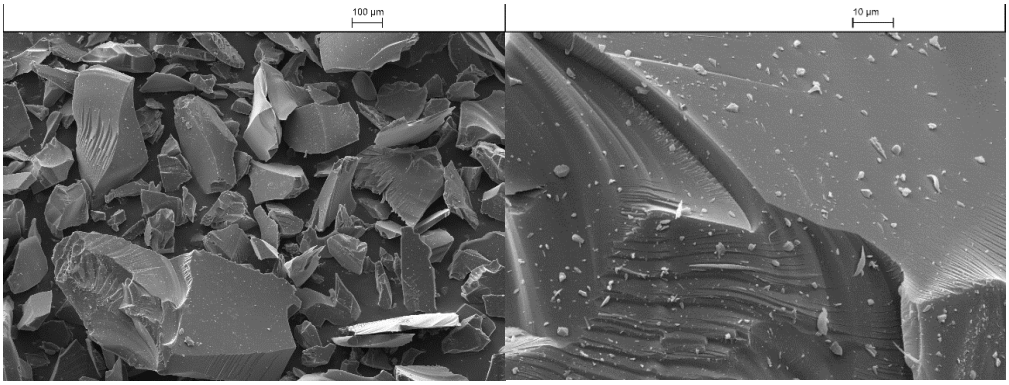

Figure 77 – SEM images of porphyrin-polyviologen entrapped in silica matrix.

The analysis of these silica supports *via* SEM proved challenging, due to their brittle properties. The SEM images did not show a porous structure of the material; even when analysed directly after formation and before drying in the oven. The brittle properties seen were similar to those noted by Artarsky *et al*. and Rychtarikova *et al*. when they used either TMOS or TEOS.[84,224] The properties differ to those seen previously when THES was used as the support, with the four hydroxyl groups present in THES allowing for generation of a more hydrophilic support and the formation of a more gel-like network.

Due to the non-porous structure, leaching, and the brittle nature of the silica support, no further evaluation of this support for porphyrin-polyviologen hybrid entrapment was carried out. In contrast, the polyacrylamide support had many advantages over the silica support, offering mouldability, more rapid synthesis and reduced toxicity, and most importantly the ability to form a porous structure when a polyacrylamide hydrogel is formed.[205]

4.2.4 Synthesis of polyacrylamide hydrogels with porphyrin and viologen entrapped in the matrix

Immobilisation without covalent attachment was the first method attempted in order to constrain porphyrins and viologens in close proximity, with this methodology offering a facile alternative to the use of conjugation methodologies. Entrapping of the porphyrin and viologen in a poly(acrylamide) based gel was attempted, using a modification of the methods developed by Giuntini *et al.*[77] and Spagnul *et al.*[205]

The synthesis of the modified polyacrylamide hydrogels was carried out using various solvent systems depending on the solubility of the porphyrin and viologen compounds. Both the metalloporphyrins and the free-base porphyrins were used in the formation of polyacrylamide gels, with the poor solubility of the synthesised metalloporphyrins limiting the solvent system that could be utilised (**Table 7**). Different solvents were evaluated in order to find the ideal solvent to use; the ideal solvent would be one that: is miscible with water; facilitates solubility of both porphyrin and viologen; and evaporates at room temperature.

Porphyrin used (number)	Viologen used (number)	Solvent used
43	6	dioxane
43	6	THF
43	18	dioxane
43	18	THF
43	17	dioxane
43	17	THF
49	6	DMF
49	6	THF
49	6	dioxane
49	17	DMF
49	18	DMF
54	6	THF
54	6	dioxane
54	18	dioxane
57	18	DMF
57	18	DMF
57	6	DMF
53	6	dioxane
53	6	THF
56	6	DMF

Table 7 – Different combinations of porphyrins and viologens used with changing solvent systems for entrapment in polyacrylamide matrix. Red indicates a zinc complex.

Figure 78 – Examples of porphyrins and viologens entrapped in a poly (acrylamide) matrix, on the left using dioxane as the solvent system (right) with the blank on the left. The right picture on the right using THF as the solvent system, with a blank polyacrylamide gel on the left.

Three different solvents were selected to be used for the polymerisation reactions; THF, DMF and 1,4-dioxane due to their high miscibility with water and their known ability to solubilise both the porphyrin and the viologen/polyviologens. In all cases, the use of different solvent systems resulted in visible differences in gel homogeneity and texture, with these differences attributed to the volatility of the solvent. **Figure 79** shows a comparison between using THF and using 1,4-dioxane as the solvent for the formation of a porphyrin-viologen hydrogel, **43** was the porphyrin used, which is more soluble in dioxane than in THF, but still remains soluble in THF. The gel made using THF was observed to be less homogenous in comparison to the gel made using dioxane, with porphyrin precipitation observed when the THF solution was mixed with the other components that make up the polymer mixture (acrylamide, bis acrylamide, TEMED, APS).

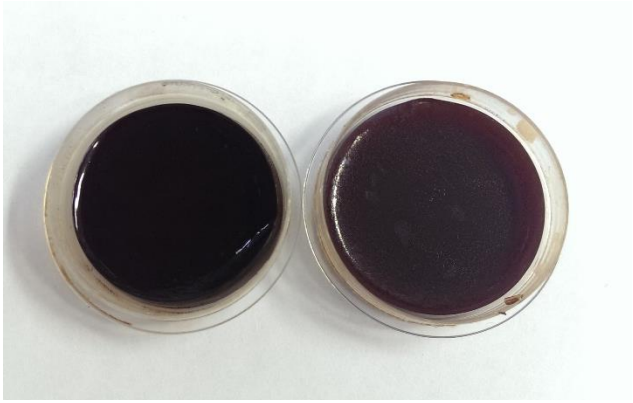

Figure 79 – Comparison of the gels formed using dioxane (left) and THF (right) as the solvent.

The poly(acrylamide) gels were made using both free base porphyrins and their metal derivatives (**Figure 80**), allowing for comparison of ROS generation between the porphyrins and metalloporphyrins.

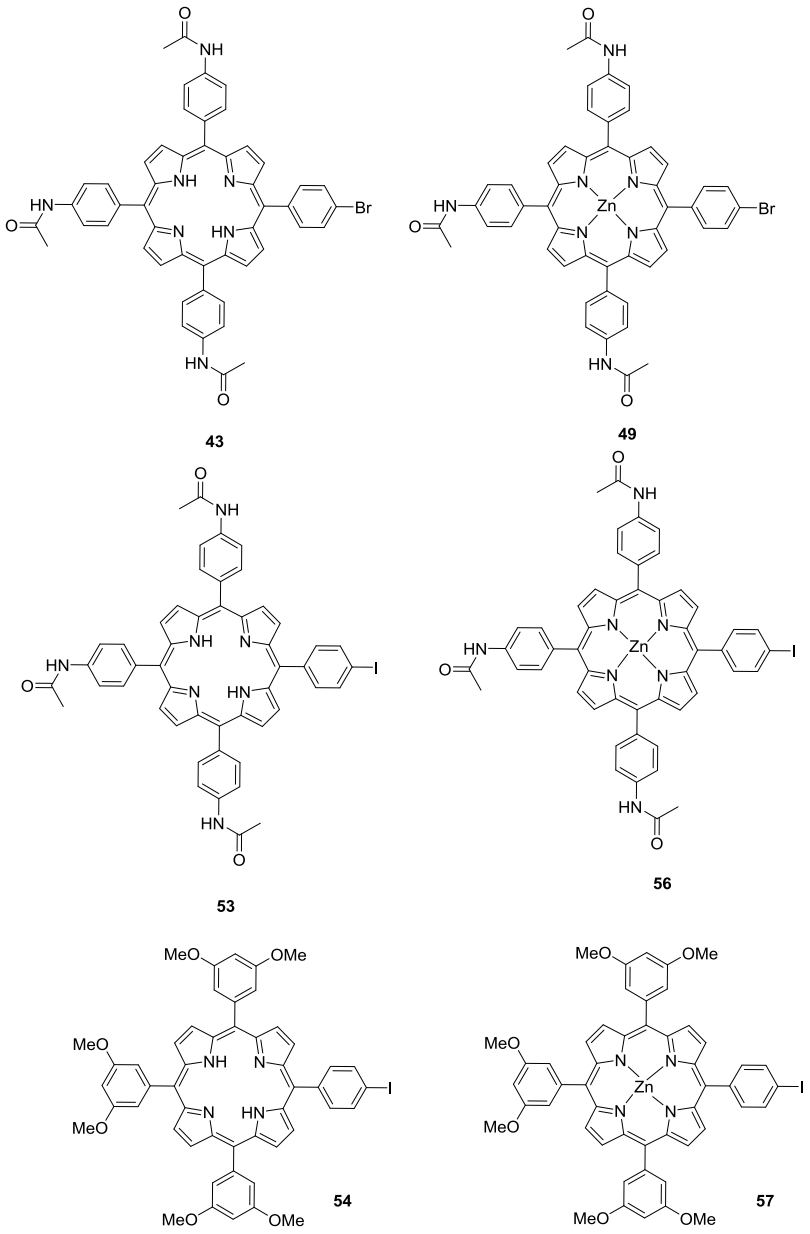

Figure 80 – Structure of porphyrin and metalloporphyrin entrapped in polyacrylamide matrix.

Production of the metalloporphyrin gels proved more challenging than for their free-base counterparts due to the reduced solubility of the metalloporphyrins. However, good solubility was obtained using both THF and DMF. THF was therefore selected where possible in order to allow a direct comparison between the metalloporphyrin and their free-base. However, for less soluble metalloporphyrins DMF was used instead (**Table 7**).

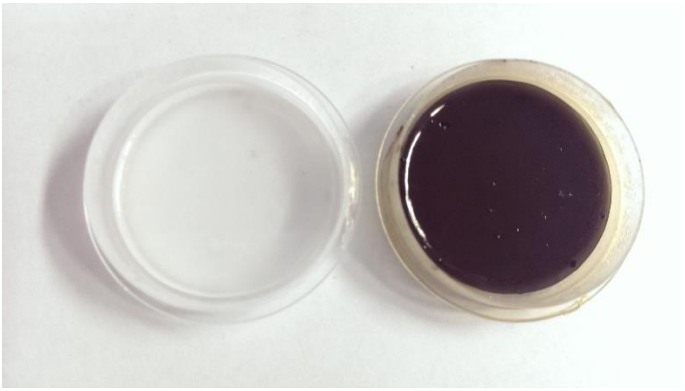

Figure 81 – Poly(acrylamide) gel formed from a metalloporphyrin using THF as the solvent.

Following gel synthesis, the hydrogels were washed multiple times with different solvents, first with the solvent that the gel formation was carried out in, and then with water in order to observe any further leaching of the vinyl monomers. The washing step was carried out multiple times until there was visually minimal to no leaching of both the porphyrin and the viologen from the gel. The washings were kept and analysed using UV-Vis spectroscopy to determine if porphyrin or viologen leaching from the gel had occurred. In all cases, spectroscopic analysis showed leaching of the porphyrin and polyviologen from the gel. These results are in accordance with the results of Kuruppuarachchi *et al.*[55] and Carvalho *et al.*[54], who also observed leaching of photosensitisers from polyacrylamide matrices.

Kuruppuarachchi *et al.* overcame the problem of leaching by grafting the photosensitiser to a large molecule,[55] this enables that the porphyrin is anchored to a large molecule so is less likely to leach. Two alternative options to minimise the leaching are; the use of a different support, or immobilisation of the photosensitiser within the hydrogel *via* covalent attachment of the photosensitiser to the polymeric support.

4.3 Synthesis of porphyrin immobilised on polyacrylamide hydrogels

Although successful formation of polyacrylamide hydrogels had been achieved, a major problem, observed when the porphyrin and polyviologen were entrapped in the polyacrylamide matrix, was leaching of the photosensitiser. In order to minimise leaching, a vinyl moiety was introduced into the porphyrin to allow it to be polymerised into the matrix *via* a vinyl free radical polymerisation method.

4.3.1 Vinyl free radical polymerisation method

The method uses vinyl monomers and an initiator which aids in the formation of free radicals (**Scheme 29**). The initiator used depends on the solubility required, but the process undertaken by each initiator is identical; the cascading production of radical species which are able to react with the corresponding monomer to form the product. Termination allows the coupling of radicals to allow the formation of a stable product.

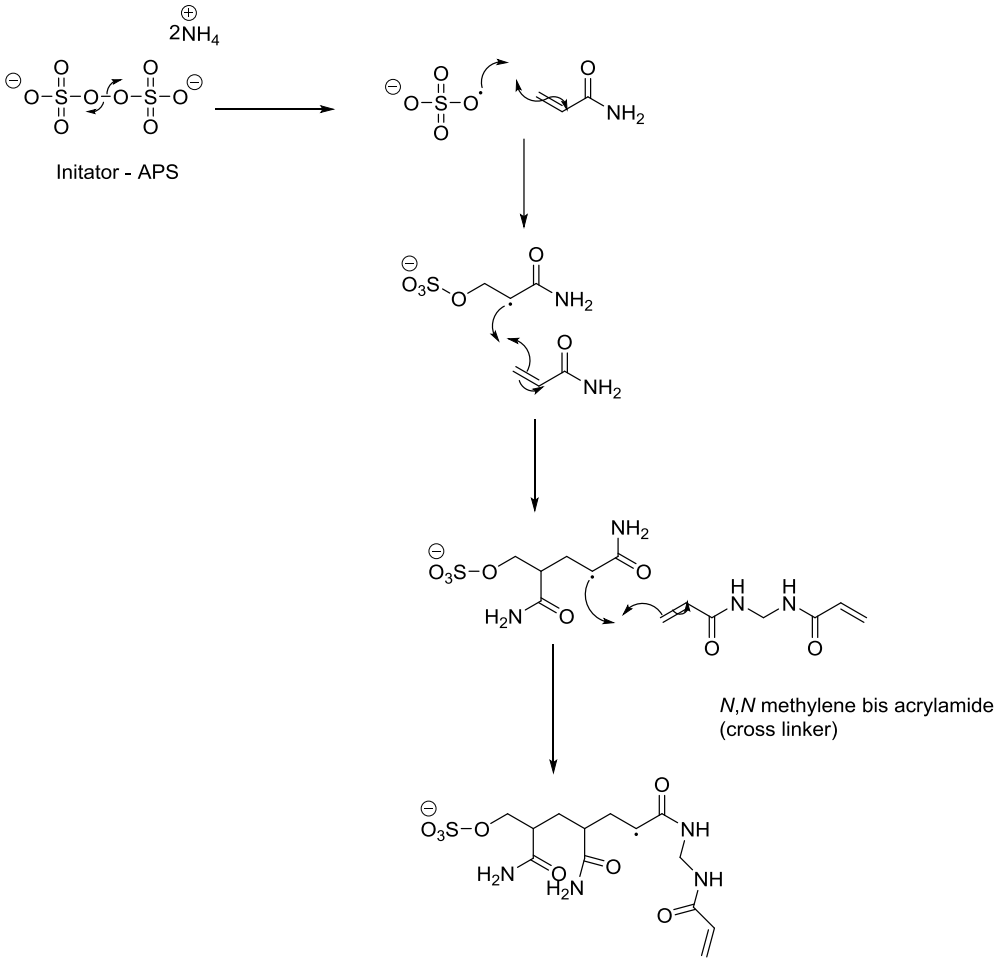

Scheme 29 – Proposed mechanism for free radical polymerisation using ammonium persulfate (APS) as the radical initiator.

4.3.2 Formation of porphyrin immobilised on polyacrylamide surfaces

Another important factor to consider when designing the porphyrin containing the vinyl handle is the solubility of the porphyrin. Previously when investigating the different solvent systems for the formation of polyacrylamide gels, the solvent played an important role in the gel formation. Ideally, the porphyrin would be water-soluble as this would allow for a more homogenous gel to be formed, which is why cationic water soluble porphyrins were synthesised. This was discussed further in Chapter 3.

Following the successful synthesis of three cationic porphyrins bearing a vinyl group (**Figure 82**), free radical polymerisation reactions were carried out to form different immobilised-porphyrin polyacrylamide hydrogels containing one of three porphyrins. The non-metallated porphyrin was selected as the control porphyrin, with the copper porphyrin representing a "switch off" scenario due to the decrease in the singlet oxygen quantum yield caused by the presence of the paramagnetic metal.[207,227] The palladium porphyrin was chosen due to the heavy atom effect, which was anticipated to increase the triplet state lifetime and hence the singlet oxygen quantum yield.

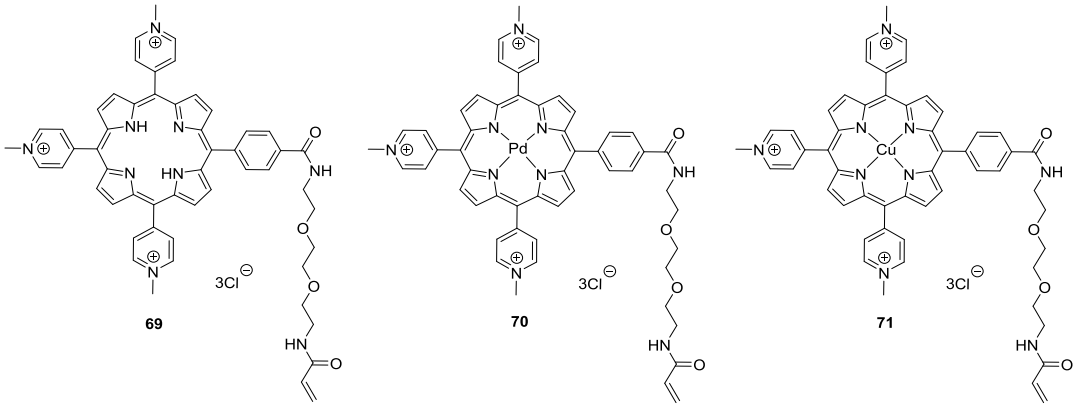

Figure 82 – Structure of three cationic porphyrins synthesised for use in formation of porphyrin immobilised on polyacrylamide hydrogels.

Figure 83 – Photograph of 1 cm^3 of the hydrogels: (a) control hydrogel (b) porphyrin hydrogel (69) with 4.0 mg of 69 (3.3 mM stock solution in PBS, pH=6.0) immobilised in it, (c) Cu(II)porphyrin hydrogel (71) with 4.1 mg of 71 (3.3 mmol L^{-1} M stock solution in PBS, pH=6.0) immobilised in it, (d) Pd(II) porphyrin hydrogel (70) with 4.4 mg of 71 (3.3 mM stock solution in PBS, pH=6.0) immobilised in it.

The optically transparent polyacrylamide hydrogels (**Figure 83**) were easily prepared by free radical polymerization of acrylamide (Am) and *N*,*N*'-methylenebisacrylamide (Bis) using ammonium persulfate (APS) and *N*,*N*,*N*',*N*'-tetramethylethylenediamine (TEMED) as the radical initiator and the catalyst, respectively.

The method used for the formation of porphyrin immobilised on polyacrylamide hydrogels followed that reported by us,[227] and Spagnul *et al.*[205] Briefly, the porphyrin was dissolved in water, to a fixed molarity (M = 3.3 mM) and added to the solution of monomers. A surfactant (SDS) was added to the mixture to prevent any aggregation of the photosensitiser and to aid the formation of a homogenous solution. SDS has been used frequently, for different photosensitisers, in solution as it helps to prevent aggregation of charged compounds in solution.[228]

Following the addition of the ammonium persulfate (APS) and *N*,*N*,*N*',*N*'-tetramethyl-ethylenediamine (TEMED), the homogenous and optically transparent hydrogels were obtained after 15-20 minutes. The control gel was obtained in a similar way, by adding the water without the photosensitiser. The gels were hydrated in deionised water for 24 hours, with the water being changed three times to remove any unreacted acrylic monomers. Analysis of these washings showed photosensitiser leaching in all cases, with the amount found to be 0.0174 mg/ cm^3 for **69**, 0.0204 mg/cm^3 for **70**, and 0.0035 mg/cm^3 for **71**. The extended stability of the gels was also tested, and after 24 h the leaching ceased, with no additional leaching occurring after this time. The amount of leaching is minimal, with **69** leaching 0.43% by mass, **70** leaching 0.5% by mass and **71** leaching 0.09% by mass.

Leaching has already been observed for other porphyrin compounds when immobilised in solid supports.[54,56–59] Carvalho *et al.* observed leaching after the formation of a

porphyrin-nanomagnet hybrid material.[54] The leaching was seen when the material was washed with water, but the amount of leaching was not quantified. Alves *et al.*[56] also observed leaching when the material was washed with solvents such as chloroform and methanol, in which the porphyrin was soluble. The washing was carried out several times until the Soret band was no longer present in the absorption spectrum. Leaching of the porphyrin from the support has been observed, but the amount was not quantified.[54,56–58] Gonzalez-Delgado *et al.*[229] measured the leaching of their porphyrin photosensitiser by measuring the decrease in absorption of the Soret band over time and they found that over six months there was a 14% decrease in the Soret band.

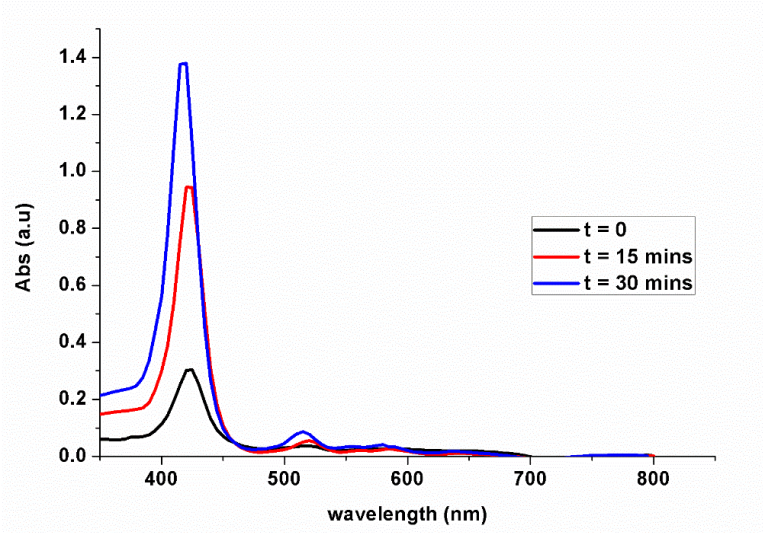

Figure 84 – UV-Vis spectra of washings of hydrogel containing 4.0 mg/cm^3 of non-metallated porphyrin in PBS pH = 7.4, with measurements taken at t = 15 minutes and t = 30 minutes showing enhanced leaching over time.

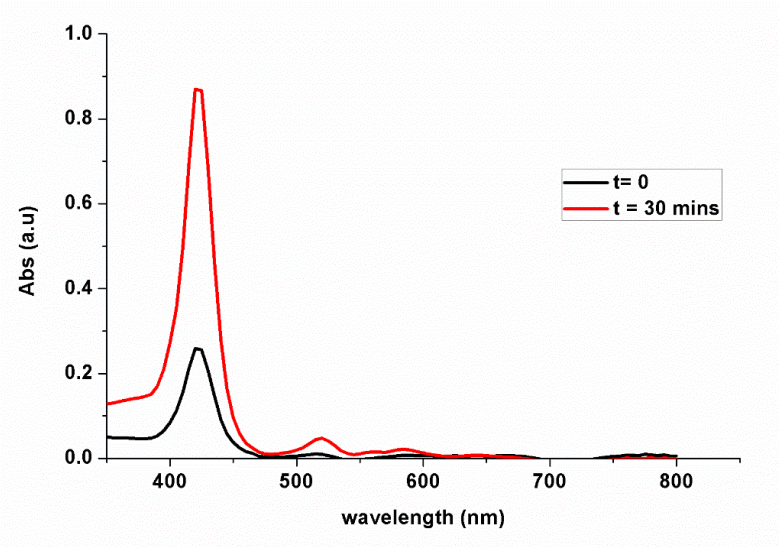

Figure 85 – UV-Vis spectra of washings of hydrogel containing 4.0 mg/cm^3 of non-metallated porphyrin in PBS pH = 7.4, following a change in the PBS solution, with measurements taken at t = 30 minutes showing less leaching compared to Figure 78.

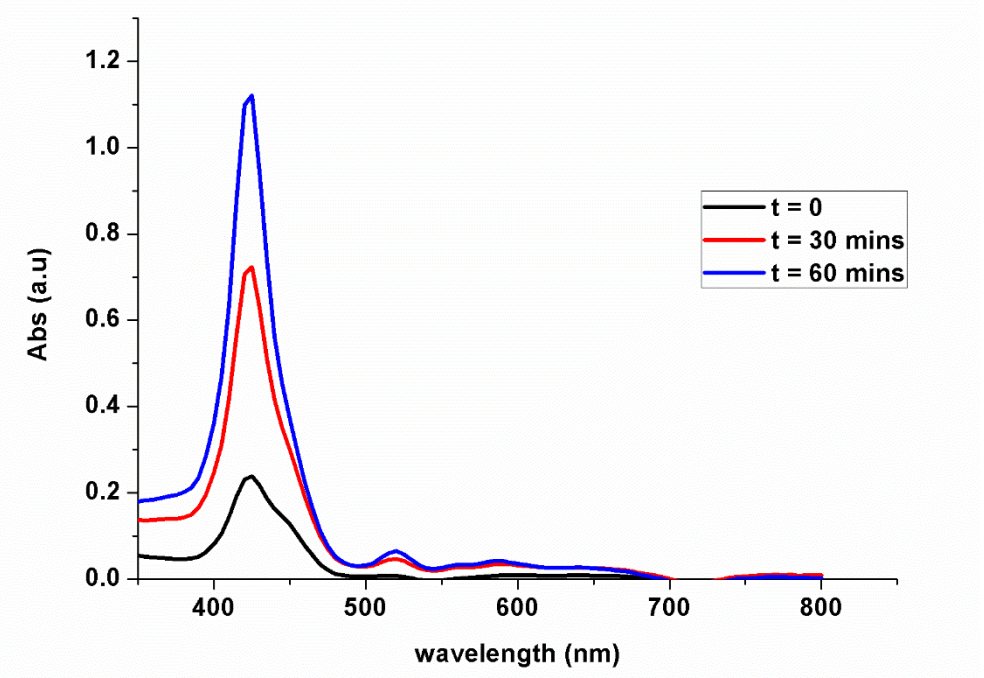

Figure 86 – UV-Vis spectra of washings of hydrogel containing 4.0 mg/cm^3 of non-metallated porphyrin in PBS pH = 6.0, with measurements taken at t = 30 minutes and t = 60 minutes showing enhanced leaching over time. The graph shows less leaching compared to Figure 79.

The leaching of the photosensitiser from the polymeric matrix was further studied in order to find a solution to minimise this effect. Initially, stability studies were carried out using phosphate buffer solution (PBS) pH = 7.4, as a standard pH for bacterial testing. When carrying out the stability studies at pH = 7.4, the hydrogel was found to leach photosensitiser, with 0.31% of the loaded photosensitiser found to leach per cm^3. A possible solution to this was the equilibration of the hydrogel in PBS first for 30 minutes, and then changing the PBS solution to remove any initially leached photosensitiser. Using this approach a lower amount of leaching of the photosensitiser was observed, with only 0.2% per cm^3 of the photosensitiser leaching by mass, following the change in PBS solution.

An alternative to changing the solution following equilibration, was the use of a different pH within the functional range of the *E.coli* test bacteria (pH 6-9). Leaching studies were carried out using PBS pH = 6.0 and the amount of leaching was found to be less than that of PBS pH = 7.4. Leaching of 0.15% per cm^3 of the porphyrin by mass was seen at pH = 6.0, in comparison to 0.2% per cm^3 at pH = 7.4, which is why PBS pH = 6.0 was chosen for bacterial testing.

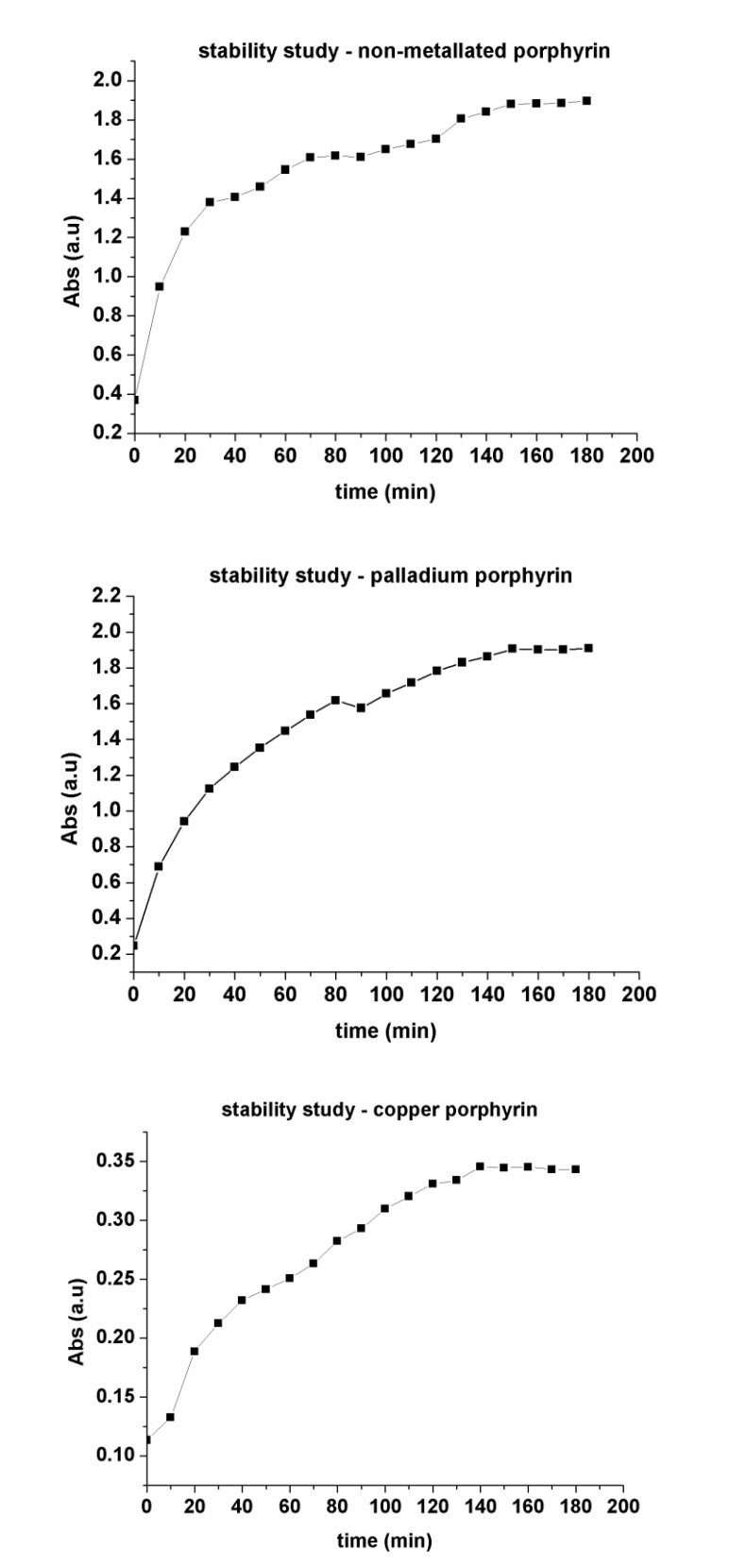

Figure 87 – Graphs showing leaching studies of 69, 79 and 71.

Stability studies were also carried out to investigate the leaching of the porphyrin from the polyacrylamide support over 3 hours (**Figure 87**). The amount of leaching was studied when the gel had been cut into a 1 cm square, which was then cut into four pieces of equal

size (0.25 cm^2). All four quarters of the gel was placed in 2 mL of PBS pH = 6.0 and the UV-Vis spectra were recorded, with readings were taken every 10 minutes. For all three porphyrins investigated, the amount of porphyrin being released reached a plateau, which indicates that no further porphyrin was being released from the matrix. For the non-metallated porphyrin and the palladium porphyrin a plateau was reached at 150 minutes, whereas for the copper porphyrin a plateau was reached after 140 minutes. The amount of time taken to reach a plateau was similar for all three porphyrins.

In order to study the effect of the UV-Vis absorption spectra when the porphyrin was immobilised in the polymeric matrix, the solid absorption spectra was obtained *via* the formation of the hydrogel inside the cuvette. The hydrogel was synthesised using the same method. However, these experiments were conducted on a smaller scale to fit the 3 mL cuvette. In general, the UV-Vis spectra for the porphyrins as a solid gave slightly broader peaks compared to the spectrum seen in solution. The slight broadening of the peaks could be due to the aggregation of the porphyrin when it is immobilised in a solid support.

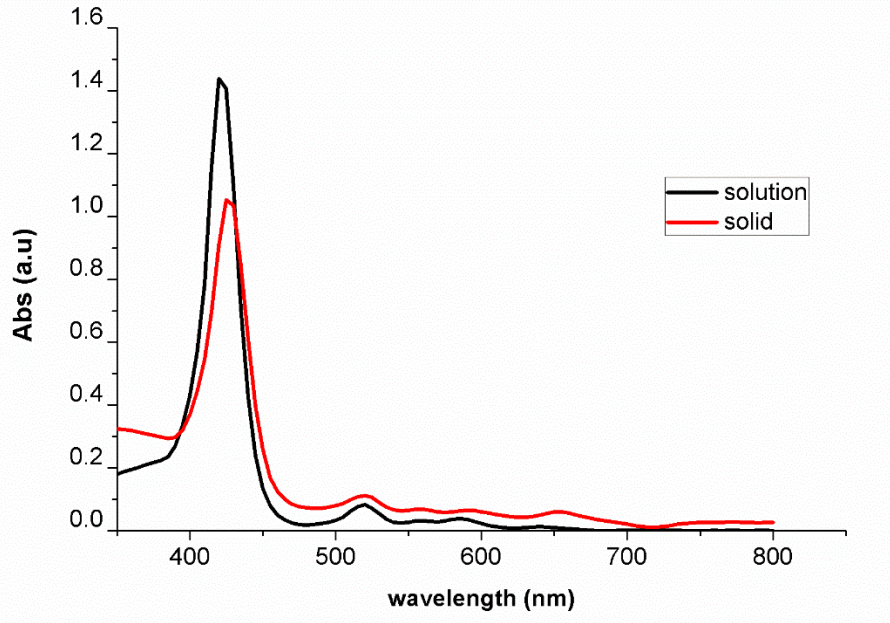

Figure 88 – UV-Vis absorption spectrum of porphyrin 69 in solution and as solid.

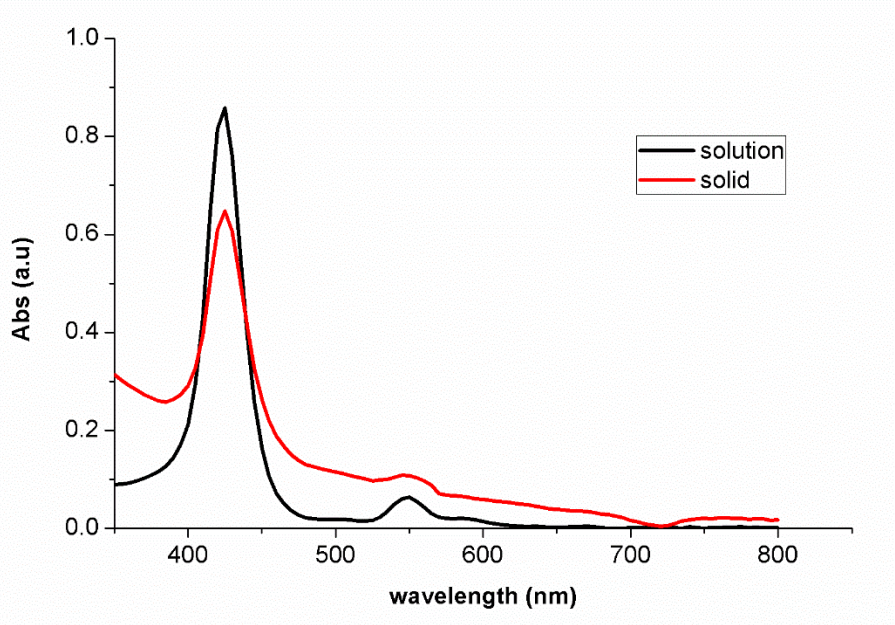

Figure 89 – UV-Vis spectrum of porphyrin 70 in solution and as solid.

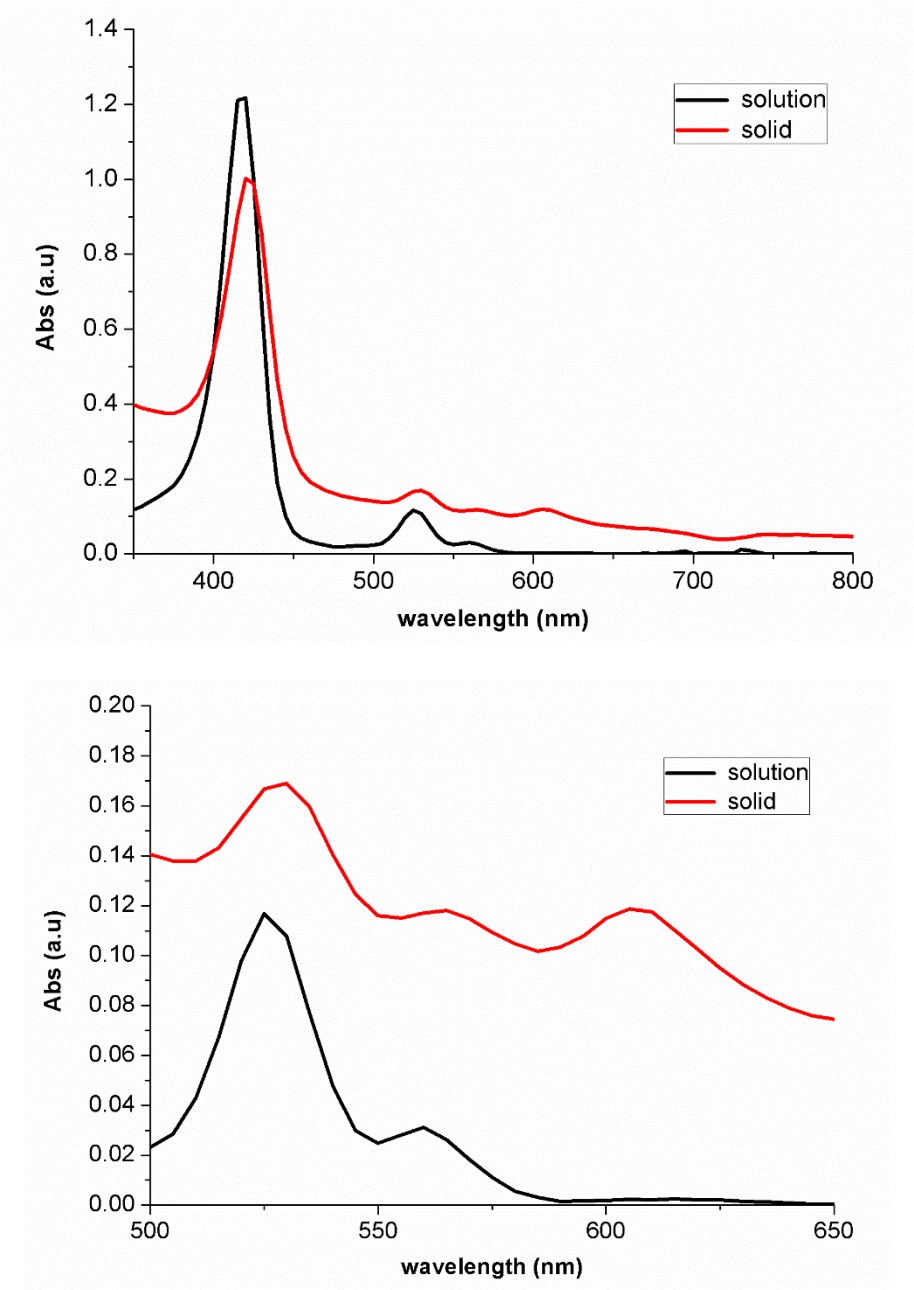

Figure 90 – UV-Vis spectrum of porphyrin 71 in solution and as solid.

The UV-Vis spectrum of porphrin **69** as a solid shows a spectrum characteristic for a porphyrin, with the Soret band at 425 nm, which has been red-shifted by 5 nm compared to **69** in PBS solution (pH = 6.0) (**Figure 88**). The absorption spectrum also shows the typical four Q-bands: the final two have been red shifted from 560 nm to 565 nm and from 645 to 650 nm, respectively.

The UV-Vis spectrum of porphyrin **70** as a solid shows a spectrum characteristic for a porphyrin, with the Soret band at 420 nm, which is the same as that of **70** in PBS solution (pH = 6.0) (**Figure 89**). The UV-Vis spectrum also shows the typical two Q-bands expected for a palladium porphyrin: the first Q-band is red-shifted by 5 nm from 525 nm

to 530 nm and the second Q-band remains the same as for the spectrum of **70** in PBS (pH = 6.0), at 560 nm. The UV-Vis spectrum is similar to **70** in PBS (pH = 6.0) which shows peaks at 420 nm, 525 nm and 560 nm, but the absorption spectrum of the solid also shows the formation of a third Q-band at 610 nm, which is not seen for the palladium porphyrin in solution. It was speculated that this is due to a change in symmetry of the porphyrin. Palladium usually sits co-planar in the porphyrin,[57,172,230] but when in solid phase the symmetry may change due to distortion of the porphyrin molecule which could be due to the polymerisation step or the different subtituents in the *meso* positions.

The UV-Vis spectrum of porphyrin **71** as a solid shows the Soret band at 425 nm, which is the same compared to **71** in PBS solution (pH = 6.0) (**Figure 90**), and the typical two Q-bands expected for a Cu(II)porphyrin, the first Q-band remains at 550 nm but the second Q-band has been blue shifted from 575 nm to 570 nm. The UV-Vis spectrum is similar to **71** in PBS (pH = 6.0) which shows peaks at 425 nm, 550 nm and 575 nm.

4.3.3 Analysis of polymeric material using scanning electron microscopy

Following UV-Vis spectroscopic analysis of the porphyrins immobilised on polyacrylamide hydrogels, analysis of the hydrogel porosity was also carried out using scanning electron microscopy (SEM).

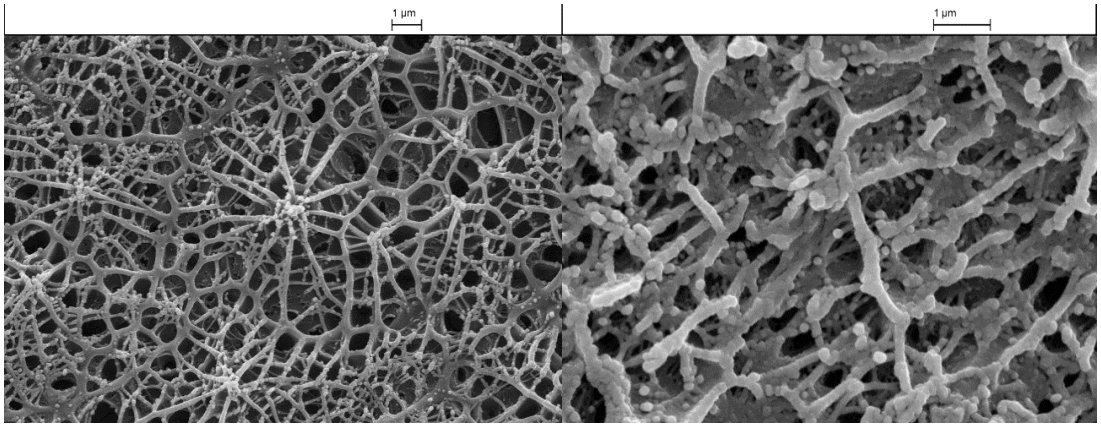

Figure 91 – Scanning electron microscope (SEM) image of control hydrogel (left). Scanning electron microscope (SEM) image of photoantimicrobial hydrogel containing porphyrin 69 (right).

The morphologies of all the hydogels were first investigated. The SEM images were analysed using ImageJ,[231] which allows for the diameter of the pores to be measured. For the blank hydrogel containing no photosensitiser a continous and non-ordered microporous mesh like network was observed with a mean diameter of 122 ± 14 nm (**Figure 91**). Similarly, the SEM of **69** showed a continous and porous mesh like structure,

but with less order. Within this less ordered structure there is a finer mesh like non-ordered porous structure. The mean pore diamater was found to be 140 ± 31 nm (**Figure 91**).

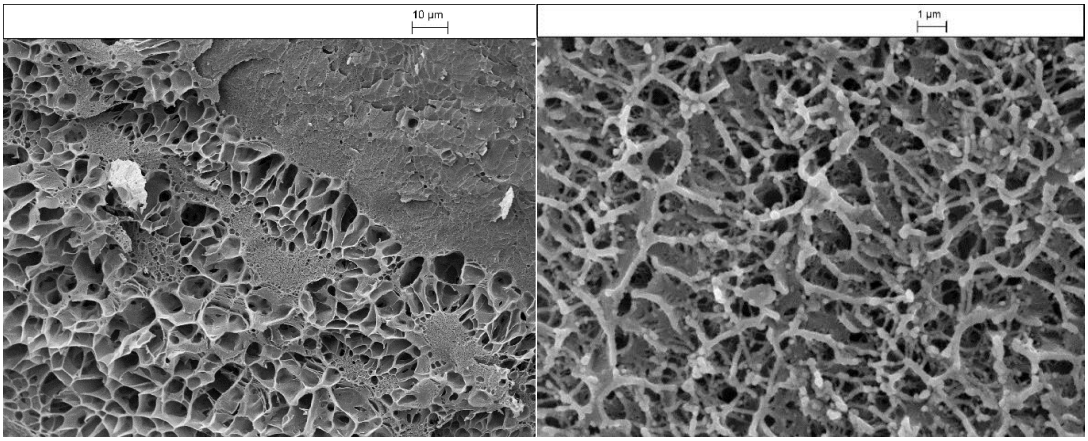

Figure 92 – Scanning electron microscope (SEM) image of photoantimicrobial hydrogel containing porphyrin 70 (left). Scanning electron microscope (SEM) image of photoantimicrobial hydrogel containing porphyrin 71 (right).

Analysis of the photoantimicrobial hydrogels containing photosensitisers **70** and **71** showed similar results to those of **69** with a porous structure and a finer mesh like structure. The hydrogel containing the palladium porphyrin (**Figure 92**) (**70**) had a pore diameter of 204 ± 72 nm, the hydrogel containing the copper porphyrin (**Figure 92**) (**70**) had a pore diameter of 128 ± 32 nm. The pore diameter sizes were within the same range when comparing the different porphyrins immobilised in the hydrogels, which shows consistency in the formation of the homogenous gels.

4.4 Analysis of ROS generation using porphyrin immobilised on polyacrylamide support

Following successful formation of three different cationic porphyrins immobilised on polyacrylamide hydrogels, the formation of reactive oxygen species was investigated.

Porphyrins are known to produce singlet oxygen upon irradiation of light of a specific wavelength in the presence of ground state molecular oxygen.[232,169] A common way to detect singlet oxygen is either through singlet oxygen probes such as singlet oxygen sensor green (SOSG), or *via* molecules which react with singlet oxygen to cause a spectroscopic change that can be monitored using UV-Visible spectroscopy, such as 9,10-Anthracenediyl-bis(methylene)dimalonic acid (ABDA), and the formation of its corresponding endoperoxide (**Figure 93**).[233]

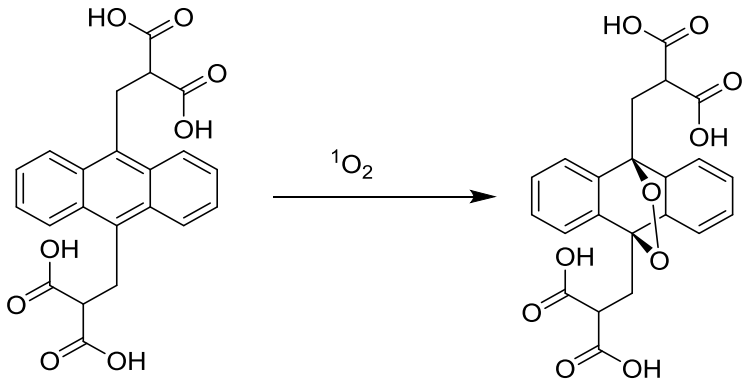

Figure 93 – 9, 10-Anthracenedicyl-bis(methylene)dimalonic acid as a singlet oxygen detector, showing changes in molecular structure upon reaction with singlet oxygen.

Due to ease of analysis using UV-Vis spectroscopy, ABDA was selected as the singlet oxygen detector. The measurements were carried out using irradiation with a cut on filter (> 550 nm), which is in within the range of the UV-Visible spectra of the porphyrins synthesised. The gels formed were cut into 1 cm squares and then divided further into four pieces to maximise the surface area of the gel for the formation of singlet oxygen.

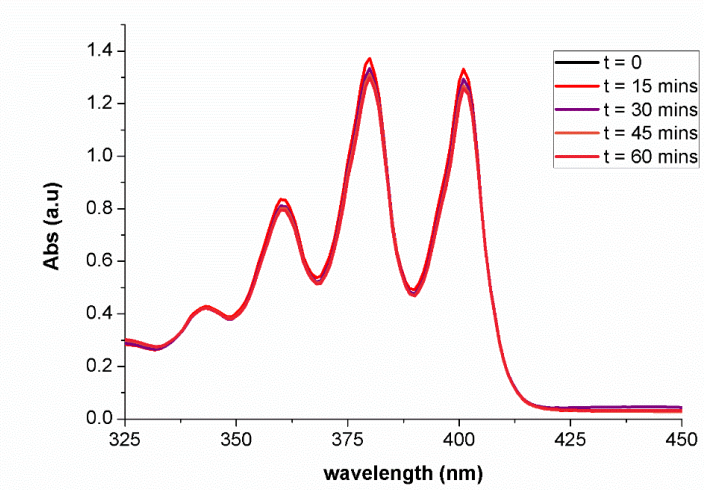

Figure 94 – Singlet oxygen testing using blank polyacrylamide hydrogel.

Initially the blank hydrogel was tested for the production of singlet oxygen, as it was crucial to prove that the gel itself does not produce singlet oxygen (**Figure 94**). The graph shows no decrease in absorbance for the ABDA peaks, which indicates that there is no singlet oxygen being produced, which is expected as reported by Spagnul *et al.*[205]

Following this, the photo-antibacterial hydrogels were evaluated for the production of singlet oxygen. Both the non-metallated porphyrin and the palladium porphyrin showed the same decrease in absorbance indicating the production of singlet oxygen (**Figure 95**),

which was expected for both porphyrins. The palladium porphyrin on the polyacrylamide support showed a different spectrum compared to the non-metallated porphyrin: the decrease in absorbance was sharp: furthermore, the production of a new peak at 430 nm was faster. Indeed, after 30 minutes of irradiation the peaks for the ABDA were no longer distinctive and the formation of the new peak at 430 nm was seen, demonstrating the palladium porphyrin is more efficient in the production of singlet oxygen.

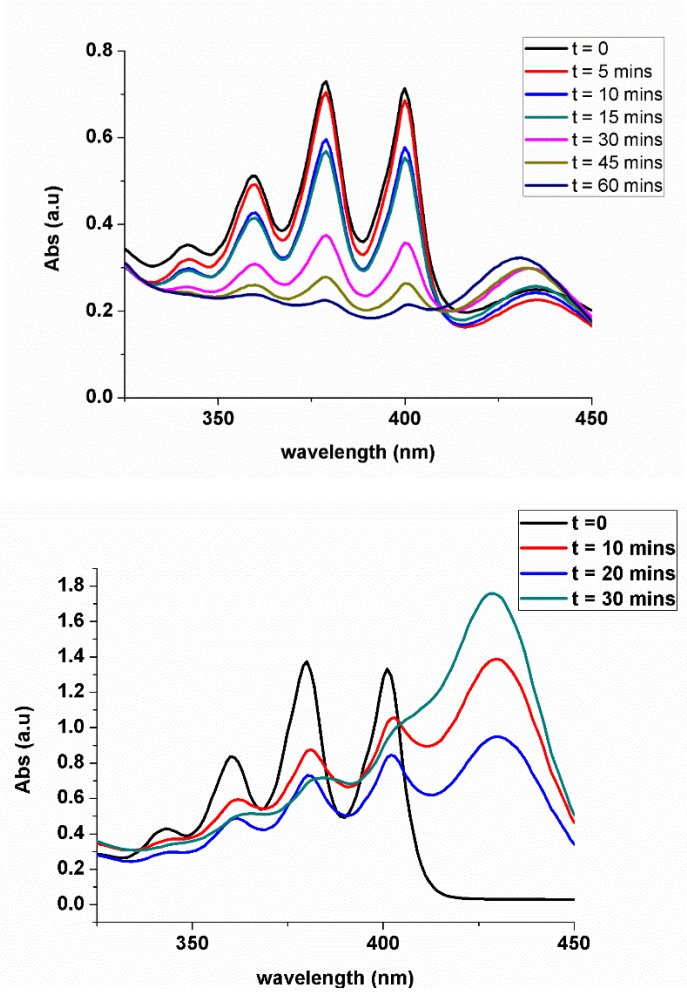

Figure 95 – Singlet oxygen testing using porphyrin photobacterial hydrogel containing porphyrin 69 (top) and porphyrin 70 (bottom).

The copper porphyrin showed different results compared to the free-base and the palladium porphyrin immobilised on polyacrylamide (**Figure 96**), with less than a 0.2 absorbance decrease, indicating the production of singlet oxygen but less than that of the free base and the palladium porphyrin when immobilised on polyacrylamide. The presence of the paramagnetic metal is known to decrease the singlet oxygen quantum yield.[38] Interestingly, the decrease in absorbance was only seen after 20 minutes of irradiation with white light, so the paramagnetic metal seems to be delaying the production of singlet oxygen.

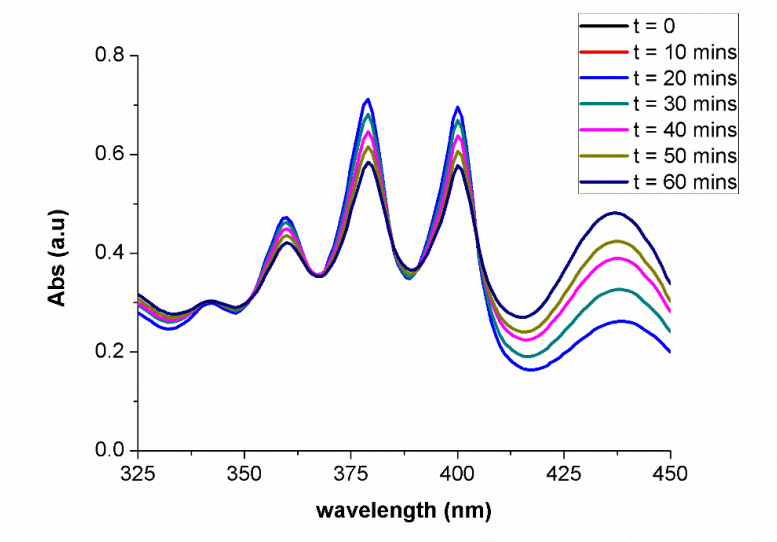

Figure 96 – Singlet oxygen testing using porphyrin photobacterial hydrogel containing porphyrin 71.

The increase in the peak seen in all three UV-Vis spectra at approximately 430 nm is speculated to be due to the small amount of leaching of the porphyrin from the matrix, but this wavelength is slightly shifted compared to the reported wavelength for the Soret band, this might be due to the presence of the porphyrin in solid support, the absorbance value is minimal.

Overall the synthesis of the three different porphyrins immobilised on the polyacrylamide support was successful, and it allows a direct comparison between the three porphyrins to be carried out. The study shows that the presence of the heavy atom palladium does increase the production of singlet oxygen and the presence of copper does hinder the presence of singlet oxygen. The porosity of the materials, and the mouldability makes them ideal for use in any situation where a sterilising surface is required.

The next step was the analysis of the photoactive hydrogels against bacteria, firstly in a bacterial broth solution and then as a more complex system. Biological evaluation will allow more information to be collected on the different behaviours on the three porphyrins used for immobilisation, it will give a better idea of the activity of the copper porphyrin against bacteria and will show how much the presence of the palladium in the porphyrin affects the bacterial killing.

4.5 Conclusions

In conclusion investigations have been carried out into the use of two different polymeric supports for the immobilisation of porphyrins; firstly silica and secondly polyacrylamide. The two supports had already been reported in the literature and showed promise for the immobilisation of photosensitisers.

The silica support showed promise in the entrapment of the porphyrin and polyviologen, but the main problem was that there was leaching observed of the porphyrin from the silica matrix. Another problem experienced with the silica matrix was the glassy-like texture making it more difficult to work with, compared to the polyacrylamide.

The polyacrylamide support was used, both for the entrapment of polyviologens and porphyrins and also for the covalent attachment of porphyrins *via* a peptide bond. The entrapment of porphyrin and polyviologen in the polyacrylamide matrix was challenging, as non-water soluble porphyrins were used to allow for the comparison of non-metal and metallated porphyrins. The hydrogels formed were found to leach porphyrin from the matrix, suggesting a need for covalent attachment of the porphyrin to the acrylamide matrix *via* a vinyl moiety on the porphyrin. The formation of the covalently bound porphyrin to the polyacrylamide was successful and allowed comparison between a metal free, copper and a palladium porphyrin in the production of reactive oxygen species. The photobacterial hydrogels have been analysed by SEM to study the pore structure and diameter, which was found to be porous with similar pore sizes found for the different porphyrins immobilised as well as the blank hydrogel. Following the successful analysis of the photoactive hydrogels in the production of singlet oxygen they were tested against bacteria to study the bacterial killing of the photoactive hydrogels formed.

5 Biological evaluation of three different cationic porphyrins immobilised on polyacrylamide hydrogels.

5.1 Introduction

The use of photosensitisers immobilised on polymeric surfaces to combat healthcare-associated infections is a flourishing area of research. There is a desperate need for a solution to this deadly problem which is estimated to cause 300,000 infections in the United Kingdom every year.[2,5,149] In Europe antibiotic resistant bacteria causes 25,000 deaths a year, the number is expected to increase unless drastic measures are taken to reduce poor hygiene.[2,3] Healthcare associated infections (HAIs) are a massive threat to the NHS and other healthcare services across the world.[1] HAIs occur due to both Gram-positive and Gram-negative bacteria, with the most common in hospital settings being *S.aureus* and its methicillin resistant strain *MRSA*, and *E.coli*.[5,149]

The immobilisation of photosensitisers on polymeric supports offers many advantages over conventional methods of antimicrobial PDT, whereby the photosensitiser was in a solution or cream. Advantages include; decreased toxicity, since when the photosensitiser is immobilised on a polymeric support the amount of leaching is negligible. Another advantage is the reusability of the photoactive material. A number of different materials have been investigated for the immobilisation of photosensitisers including both natural and synthetic supports.[32] Recently, the biological evaluation of photosensitisers immobilised on polymeric supports has become increasingly important due to the need of new solutions to the antibiotic problem.

Bacteria can be divided into two main categories; Gram-positive and Gram-negative bacteria, based on the structure of the bacterial cell wall. Gram-positive bacteria such as *S.aureus*, have a simple bacterial cell wall, compared to Gram-negative bacteria such as *E.coli*, making them less challenging to inactivate. Porphyrin-mediated photosensitisation has been shown to be more toxic towards Gram-positive bacteria than Gram-negative bacteria.[234]

5.1.1 Immobilisation of porphyrins on polymeric supports

Recently biological testing of photoactive surfaces has been carried out against both Gram-positive and Gram-negative bacteria.[32,54,57–59,64,65,67,69,70,78,84,234–240] This project focused on the investigation of porphyrins immobilised on polymeric supports against *E.coli*. This Gram-negative strain of bacteria was chosen because it is known to be harder to inactivate compared to Gram-positive bacteria.

A number of different polymeric supports have previously been investigated for the immobilisation of porphyrins against *E.coli* including; carbon nanotubes,[234] cellulose (cotton),[59,65,67,69,238] polystyrene,[236,237] polyurethane,[235] chitosan[70] and silica.[54,57,84]

5.1.2 Bacterial testing on porphyrins immobilised on carbon nanotubes

Banerjee *et al.* evaluated the photoinactivation of both *S.aureus* and *E.coli* when protoporphyrin IX was covalently bound to carbon nanotubes.[234] Functionalisation of PPIX was carried out to incorporate an amine group, which was used for the covalent attachment to the carboxylic acid-functionalised carbon nanotubes. The film formed was found to be successful in killing *S.aureus*, with only a few viable cells remaining following incubation of the conjugate at a concentration of 0.1 mg/mL and exposure to visible light for 15 minutes. Following 5 minutes of irradiation, 50% of the bacterial cells survived; and following 10 minutes of irradiation, only 10% of the bacterial cells survived. When the PPIX conjugate was tested against Gram-negative bacteria *E.coli* it was found to be unsuccessful, even after an increase in the porphyrin concentration to 4.0 mg/mL and irradiation times as long as 2 hours there was no inactivation of *E.coli* observed. The results in this paper support the proposal that porphyrins are able to inactivate Gram-positive bacteria with more ease than Gram-negative bacteria.

5.1.3 Bacterial testing on porphyrins immobilised on chitosan

Chitosan is a natural polymer, and therefore the covalent attachment of porphyrin can be more challenging. Bonnett *et al.* investigated the immobilisation of two porphyrins (**Figure 97**) on chitosan for biological testing against *E.coli*.[70]

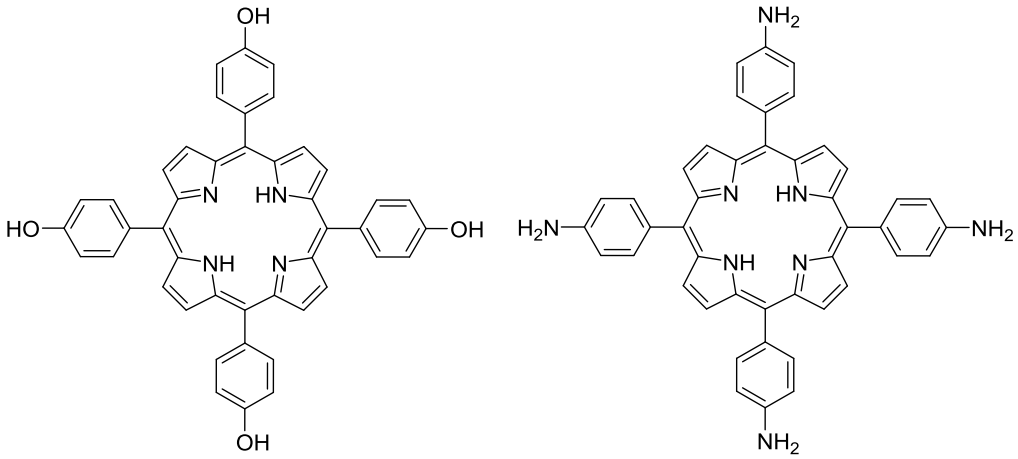

Figure 97 – Structure of two porphyrins that have been immobilised on chitosan (5,10,15,20-tetra[4-hydroxyphenyl] porphyrin) and (5,10,15,20-tetra[4-aminophenyl]porphyrin) by Bonnett *et al.*[70]

A comparative study was carried out between the two porphyrins to study how effective they were at inactivating *E.coli* using a 500 W halogen lamp. The concentration of porphyrin in the chitosan membrane was estimated to be 5.7 µg cm^{-2}.The use of 5,10,15,20-tetra[4-aminophenyl]porphyrin showed complete bacterial cell death after 90 minutes, whereas the 5,10,15,20-tetra[4-hydroxyphenyl showed a slower rate of bacterial cell death, although complete killing was also observed after 90 minutes. This paper shows promising results for the inactivation of the Gram-negative bacteria, *E.coli* using a neutral porphyrin and a protonated amino porphyrin immobilised on a surface.

5.1.4 Bacterial testing on porphyrins immobilised on cellulose

The use of cellulose as a support for the immobilisation of porphyrins and their bacterial evaluation has proven popular.[59,65,67,69,238]

Krouit *et al.* investigated the immobilisation of PPIX on lipophilic cellulose esters. They then investigated the production of singlet oxygen by the porphyrin hybrid material and following this evaluated the activity against *E.coli*.[65] The chosen porphyrin, PPIX, was covalently bound to the polysaccharide polymer (**Figure 98**). The porphyrin was shown to produce singlet oxygen by testing ergosterol acetate photo-peroxidation.

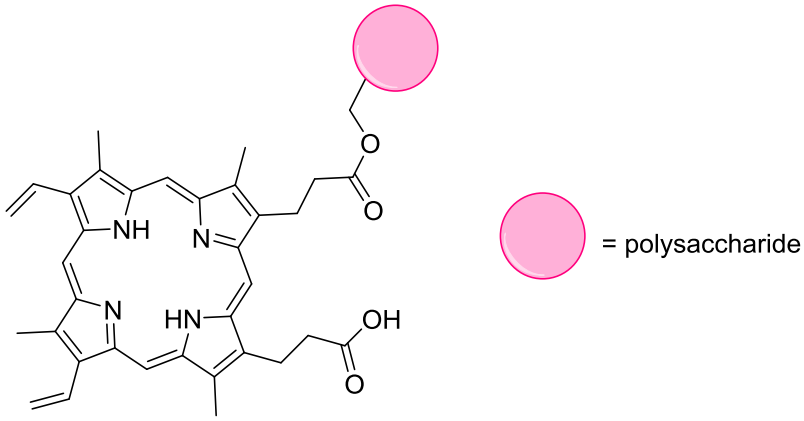

Figure 98 – Structure of PPIX covalently attached to polysaccharide polymer by Krouit *et al.*[65]

Biological testing of PPIX covalently attached to polysaccharide was carried out using four 150 W tungsten bulbs with a total fluence rate of 1.7 mW cm^{-2}, and with several different porphyrin concentrations immobilised ranging from 0.19-1.1%. Even the lowest concentration of immobilised porphyrin allowed the complete inactivation of *S.aureus*, but for the inactivation of *E.coli* only the surfaces containing 0.52-1.1% loading of porphyrin were found to be efficient for the inactivation of *E.coli*. This particular example

shows promise for the use of immobilised commercially available photosensitisers for the inactivation of *E.coli* and *S.aureus*.

Continuing their interest in this area Krouit *et al.* decided to explore the effect of the length of the spacer arm between the porphyrin and support to determine if this has an effect on the photoantibacterial properties.[67] The two porphyrins used had varying chain lengths (between 1 and 8 carbon chain length) for conjugation to the cellulose support. Following successful conjugation, the two photoactive supports were tested for the production of singlet oxygen using the same method as previously described by Krouit *et al.*[65] Biological testing was carried out by cutting out the plastic discs and placing them on nutrient agar which has been seeded with the two different bacterial strains (*S.aureus* and *E.coli*). The two different supports were tested both in the dark and under illumination with light from four 150W tungsten bulbs with a total fluence rate of 1.7 mW cm^{-2}. Both of the porphyrin-cellulose laurate ester materials showed similar photoactivity against both strains, but only if the grafting percentage was higher than 0.16. The results showed that the length of the spacer did not have a significant effect of the inactivity of the two bacterial strains.

A different approach was taken by Feese *et al.* whereby the click reaction was used to immobilise an alkyne functionalised porphyrin on cellulose nanocrystals that have been pre-functionalised with azide groups (**Figure 99**).[59]

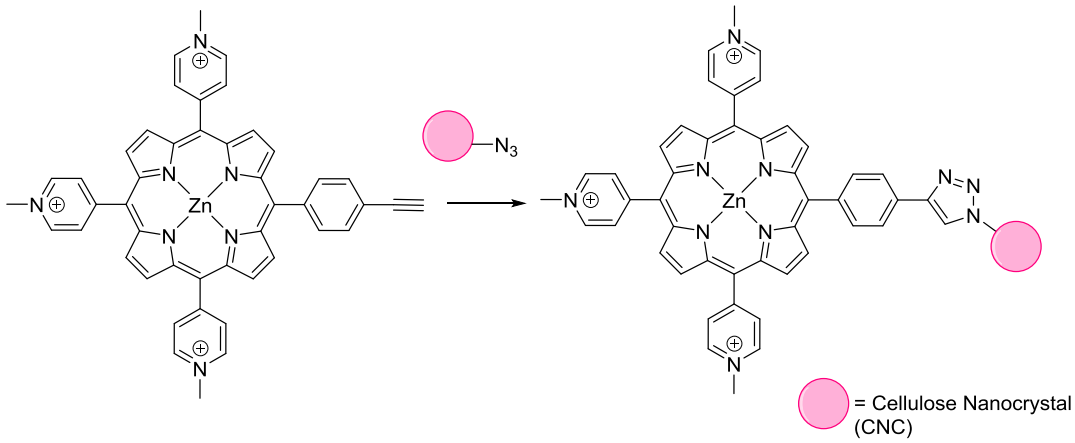

Figure 99 – Cationic porphyrin immobilised on CNC by Feese *et al.*[59]

Biological evaluation of the system was carried out using cell survival assays and the plating technique, where a maximum of a 6 log reduction could be detected. The CNC-porphyrin conjugate was tested against three different strains of bacteria; *E.coli*,

M.smegmatis and *S.aureus*, a fluence rate of 60 mW cm^{-2} was used for 15 mins or 30 mins of irradiation which is equivalent to a total fluence of 54 or 108 J cm^{-2} respectively. Following bacterial testing *E.coli* was found to be the least susceptible to photodynamic inactivation at a porphyrin concentration of 20 μM, there was no statistically significant inactivation of *E.coli* following 15 minutes of illumination. However, when the time was increased to 30 minutes a 1-2 log reduction was observed. There was no toxicity towards *E.coli* seen in the dark. Both *M.smegmatis* and *S.aureus* showed higher bacterial inactivation than *E.coli*. Even though the photodynamic inactivation of *E.coli* was lower than that observed for the other two bacterial strains, the amount of inactivation shows promise for the use of immobilised porphyrins against *E.coli*.

Memmi *et al.* also investigated the covalent attachment of two different porphyrins bearing an alkyne functionality to azide functionalised cellulose.[238] The two porphyrins chosen were protoporphyrin IX (PPIX) modified with an alkyne functionality and tritritoylporphyrin with a benzylethoxy alkyne substituent (**Figure 100**).

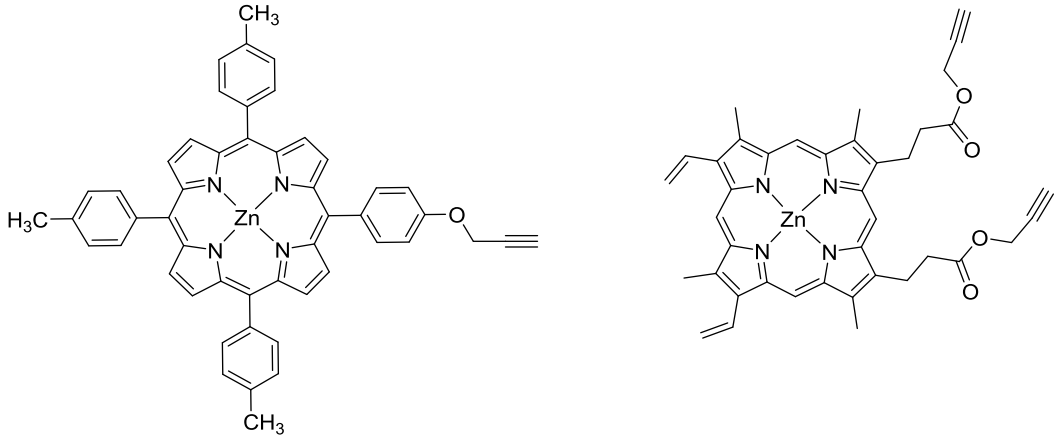

Figure 100 – Structure of two alkyne functionalised porphyrins used in a click reaction by Memmi *et al.*[238]

The porphyrinated films prepared by Memmi *et al*. were tested against three strains of bacteria; Gram-positive *S.aureus*, Gram-negative *E.coli* and Gram-negative *P.aeruginosa* to study their ability to photoinactivate the bacteria. The testing was carried out by cutting a disc out from the porphyrinated film and depositing it on the nutrient agar which had been seeded with the target strain. A fluence rate of 1.7 mW cm^{-2} was used, and following irradiation the results showed that the film containing PPIX with only 0.76 % porphyrin encorporated was not able to kill any of the three strains of bacteria, but with incorporation above 1% both porphyrins were able to inactive all three strains of bacteria successfully. No comparison was made regarding the time taken to inactive the three

different strains of bacteria, so there is no indication of the ease of killing of the *E.coli* compared to the other two bacteria.

Mbakidi *et al.* investigated the use of a cationic porphyrin (**Figure 101**) for the immobilisation on cellulose paper, and studied the bacterial inactivation against *S.aureus* and *E.coli*.[69]

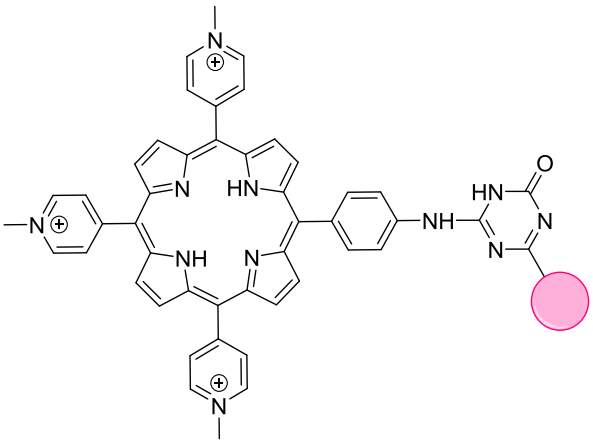

Figure 101 – Structure of porphyrin used for immobilisation on cellulose paper by Mbakidi *et al.*[69]

The grafting yield of the porphyrin to the cellulose paper was reported to be 55% (0.03µmol/mg of paper). Following successful grafting of the porphyrin to the cellulose paper the material was tested for its antibacterial activity against both *S.aureus* and *E.coli*. Following a 24 hour exposure to light with a total fluence of 9.5 J cm^{-2} there was no surviving bacteria present for either *S.aureus* or *E.coli*. The synthesised materials show good preliminary results against both the Gram-positive and Gram-negative bacteria, but further testing would be required.

5.1.5 Bacterial testing on porphyrins immobilised on silica supports

The use of silica as a support has become increasingly popular due to the versatility of this material; it can be used either in the form of micro or nanoparticles, or for the formation of glassy-like materials using TEOS, THES or TMOS as discussed in the previous chapter.[54,57,84]

Magaraggia *et al.* investigated the encapsulation of a tetracationic meso-substituted amphiphilic porphyrin in silica microparticles to give a conjugate which has a mean particle diameter of 0.9 µm. These researchers then studied the production of singlet oxygen using ADPA as well as carrying out biological evaluation against both Gram-positive (*MRSA*) and Gram-negative bacteria (*E.coli*).[57] When studying the singlet

oxygen testing using ADPA the graph showed an increase in absorbance around that seen for the Soret band of a porphyrin, which could indicate leaching of the photosensitiser although there was no report of this. The two strains of bacteria were evaluated with a fluence rate of 100 J cm^{-2} during irradiation. The Gram-positive bacteria methicillin-resistant *Staphylococcus aureus* (*MRSA*) was found to have a 4 log reduction following exposure to visible light for 20 minutes, a similar decrease was observed for *E.coli* but this required 30 minutes of illumination. When the porphyrin-microparticle conjugates were analysed in the dark they were found to be non-toxic. The results obtained show promise for the use of silica-porphyrin conjugates for PACT.

Carvalho *et al.* decided to take a different approach and use magnetic nanoparticles surrounded by a silica shell for the attachment of cationic porphyrins.[54] The immobilisation method was discussed previously in chapter 4. Briefly, the porphyrin used was a cationic porphyrin that was covalently attached to the silica outer shell *via* a pentafluorobenzene linker. The amount of porphyrin covalently bound was found to be between 4-5%. Before biological evaluation was carried out against *E.coli* the support was tested for the production of singlet oxygen using 1,3-diphenylisobenzofuran (DPiBF), this method is a qualitative technique but still showed that singlet oxygen was being produced. Following the detection of singlet oxygen the materials were tested again Gram-negative bacteria *E.coli*, the cationic porphyrins were the most effective against *E.coli*, as predicted.[241] Irradiation with white light at a fluence rate of 40 mW m^{-2} for 270 minutes with a total light dose of 64.8 J cm^{-2} showed a 4.8 log reduction for *E.coli* when the concentration of the porphyrin-hybrid was 200 μm. The results in this paper show a direct comparison between cationic and neutral porphyrins immobilised on surfaces, and enabled the conclusion that the cationic charge on the porphyrin aids in the photodynamic inactivation of *E.coli*.

Rychtarikova *et al.* also investigated the use of silica gels for the immobilisation of porphyrins, and carried out biological testing against *E.coli*.[84] A tetrasubstituted cationic porphyrin was chosen for immobilisation on silica, comparing two different sources of silica support, TMOS and THES. Firstly the supports were tested for the production of singlet oxygen *via* the iodometric method which was found to be successful. Following this, anti-bacterial testing was carried out using genetically modified organism (GMO) *E.coli* BL21 (DE3) producing red fluorescent protein in a medium with ampicillin and lactate. Bacterial testing was carried out both under illumination with light and in the dark. There was found to be no bacterial killing the dark, and in the light the THES

composites with the lower specific surface area were found to be more successful than the TMOS analogues.

5.1.6 Bacterial testing on porphyrins immobilised on alternative supports

Polyurethane (PUR) has been investigated by Mosinger *et al.* for the immobilisation of porphyrins for PACT.[235] Tetraphenylporphyrin was immobilised on PUR to give a nanofabric with a thickness of 0.03 mm and a loading of 0.12% of tetraphenylporphyrin. Bacterial evaluation was carried out for the porphyrin-nanofabric against Gram-negative bacteria *E.coli*. Small pieces of the nanofabric were cut for testing against GMO *E.coli* DH5α with plasmid PGEM11z which produces β-galactosidase which causes the bacterial cells to turn blue-green once they have been inactivated. Illumination was carried out with a white light (150 W halogen bulb) for 60 minutes and the porphyrin-nanofabric showed photoinactivation of the *E.coli*, but no specific data was given on the amount of inactivation.

The use of polystyrene as a polymeric support for the immobilisation of porphyrins has been investigated by Henke *et al.*, who utilised tetraphenylporphyrin on electrospun polystyrene fibres to study antibacterial effect.[236] This specific study investigated the effect of wettability and hydrophobicity on the antibacterial activity of the porphyrin-polystyrene fibres. Three different treatments were carried out; i) sulfonation, ii) cold oxygen plasma treatment and iii) coating of PDA on the surface of the material. When evaluated against Gram-negative bacteria *E.coli*, the results showed that the best bacterial killing was seen following sulfonation with complete inactivation occurring after 20 minutes of irradiation by a 400 W solar simulator. The other two treatments also showed inactivation of *E.coli*, with only 20% colony forming units (CFU) remaining following irradiation for 20 minutes. The increase in wettability was found to increase the antibacterial activity of the surface. The use of polystyrene shows promise for the immobilisation of porphyrins, as irradiation caused killing of *E.coli*.

Jesenska *et al*. also investigated the use of electrospun fibres for the immobilisation of tetraphenylporphyrin for use in the photoinactivation of bacteria.[237] This particular study compared three different electrospun fibres; polyurethane, polystyrene, polycaprolactone and polyamide 6 with respect to production of singlet oxygen and the inactivation of bacteria. Singlet oxygen production was monitored using iodometric analysis, and all three supports were found to produce singlet oxygen. Antibacterial evaluation was carried out against GMO *E.coli* DH5α containing the PGEM11Z plasmid, which allowed for easy

detection of inactivation. The amount of porphyrin grafted to the support was 1%, and the results, showed that following irradiation with white light (150W halogen bulb) for 90 minutes there was strong inhibition of bacterial colony growth on the polyurethane support. Similar results were obtained for polystyrene and polycaprolactone, but the polyamide 6 did not show such high levels of inactivation.

5.2 Motivation

Following the research that has already been carried out, the main issue in the inactivation of Gram-positive and Gram-negative bacteria seems to be finding a surface that is able to inactive both Gram-positive and Gram-negative bacteria. The formation of this particular surface has proved challenging due to the complex cell structure of Gram-negative bacteria making it more difficult to inactivate.[9]

The use of porphyrins immobilised on supports has proven interesting, with bacterial studies being carried out on Gram-positive bacteria *S.aureus* and Gram-negative bacteria *E.coli*. It was thought that positively charged photosensitisers were more likely to inactivate Gram-negative bacteria,[54,241] and this was proven true when a study was carried out by Carvalho *et al.* who compared the bacterial activity of both neutral and cationic porphyrins. The cationic porphyrin showed better activity against *E.coli* when compared to neutral porphyrins.[54] A recent study carried out by Spagnul *et al.* investigated the use of methylene blue (MB) immobilised on polyacrylamide for use in PACT.[205] The study compared the inactivation of both the Gram-positive and Gram-negative bacteria, and the results showed that there was greater inactivation of the Gram-positive bacteria than the Gram-negative bacteria.

Another important factor to consider when designing a photoactive support is the reusability of the support. This is important as it would allow the same surface to be used multiple times without the need of reapplication. Of the literature investigated, reusability was mentioned only by Spagnul *et al*. who tested the number of cycles that the methylene blue-polyacrylamide hybrid was viable for, and found that the material gave significant anti-bacterial activity for five cycles (150 minutes).

5.3 Biological evaluation of three cationic porphyrins immobilised on polyacrylamide against *Escherichia coli*.

Biological testing of porphyrins immobilised on polyacrylamide hydrogels was carried out as a collaboration with Professor John Greenman, Department of Life Sciences, University of the West of England, Bristol, with assistance from Dr. Cinzia Spagnul.

Biological testing was carried out against a genetically modified organism (GMO) *E.coli* DH5α containing the plasmid pGLITE, a derivative of pBBR1MCS-2 containing the lux CDABE operon of *photorhabdus luminescens*. It was maintained from frozen stock on nutrient agar, with the addition of kamomycin to help maintain the lux plasmids.[242] The use of genetically modified *E.coli* allowed for detection of bacterial death by bioluminescence using a luminometer. This allowed for more rapid detection of bacterial inactivation.[205]

Bacterial evaluation of the three porphyrins immobilised on polyacrylamide was carried out to study the porphyrin-polyacrylamide hybrids in real-life scenarios, and to evaluate their activity against *E.coli*. Three different cationic porphyrins were chosen: a free-base, a palladium porphyrin and a copper porphyrin (**Figure 102**). The three different porphyrins were chosen to study the effect of the complexation of a metal on anti-bacterial activity. It was anticipated that the palladium porphyrin would increase the bacterial activity due to the heavy atom effect, and that the copper porphyrin would have negligible activity against bacteria due to the presence of the paramagnetic metal. [204, 207,208]

The paramagnetic nature of copper porphyrins has meant that in some cases the phototoxicity has been decreased,[208] and the copper porphyrin has either no effect or little effect on enzyme activity. There has also been research that shows a copper porphyrin with activity but *via* a different mechanism. Antoni *et al.* investigated the activity of non-metallated porphyrins, zinc porphyrins and copper porphyrins. It is known in the literature that copper porphyrins, due to their paramagnetic properties, are not luminescent and do not produce singlet oxygen,[208,168] but the study carried out by Antoni *et al*. showed evidence of a copper porphyrin producing hydroxyl radicals ($OH^{\cdot}$) after irradiation with light.

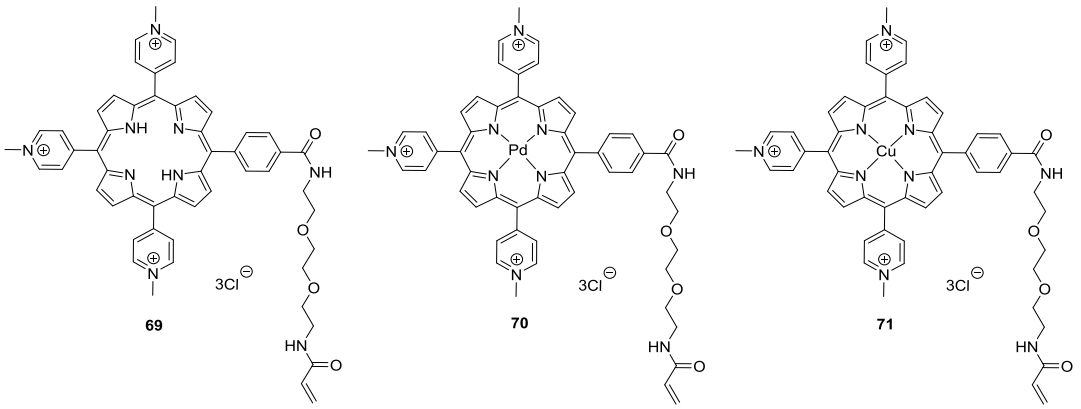

Figure 102 – Structure of three different porphyrin conjugates synthesised used for immobilisation.

Initially tests were carried out to study the effect of using white light on the *E.coli*. These tests were carried out to ensure that the light was not killing the bacteria itself, and that the bacteria are stable in the intensity of light used. The test was also carried out to ensure that bacteria were not being inactivated in a medium of pH = 6.0, which is the pH proposed for testing. To carry out the testing, a standard method was used; a solution of *E.coli* (100 µL *E.coli* and 1900 µL phosphate buffer solution (PBS), pH = 6.0) was placed in a tube, and the measurements were taken every minute for both the sample under irradiation with white light and the sample in the dark.

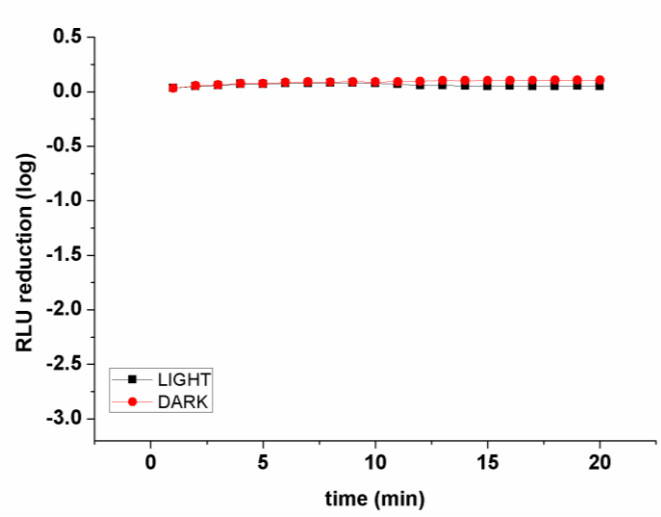

Time (mins)	Log killing (light)	Log killing (dark)
10	+0.0765	+0.0905
20	+0.0508	+0.105

Figure 103 – Kill curve obtained for *E.coli* control test with no polyacrylamide hydrogel present both in the light and in the dark using PBS at pH = 6.0.

The test showed growth of the bacteria under both light and dark conditions. After 20 minutes +0.0508 log growth was seen in the light, and in the dark + 0.105 log growth was seen. The test also confirmed that the use of PBS pH = 6.0 has no effect on the killing of

the bacteria, which meant that this pH could be used for further testing as it allowed the amount of leaching of the photosensitiser to be minimalised.

Following on from the previous experiment, which tested the effect of light and pH on the growth of the bacteria. Testing was then carried out with the blank hydrogel containing no photosensitiser was against *E.coli*, to see if there was any effects associated with the support itself. A 1 cm square was cut from the hydrogel, which was then cut into four pieces and placed in PBS (pH = 6.0), measurements were taken every minute both in the light and the dark. The results showed a log killing of -0.599 in the light and a -0.0436 in the dark after 20 minutes.

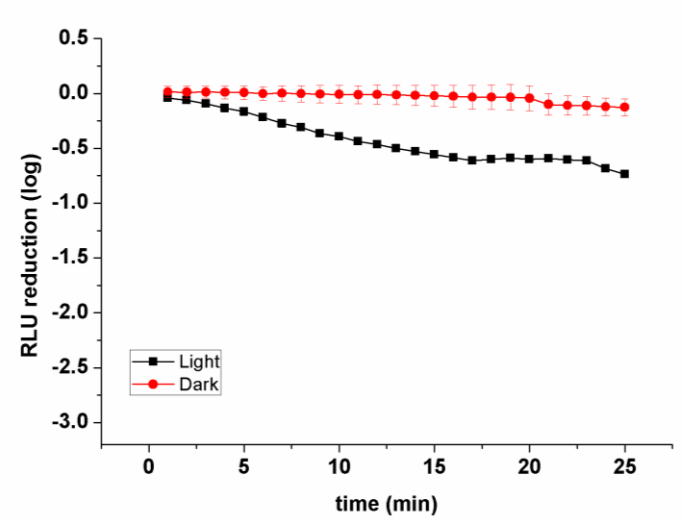

Time (mins)	Log killing (light)	Log killing (dark)
10	-0.393	-0.00796
20	-0.599	-0.0436
25	-0.736	-0.127

Figure 104 – Kill curve for *E.coli* control polyacrylamide hydrogel both in the light and the dark.

Following testing of experimental conditions on both the *E.coli* and the blank polyacrylamide hydrogel, the initial testing of the porphyrin involved finding the optimum concentration of porphyrin loading in the hydrogel for bacterial inactivation. Investigations were carried out using three different polyacrylamide gels containing different concentrations of the non-metallated porphyrin (**69**). The different concentrations tested were 1.0 mg cm^{-3}, 2.0 mg cm^{-3} and 4.0 mg cm^{-3}. The main aim of this test was to determine the effect of increasing the concentration of porphyrin on bacterial killing, both in the light and in the dark, using the conditions previously used for light and hydrogel only.

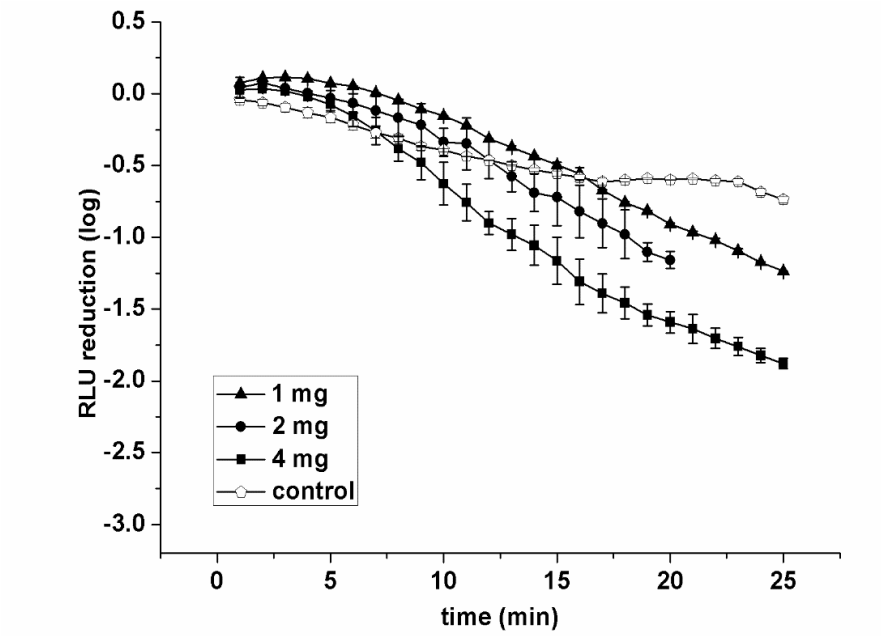

Time (mins)	Control gel log killing	1.0 mg cm^{-3} gel log killing	2.0 mg cm^{-3} gel log killing	4.0 mg cm^{-3} gel log killing
10	-0.393	-0.155	-0.337	-0.337
20	-0.599	-0.908	-1.16	-1.59

Figure 105 – Kill curve showing the effect of increasing porphyrin concentration on *E.coli* inactivation, and a table showing the three different concentrations used and the log killing over 20 minutes.

The results in **Figure 105** show that the 4.0 mg cm^{-3} gel gives the highest amount of bacterial killing, with a log reduction of -1.59 after 20 minutes of irradiation with light. When comparing the loading of photosensitiser with the study carried out by Spagnul *et al.*, the loading required for a similar log reduction of -1.6 after 20 minutes was 1.0 mg cm^{-3}, which is significantly less than the amount required for the immobilised porphyrin to have the same effect on bacterial killing.[205]

Biological evaluation was also carried out for varying concentrations in the dark (**Figure 106**). The amount of bacterial killing in the dark is significantly less than that observed by Spagnul *et al.*, who found a 1 log reduction in the dark using a 1.0 mg cm^{-3} gel. The experimental data collected in this project showed only a -0.0792 log reduction in the dark after 20 minutes, with the 4.0 mg cm^{-3} gel showing a -0.374 log reduction in the dark after 20 minutes, which is still significantly less than that observed for methylene blue. A low level of dark killing is especially important as this allows the system to be used in a switch on/switch off scenario whereby the system is activated by the use of light and the amount of bacteria killed in the dark is minimal.

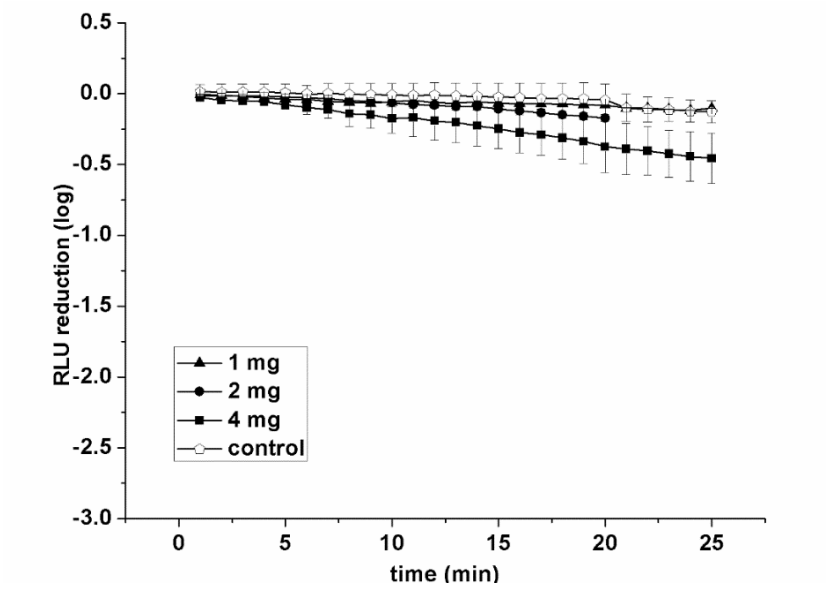

Time (mins)	Control gel log killing	1.0 mg cm^{-3} gel log killing	2.0 mg cm^{-3} gel log killing	4.0 mg cm^{-3} gel log killing
10	-0.00796	-0.0579	-0.0633	-0.174
20	-0.374	-0.0792	-0.171	-0.374

Figure 106 – **Kill curve for *E.coli* comparing increasing porphyrin immobilised on polyacrylamide in the dark, and table showing the three different concentrations of porphyrin and the log killing over time.**

After evaluating the three different concentrations of porphyrin immobilised on polyacrylamide it was decided that the 4.0 mg cm^{-3} gel (molarity = 3.3 mM) would be used for further testing. Due to the slight differences in molecular weight of the three porphyrins, the amount of porphyrin required was slightly different for all of the porphyrins tested (**Table 8**), but the molarity was always kept constant.

	Amount of porphyrin (mg cm^{-3})	moles	Molarity (mmol L^{-1})
Non-metallated porphyrin	4.0	3.6×10^{-6}	3.3
Copper porphyrin	4.1	3.9×10^{-6}	3.3
Palladium porphyrin	4.4	4.0×10^{-6}	3.3

Table 8 – Comparison study showing the amounts of the three different porphyrins required for formation of the equivalent hydrogel concentration.

The testing of the three different hydrogels was carried out using the same method as before, while equilibrating in PBS for 30 minutes before adding the gel to an *E.coli* solution (100 µL *E.coli*, 1900 µL PBS (pH = 6.0)).

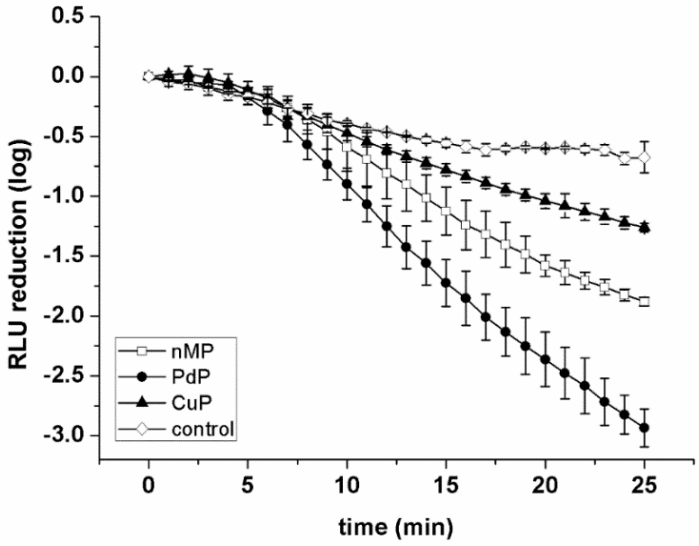

Time (mins)	Non-metallated porphyrin (nMP) log killing	Palladium porphyrin (PdP) log killing	Copper porphyrin (CuP) log killing	Control log killing
10	-0.590	-0.897	-0.402	-0.366
20	-1.58	-2.36	-0.989	-0.590
25	-1.88	-2.94	-1.26	-0.674

Figure 107 – Kill curve for *E.coli* comparing three porphyrins immobilised on polyacrylamide activated with light, and a table comparing the log killing of the three different porphyrins over time.

The results from the comparison test shown in **Figure 105** correspond with the expected trend, the palladium porphyrin showed the highest amount of bacterial killing with a -2.36 log reduction seen after 25 minutes (kill rate of 0.106, and a 1 log reduction after 11 minutes), compared to the non-metallated porphyrin which showed a log reduction of log reduction of -1.88 after 25 minutes (kill rate of 0.0694 and a 1 log reduction seen after 14 minutes), the palladium porphyrin shows approximately 1.5 times more bacterial killing compared to the non-metallated porpyrin. Interestingly, the copper porphyrin showed some bacterial killing with a log reduction of -1.26 seen after 25 minutes (kill rate of 0.047 and a 1 log reduction after 20 minutes). This is lower than the non-metallated porphyrin. This result is not expected, as the presence of the paramagnetic metal in the porphyrin has been known to suppress singlet oxygen formation, but there are also reports that suggest metallation with copper can still show some activity.[207] It is speculated that the copper porphyrin could be causing bacterial death by an alternative method.

The same experiment comparing the three different porphyrins, was carried out in the dark (**Figure 108**). Interestingly, the palladium porphyrin showed the lowest dark killing with a -0.534 log reduction seen after 25 minutes whereas the copper porphyrin showed the highest bacterial killing in the dark with a -1.00 log reduction seen after 25 minutes (kill rate of 0.0404 and a 1 log reduction seen after 20 minutes).

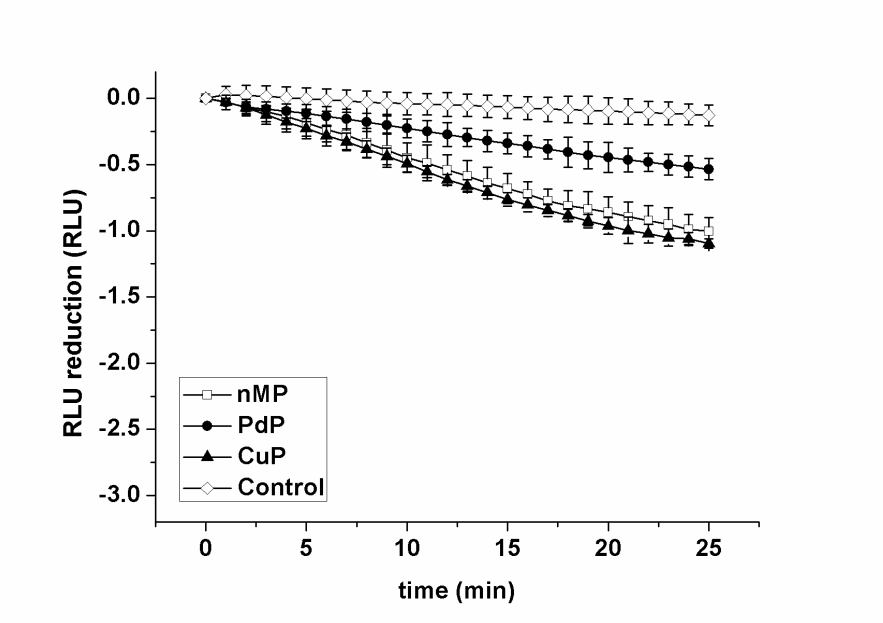

Time (mins)	Non-metallated porphyrin gel (nMP) log reduction	Palladium porphyrin gel (PdP) log reduction	Copper porphyrin gel (CuP) log reduction	Control gel log reduction
10	-0.390	-0.202	-0.438	-0.0351
20	-0.834	-0.431	-0.926	-0.0876
25	-1.00	-0.534	-1.10	-0.127

Figure 108 – **Kill curve for *E.coli* comparing three porphyrins immobilised on polyacrylamide in the dark and a table comparing the log killing of the three different porphyrin hydrogels and the control.**

The results obtained when testing the three different porphyrins immobilised on polyacrylamide, both irradiated with white light and non-irradiated, suggest that the palladium porphyrin has the best properties, as it demonstrates the highest bacterial killing in the light and the lowest bacterial killing in the dark.

In order to determine whether the immobilisation process affects the ability of the porphyrin to kill bacteria, the same experiment was carried out comparing the three different porphyrins free in solution. The same method was used as before, but instead of using porphyrin immobilised gel, the corresponding free porphyrin was dissolved in PBS

(pH = 6.0) and added to the *E.coli* broth. The results show that the porphyrins free in solution are able to inactivate the bacteria more effectively. The non-metallated porphyrin showed a -2.31 log reduction after 20 minutes (kill rate of 0.0936, with a 1 log reduction after 12 minutes), when free in solution, compared to a log reduction of -1.58 after 20 minutes when immobilised on polyacrylamide. The palladium porphyrin in solution showed a -2.83 log reduction after 20 minutes (kill rate of 0.121, with a 1 log reduction after 10 minutes), compared to the -2.36 log reduction when the porphyrin was immobilised in the polyacrylamide gel (kill rate of 0.106, and a 1 log reduction after 11 minutes). The copper porphyrin showed a -0.572 log reduction after 20 minutes (kill rate of 0.0198), which is lower than the reduction seen when the copper was immobilised (-0.926 log reduction seen after 20 minutes). These results show that the porphyrin free in solution gives better photoactivity against *E.coli*, but the activity is not dramatically hindered by immobilisation.

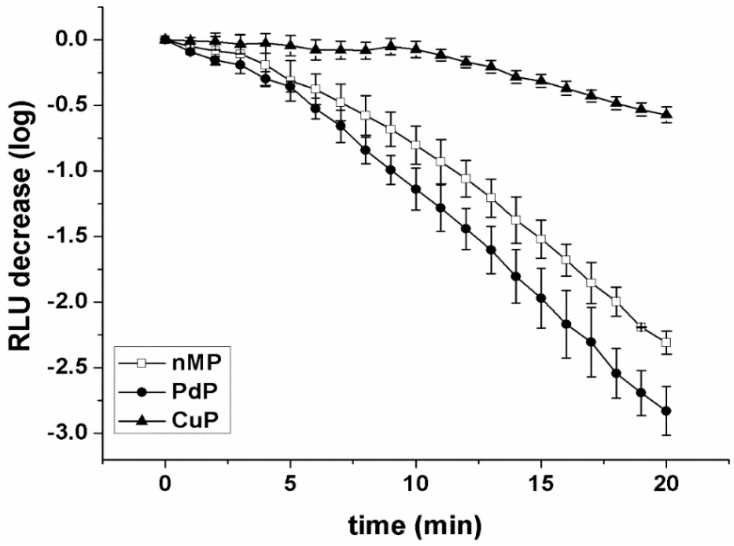

Time (mins)	Non-metallated porphyrin (nMP) log reduction	Palladium porphyrin (PdP) log reduction	Copper porphyrin (CuP) log reduction
10	-0.804	-0.992	-0.0517
20	-2.31	-2.83	-0.572

Figure 109 – Kill curve for *E.coli* comparing the three different porphyrins in solution with irradiation using white light, a table comparing the log killing of the bacteria.

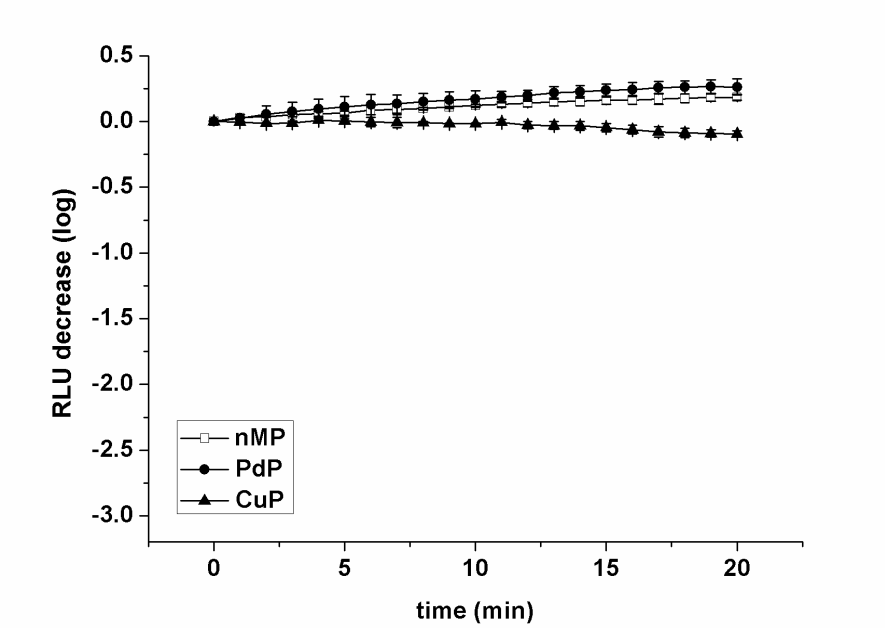

Time (mins)	Non-metallated porphyrin (nMP) log reduction	Palladium porphyrin (PdP) log reduction	Copper porphyrin (CuP) log reduction
10	+ 0.124	+ 0.171	-0.0162
20	+ 0.185	+ 0.262	-0.0934

Figure 110 – Kill curve for *E.coli* comparing the three different porphyrins in solution in the dark.

The results obtained for the study of the porphyrins free in solution are promising, as none of the porphyrins show any significant bacterial killing in the dark, compared to the same porphyrin immobilised on the polyacrylamide support, where the dark killing was found to be -0.834 log reduction for the non-metallated porphyrin, and even higher (-0.926 log reduction) for the copper porphyrin. Interestingly, the control gel with no porphyrin immobilised only showed a -0.0436 log reduction in the dark after 20 minutes, which indicates that it is not the presence of either the support or the copper porphyrin that gives the high dark toxicity, but rather that a synergistic effect is responsible. The copper porphyrin showed interesting results, as when the copper porphyrin gel was tested for the formation of singlet oxygen it was found to only show a minimal decrease in the ABDA peaks. It was speculated that the bacterial death could be due to a different mechanism killing, similar results were shown by Antoni *et al.* who saw copper activity *via* the formation of hydroxide radicals.[207]

The porphyrins immobilised on the gel gave some promising results against the Gram-negative bacteria, but the most important factor is, perhaps, the reusability of the material and how long the material can remain active for. The capacity test effectively quantifies

how reusable the material is. This involves using the same gel, with a fresh colony of bacteria each time, to determine loss of activity over time.

5.4 Testing the reusability of the photoactive hydrogels

The reusability of the photoactive hydrogels is an important factor to consider, as this gives an indication of how long the surface is able to maintain effective anti-bacterial activity for. Ideally, the amount of time a specific surface is active for should be as long as possible.

In order to test the reusability of the photoactive materials, capacity tests were carried out for both the non-metallated porphyrin and the palladium porphyrin, as these materials showed the most promise in terms of bacterial killing. The capacity tests were carried out by following the standard method: the photoactive hydrogel was cut into a 1 cm square which was then cut into four and placed in an Eppendorf tube with the *E.coli* solution (100µL *E.coli* and 1900µL of PBS (pH = 6.0)). The sample was then irradiated for 20 minutes, and following completion the *E.coli* solution was discarded and the photoactive material was challenged with a fresh *E.coli* solution (100µL *E.coli* and 1900µL of PBS (pH = 6.0)). This was repeated for five cycles, with measurements being carried out both in the light and in the dark.

5.4.1 Evaluating the reusability of the free base porphyrin photoactive hydrogel

Firstly the non-metallated porphyrin (**69**) was tested for reusability, both in the light and in the dark (**Figure 111** and **Figure 112**).

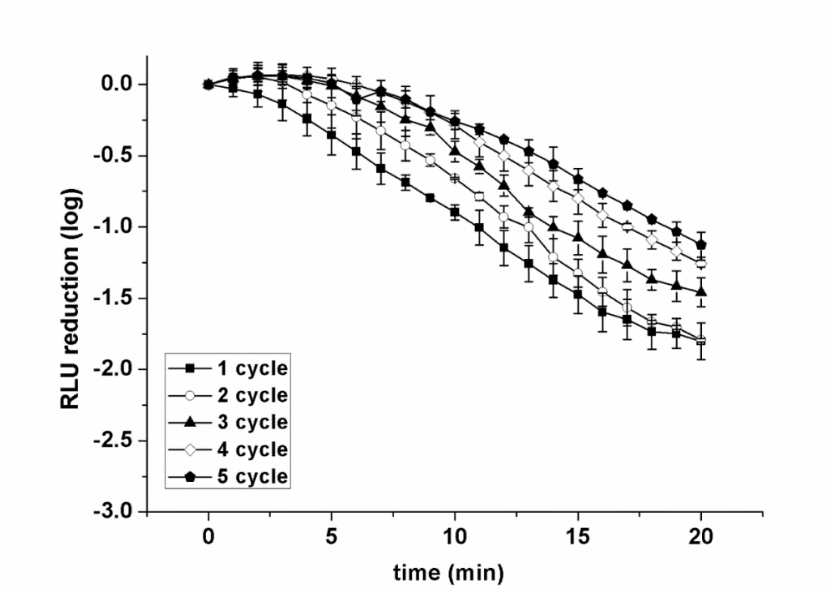

Time (mins)	Cycle 1 log reduction	Cycle 2 log reduction	Cycle 3 log reduction	Cycle 4 log reduction	Cycle 5 log reduction
10	-0.897	-0.660	-0.444	-0.444	-0.243
20	-1.80	-1.79	-1.43	-0.768	-0.740

Figure 111 – Kill curve for *E.coli*, non-metallated porphyrin capacity test in the light.

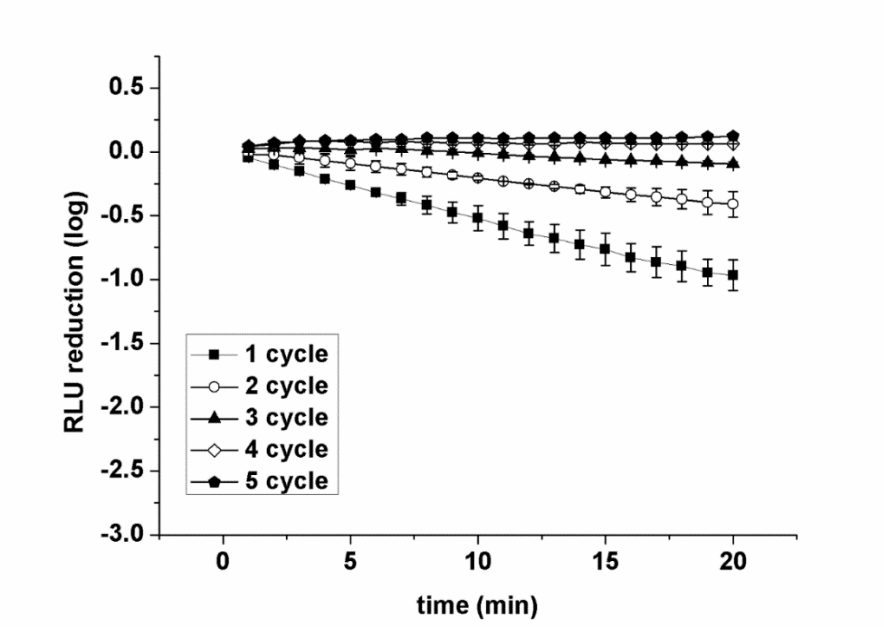

Time (mins)	Cycle 1 log reduction	Cycle 2 log reduction	Cycle 3 log reduction	Cycle 4 log reduction	Cycle 5 log reduction
10	-0.520	-0.205	-0.0103	0.0717	0.107
20	-0.967	-0.410	-0.0934	0.0624	0.121

Figure 112 – Kill curve for *E.coli*, non-metallated porphyrin capacity test in the dark.

Figure 111 shows the results obtained for the non-metallated porphyrin capacity test in the light. The first cycle of 20 minutes irradiation showed a log reduction of -1.80, which decreased to a log reduction of -1.79 after the second cycle. The third cycle showed a -1.43 log reduction after 20 minutes, which is + 0.3 log higher than cycles one and two. Cycles four and five only showed half the activity of cycle three with log reductions of -0.768 and -0.740 respectively. Overall the material was found to be active for five consecutive cycles when irradiated with light. When comparing the results with those obtained by Spagnul *et al*., where a -1.8 log reduction was seen for the first cycle, results for the non-metallated porphyrin are similar. The second cycle, when using methylene blue, showed a -0.8 log decrease, compared to a -1.8 log decrease for the porphyrin. The bacterial inactivation is higher for the porphyrin therefore, than methylene blue, but the concentration of porphyrin is four times higher. The third cycle showed a decrease in killing for both the porphyrin (-1.43 log decrease) and for the methylene blue (-0.4 log decrease). The porphyrin shows more appreciable killing of the bacteria compared to the methylene blue. The fourth cycle showed a slight decrease for the methylene blue (-0.3 log decrease) compared to a larger decrease in activity seen for the porphyrin (-0.7 log

decrease). The final cycle for the methylene blue showed minimal bacterial killing, with some bacterial growth occuring after 20 minutes of irradiation, when compared to the porphyrin which showed a -0.740 log decrease under the same conditions. The porphyrin immobilised hydrogel still showed appreciable killing even after five consecutive cycles, with a total irradiation time of 100 minutes, whereas the level of activity shown for the methylene blue was minimal in the fifth cycle.

The results obtained for the material in the dark are shown in **Figure 112**. The first cycle showed a log reduction of -0.967, compared to the methylene blue hydrogel that showed a -1.0 log decrease in the dark after 20 minutes. The second cycle still showed bacterial killing for the porphyrin photoactive hydrogel (-0.410 log decrease), with similar values being observed for methyelene blue (-0.4 log decrease). The third cycles for both photosensitisers showed minimal killing, and following this cycle minimal bacterial killing and bacterial growth was observed. Overall the dark experiment showed minimal killing in the dark for three cycles, and then the last two cycles showed bacterial growth.

The non-metallated porphyrin photoactive hydrogel showed good results for reusability of the material following five consecutive cycles, which supports the potential for the use of this material in real-life situations.

5.5 Evaluating the reusability of the palladium porphyrin photoactive hydrogel

Following the successful evaluation of the reusability of the non-metallated porphyrin hydrogel, the reusability of the palladium porphyrin hydrogel was investigated.

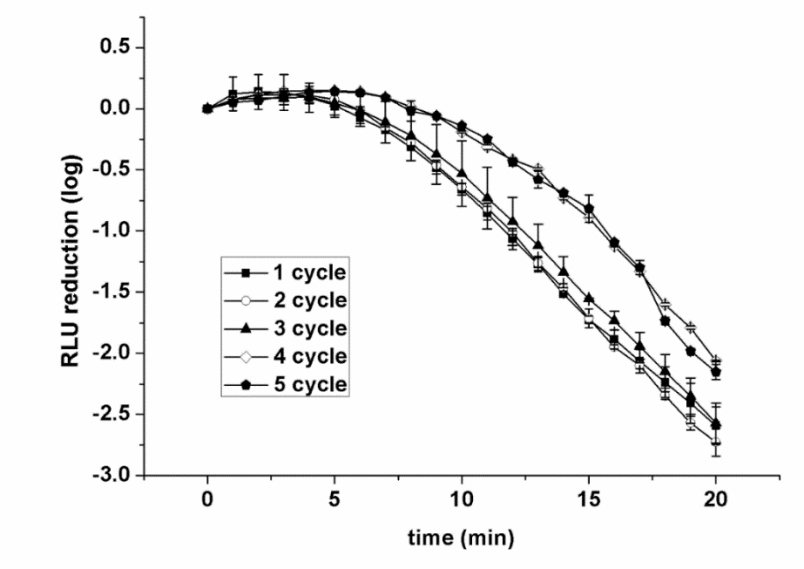

Time (mins)	Cycle 1 log reduction	Cycle 2 log reduction	Cycle 3 log reduction	Cycle 4 log reduction	Cycle 5 log reduction
10	-0.659	-0.465	-0.372	-0.0604	-0.0586
20	-2.59	-2.73	-2.57	-2.06	-2.15

Figure 113 – Kill curve for *E.coli*, palladium porphyrin capacity test in the light.

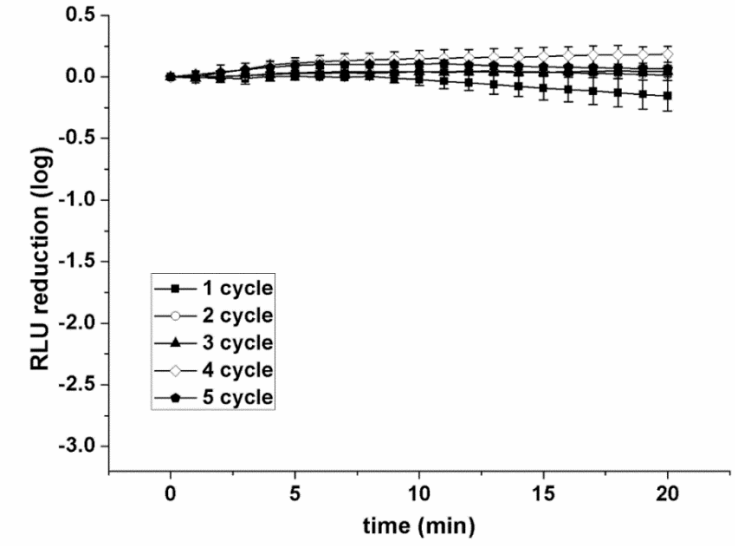

Time (mins)	Cycle 1 log reduction	Cycle 2 log reduction	Cycle 3 log reduction	Cycle 4 log reduction	Cycle 5 log reduction
10	-0.0224	0.0397	0.0397	0.149	0.103
20	-0.154	0.0165	0.0438	0.184	0.0658

Figure 114 – Kill curve for *E.coli*, palladium porphyrin capacity test in the dark.

The palladium porphyrin hydrogel showed activity for five consecutive cycles following irradiation with light (**Figure 113**). The first three cycles showed similar bacterial killing,

cycle one showed a -2.59 log decrease; the second cycle showed a slight increase in bacterial killing with a -2.73 log decrease; and the third cycle showed a -2.57 log decrease. When comparing the results to the non-metallated porphyrin hydrogel, the activity of the palladium hydrogel was maintained for the first three cycles, whereas the non-metallated porphyrin hydrogel began to show a decrease in activity in the third cycle. The palladium porphyrin hydrogel showed a slight decrease in activity for the fourth cycle, with a -2.06 log decrease which remained similar for the fifth cycle (-2.15 log decrease). The palladium porphyrin hydrogel showed a 2 log decrease even after five consecutive cycles, which is more than double the activity of the non-metallated porphyrin hydrogel after the same number of cycles. The only difference between the two photoactive hydrogels tested was the insertion of palladium into the porphyrin. The palladium insertion in the porphyrin allows the material to show a 2 log decrease after five consecutive cycles, which shows real promise for use in real world applications.

The same experiments were also carried out in the dark for five consecutive cycles (**Figure 114**). The results show minimal dark killing for the first cycle, and following this the next four cycles show no dark killing with small amounts of bacterial growth. Comparing the results to those of the non-metallated porphyrin hydrogel, which showed dark killing for three cycles and then started to show bacterial growth, the palladium porphyrin hydrogel shows lower dark killing. Overall, the palladium porphyrin hydrogel shows better bacterial killing compared to the non-metallated porphyrin when irradiated with light, and the dark killing observed is lower.

5.5.1 Study of the initial kill rates from the capacity tests carried out

In order to directly compare the kill curves for the non-metal and the palladium porphyrin when carrying out the capacity tests the kill rates were compared. The initial kill rate is the rate at which the bacteria is killed over a stated period of time, and the total kill rate is the rate at which the bacteria is inactivated over the total time for the experiment. The equation used for the calculation of the kill rate is;

$$-K = (\log RLU_0 - \log RLU_1)/(t_1 - t_0)$$

Where RLU is the relative lux units, and t is time.

Equation 2 – Calculation of initial kill rate and total kill rate

5.5.2 Comparison of the initial rate of kill for the non-metallated porphyrin and the palladium porphyrin capacity test

Firstly the initial rate of kill was studied, as this showed how the gel reacted over the first 10 minutes of irradation and in the dark.

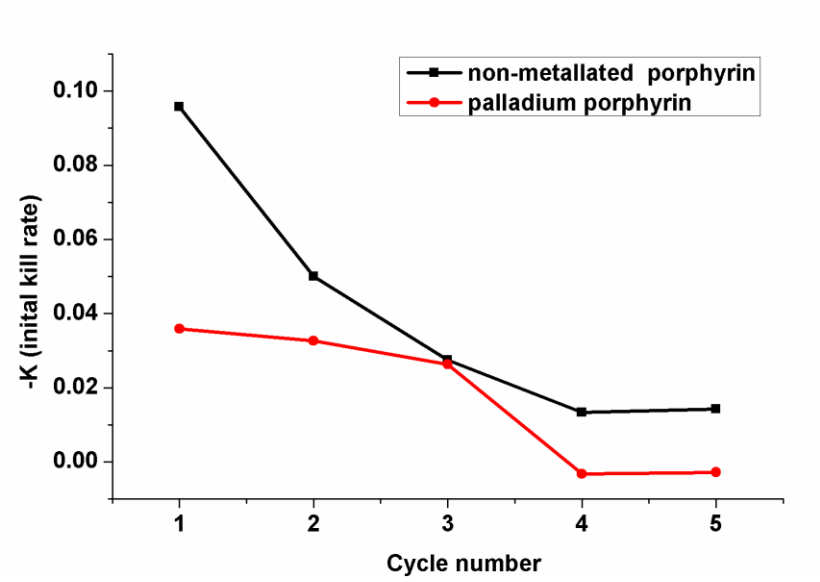

	Initial kill rate (-K initial)	
Cycle number	**Non-metallated porphyrin**	**Palladium porphyrin**
1	0.0958	0.0359
2	0.0500	0.0327
3	0.0275	0.0263
4	0.0134	-0.0032
5	0.0143	-0.0028

Figure 115 – Comparison of the initial kill rates for the non-metallated porphyrin capacity test and the palladium porphyrin capacity test in the light.

Figure 115 shows a comparison of the initial kill rates for the capacity tests of the non-metallated porphyrin and the palladium porphyrin. The initial kill rate was taken over the first 10 minutes of irradiation with light. When comparing the non-metallated porphyrin and the palladium porphyrin, there is a difference in the initial kill rate, with the non-metallated porphyrin causing a higher log reduction (-K) in the first ten minutes compared to the palladium porphyrin for the first two cycles; with initial kill rates of 0.0958 and 0.0500 for the non-metallated porphyrin and initial kill rates of 0.0359 and 0.0327 seen for the palladium porphyrin. The non-metallated porphyrin shows a higher initial kill rate than the palladium porphyrin over the first two cycles, in the following cycles the

palladium porphyrin shows a higher initial kill rate due to the loss of activity of the non-metallated porphyrin.

5.5.3 Comparison of the total kill rate (-K total) for the non-metallated porphyrin and the palladium porphyrin capacity tests

In order to investigate further the bacterial killing of the non-metallated porphyrin and the palladium porphyrin throughout the capacity tests the total kill rate was also compared. The palladium porphyrin was found to give a higher log reduction over 20 minutes than the non-metallated porphyrin, but the initial kill rate was found to be lower for the first and second cycles.

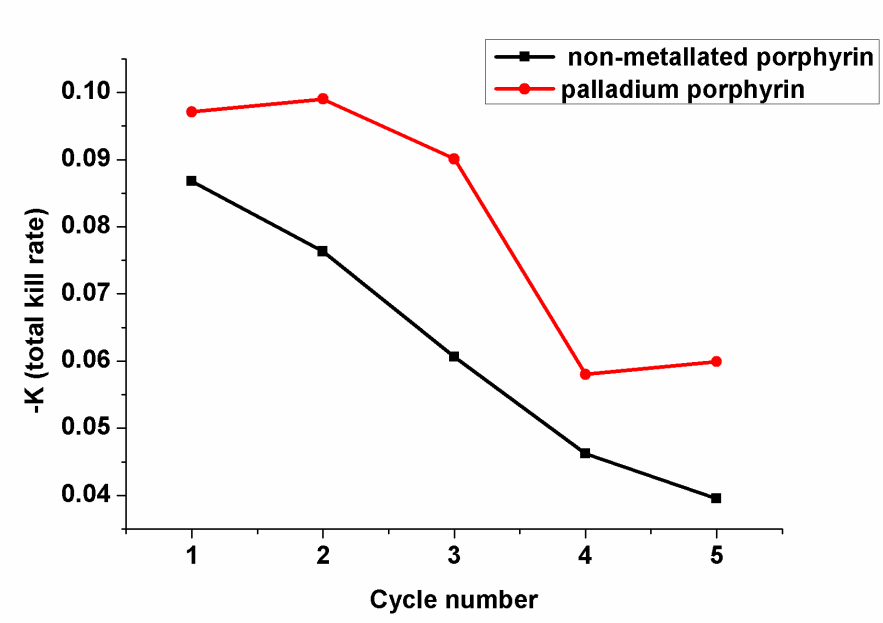

	Total kill rate (-K total)	
Cycle number	**Non-metallated porphyrin**	**Palladium porphyrin**
1	0.0868	0.0971
2	0.0763	0.099
3	0.0606	0.0901
4	0.0462	0.058
5	0.0395	0.0599

Figure 116 – Comparison of the initial kill rates for the non-metallated porphyrin capacity test and the palladium porphyrin capacity test in the light.

Figure 116 shows a comparison between the total kill rates (-K total) for the non-metallated porphyrin and the palladium porphyrin. For all five cycles the palladium porphyrin shows a higher killing rate than the non-metallated porphyrin, which is the

opposite of what was seen for the initial kill rate. Interestingly, the palladium porphyrin shows higher activity with a lower initial kill rate for cycles 1 and 2 which indicates that the palladium porphyrin may have a delay in the production of singlet oxygen for killing bacteria.

5.6 Conclusions

Following biological testing against Gram-negative *E.coli* bacteria the 4.0 mg cm^{-3} porphyrin loaded gel was found to be the most active when tested against the 1.0 mg cm^{-3} and the 2.0 mg cm^{-3} analogues, the 4.0 mg cm^{-3} gel showed a -1.59 log reduction following 20 minutes of irradiation. A comparative study was carried out between the three different porphyrins, metal free porphyrin, copper porphyrin and palladium porphyrin, and the palladium porphyrin was found to be the most active with a -2.94 log decrease seen following 20 minutes of irradiation with light. Interestingly, the copper porphyrin showed activity with a -1.26 log decrease following 20 minutes of irradiation. The palladium porphyrin showed little bacterial killing in the dark (-0.534 log reduction), whereas the non-metallated and the copper porphyrin showed a 1 log reduction after 20 minutes. The three porphyrins were also tested in solution, to determine whether the immobilisation hinders the bacterial killing. The porphyrins free in solution showed higher levels of bacterial killing in the light than those immobilised in polyacrylamide: the dark killing was also lower.

The reusability of the non-metallated porphyrin hydrogel and the palladium porphyrin hydrogel was tested to gauge material lifetime. Both of the porphyrin hydrogels were found to be reuseable following five consecutive cycles of testing the same hydrogel with a fresh sample of *E.coli*.

The results obtained show great promise for the formation of an antibacterial surface that is reusable. Further research could be carried out into the testing of these porphyrin hydrogels against different bacteria, and also against planktonic bacteria on a thin film to obtain more data on bacterial killing on surfaces.

6 Overall conclusions

This project has investigated a number of possibilities for the formation of a porphyrin and an electron acceptor immobilised on a polymeric support for use against bacteria. This project has allowed the formation of a sterilising surface to be formed *via* the parallel synthesis of porphyrins and polyviologens.

Primarily research was focused on the formation of a material that contained an electron donating component and an electron accepting component. A library of polyviologen molecules were synthesised for use as an electron acceptor. These were utilised with, firstly, titanium dioxide, and then further investigated with an organic photosensitiser, a porphyrin, acting as photoelectron donors. A library of conjugatable viologens was synthesised for use in click reactions and palladium catalysed coupling reactions, but with minimal success for such coupling.

A library of porphyrins and their metal derivatives was synthesised for use in conjugation to viologen molecules. Unfortunately, the conjugation was again unsuccessful. Attempts were made to entrap both the polyviologen and the porphyrin in two different polymeric matrices. The two different supports that were investigated were polyacrylamide and silica. The entrapment was unsuccessful, with the support leaching both the polyviologen molecule and the porphyrin, which is not ideal for the desired application.

A secondary aim of the project was the formation of a reusable antibacterial surface. In this respect, the project made an important advancement in the formation of a sterilising surface for use in photodynamic antimicrobial chemotherapy (PACT). The PACT field has struggled with the formation of photosensitisers immobilised on polymeric supports for numerous reasons including leaching, low loading and the inability to inactive Gram-negative bacteria. This project achieved the formation of a porphyrin-acrylamide support that allowed the fine tuning of antibacterial activity, depending on the metal coordinated by the porphyrin, this fine-tuning allowed the support to be studied in both “switched on” and “switched off” scenarios. The support was also found to be reusable for five consecutive cycles with minimal loss of activity, indicating that the material is applicable to real life situations. The palladium porphyrin showed enhanced photo-bacterial killing when tested against genetically modified *E.coli*, when compared with the non-metallated porphyrin, which supports the fact that the introduction of a heavy atom enhances the production of singlet oxygen, and bacterial killing. Interestingly, the copper porphyrin showed bacterial killing, which was not expected for a paramagnetic porphyrin complex.

6.1 Future work

In the short term, the future work for this project could involve the bacterial testing of the porphyrin-polyacrylamide supports against Gram-positive bacteria to study the effect of the porphyrin on photoinactivation of the Gram-positive bacteria such as *S.aureus*. Moving on from this, the system could be evaluated against planktonic bacteria, and also tested as a coating, in order to give a better assessment of its potential in a real life situation for hospital applications. Another area of interest could be bacterial evaluation against *salmonella* and also *MRSA*, as these are some of the most common microorganisms associated with healthcare-associated infections. Further investigations could be carried out into the lifetime of the system, carrying out more tests to study how long the material remains active for. Another factor to consider is the shelf-life of the material, i.e how long the material can be used without the polymeric support degrading. The shelf-life of the material is important as the limiting amount of time between gel formation and use of the gel for bacterial killing should be known, this would give a good indication of how long these materials could be stored before use.

Another short-term investigation could be carried out on the use of alternative cationic photosensitisers for immobilisation, as the system is versatile and the photosensitiser would require only the insertion of the vinyl functionality. The study of different photosensitisers could allow for the comparison of a number of different factors; including the number of positive charges on the photosensitiser, and also the size of the photosensitiser. The size of the photosensitiser could have an effect on the loading of the support, and also the pore size of the material which is important for the production of reactive oxygen species.

The polymeric support currently uses bisacrylamide for the cross-linking agent, the ratio of the cross linker to monomer could be altered, along with the cross linker itself to find the optimum material required. Ideally, the application of the surface would be carried out using either a spray-on or a brush-on coating. This could require a change in the monomer concentration, and perhaps a change in the polymeric support itself to meet these requirements.

Another possible area of further research could involve investigating other polymeric supports for the palladium water soluble porphyrin containing the acrylamide functionality. For example, supports such as polyHEMA, which is already used in contact lenses, could be explored due to its excellent biocompatibility and similar properties to polyacrylamide. It would be interesting to compare the different supports with the same

flexibility on the photoinactivation of bacteria. The porosity of the material could be altered, by changing the cross-linking ratios and the cross-linker itself, and comparisons could be made with the effect of porosity of the material on production of singlet oxygen and also the inactivation of both Gram-positive and Gram-negative bacteria.

Once optimisation of the system has been carried out, so that a sterilising surface is available, incorporation of the viologen molecule could be attempted again. The viologen molecule could be incorporated either with a vinyl group, *via* the polymerisation method, or the viologen could be conjugated to the porphyrin *via* a spacer group to minimise steric hindrance. This could be carried out by investigating different conjugation methods and optimising the coupling, or by attempting the polymerisation reaction with both the porphyrin and viologen with a vinyl functionality.

Investigations could also be carried out into the use of alternative molecules that carry out electron transfer with a porphyrin, for example Ru(bipy), which has been widely used for electron transfer. This could be used for comparison with the porphyrin-viologen conjugates.

6.2 Contributions to the field of research

The immobilisation of photosensitisers on polymeric supports is needed for the PACT community in the context of healthcare associated infections. More specifically the immobilisation of photosensitisers that are able to inactivate Gram-negative bacteria is particularly important as Gram-negative bacteria are more challenging to kill compared to Gram-positive bacteria.

The immobilisation of three different porphyrins on polyacrylamide for the inactivation of *E.coli* has been carried out. The study investigates the effect of metal insertion on bacterial inactivation: this allows a "switch on" and "switch off" scenario to be used. The amount of leaching was found to be minimal, compared to those systems reported in the literature, and the log killing of bacteria was found to be high with an almost 3 log decrease for the palladium porphyrin immobilised seen after 20 minutes of irradiation. The photoactive materials were also tested for reusability and were found to be active for five cycles, with minimal dark killing. The reusability of the materials shows excellent promise for the use of these materials in real life situations. The activity level was found to decrease after the first two cycles for the non-metallated porphyrin but for the palladium porphyrin the activity was found to be similar over the five consecutive cycles with a 2 log decrease seen after five cycles.

Investigations into the formation of a self-sterilising surface were also carried out with the incorporation of a porphyrin and viologen molecule in a polymeric support. Although this approach was not successful, it shows promise for a system that could work with an alternative conjugation methodology of both components in a polymeric matrix. The viologen has previously demonstrated reversible electron transfer properties, and thus optimisation of the conditions could be carried out prior to immobilisation on polymeric supports.

7 Experimental

General Information

Mono and bidimensional (H–H COSY), ^{1}H NMR spectra were recorded at ambient temperature on JEOL Eclipse 400 and JEOL Lambda 400 spectrometers (operating at 400 MHz for ^{1}H and 100 MHz for ^{13}C). In all the solvents chemical shifts were referenced to the peak of residual non deuterated solvent (d = 7.26 for $CDCl_3$, 4.89 for D_2O, 2.50 for DMSO-d_6, 3.35 and 4.78 for THF-d_8, 8.03, 2.92 and 2.75 for DMF-d_7, 3.35 and 4.78 for Methanol-d_4). Coupling constants (J values) are reported in Hertz (Hz) and are H–H coupling constants unless otherwise stated. Assignments were performed through conventional 2D correlation spectra.

Splitting patterns are designated as s (singlet), d (doublet), t (triplet), q (quartet), quin (quintet), m (multiplet) and br s (broad singlet). All mass spectrometry data was obtained from the EPSRC Mass Spectrometry Service, Swansea. Melting points were obtained using a Stuart SMP10 melting point apparatus without correction. CHN analysis was performed using a CHN analyser EA1108 (Carlo Erba). UV-Vis spectra were measured on a Varian Cary 50 Bio UV-Vis spectrophotometer. Reagents were purchased from Alfa Aesar, Fluorochem and Sigma Aldrich, and used as received. Dry solvents were obtained from drying solvents over molecular sieves according to the method of Williams *et al.*[243] All other solvents were used as purchased. All reactions were monitored by TLC using Fluka analytical 0.2 mm layer thickness 60 Å pore size silica gel plates with or without UV indicator (F-254). Silica gel (Fluorochem 60-40 µm) and neutral Alumina (Sigma Aldrich) pore size 58 Å were used for column chromatography. All microwave reactions were carried out on a CEM discover SP microwave reactor, using 200 W power and 20 bar pressure unless stated otherwise. High performance liquid chromatography (HPLC) analysis was carried out on a Jasco system equipped with a Jasco PU-1580 dual pump, Jasco MD-1515 multi-wavelength detector and a Gemini- NX C18 column (100 A, 150 x 4.6 mm) using as the mobile phase 0.1% trifluoroacetic acid in water (solvent A) and 0.1% trifluoroacetic acid in acetonitrile (solvent B). The gradient elution was 5% A to 95% B in 18 mins with a flow rate of 1.00 mL min^{-1} and the injection volume was 10.00 µL. Powder X-ray diffraction was carried out on materials using a PANalytical empyrean X-ray diffractometer using Cu Kα1radiation. The results were recorded using the instruments built-in software. The obtained patterns were analysed using PANalytical Highscore Plus software.

The morphology of the hydrogels was characterized by field-emission scanning electron microscopy. Scanning electron microscope (SEM) images of the hydrogel alone or in the presence of the porphyrin compound were obtained using a EVO60 scanning electron microscope (Zeiss) fitted with a cryo-preparation system-model: PP3010T, manufacturer: Quorum Technologies. After plunge-freezing in liquid nitrogen the sample was transferred (under vacuum) to the cryo system preparation chamber. Most of the water-ice was removed by sublimation by increasing the temperature of the sample from -140 °C to – 60 °C at a pressure of 5 x 10^{-5} mbar for 10 minutes. After this, the temperature of the sample was reduced to -140 ° C and a pressure of approximately 5 x 10^{-7} mbar. The sample was then sputter coated with about 2 nm of platinum and then transferred to the SEM for examination. The SEM electron beam accelerating voltage used was 15 kV at a probe current of 20–35 pA. The diameters of the gel pores were determined using the Image J program.

Synthetic Methods

Ethane-1,2-diyl bis (4-methylbenzenesulfonate) (1)

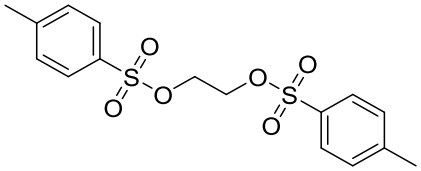

Ethylene glycol (3.100 g, 49.94 mmol, 1 equiv.) and pyridine (8.118 g, 102.6 mmol, 2 equiv.) were dissolved in dichloroethane (40.00 mL). The solution was then cooled to 0 °C and *p*-toluenesulfonylchloride (19.07 g, 100.0 mmol, 2 equiv.) was added gradually with stirring for 30 mins. Following this, the solution was left at 0 °C for 12 h and then aqueous saturated sodium bicarbonate was added (100.0 mL). The crude product was extracted with CH_2Cl_2 (2 x 100.0 mL) and the organic fractions were washed again with aqueous saturated sodium bicarbonate (50.00 mL). The excess solvent was removed under reduced pressure and the crude product was recrystallized from methanol to give a white powder (12.55 g, 68% yield).

^{1}H-NMR ($CDCl_3$): δ 2.46 (6H, br s, 2 x CH_3), 4.18 (4H, s, CH_2-CH_2), 7.34 (4H, d, 3,5Ph, J = 8.0 Hz, 7.73 (4H, d, 2,6 Ph, J = 8.0 Hz).^{13}C- NMR ($CDCl_3$): δ 21.8, 66.8, 128.1, 130.1, 132.4, 145.4. MS:(ESI) m/z 388 (100$[M+NH_4]^+$), HRMS: calcd. for $C_{16}H_{22}O_6S_2N_1$: 388.0883 found 388.0884. Mp: 127 °C compared to a literature value of 128 °C. Anal. calcd for $C_{16}H_{18}O_6S_2$: C, 51.88; H, 4.90; N, 0.00 ; S, 17.31 found: C, 51.77; H, 4.82; N, 0.00, ;S, 17.31.

Ethane-1, 2-diyl dimethanesulfonate[244] (2)

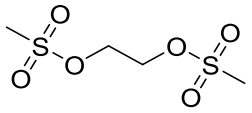

Ethylene glycol (0.569 g, 9.16 mmol, 1 equiv.) was dissolved in dry dichloromethane (100.0 mL), and triethylamine (1.00 mL) was added to the mixture which was subsequently cooled to 0 °C under nitrogen. Once the reaction mixture had cooled methanesulfonylchloride (7.00 mL, 9.16 mmol, 1 equiv.) was added drop wise *via* syringe, and the mixture was bought up to rt and stirred until completion, which was monitored using TLC. The mixture was washed with saturated sodium bicarbonate (100.0 mL) and extracted with CH_2Cl_2 (100.0 mL). The excess solvent was removed under reduced pressure to give a near colourless oil, which was purified using column chromatography (silica) hexane: ethylacetate (97:3) to give a colourless oil (1.500 g, 75% yield).

^{1}H-NMR ($CDCl_3$): δ 3.04 (6H, s, 2 x C*H*$_3$), δ 4.40 (4H, s, 2 x C*H*$_2$). This matches the ^{1}H-NMR data given in the literature.

1, 4-Phenylenedimethanol[245] **(3)**

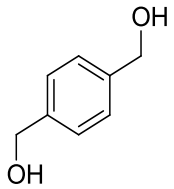

$LiAlH_4$ (5.490 g, 144.8 mmol, 10 equiv.) was added to a solution of dry THF (100.0 mL), the mixture was cooled to 0 °C and stirred under nitrogen. Once cooled dimethylterephthalate (2.810 g, 14.48 mmol, 1 equiv.) was added gradually and the reaction stirred at 0 °C for 1 h, then bought up to rt and stirred for 5 h. Following this, water (21.00 mL) was added followed by sodium hydroxide solution (1.00 mL). The crude product was then filtered under vacuum, and extracted with dichloromethane (100.0 mL) and water (20.00 mL). The excess solvent was removed under reduced pressure to give the product as a white solid (1.150 g, 58% yield).

^{1}H-NMR (CD_3OD): δ 4.59 (4H, s, 2 x C*H*$_2$-OH), 7.32 (4H, s, Ph).^{13}C-NMR (CD_3OD): δ 63.7, 126.7, 140.4. MS: (ESI) m/z 138 (100[M+NH_4OAc]) HRMS: calcd. for $C_8H_{10}O_2$: 138.01910 found 138.0913.

1, 4-Phenylenebis (methylene) bis (4-methylbenzenesulfonate) (4)

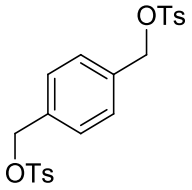

1, 4-Phenylenedimethanol (1.000 g, 7.241 mmol) and pyridine (1.145 g, 7.240 mmol, 1 equiv.) were dissolved in dichloroethane (20.00 mL). The solution was cooled to 0 °C and *p*-toluenesulphonylchloride (2.759 g, 14.48 mmol, 2 equiv.) was added slowly with stirring for 30 mins. The solution was maintained under these conditions for 12 h and then bought up to rt. Following this, the solution was extracted with saturated aqueous sodium bicarbonate (50.00 mL) and CH_2Cl_2 (100.00 mL). The excess solvent was removed under reduced pressure. The desired product was not isolated.

1, 4-Phenylenebis (methylene) dimethanesulfonate (5)

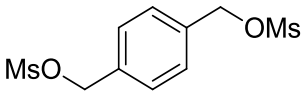

1, 4-Phenylenedimethanol (2.000 g, 14.48 mmol, 1 equiv.) was dissolved in dry dichloromethane (150.00 mL), triethylamine (1.00 mL) was added to the reaction mixture which was then stirred under nitrogen and cooled to 0°C. Once cooled, methanesulfonylchloride (2.25 mL, 28.95 mmol, 2 equiv.) was added dropwise *via* syringe and the reaction returned to room temperature and stirred for 8 h. The desired product was not isolated.

Poly(p-xylylviologen dibromide) [98] **(6)**

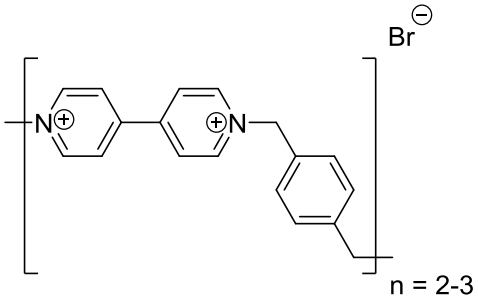

4,4'-Bipyridine (2.072 g, 13.72 mmol, 1 equiv.) and dibromo-*p*-xylene (3.538 g, 13.40 mmol, 1 equiv.) were dissolved in acetonitrile (95.00 mL). The solution was stirred overnight at rt for polymerisation to occur. The crude mixture was precipitated with acetone to give a white solid (2.534 g).

^{1}H-NMR (C_2D_6SO): δ 4.72 (4H, s, Ph–C*H*$_2$), 5.89 (2H, m), 7.55 (4H, q), 7.68 (4H, m), 8.02 (4H, d), 8.64 (4H, d), 8.75 (4H, m), 8.88 (4H, d), 9.35 (4H, d), 9.56 (4H, m).^{13}C-NMR (C_2D_6SO): δ 122.6 145.9, 151.5.MS (NSI): m/z 1456.

Poly(ethylviologen ditosylate) (7)

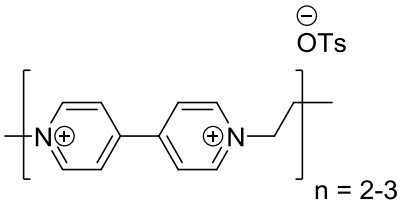

A solution of 4,4' bipyridine (2.033 g, 13.02 mmol) and 1,2-ethane ditosylate (4.816 g, 13.00 mmol) in acetonitrile (100.0 mL) was heated at reflux for 21 h under nitrogen. The product was precipitated from ethyl acetate (300.0 mL) to give a yellow solid (1.416 g).

^{1}H-NMR (CD_3OD): δ 2.3 (4H, s), 4.7 (4H, d), 2.8 (3H, d), 7.2 (3H, d), 7.33 (3H, d), 7.68 (6H,t), 7.99 (3H, m), 8.46 (3H, d), 8.85 (3H, m), 9.02 (3H, d).^{13}C-NMR (CD_3OD): δ 20.0, 59.6, 68.1, 68.1, 122.2, 125.7, 130.0, 145.8, 150.6 **.** MS (NSI): m/z 1407

Poly(ethylviologen) dibromide (8)

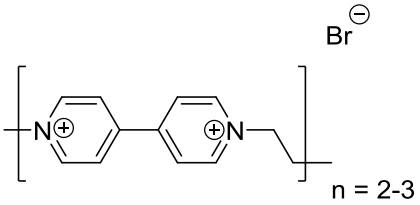

A solution of 4,4’ bipyridine (2.000 g, 0.01280 mmol) and 1,2-dibromoethane (2.410 g, 0.01280 mmol) in dry acetonitrile (85.00 mL) was heated at reflux for 21 h under nitrogen. The crude product was precipitated out of solution using ethyl acetate (300.00 mL) to give a brown solid. (1.828 g).

^{1}H-NMR (C_2D_6OS): δ 4.13-4.20 (2H, t, CH_2), 5.07-5.14 (2H, t, CH_2), 8.06-8.17 (4H, m, m-Py), 8.88-8.95 (4H, m, o-Py).^{13} C-NMR (C_2D_6OS): δ 124.52, 125.62, 128.52, 145.40. MS (NSI): m/z 970.93

Poly (ethylviologen) dichloride (9)

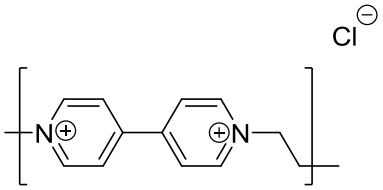

A solution of 4,4’ bipyridine (2.000 g, 12.80 mmol) and 1,2-dichloroethane (0.82 mL, 12.80 mmol) in acetonitrile (100.0 mL) was refluxed for 21 h under nitrogen. Following this the crude product was washed with acetone (300.0 mL), the desired product was not isolated.

Poly(benzyl viologen) dichloride (10)

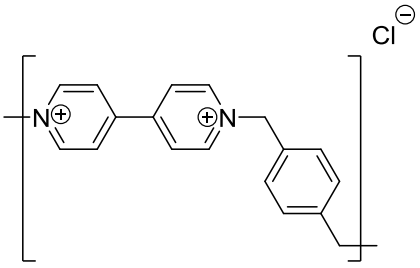

4,4’-bipyridine (2.000 g, 12.80 mmol, 1 equiv.) and dichloro-*p*-xylene (2.227 g, 12.80 mmol, 1 equiv.) were dissolved in acetonitrile (95.00 mL). The solution was stirred overnight at room temperature for polymerisation to occur, but the desired product was not isolated.

1, 1'-Diallyl-[4, 4'-bipyridine]-1, 1'-diium [146] (11)

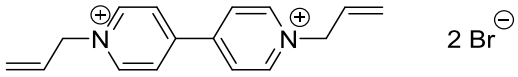

To a solution of 4,4'bipyridine (0.320g, 2.000 mmol, 1 equiv.) in dry acetonitrile (50.00 mL) was added *via* syringe allyl bromide (1.77 mL, 20.00 mol, 10 equiv.), and the reaction mixture was heated at reflux for 4 h. Once cooled the product mixture was isolated *via* filtration, and the filter cake was washed with cold ethanol (20.00 mL) and placed in the freezer to crystallise, to give the title compound as a yellow solid (0.544 g, 65% yield).

^{1}H-NMR (CD_3OD): δ 5.40 (4H, d, 2x CH=C*H*$_2$, J = 8.0 Hz), 5.58-5.66 (4H, m, 2x C*H*$_2$-CH), 6.17-6.32 (2H, m, 2x C*H*-CH_2) 8.71 (4H, d, *m*Py, J = 7.6 Hz), 9.26 (4H, d, *o*Py, J = 7.2 Hz).^{13}C-NMR (CD_3OD): δ 63.5, 123.0, 127.1, 130.2, 145.8, 150.3. MS: (ESI) m/z 238 (100[M-H]) HRMS: calcd. for $C_{16}H_{18}N_2^{2+}$: 237.1387 found 237.1386.MP: 178-180 °C.

1, 4-Bis (allyloxy) benzene [147] **(12)**

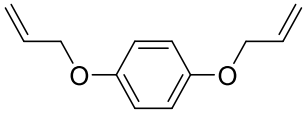

To a stirred mixture of allyl bromide (40.00 g, 330.0 mmol, 3 equiv.) and potassium carbonate (34.50 g, 249.6 mmol, 2.5 equiv.) in acetone (200.0 mL) was added hydroquinone (11.00 g, 99.00 mmol, 1 equiv.). The reaction mixture was heated at reflux for 5 h, and then cooled to rt. The crude product was then collected *via* filtration and recrystallised from hexane to give the product as a yellow solid (7.20 g, 38% yield).

^{1}H-NMR ($CDCl_3$): δ 4.45-4.53 (4H, m, 2 x O-C*H*$_2$), 5.20-5.45 (4H, m, 2 x CH-C*H*$_2$), 5.99-6.13 (2H, m, 2 x C*H*-CH_2), 6.85 (4H, s, Ph).^{13}C-NMR ($CDCl_3$): δ 69.5, 115.7, 117.6, 133.7, 152.9. MS (ASAP): m/z 190 (100[M+H]) HRMS: calcd. for $C_{12}H_{14}O_2$ 191.1066 found 191.1067. Anal. calcd for $C_{12}H_{14}O_2$: C, 75.76; H, 7.46 Found: C, 75.86; H, 7.64.

(Allyloxy) benzene[148] **(13)**

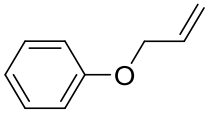

To a stirred solution of phenol (9.410 g, 0.1000 mol, 1 equiv.) and potassium carbonate (27.64 g, 0.200 mol, 2 equiv.) in acetone (100.00 mL) was added, *via* syringe, allyl bromide (10.4 mL, 0.120 mol, 1.2 equiv.). The mixture was heated at reflux for 12 h, and then cooled. The mixture was then filtered and the filtrate was washed with ethyl acetate (100.0 mL) Following this, the excess solvent was removed under reduced pressure and the crude product was purified *via* column chromatography (silica) eluting with hexane:ethyl acetate (10:1) to yield a nearly colourless, light yellow oil (6.50 g, 53%).

^{1}H-NMR ($CDCl_3$): δ 4.51-4.57 (2H, m, CH=C*H*$_2$), 5.28-5.33 (1H, m, C*H*=CH_2), 5.41-5.48 (1H, m, C*H*=CH_2), 6.01-6.17 (1H, m, CH), 6.91-7.05 (3H, m, *m*Ph), 7.25-7.37 (2H, m, *o*Ph).^{13}C-NMR ($CDCl_3$): δ 68.8, 114.8, 117.8, 120.9, 129.6, 133.5, 158.7. MS: (ASAP) m/z 134 (100[M+H]) HRMS: calcd. for $C_9H_{10}O$: 135.0802 found 135.0804.

Co-polymerisation of three monomers [82] **(14)**

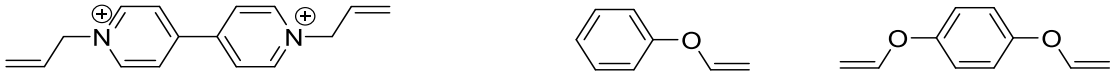

A solution of deionised water (200.0 mL) was acidified to pH = 2.0 with sulphuric acid and purged with nitrogen for 30 minutes. The solution was heated at 70°C for 20 mins, following this (allyloxy) benzene (10.00 g, 0.07453 mol), 1,4-bis(allyloxy)benzene (100 mg, 0.5257 mmol), 1,1'-diallyl-[4,4'-bipyridine]-1,1'-diium (10.0 mg, 0.0420 mmol) were added rapidly and the system was left under inert atmosphere. Whilst stirring, a solution of potassium peroxodisulfate (120.0 mg, .0444 mmol) in water (10.00 mL) was added in one portion *via* syringe. The mixture was stirred under nitrogen overnight under these conditions, and then quenched with methanol (20.0 mL). The mixture was centrifuged at 3000 rpm for 30 mins and then extracted with dichloromethane (100.0 mL). The water mixture was tested for polymerisation using a dialysis membrane with a cut-off of 10 KDa., but the ideal product was not isolated.

Polymerisation using protoporphyrin IX [82] **(15)**

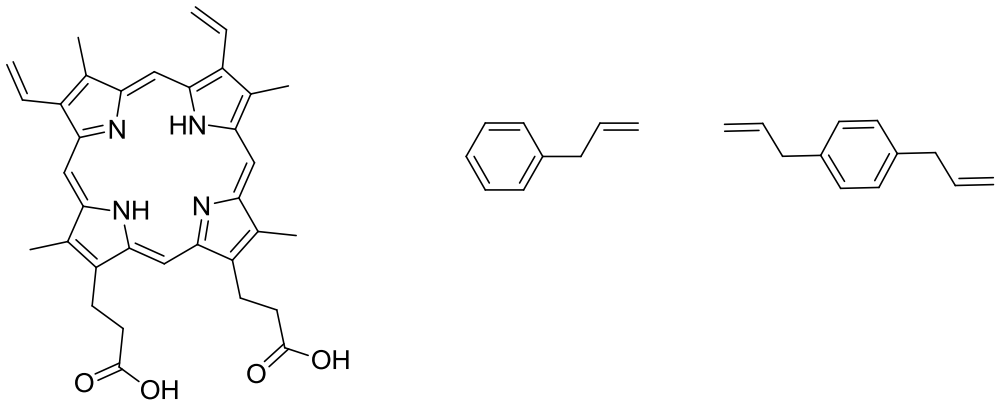

A solution of deionised water (200.0 mL) was acidified to pH = 2.3 with sulphuric acid, and then purged with nitrogen for 20 mins. Following this, protoporphyrin IX (10.00 mg, 0.00178 mmol), styrene (10.00 g, 0.09602 mol), and divinylbenzene (100.0 mg, 0.7692 mmol) were added and the mixture was stirred under nitrogen whilst a solution of potassium peroxodisulfate (120.0 mg, 0.4439 mmol) in water (10.00 mL) was added. The mixture was left to polymerise for 7 h and then quenched with methanol. The ideal product was not isolated.

Co-polymerisation of one monomer with styrene and divinylbenzene (16)

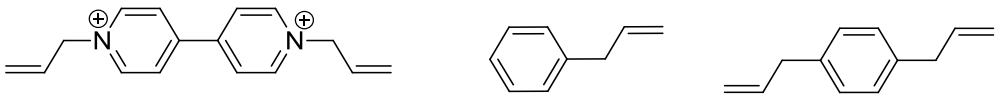

A solution of deionised water (200 mL) was acidified to pH = 2.3 with sulphuric acid, and the solution was purged with nitrogen and heated to 70 °C for 20 mins. Following this, styrene (10.00 g, 0.09600 mol), divinylbenzene (0.100 g, 0.7681 mmol) and protoporphyrin IX (0.01 g, 0.0178 mmol) were added and the reaction maintained under nitrogen. Whilst stirring, potassiumperoxodisulfate (120.0 mg, 0.4439 mmol) in water (10.00 mL) was added. The solution was stirred for 7 h, and then allowed to cool to room temperature before being quenched with methanol (50.00 mL). The resulting particles were separated using centrifugation at 3000 rpm for 30 mins, and a white precipitate was formed, which was washed with dichloromethane to remove any unreacted monomers. The particles were filtered and dried *in vacuo* at 40 °C to yield an insoluble white solid (10.657 g) which was not able to be analysed. The ideal product was not isolated.

1-(2-Boronobenzyl)-[4, 4'-bipyridin]-1-ium bromide (17)

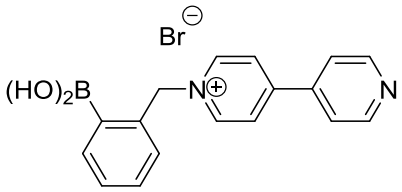

To a solution of 2-bromomethylphenylboronic acid (0.400 g, 1.86 mmol, 1 equiv.) in acetone (50.00 mL) was added 4,4'-bipyridine (1.160 g, 7.400 mmol, 4 equiv.). The reaction mixture was heated at reflux temperature for 15 mins. After cooling to rt, diethyl ether (100.0 mL) was added to the reaction mixture to precipitate the product, which was then isolated *via* filtration, and washed with acetone (2 x 20.00 mL) to give a yellow solid (0.521 g, 24% yield).

^{1}H-NMR ($CDCl_3$): δ 3.29-3.31 (2H, m, C*H*$_2$), 7.46-7.61 (3H, m, *m*Py),7.79-7.88 (1H, m, *Ph*-B(OH)$_2$), 7.96-8.04 (2H, m, *o*Py), 8.50 (2H, d, *o*Py, J = 8.0 Hz), 8.78-8.84 (2H, m, Py), 9.04 (2H, d, Py, J = 7.8 Hz).^{13}C-NMR ($CDCl_3$): δ 64.2, 122.2, 125.4, 129.1, 131.2, 136.2, 142.3, 145.1, 149.8, 150.5, 153.8. MS (ESI): m/z 291 (100[M+H]$^+$) HRMS: calcd. for $C_{17}H_{16}O_2N_2B$: 290.1340 found 290.1336. MP: 128-132 °C.

1-(4-Boronobenzyl)-[4, 4'-bipyridin]-1-ium bromide (18)

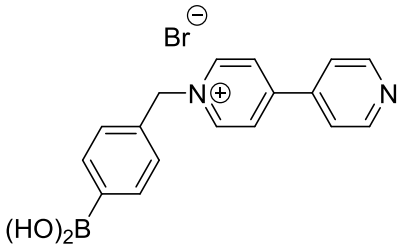

To a solution of 4-bromomethylphenylboronic acid (0.400 g, 1.86 mmol, 1 equiv.) in acetone (50.00 mL) was added 4, 4'-bipyridine (1.160 g, 7.400 mmol, 4 equiv.). The reaction was heated at reflux temperature for 15 mins and then cooled to rt. After cooling, diethyl ether (100.0 mL) was added and the resulting precipitate was isolated *via* filtration and washed with acetone and diethyl ether to give a green solid (231 mg, 43% yield).

^{1}H-NMR (CD_3OD): δ 3.29-3.33 (2H, m, C*H*$_2$), 7.66-7.69 (2H, m, Py), 7.84-7.88 (2H, m, Py), 8.41-8.45 (2H, m, Ph), 8.64–8.67 (2H, m, Py), 8.78-8.82 (2H, m, Ph). ^{13}C-NMR (CD_3OD): δ 64.5, 122.0, 126.2, 128.2, 135.1, 141.8, 145.3, 146.1 149.9, 150.8, 154.3. MS (ESI): 291 m/z (100[M+]) HRMS: calcd. for $C_{17}H_{16}BN_2O_2$: 290.1342 found 290.1336.MP: 128-132 °C.

1-(But-3-yn-1-yl)-[4, 4'-bipyridin]-1-ium bromide (19)

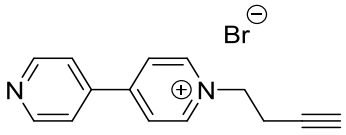

To a solution of 4,4'-bipyridine (0.400 g, 2.56 mmol, 1 equiv.) in DMF (50.00 mL) was added 1-bromo-4-butyne (0.30 mL, 3.1 mmol, 1 equiv.), the reaction mixture was heated to 80 °C overnight. Following this, acetonitrile (100.0 mL) was added to precipitate out the product, which was obtained as a brown solid (158 mg, 30% yield).

^{1}H-NMR (CD_3OD): δ 2.60-2.65 (1H, m, C*H*), 3.02-3.09 (2H, m, CH-C*H*$_2$), 4.83-4.86 (2H, m, CH_2-CH_2), 8.02 (2H, dd, *m*Py, J = 7.2 Hz, J = 2.7 Hz), 8.57 (2H, d, *o*Py, J = 7.2 Hz), 8.84 (2H, dd, *m*Py, J = 7.2 Hz, J = 2.8 Hz), 9.18 (2H, d, *o*Py, J = 7.2 Hz).^{13}C-NMR (CD_3OD): δ 20.5, 59.4, 73.7, 77.7, 122.3, 125.7, 142.3, 145.5, 150.5, 154.4. MS (NSI): m/z 209 (100 [M]+) HRMS: calcd. for $C_{14}H_{13}N_2$: 209.1072 found 209.1073.

1-Bromo-3, 6, 9, 12-tetraoxapentadec-14-yne (20)

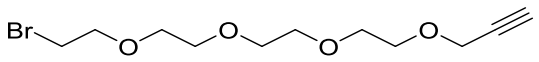

To a solution of 3,6,9,12-tetraoxapentadec-14-yn-1-ol (0.200 g, 0.861 mmol) in dry dichloromethane (50.00 mL) was added dropwise, *via* syringe, PBr_3 (1.32 mL, 1.72 mmol). The reaction mixture was stirred at rt overnight under nitrogen. Following this the solution was diluted using sat. sodium bicarbonate (50.00 mL) and subsequently extracted using water (2 x 20.00 mL) and dichloromethane (2 x 50.00 mL). The combined organic layers were dried over magnesium sulphate and the excess solvent was removed under reduced pressure to give a yellow oil (0.200 g, 78% yield).

^{1}H-NMR ($CDCl_3$): δ 2.42-2.45 (1H, m, C*H*), 3.47 (2H, t, CH_2, J = 6.0 Hz), 3.64-3.73 (12H, m, 6 x CH_2), 3.81 (2H, t, CH_2, J = 7.2 Hz), 4.21 (2H, d, CH_2-CH, J = 4.2 Hz).^{13}C-NMR ($CDCl_3$): δ 18.4, 52.6, 58.6, 69.2, 70.5, 70.6, 70.7, 71.3. MS (NSI): m/z 295 (100[M+NH_4]$^+$) HRMS: calcd. for $C_{11}H_{23}BrO_4N$: 312.0805 found 312.0805.

1-(3, 6, 9, 12-Tetraoxapentadec-14-yn-1-yl)-[4, 4'-bipyridin]-1-ium (21)

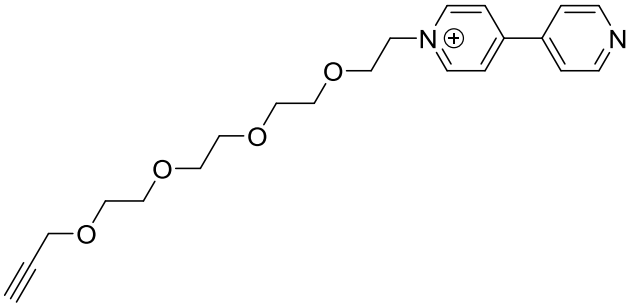

A solution of 1-bromo-3, 6, 9, 12-tetraoxapentadec-14-yne (0.200 g, 0.678 mmol, 1.2 equiv.) and 4, 4'-bipyridine (0.088 g, 0.56 mmol, 1 equiv) in DMF was heated at 80 °C overnight. The mixture was cooled and then the excess solvent was removed under reduced pressure to give a brown solid (0.150 g, 72% yield).

^{1}H-NMR ($CDCl_3$): δ 2.93-3.29 (16H, m,CH_2*Peg*), 3.29-3.33 (1H, m, CH), 3.55-3.69 (2H, m, OC*H*$_2$-CH), 7.49-7.60 (4H, m, *m*Py), 8.59-8.73 (4H, m, *o*Py). ^{13}C-NMR ($CDCl_3$): δ 48.8, 48.9, 49.2, 49.4, 49.6, 121.8, 146.0, 150.2. MS (NSI): m/z 371 (100[M]+) HRMS: calcd. for $C_{21}H_{27}O_4N_2$: 371.1973 found 371.1965.

Synthesis of titanium dioxide nanoparticles

To a solution of titanium(IV)isopropoxide (20.00 mL) was added dropwise distilled water (5.00 mL) under continuous stirring until a homogenous mixture was achieved. The white solid was placed in an oven at 100 °C for 24 h, and then removed and placed in a furnace at 400 °C for 5 hours to give the resulting white solid (5.300 g).

Analysis using pXRD;

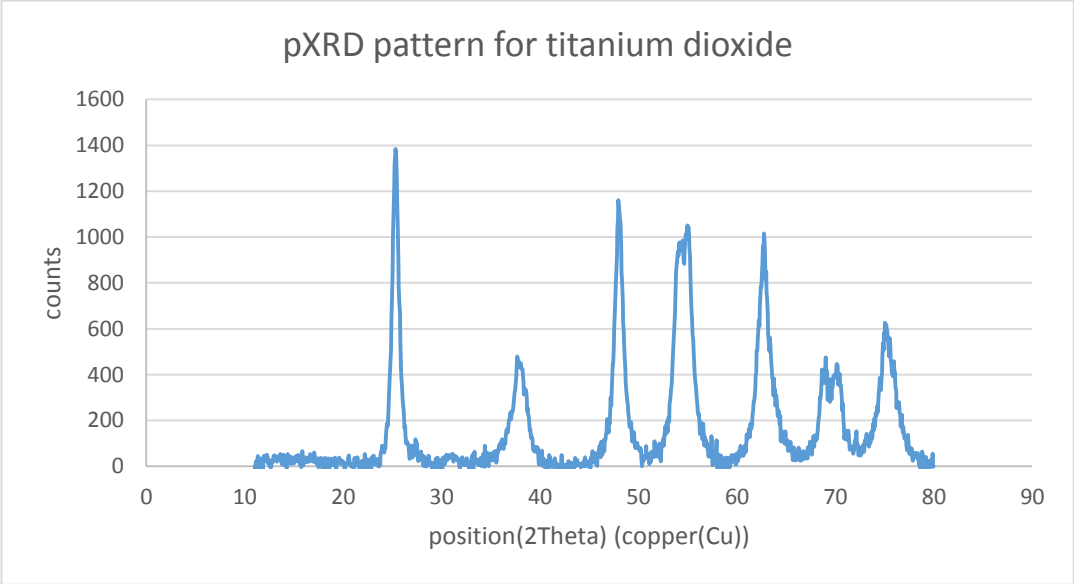

Synthesis of amine modified titanium dioxide

Titanium dioxide (0.500 g) was placed in a furnace at 200 °C with ammonium gas bubbling through for 2h. Following this the sample was left to cool and the product, the fluorescence of the sample was tested and analysis was carried out by pXRD.

pXRD;

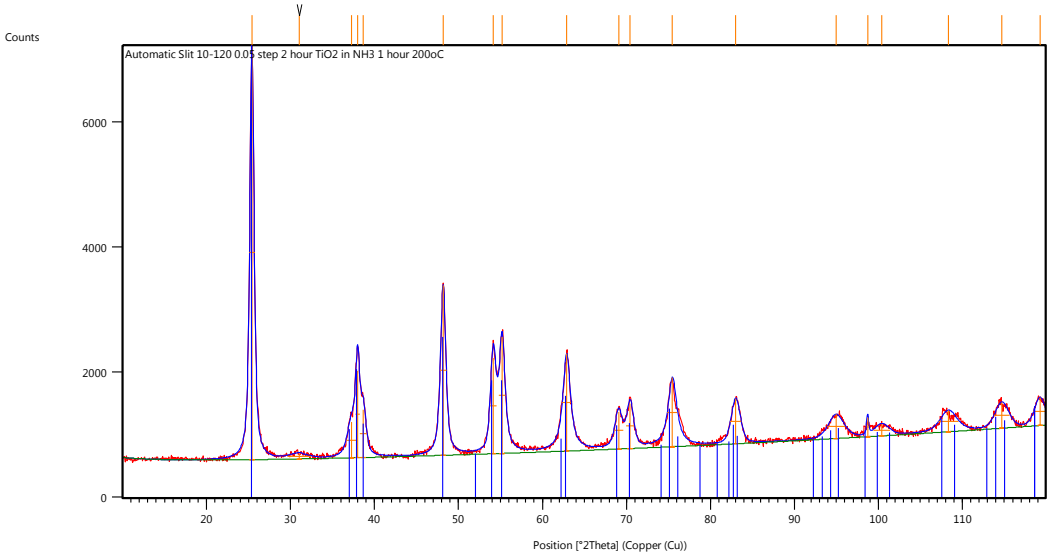

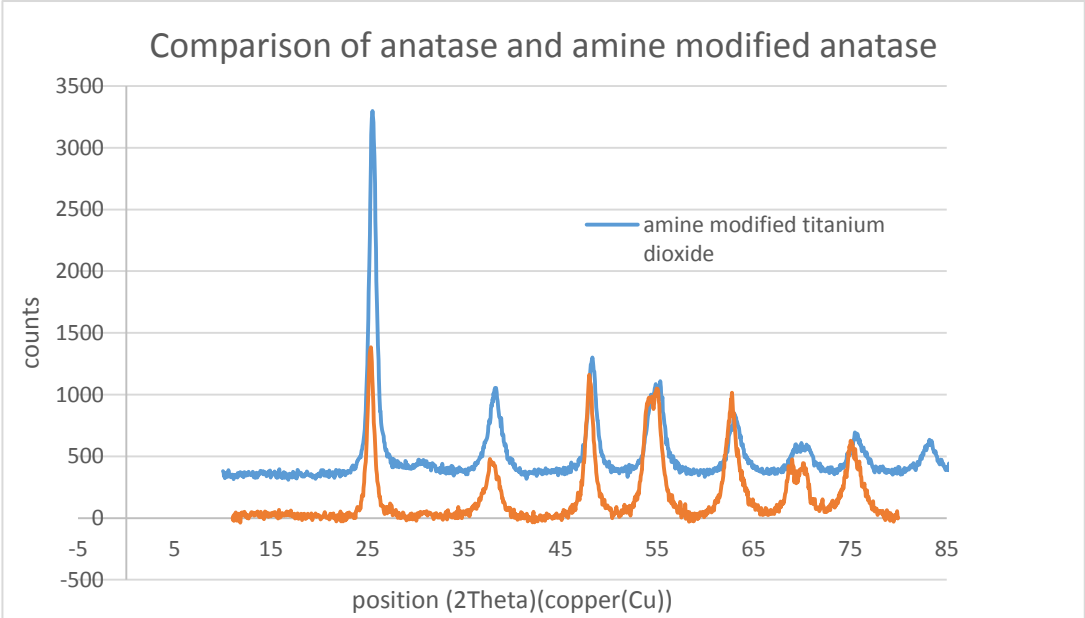

Di (1H-pyrrol-2-yl) methane (22) [175]

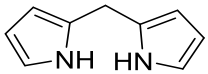

A solution of formaldehyde (33% w/w solution in water, 8.10 mL, 90.0 mmol, 45 equiv.) and pyrrole (150.0 mL, 2.161 mmol, 1 equiv.) was degassed by stirring under reduced pressure and flushing with nitrogen. Following this, trifluoroacetic acid (0.81 mL, 11 mmol, 5 equiv.) was added dropwise with vigorous stirring for 5 mins. Following this dichloromethane (150.0 mL) was added, followed by the addition of sat. Na_2CO_3 solution. The reaction mixture was extracted with dichloromethane (2x 100.0 mL) and water (100.0 mL). The crude product was purified by column chromatography (neutral alumina) eluting with dichloromethane and ethyl acetate (10:1). The desired product was not isolated.

Methyl-4(di-(1H-pyrrol-2-yl) methyl) benzoate (23) [178]

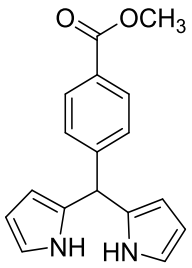

Pyrrole (9.31 mL, 136 mmol) and methyl-4-formylbenzoate (1.120 g, 6.810 mmol) were added to a reaction flask, which was then degassed with nitrogen for 20 mins. Following this, trifluoroacetic acid (0.06 mL, 0.084 mmol) was added and the reaction mixture was stirred at rt for 40 mins under nitrogen, protected from light. Excess pyrrole was removed under reduced pressure to give a brown oil. Following this, the crude product was purified by column chromatography (silica) eluting with CH_2Cl_2: CH_3OH (100:0.5) to yield a white solid (1.050 g, 55% yield).

^{1}H-NMR ($CDCl_3$): δ 3.90 (3H, s, C*H*$_3$), 5.53 (1H, s, bridging H), 5.87-5.91 (2H, m, *m*NH), 6.15-6.18 (2H, m, *m*NH), 6.71-6.74 (2H, m, *o*NHpyrrole), 7.29 (2H, d, *oAr*$COOCH_3$, J = 8.0 Hz), 7.98 (2H, d, *m*Ph, J = 8.0 Hz).^{13}C-NMR ($CDCl_3$): δ 44.1, 52.2, 107.6, 108.7, 117.7, 128.5, 130.0, 131.7, 147.4 (C=O), 177.4. MS: (ESI) m/z 280 (100[M+NH_4OAc]) HRMS: calcd. for $C_{17}H_{16}N_2O_2$:281.1288 found 281.1285.Anal. calcd for $C_{17}H_{16}N_2O_2$: C, 72.84; H, 5.75; N, 9.99. found: C, 71.80; H, 5.72; N, 9.80.

4-(Di (1H-pyrrol-2-yl) methyl) pyridine (24) [177]

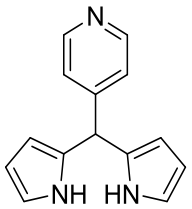

A solution containing 4-pyridinecarboxaldehyde (1.90 mL, 20.0 mmol, 1 equiv.) and pyrrole (20.00 mL, 290.0 mmol, 10 equiv.) was stirred for 15 h at 85 °C under nitrogen. The excess solvent was then removed under reduced pressure, and the crude product was purified by column chromatography eluting with CH_2Cl_2: ethyl acetate 50:50. The product was dissolved in CH_2Cl_2 and precipitated using hexane to give a brown solid (1.863 g, 41% yield).

^{1}H-NMR ($CDCl_3$): δ 5.46 (1H, s, bridging H), 5.84-5.94 (2H, m, *m*pyrrole), 6.15-6.22 (2H,q, *m*pyrrole), 6.72-6.74 (2H, m, *o*pyrrole), 7.13 (2H, d, *m*Py, J = 6.8 Hz), 8.02 (2H, bs, NH), 8.53 (2H, d, *o*Py, J = 6.8 Hz).^{13}C-NMR ($CDCl_3$): δ 43.5, 107.8, 108.8, 118.0, 123.6, 130.7, 150.2. MS (ESI): m/z 223 (100[M+NH_4OAc]) HRMS: calcd. for $C_{14}H_{13}N_3$: 224.1191 found 224.1192. Anal. calcd for $C_{14}H_{13}N_3$: C, 75.31; H, 5.87; N, 18.82. found: C, 74.60; H, 5.95; N, 18.41.

2, 2'-(Phenylmethylene) bis (1H-pyrrole) (25) [179]

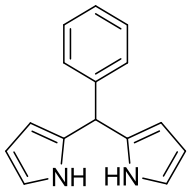

To a stirred and degassed solution of pyrrole (15.60 mL, 22.40 mmol, 2 equiv.) and benzaldehyde (1.20 mL 11.2 mmol, 1 equiv.) was added dropwise, *via* a syringe, trifluoroacetic acid (1.00 mL, 0.0131 mol). The crude mixture was stirred at room temperature for 1 h protected from the light. Excess pyrrole was removed under reduced pressure to give a brown oil which was purified *via* column chromatography (silica) eluting with CH_2Cl_2: hexane (2:1) to give a brown solid (1.911 g, 77%).

^{1}H-NMR ($CDCl_3$): δ 5.49 (1H, s, C-H-ArH), 5.62-5.95 (2H, m, *o*NHpyrrole), 6.07-6.23 (2H, m, *m*NHAr), 6.58-6.78 (2H, m, *m*NHAr), 7.18-7.40 (5H, m, Ph).^{13}C-NMR ($CDCl_3$): δ 44.1, 107.3, 108.5, 117.3, 117.7, 127.1, 128.8, 132.6, 142.2. MS (APCI): m/z 222 [M+] HRMS calcd. for $C_{15}H_{15}N_2$: 223.1227 found 223.1230. Anal. Calcd. for $C_{15}H_{15}N_2$: C, 79.33; H, 6.22; N, 12.28. found: C, 79.24; H, 6.62; N, 12.42.

Dimethyl 4, 4'-(porphyrin-5, 15-diyl) dibenzoate (26)

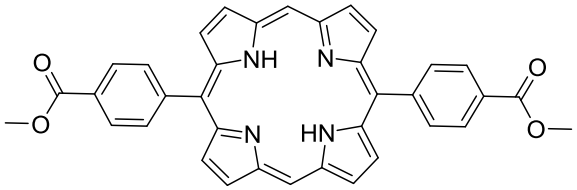

Methyl-4(di-(1H-pyrrol-2-yl) methyl) benzoate (645 mg, 2.30 mmol) was dissolved in dry CH_2Cl_2 (630 mL), and trimethylorthoformate (18.0 mL, 165 mmol, 70 equiv.) was then added to the reaction mixture in one portion. A solution of trichloroacetic acid (8.83 g, 54.0 mmol, 24 equiv.) in dry CH_2Cl_2 (230.0 mL) was added to the reaction mixture dropwise over 15 mins. The resulting solution was stirred in the dark for 4 h. Following this, excess acid was quenched by adding pyridine (15.6 mL, 0.194 mmol) in one portion. The solution was then stirred for 17 h protected from light, followed by 4 h open to light. Excess solvent was then removed under reduced pressure and the crude product purified by column chromatography eluting with (silica) CH_2Cl_2: hexane (3:1). Excess solvent was removed under reduced pressure and the product was precipitated from methanol over dichloromethane to give a purple solid (10 mg, 0.75%). The product was found to be insoluble in all common NMR solvents.

MS (ESP): m/z 578 (100(M+H)) HRMS calcd. for $C_{36}H_{26}N_4O_4$: 579.2022 found 579.2027.

5, 15-Di (pyridin-4-yl) porphyrin (27)

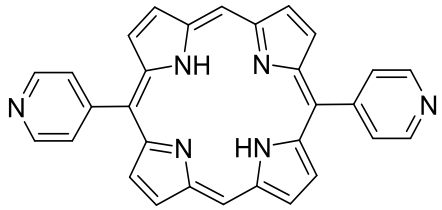

To a stirred solution of 5-(4-pyridyl) dipyrromethane (500 mg, 2.24 mmol, 1 equiv.) and trimethylorthoformate (18.0 mL, 170 mmol, 75 equiv.) in dry CH_2Cl_2 (630 mL) was added dropwise, *via* syringe, over 15 mins, a solution of trichloroacetic acid (8.83 g, 54.0 mmol, 24 equiv.) in dry CH_2Cl_2 (227.0 mL). The solution was stirred in the dark at room temperature for 4 h before being quenched with pyridine (15.6 mL, 0.194 mmol) and then stirred in the dark for a further 17 h. Following this the solution was stirred in the light and open to air for 4 h. The excess solvent was removed under reduced pressure and then the crude product was purified using column chromatography (silica) with CH_2Cl_2: CH_3OH (10:1) to give a purple solid (5.5 mg, 0.45% yield).

^{1}H-NMR ($CDCl_3$): δ 8.23 (4H, d, *o*Py, J = 6.0 Hz), 9.07 (4H, d, βH, J = 6.0 Hz), 9.10 (4H, d, *m*Py, J = 6.0 Hz), 9.47 (4H, d, βH, J = 6.0 Hz), 10.40 (2H, s, 10,20 *meso*).^{13}C-NMR ($CDCl_3$): δ 106.1, 127.2, 129.8, 130.7, 132.5, 134.9, 136.9, 148.6, 149.6. MS (EI): m/z 464 (100[M^+]) HRMS: calcd. for $C_{30}H_{20}N_6$: 464.1737 found 464.1744.

5, 15-Diphenylporphyrin (28)

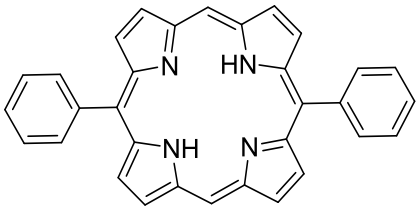

To a stirred solution of 5-phenyl dipyrromethane (500 mg, 2.25 mmol, 1 equiv.) and trimethylorthoformate (18.0 mL, 165 mmol, 70 equiv.) in dry CH_2Cl_2 (630.0 mL) was added dropwise *via* syringe a solution of trichloroacetic acid (8.83 g, 54.0 mmol, 24 equiv.) in CH_2Cl_2 under nitrogen. The solution was stirred in the dark at room temperature for 4 h before being quenched with pyridine (15.6 mL, 0.194 mmol) and stirred in the dark again for 17 h. The solution was then purged with air for 10 mins and stirred in the light for a further 4 h. The excess solvent was removed under reduced pressure and the residue purified by column chromatography eluting with (silica): CH_2Cl_2: hexane (1:1) to give a purple solid (100 mg, 9.61%)

UV-Vis (CH_2Cl_2): λ_{max} (nm): 405, 505, 540, 585, 635, ε (414 nm) = 577109 M^{-1} cm^{-1}.^{1}H-NMR ($CDCl_3$): δ 7.77-7.90 (6H, m, *m* + *p*Ph), 8.24-8.35 (4H, m, *o*Ph), 9.05-9.48 (8H, m, βH), 10.32 (2H, s, 10,20 *meso*).[13] C-NMR ($CDCl_3$): δ 105.4, 119.2, 127.1, 127.8, 131.2, 131.7, 134.9, 141.5, 145.3, 147.3. MS (NSI): m/z 462 (100$[M+H]^+$) HRMS: calcd. for $C_{32}H_{23}N_4$: 463.1904 found 463.1917.

5,15-di-[4-Carbomethoxyphenyl],10,20-di-(phenyl) porphyrin (29)

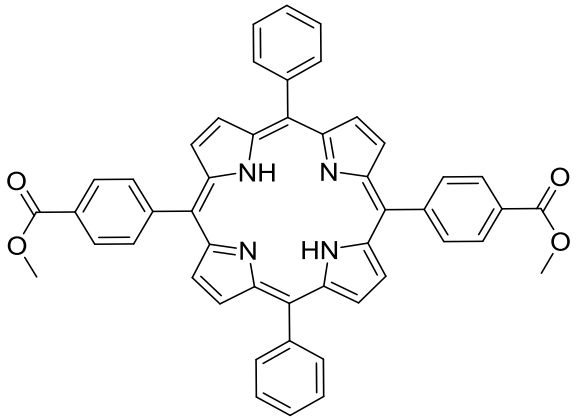

To a refluxing mixture of methyl-4-formylbenzoate (4.39 g, 27.0 mmol, 1 equiv.) and benzaldehyde (4.35 g, 41.0 mmol, 1.5 equiv.) in propionic acid (500.0 mL) was added dropwise, *via* syringe, pyrrole (4.75 mL, 0.105 mol, 4 equiv.). The crude mixture was heated at reflux temperature for an hour and then cooled to rt. Following this, the excess solvent was removed under reduced pressure, and subsequently the crude mixture was purified using a pre-column of CH_2Cl_2: CH_3OH (98:2). Further purification was carried out by column chromatography eluting with (silica) CH_2Cl_2. Finally, the pure product was precipitated from methanol over dichloromethane, then filtered to give a purple solid (175 mg, 0.58 % yield).

UV-Vis (CH_2Cl_2): λ_{max} (nm): 420, 517, 556, 591, 642, ε (420 nm) = 914818 M^{-1} cm^{-1}.^{1}H-NMR ($CDCl_3$) δ 4.12 (6H, s, 2 x C*H*$_3$), 7.72-7.83 (6H, m, *m* + *p*Ph), 8.18-8.25 (4H, m, *o*Ph), 8.32 (4H, d, *o*Ph, J = 8.0 Hz), 8.46 (4H, d, *m*PhCOOCH$_3$, J = 8.0 Hz), 8.76-8.92 (8H, m, βH).^{13}C-NMR ($CDCl_3$) δ 65.5, 119.9, 120.3, 125.4, 126.8, 127.8, 131.3, 134.7, 134.8, 134.8, 140.3, 141.6, 142.2. MS (NSI): m/z 730 (100[M+H]) HRMS: calcd. for $C_{48}H_{34}N_4O_4$:731.2637 found 731.2653.

5,15-di-[4-Methan-1-ol-phenyl],10,20-di-(phenyl) porphyrin (30)

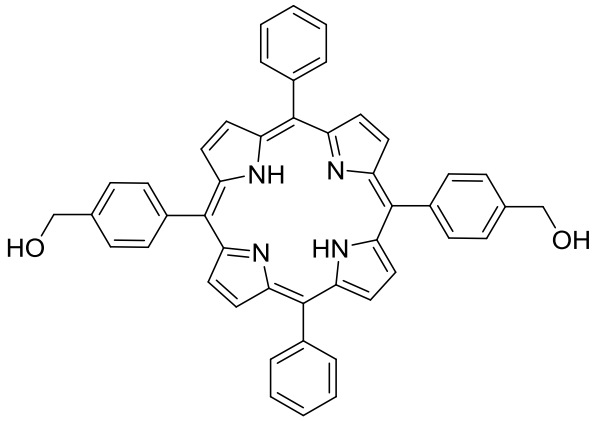

$LiAlH_4$ (77.64 mg, 2.047 mmol, 10 equiv.) was added to dry THF (50.0 mL) and the mixture was stirred under nitrogen for 1 h. To this solution 5,15-di-[4-carbomethoxyphenyl],10,20-di-(phenyl) porphyrin (150 mg, 0.0205 mmol, 1 equiv.) was added and the reaction mixture was stirred under nitrogen for 5 h at rt. Following this, water (21.0 mL) and sat. sodium hydroxide (1.0 mL) were added, and the solution was extracted with CH_2Cl_2 (2 x 50.0 mL). The combined organic fractions were then washed with water (2 x 20.0 mL), and the solvent then removed in *vaccuo*. The crude product was purified by column chromatography (silica) eluting with CH_2Cl_2: CH_3OH (98:2) to yield a purple solid (30 mg, 20% yield).

UV-Vis (CH_2Cl_2): λ_{max} (nm): 416, 521, 556, 602, 654, ε (420 nm) = 464183 M^{-1} cm^{-1}.^{1}H-NMR ($CDCl_3$): δ 5.06 (4H, s, 2 x C*H*$_2$OH), 7.80-7.85 (10H, m, *m*Ph), 8.19-8.22 (8H, m, βH), 8.80-8.89 (8H, m, *o*Ph).^{13}C-NMR ($CDCl_3$): δ 64.5, 125.4, 126.8, 127.8, 134.6, 134.8, 140.4, 141.6, 142.2. MS (NSI): m/z 674 (100[M+H]$^+$) HRMS: calcd. for $C_{46}H_{35}O_2N_4$: 675.2752 found 675.2755.

5,15-[4-Tosylmethylphenyl],10,20-di-(phenyl) porphyrin (31)

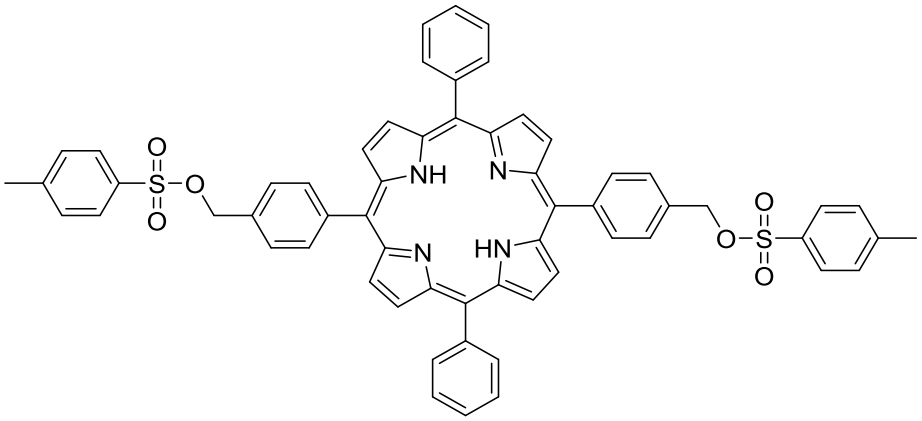

To a solution of 5,15-[4-methan-1-ol],10,20-di-(phenyl) porphyrin (20.0 mg, 0.0298 mmol) in CH_2Cl_2 (50.0 mL) was added triethylamine (1.0 mL). The reaction mixture was cooled to 0 °C, and following this *p*-toluene sulfonylchloride (11.4 mg, 0.0598 mmol, 2 equiv.) was added with stirring for 30 mins. The solution was stirred at 0 °C for 12 h and then diluted with saturated sodium bicarbonate. Following this the solution was extracted with dichloromethane and excess solvent was removed under reduced pressure. The desired product was not isolated.

5,15-di-[4-Mesylmethylphenyl],10,20-di-(phenyl) porphyrin (32)

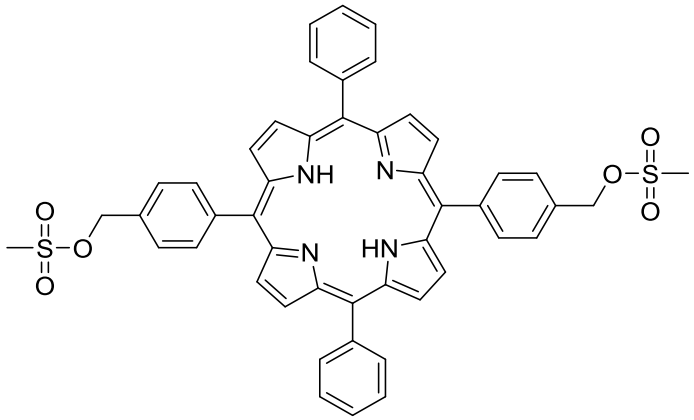

A solution of 5,15-di-[4-methan-1-ol-phenyl],10,20 di-(phenyl) porphyrin (100.0 mg, 0.1484 mmol) in dry dichloromethane (100.0 mL) was cooled to 0°C under nitrogen. Following this, methanesulfonylchloride (1.0 mL, 13 mmol) was added drop-wise and the mixture was warmed to rt and stirred overnight. The crude mixture was washed with saturated sodium bicarbonate and water, then dried over magnesium sulphate and excess solvent removed under reduced pressure, but the desired product was not isolated.

5,15-di-[4-Bromomethylphenyl],10,20-di-(phenyl) porphyrin (33)

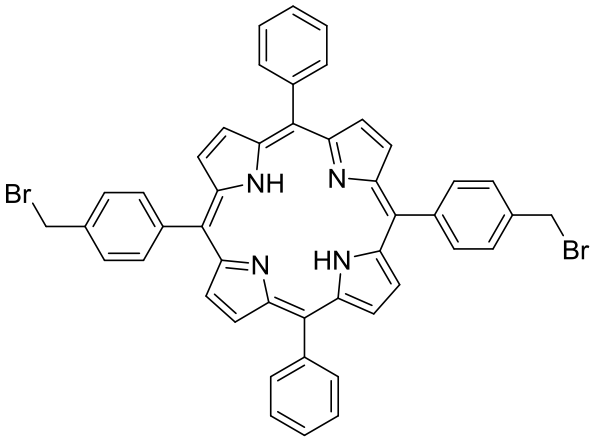

To a stirred solution of 5,15-[4-methan-1-ol-phenyl],10,20-di-(phenyl) porphyrin (160.0 mg, 0.2833 mmol) in dry CH_2Cl_2 (100.0 mL) was added dropwise, *via* syringe, phosphorus tribromide (2.00 mL, 0.0213 mol, 100 equiv.). The mixture was stirred overnight at room temperature under nitrogen. The crude product was neutralised using saturated sodium bicarbonate and then partitioned between dichloromethane and water. The organic layer was dried over magnesium sulphate and the solvent removed under reduced pressure. The product was precipitated from CH_3OH over CH_2Cl_2 to give a purple solid after isolation *via* filtration. (100.0 mg, 44 % yield).

UV-Vis (CH_2Cl_2): λ_{max} (nm): 420, 518, 559, 594, 651, ε (420 nm) = 528187 M^{-1} cm^{-1}.^{1}H-NMR ($CDCl_3$): δ 4.79-4.96 (4H, s, 2 x C*H*$_2$), 7.68-7.84 (10H, m, Ph), 8.12-8.27 (8H, m, PhBr), 8.77-8.94 (8H, m, βH).^{13}C-NMR ($CDCl_3$): δ 53.6, 117.6, 118.9, 120.4, 126.8, 127.8, 131.2, 134.6, 135.8, 139.0, 139.9, 140.2. MS (NSI): m/z 800 (100[M+H]) HRMS calcd. for $C_{46}H_{32}Br_2N_4$: 799.1066 found 799.1066.

5, 15-[Diphenyl],10, 20-di-[4-pyridyl] porphyrin (34)

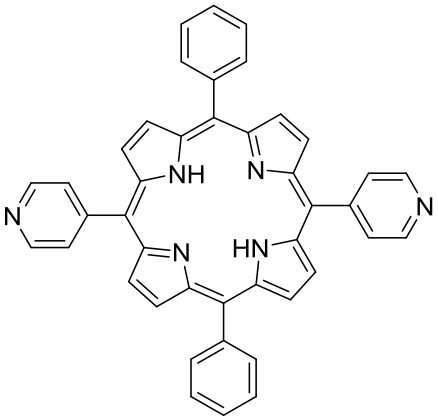

4-(Di(1H-pyrrol-2-yl) methyl) pyridine (500 mg, 2.24 mmol) and benzaldehyde (238 mg, 2.24 mmol) were dissolved in dry dichloromethane (350.0 mL). The mixture was cooled to 0 °C and then trifluoroacetic acid (7.15 mL, 96.3 mmol) was added dropwise, *via* syringe, and the mixture stirred at 0°C for 20 mins. Following this 2,3-dichloro-5,6-dicyano-1,4-benzoquinone (1.015 g, 4.480 mmol) was added and the mixture was stirred at rt for an hour. The solution was then extracted with sodium bicarbonate and water, and the organic layer dried over Na_2SO_4. The crude product was purified *via* column chromatography (silica) eluting with CH_2Cl_2: CH_3OH (98:2). Following this, the excess solvent was removed under reduced pressure and the product was recrystallized from hexane over dichloromethane to give a purple solid after isolation *via* filtration. (655 mg, 47 % yield).

UV-Vis (CH_2Cl_2) λ_{max} (nm): 416, 520, 556, 600, 655 ε (416 nm) = 989213 M^{-1} cm^{-1}.^{1}H-NMR ($CDCl_3$): δ 7.73-7.86 (6H, m, *m* + *p*Ph), 8.17(4H, d, *o*Py, J = 6.2 Hz), 8.22 (4H, d, *o*Py, J = 6.0 Hz), 8.77-8.96 (8H, m, βH), 9.05 (4H, d, *m*Py, J = 6.0 Hz).^{13}C-NMR ($CDCl_3$): δ 116.3, 121.7, 126.8, 128.1, 129.9, 134.5, 141.6, 147.6, 151.2. MS (ASAP): m/z 617 (100$[M+H]^+$) HRMS: calcd. for $C_{42}H_{28}N_6$: 617.2437 found 617.2448.

4,4'-(10,20-Diphenylporphyrin-5,15-diyl)bis(1-(4-(bromomethyl)benzyl)pyridin-1-ium) (34a)

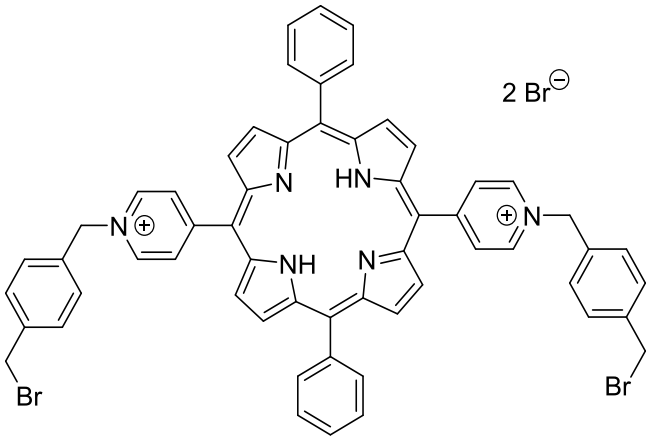

Method one

To a solution of 5,15-diphenyl-10,20-di-(pyridin-4-yl) porphyrin (100.0 mg, 0.1622 mmol, 1 equiv.) in acetonitrile (20.0 mL) was added dibromo-*p*-xylene (0.0428 g, 0.162 mmol, 1 equiv.). The reaction mixture was stirred at rt overnight under nitrogen. Following this the mixture was filtered and washed with acetone, but the desired product was not isolated.

Method two

To a solution of 5,15-diphenyl-10,20-di (pyridin-4-yl) porphyrin (100 mg, 0.162 mmol, 1 equiv.) in acetonitrile (20.0 mL) was added dibromo-*p*-xylene (0.0428 g, 0.162 mmol, 1 equiv.). The reaction mixture heated at reflux overnight under nitrogen. Following this the mixture was filtered and washed with acetone, but the desired product was not isolated.

4,4'-(10,20-Diphenylporphyrin-5,15-diyl)bis(1-(2-(tosyloxy)ethyl)pyridin-1-ium) (34b)

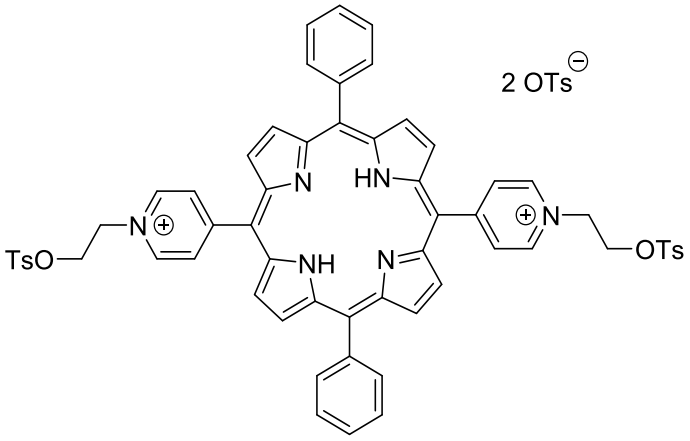

To a solution of 5,15-di-[phenyl]-10,20-di-(pyridin-4-yl) porphyrin (100.0 mg, 0.1622 mmol, 1 equiv.) in acetonitrile (20.0 mL) was added 1,2-ethaneditosylate (60.0 mg, 0.162 mmol, 1 equiv.). The reaction mixture was stirred at rt overnight under nitrogen. Following this the mixture was filtered and washed with acetone, but the desired product was not isolated.

Zinc 5, 15-[diphenyl],10, 20-di-[4-pyridyl] porphyrin (35)

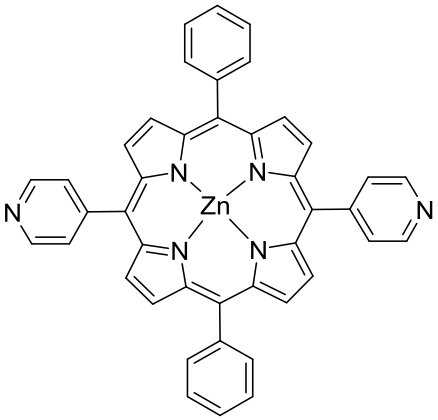

To a stirred solution of 5,15-di-[phenyl]-10,20-di-(4-pyridyl) porphyrin (20.0 mg, 0.0324 mmol) in dichloromethane was added zinc acetate (20.0 mg, 0.109 mmol) in methanol (1.0 mL). The reaction was stirred at room temperature for 1 h. Following this, the excess solvent was removed under reduced pressure and the crude product was precipitated from methanol over dichloromethane to yield a purple solid after isolation *via* filtration. (23 mg, 96% yield).

UV-Vis (CH_2Cl_2): λ_{max} (nm): 420, 559, 606 ε (420 nm) = 484975 M^{-1} cm^{-1}.^{1}H-NMR ($CDCl_3$): δ 7.01-7.24 (4H, m, *o*Py), 7.65-7.75 (8H, m, *m*Ph), 8.09-8.24 (8H, m, βH), 8.70-8.85 (6H, m, *o*Ph).^{13}C-NMR ($CDCl_3$): δ 116.3, 121.7, 126.8, 128.1, 129.9, 134.5, 141.6, 147.6, 151.2. MS (ESI): m/z 680 (100[M+H]) HRMS: calcd. for $C_{42}H_{26}N_6Zn$: 678.1512 found 678.1505.

Manganese 5, 15-[diphenyl],10, 20-di-[4-pyridyl] porphyrin (36)

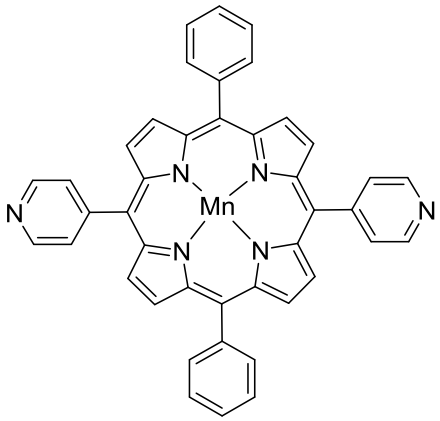

To a 10.00 mL microwave tube was added 5,di-[phenyl]-10,20-di-(4-pyridyl) porphyrin (30.0 mg, 0.0487 mmol) and manganese acetate tetrahydrate (30.0 mg, 0.173 mmol) in DMF (7.0 mL). The reaction was heated and stirred in the microwave for 30 mins at 165°C (300 W, 300 KW). The excess solvent was removed under reduced pressure and the product was precipitated from hexane over dichloromethane to yield a dark green solid that was isolated *via* filtration (31.0 mg, 95% yield).

UV-Vis (CH_2Cl_2) λ_{max} (nm): 472, 594, 622, ε (472 nm) = 100758 M^{-1} cm^{-1}.^{1}H-NMR ($CDCl_3$): δ 5.11-5.43 (4H, m, *o*Py), 7.01-7.55 (8H, m, *m*Ph), 7.77-8.55 (6H, m, *o*Ph). MS (NSI): m/z 669 (100[M+H]) HRMS: calcd. for $C_{42}H_{26}MnN_6$ 669.1588 found 669.1594.

Cobalt 5, 15-[diphenyl],10, 20-di-[4-pyridyl] porphyrin (37)

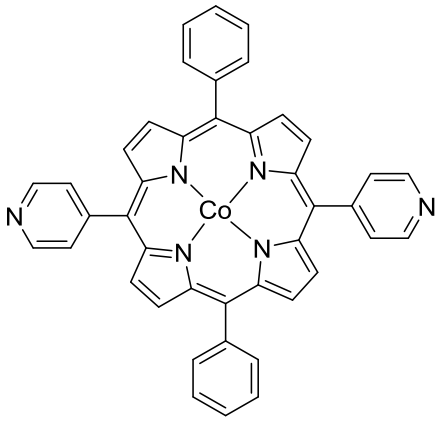

To a 10.00 mL microwave tube was added 5,15-di-[phenyl],10,20-di-[4-pyridyl] porphyrin (30.0 mg, 0.0487 mmol) and $Co(OAc)_2$ (30.0 mg, 0.120 mmol dissolved in DMF. The mixture was stirred and heated at 165 °C for 30 mins. After this the excess solvent was removed under reduced pressure and the product was precipitated from CH_3OH over CH_2Cl_2 to give a purple solid that was isolated *via* filtration (30.0 mg, 98% yield).

UV-Vis (CH_2Cl_2) λ_{max} (nm): 410, 530, 662, ε (472 nm) = 271816 M^{-1} cm^{-1}. MS (ESI): m/z 673 (100 $[M]^+$) HRMS calcd. for $C_{42}H_{26}CoN_6$: 673.1532 found 673.15

Tetraphenylporphyrin (38)

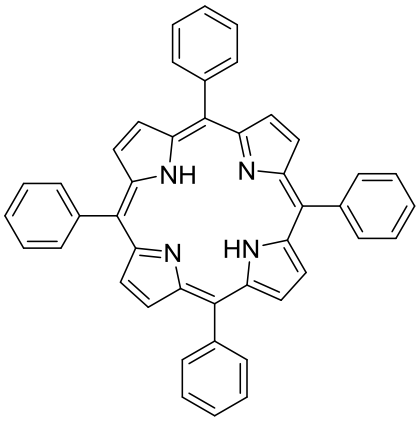

To a refluxing solution of benzaldehyde (8.1 mL, 80 mmol) in propionic acid (500.0 mL) was added dropwise, *via* syringe, pyrrole (5.54 mL, 80 mmol), and the mixture was heated at reflux for 1 h protected from light. The crude reaction mixture was then cooled to room temperature and the excess solvent removed under reduced pressure. The crude product was purified by column chromatography (silica) eluting with CH_2Cl_2, and the product was precipitated from methanol over dichloromethane to give a purple solid which was isolated *via* filtration (3.04 g, 25% yield).

UV-Vis (CH_2Cl_2): λ_{max} (nm): 417, 520, 559, 598, 558, ε (417 nm) = 930998 M^{-1} cm^{-1}.^{1}H-NMR ($CDCl_3$): δ 7.71-7.82 (12, m, *m*+ *p*Ph), 8.18-8.22 (8H, m, *o*Ph), 8.81-8.85 (8H, m, βH).^{13}C-NMR ($CDCl_3$): δ 120.2, 126.8 (βC), 127.8, 128.12, 128.44, 130.0, 134.7 (βC), 139.1, 140.0, 142.3, 146.1. MS (ASAP): m/z 615 (100[M+H]) HRMS calcd. for $C_{44}H_{33}N_4$: 615.2538 found 615.2543.

5-[4-Nitrophenyl]-10,15,20-(triphenyl) porphyrin (39)

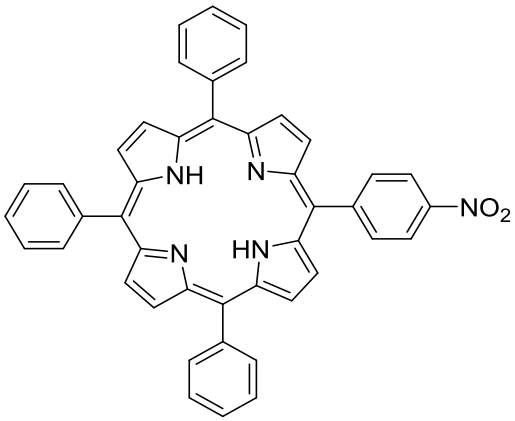

To a cooled solution of tetraphenylporphyrin (245 mg, 0.399 mmol) in trifluoroacetic acid (10.0 mL, 0.131 mol) was added sodium nitrate (28.0 mg, 0.411 mmol). The reaction was warmed to room temperature and stirred for 8 mins. Following this, the reaction mixture was added to water (600.0 mL) and neutralised with sodium carbonate. The solution was then extracted with dichloromethane and dried using magnesium sulphate. The crude product was purified using column chromatography (silica) eluting with (CH_2Cl_2: hexane) 50:50 and precipitated from methanol over dichloromethane to give a purple solid which was isolated *via* filtration. (211 mg, 80% yield).

Rf: (silica, CH_2Cl_2: hexane (1:1)) = 0.22. UV-Vis (CH_2Cl_2): λ_{max} (nm): 418, 516, 552, 590, 646 ε (418 nm) = 406211 M^{-1} cm^{-1}. ^{1}H-NMR ($CDCl_3$): δ 7.69-7.84 (9H, m, *m* + *p*Ph), 8.17-8.27 (6H, m, *o*Ph), 8.39 (2H, d, *o*PhNO_2, J = 8.4 Hz), 8.59-8.68 (2H, d, *m*PhNO_2, J = 8.4 Hz), 8.70-8.94 (8H, m, βH). ^{13}C-NMR ($CDCl_3$): δ 120.8, 121.9, 126.9, 127.9, 131.5, 134.6, 135.2, 141.9, 147.8, 149.3, 165.4. MS (APCI): m/z 659 (100$[M+H]^+$) HRMS: calcd. for: $C_{44}H_{30}N_5O_2$: 660.2382 found 660.2394

5-[4-Nitrophenyl]-10,15,20-triphenylporphyrin (39b)

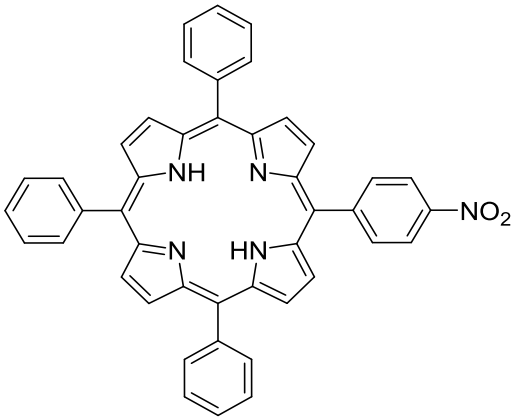

To a refluxing solution of 4-nitrobenzaldehyde (9.81 mL, 90 mmol) and benzaldehyde (9.5 mL, 90 mmol) in propionic acid (500 mL) was added dropwise, *via* syringe, pyrrole (12.5 mL, 180 mmol). The solution was heated at reflux for 3h and then cooled to rt. The excess solvent was removed under reduced pressure and the crude product was purified firstly using a pre-column (silica) in CH_2Cl_2. The crude product was further purified using column chromatography (silica) eluting with CH_2Cl_2: hexane (1:1). The product was precipitated from methanol over dichloromethane to give a purple solid which was isolated *via* filtration (400 mg, 0.7%)

Rf: (silica, CH_2Cl_2: hexane (1:1)) = 0.22.UV-Vis (CH_2Cl_2): λ_{max} (nm): 418, 516, 552, 590, 646, ε (418 nm) = 406211 M^{-1} cm^{-1}.^{1}H-NMR ($CDCl_3$): δ 7.69-7.84 (9H, m, *m* + *p*Ph), 8.17-8.27 (6H, m, *o*Ph), 8.39 (2H, d, *o*PhNO_2, J = 8.4 Hz), 8.59-8.68 (2H, d, *m*PhNO_2, J = 8.4 Hz), 8.70-8.94 (8H, m, βH).^{13}C-NMR ($CDCl_3$): δ 120.8, 121.9, 126.9, 127.9, 131.5, 134.6, 135.2, 141.9, 147.8, 149.3, 165.4. MS (APCI): m/z 659 (100 $[M+H]^+$) HRMS: calcd. for: $C_{44}H_{30}N_5O_2$: 660.2382 found 660.239.

5-[4-Aminophenyl]-10,15,20-tri-(phenyl)porphyrin (40)

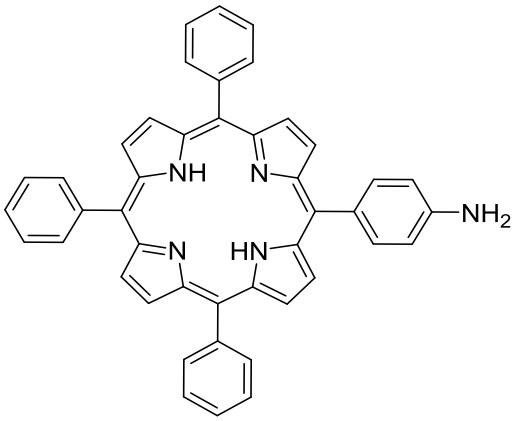

To a solution of 5-[4-nitrophenyl]-10,15,20-tri-(phenyl)porphyrin (434 mg, 0.616 mmol) in HCl (36% in water, 200.0 mL) was added tin (II) chloride (417 mg, 1.85 mmol). The mixture was stirred at 60 °C under nitrogen for 1 h. The excess solvent was removed under reduced pressure and the residue then dissolved in DCM/TEA (9:1) (200.0 mL) and stirred for 10 mins at rt. The solution was washed with water and the organic layer was subsequently dried with magnesium sulphate. The excess solvent was removed under reduced pressure and the product was then precipitated from methanol over dichloromethane to give a purple solid which was isolated *via* filtration (391 mg, 98% yield).

Rf: (silica, CH_2Cl_2: hexane (1:1)) = 0.45. UV-Vis (CH_2Cl_2): λ_{max} (nm): 418, 517, 556, 594, 650, ε (418 nm) = 962563 M^{-1} cm^{-1}.^{1}H-NMR ($CDCl_3$): δ 4.01 (2H, bs, NH_2), 7.06 (2H, d, *o*PhNH_2, J = 8.8 Hz), 7.68-7.83 (9H, m, *m* + *p*Ph), 7.99 (2H, d, *m*PhNH_2, J = 8.2 Hz), 8.21 (6H, d, *o*Ph, J = 8.0 Hz), 8.71-8.89 (8H, m, βH).^{13}C-NMR ($CDCl_3$): δ 116.9, 120.7, 121.2, 121.9, 126.9, 127.9, 134.6, 135.2, 141.9, 147.8, 149.3. MS (NSI): m/z 629 (100$[M+H]^+$) HRMS: calcd. for $C_{44}H_{32}N_5$: 630.2638 found 630.2652.

5-(4-Azidophenyl)-10,15,20-tri-(phenyl) porphyrin (41)

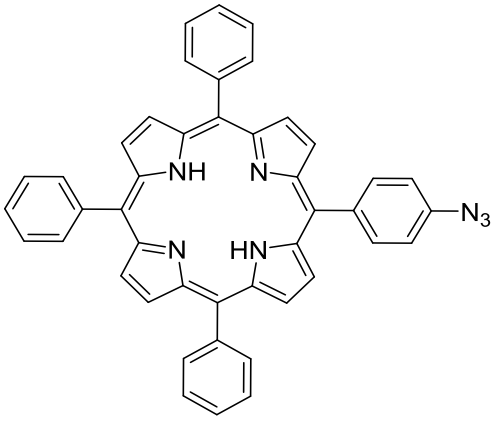

To a stirred solution of 5-[4-aminophenyl]-10,15,20-tri-(phenyl)porphyrin (350 mg, 0.543 mmol) in TFA at 0°C was added a solution of sodium nitrite (75 mg, 1.0 mmol) in H_2O (3.0 mL). The mixture was stirred for 15 mins at 0°C. Following this, a solution of sodium azide (141 mg, 2.17 mmol) in water (2.0 mL) was added drop-wise *via* syringe. The reaction mixture was stirred at 0°C for 1h and after this time the solution was diluted with water and neutralised using sodium hydrogen carbonate. The solution was then extracted with dichloromethane, and the organic layer dried over magnesium sulphate. Excess solvent was removed under reduced pressure and the product was precipitated from methanol over dichloromethane to give a purple solid after isolation *via* filtration (328 mg, 92% yield).

Rf: (silica, CH_2Cl_2: hexane (1:1)) = 0.35. UV-Vis (CH_2Cl_2): λ_{max} (nm): 418, 515, 556, 594, 650, ε (418 nm) = 515509 M^{-1} cm^{-1}.^{1}H-NMR ($CDCl_3$): δ 7.43 (2H, d, *m*PhN_3, J = 8.0 Hz), 7.70-7.85 (9H, m, *m* + *p*Ph), 8.16-8.29 (8H, m, *o*Ph + *o*PhN_3), 8.71-8.95 (8H, m, βH).^{13}C-NMR ($CDCl_3$): δ 113.9, 117.5, 118.9, 120.3, 126.8, 127.7, 131.3, 134.6, 135.8, 139.0, 142.2. MS (ESI): m/z 655 (100[M+H]) HRMS: calcd. for $C_{44}H_{29}N_7$: 656.2552 found 656.2552.

Zinc 5-(4-Azidophenyl)-10,15,20-tri-(phenyl) porphyrin (41b)

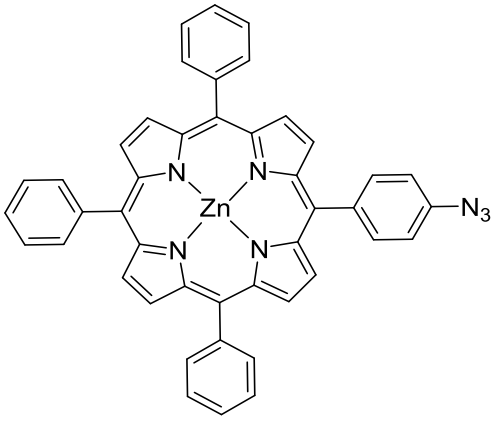

To a solution of 5-(4-azidophenyl)-10,15,20-tri-(phenyl) porphyrin (200 mg, 0.911 mmol) in dichloromethane was added zinc acetate (200 mg, 1.09 mmol). The solution was heated at 40 °C for 4h, and then cooled. Following this excess solvent was removed under reduced pressure and then the product was precipitated from hexane over dichloromethane to give a purple solid (191 mg, 89 % yield).

Rf (CH_2Cl_2: hexane 6:4) = 0.576. UV-Vis (CH_2Cl_2): λ_{max} (nm): 415, 550, 595, ε (415 nm) = 913021 M^{-1} cm^{-1}.^{1}H-NMR ($CDCl_3$): δ 7.37-7.45 (2H, m, *m*PhN_3), 7.71-7.84 (9H, m, *m*Ph), 8.17-8.31 (8H, m, *o*Ph), 8.90-9.03 (8H, m, βH).^{13}C-NMR ($CDCl_3$): δ 117.4, 119.9, 121.3, 126.7, 127.6, 131.8, 132.2, 134.5, 135.6, 139.7, 142.8, 150.4. MS (NSI): m/z 719 (100$[M+H]^+$) HRMS: calcd. for: $C_{44}H_{28}N_7Zn$: 718.1690 found 718.1692.

Attempted synthesis of Porphyrin-viologen hybrid (41c)

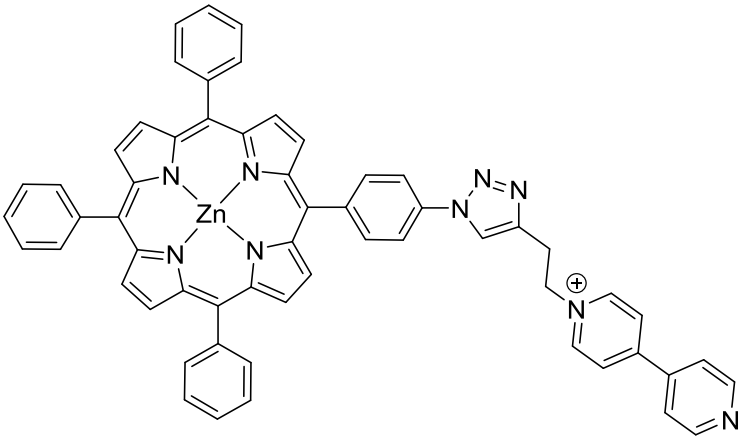

To a 10.00 mL microwave tube was added zinc (II) 5-(4-azidophenyl)-10,15,20-triphenylporphyrin and 1-(but-3-yn-1-yl)-[4,4'-bipyridin]-1-ium in the chosen solvent with copper sulphate and sodium ascorbate. The mixture was heated as shown in the table and then excess solvent was removed under reduced pressure. The desired product was not isolated.

Reaction number	Amount of porphyrin used	Amount of alkyne used	Solvent used	Amount of catalyst	Temperature	Time
1	10 mg	10 mg	THF/water (1:1)	Copper sulphate/sodium ascorbate 10 mg	80 °C	48 h on bench
2	10 mg	10 mg	THF/water (1:1)	Copper sulphate/sodium ascorbate 10 mg	50 °C	1 h in microwave followed by 1 h at 80°C in microwave
3	10 mg	10 mg	DMSO	Copper acetate 10 mg	rt, then heat to 80 °C for 48 h.	24 h
4	10 mg	10 mg	DMF	Copper iodide 15 mg	80 °C microwave	2 h.
5	10 mg	10 mg	*t*-butanol/water (9:1)	Copper sulphate/sodium ascorbate 10 mg	80 °C microwave	2 h
6	10 mg	10 mg	*t*-butanol/water (9:1)	Copper sulphate/sodium ascorbate 10 mg	80 °C microwave	4 h
7	10 mg	10 mg	*t*-butanol/water (9:1)	Copper sulphate/sodium ascorbate 10 mg	80 °C microwave	6 h
8	10 mg	10 mg	*t*-butanol/water (9:1)	Copper sulphate/sodium ascorbate 10 mg	90 °C microwave	2 h
9	10 mg	10 mg	*t*-butanol/water (9:1)	Copper sulphate/sodium ascorbate 10 mg	100 °C microwave	2 h

Attempted synthesis of Porphyrin-viologen hybrid (41d)

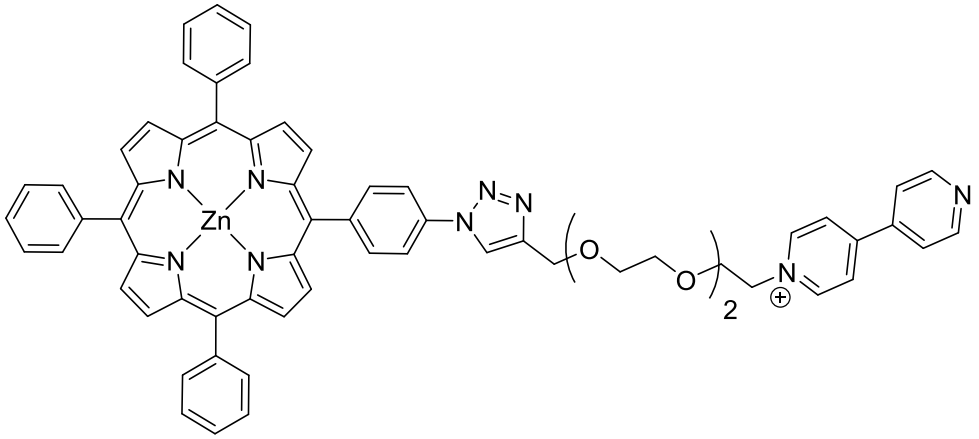

To a 10 mL microwave tube was added zinc(II) 5-(4-azidophenyl)-10,15,20-triphenylporphyrin (10.0 mg, 0.00139 mmol) and 1-(3,6,9,12-tetraoxapentadec-14-yn-1-yl)-[4,4'-bipyridin]-1-ium (10.0 mg, 0.0270 mmol) and copper(II) sulphate (10.0 mg, 0.00630 mmol) and sodium ascorbate (10.0 mg, 0.0505 mmol) in a mixture of THF/water (9:1) (10.0 mL). The mixture was heated in the microwave for 24 h at 80°C, the desired product was not isolated.

5-[4-Bromophenyl]-10, 15, 20-triphenylporphyrin (42)

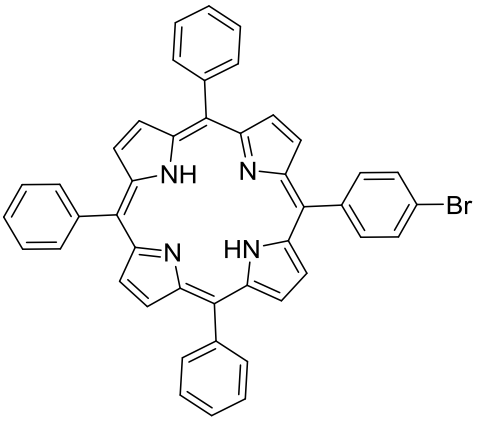

To a refluxing solution of benzaldehyde (14.33 mL, 135.0 mmol) and 4-bromobenzaldhyde (8.326 g, 45.00 mmol) in propionic acid (500.0 mL) was added dropwise, *via* syringe, pyrrole (12.5 mL, 180 mmol). The solution was stirred at reflux temperature for 3 h, and then the excess solvent was removed under reduced pressure. Subsequently the crude product was purified using column chromatography (silica) CH_2Cl_2: CH_3OH (98:2). The desired product was not isolated.

5-[4-Bromophenyl]-10, 15, 20- tri-(4-acetamidophenyl) porphyrin (43)

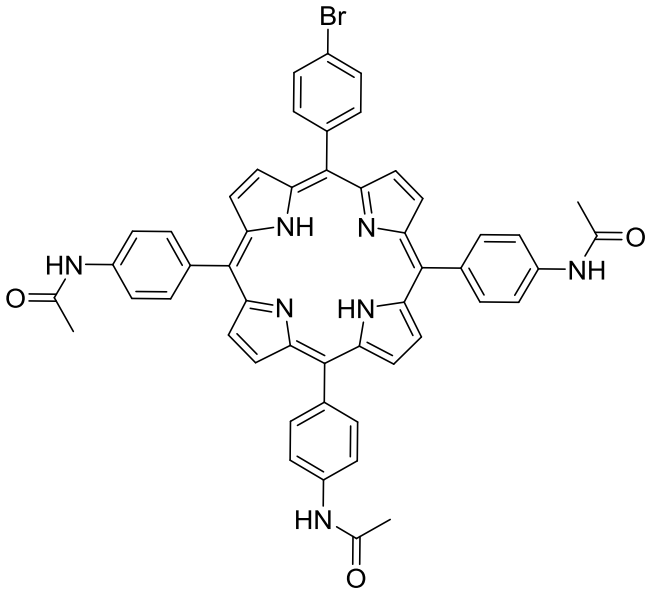

To a refluxing solution of 4-bromobenzaldehyde (3.48 g, 18.8 mmol) and 4-acetamidobenzaldehyde (9.20 g, 56.4 mmol) in propionic acid (500.0 mL) was added dropwise, *via* syringe, pyrrole (6.00 mL, 75.2 mmol). The reaction mixture was heated at reflux for 3 h and then cooled to rt. The excess solvent was removed under reduced pressure. The crude product was purified using column chromatography (silica) eluting with CH_2Cl_2:CH_3OH (4:1). The crude product was further purified by column chromatography (silica) eluting with CH_2Cl_2:CH_3OH (91:9). The product was precipitated from hexane over dichloromethane, and then isolated *via* filtration to give a purple solid (928 mg, 5.7%).

Rf: (silica, CH_2Cl_2 (9:1) CH_3OH) = 0.71. UV-Vis (CH_2Cl_2): λ_{max} (nm): 422, 522, 558, 596, 658, ε (422 nm) = 422846 M^{-1} cm^{-1}.^{1}H-NMR ($CDCl_3$): δ 2.21-2.26 (9H, m, 3 x CH_3), 7.78 (2H, d, *m*PhBr, J = 8.8 Hz), 7.82-7.89 (6H, m, *m*Ph), 7.96 (2H, d, *o*PhBr, J = 8.6 Hz), 8.03-8.08 (6H, m, *o*Ph), 8.68-8.88 (8H, m, βH).^{13}C-NMR ($CDCl_3$): δ 49.9, 118.2, 119.87, 122.4, 129.9, 135.0, 135.9, 137.6, 138.2, 170.1. MS (NSI): m/z 865 (100$[M+H]^+$) HRMS: calcd. for $C_{50}H_{39}O_3N_7Br$: 864.2291 found 864.2292.

5-[4-Bromophenyl]-10,15,20- tri-(4-carbomethoxyphenyl) porphyrin (44)

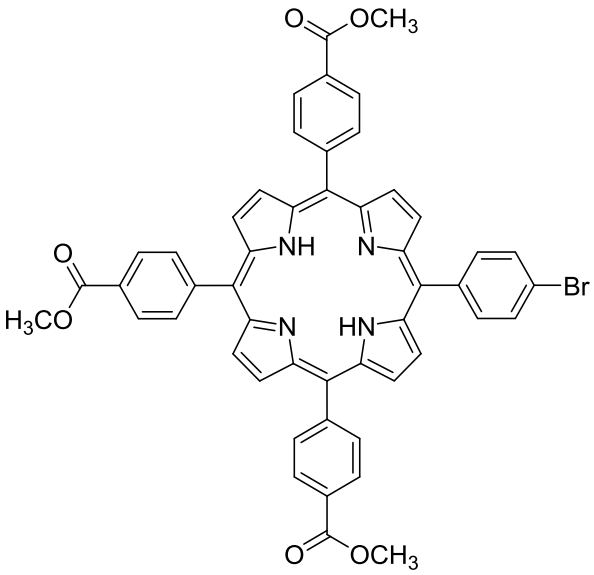

To a refluxing solution of 4-bromobenzaldehyde (4.167 g, 22.51 mmol) and methyl-4-formylbenzoate (11.08 g, 67.51 mmol) in propionic acid (250.0 mL) was added dropwise, *via* syringe, pyrrole (6.25 mL, 90.0 mmol). The solution was heated at reflux for 3 h and then the excess solvent removed under reduced pressure. The crude product was purified on a pre-column of silica eluting with CH_2Cl_2:CH_3OH (98:2). Further purification of the product was carried out using column chromatography (silica) eluting with CH_2Cl_2:CH_3OH (99.5:0.5). The desired product was not isolated.

5-[4-Bromophenyl]-10,15,20-tri-(3,5-dimethoxyphenyl) porphyrin (45)

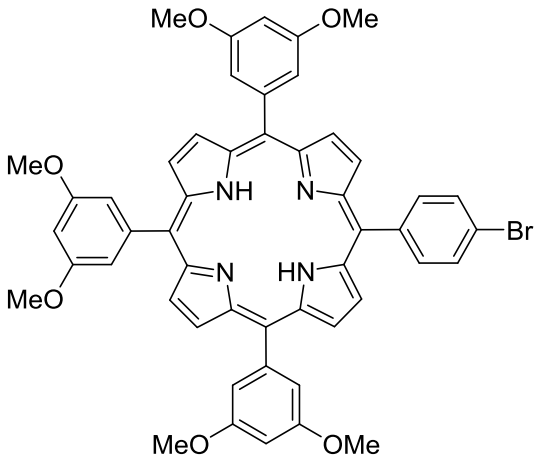

To a refluxing solution of 4-bromo-benzaldehyde (1.71 g, 9.23 mmol) and 3,5-dimethoxybenzaldehyde (4.60 g, 27.7 mmol) in propionic acid (250.0 mL) was added dropwise, *via* syringe, pyrrole (3.12 mL, 37.0 mmol). The solution was heated at reflux temperature for 3 h. Following this, the excess solvent was removed under reduced pressure. The crude product was purified using column chromatography (silica) eluting with CH_2Cl_2:CH_3OH (98:2). The product was precipitated from hexane over dichloromethane and isolated *via* filtration to give a purple solid (238 mg, 3 % yield).

Rf: (silica, CH_2Cl_2) = 0.7. UV-Vis (CH_2Cl_2): λ_{max} (nm): 418, 518, 552, 594, 652, ε (418 nm) = 822342 M^{-1} cm^{-1}.^{1}H-NMR ($CDCl_3$): δ 3.91-4.05 (18H, m, 6 x C*H*$_3$), 6.88-6.92 (3H, m, *p*Ph), 7.36-7.41 (6H, m, *o*Ph), 7.89 (2H, d, *m*PhBr, J = 8.8 Hz), 8.07 (2H, d, *o*PhBr, J = 8.6 Hz), 8.77-9.00 (8H, m, βH).^{13}C-NMR ($CDCl_3$): δ 55.7, 100.2, 113.9, 118.5, 120.1, 130.0,131.8, 135.9, 141.2, 144.0, 158.9. MS (NSI): m/z 873 (100$[M+H]^+$)HRMS: calcd. for $C_{50}H_{42}BrN_4O_6$: 873.226 found 873.2282.

5-[4-Bromophenyl]-10,15,20-tri-(4-pyridyl) porphyrin (46)

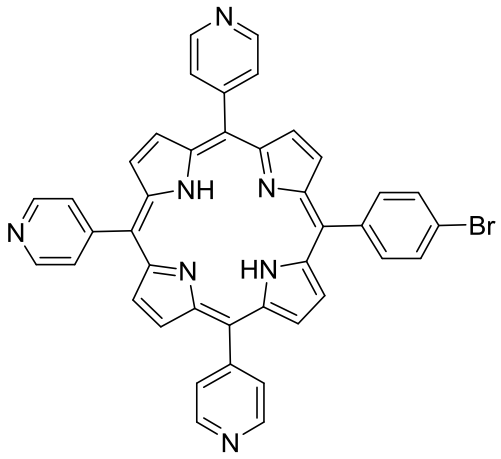

To a refluxing solution of 4-bromobenzaldehyde (4.167 g, 22.53 mmol) and 4-pyridinecarboxaldehyde (6.35 mL, 67.5 mmol) in propionic acid (250.0 mL) was added dropwise, *via* syringe, pyrrole (6.25 mL, 90.0 mmol). The solution was heated at reflux temperature in the dark for 3h. After this, the excess solvent was removed under reduced pressure. The crude product was purified using a pre-column (silica) eluting with CH_2Cl_2:CH_3OH (90:10). Further purification was carried out using column chromatography (silica) eluting with CH_2Cl_2:CH_3OH (96:4). The product was precipitated from methanol over dichloromethane and isolated *via* filtration to give a purple solid (1.068 g, 7 %).

Rf: (silica, CH_2Cl_2:CH_3OH (95:5)) = 0.42.UV-Vis (CH_2Cl_2): λ_{max} (nm): 415, 516, 556, 594, 646 ε (415 nm) = 258199 M^{-1} cm^{-1}.^{1}H-NMR ($CDCl_3$): δ 7.91 (2H, d, *o*Ph, J = 8.0 Hz), 8.07 (2H, d, *m*Ph, J = 8.4 Hz), 8.12-8.21 (6H, m, *m*Py), 8.80- 8.95 (8H, m, βH), 9.03-9.11 (6H, m, *o*Py).^{13}C-NMR ($CDCl_3$): δ 117.4, 117.7, 123.0, 129.4, 130.2, 131.6, 135.9, 140.5, 148.5, 149.97. MS (NSI): m/z 696 (100$[M+H]^+$) HRMS: calcd. for $C_{41}H_{27}BrN_7$: 696.1502 found 696.1506.

5-[4-Bromophenyl]-10,15,20-tri-(3-pyridyl) porphyrin (47)

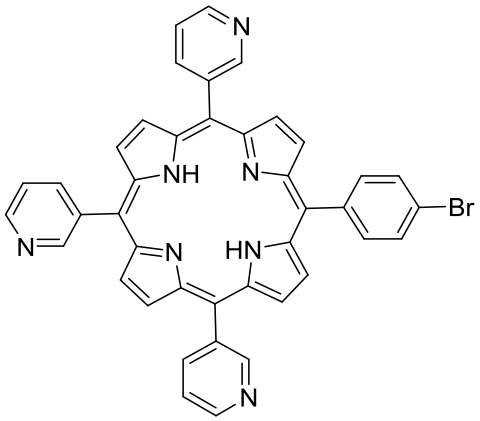

To a refluxing solution of 4-bromobenzaldehyde (4.167 g, 22.54 mmol) and 3-pyridinecarboxaldehyde (6.35 mL, 67.5 mmol) in propionic acid (250.0 mL) was added dropwise, *via* syringe, pyrrole (6.25 mL, 90.0 mmol). The solution was heated at reflux temperature for 3 h. After this, the excess solvent was removed under reduced pressure. The crude product was purified using a pre-column (silica) eluting with CH_2Cl_2:CH_3OH (90:10), further purification of the product was carried out using column chromatography (silica) eluting with CH_2Cl_2:CH_3OH (97:3) to give a purple solid after isolation *via* filtration (954 mg, 6.1% yield).

Rf: (silica, CH_2Cl_2:CH_3OH (97:3)) = 0.40.UV-Vis (CH_2Cl_2): λ_{max} (nm): 418, 522, 552, 594, 652 ε (422 nm) = 258199 M^{-1} cm^{-1}.^{1}H-NMR ($CDCl_3$): δ 7.72-7.84 (3H, m, *o*Py), 7.87-7.99 (2H, m, *o*Ph), 8.04-8.15 (2H, m, *m*Ph), 8.47-8.62 (3H, m, *o*Py), 8.79-9.19 (11H, m, 8βH + 3Py), 9.41-9.5 (3H, m, *o*Py).^{13}C-NMR ($CDCl_3$): δ 116.7, 119.8, 122.2, 122.9, 130.2, 131.3, 135.9, 137.8, 141.0, 149.4, 153.7. MS (ESI): m/z 696 (100[M+H]) HRMS: calcd. for $C_{41}H_{27}N_7Br$: 696.1502 found 696.1506.

5-[4-Bromophenyl]-10,15,20-tri-(2-pyridyl) porphyrin (48)

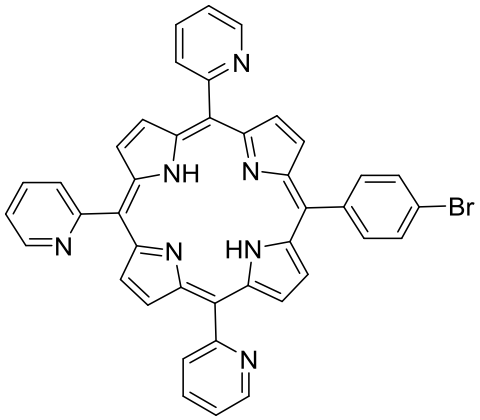

To a refluxing solution of 4-bromobenzaldehyde (4.167 g, 22.54 mmol) and 2-pyridinecarboxaldehyde (6.35 mL, 67.5 mmol) in propionic acid (250.0 mL) was added dropwise, *via* syringe, pyrrole (6.25 mL, 90.0 mmol). The solution was heated at reflux temperature in the dark for 3 h. After this the excess solvent was removed under reduced pressure. The crude product was purified using a pre-column (silica) eluting with CH_2Cl_2:CH_3OH (90:10). The desired product was not isolated.

Zinc 5-[4-Bromophenyl]-10,15,20-tri-(4-acetamidophenyl) porphyrin (49)

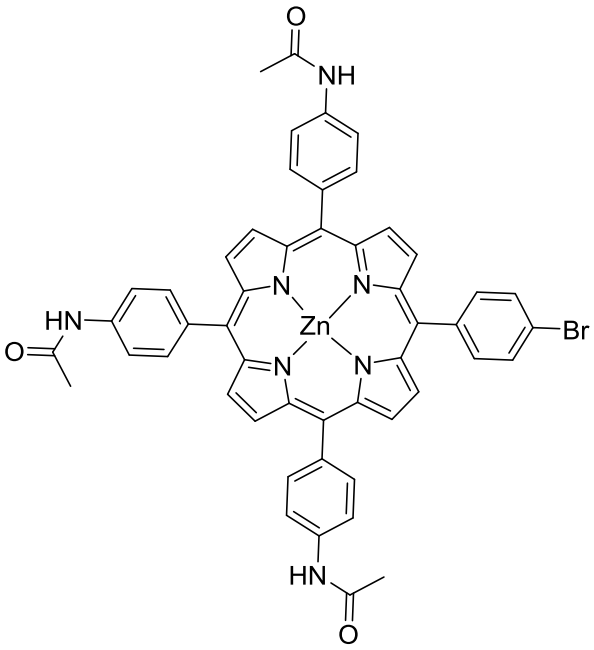

To a stirred solution of 5-[4-bromophenyl]-10,15,20-tri-(4-acetamidophenyl) porphyrin (400 mg, 0.463 mmol) in DMF (300.0 mL) was added zinc acetate dihydrate (406 mg, 1.85 mmol). The solution was stirred at 60 °C overnight. After this the excess solvent was removed under reduced pressure. The product was precipitated from water over DMF to give a purple solid after isolation *via* filtration (236 mg, 56% yield).

Rf: (silica, CH_2Cl_2:CH_3OH (95:5),) = 0.41. UV-Vis (DMF): λ_{max} (nm): 430, 562, 602 ε (430 nm) = 336362 M^{-1} cm^{-1}.^{1}H-NMR (DMF-d7): δ 2.01-2.25 (9H, m, 3x C*H*$_3$), 7.85-7.95 (6H, m, *o*Ph), 7.97-8.14 (8H, m, *m*Ph), 8.77-8.93 (2H, m, *o*PhBr).^{13}C-NMR (C_2D_6SO): δ 24.8, 31.3, 36.3, 117.6, 120.8, 130.1, 131.8, 132.1, 135.0, 136.5, 137.8, 139.3,149.4, 149.9, 162.9, 169.2. MS (NSI): m/z 928 (100$[M+H]^+$) HRMS: calcd. for $C_{50}H_{36}BrN_7O_3Zn$: 926.1423 found 926.1427.

Attempted synthesis of Porphyrin-viologen hybrid (49b)

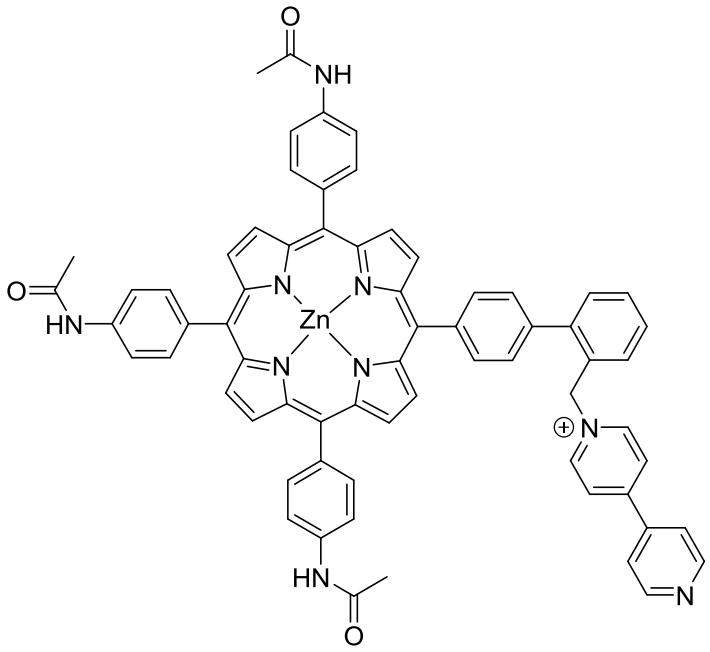

Zinc N,N',N''-((20-(4-bromophenyl)porphyrin-5,10,15-triyl)tris(benzene-4,1-diyl)) triacetamide, and 1-(2-boronobenzyl)-[4,4'-bipyridin]-1-ium were dissolved in DMF (10.0 mL). Palladium tetrakis(triphenylphosphine) was added to the reaction mixture. The reaction mixture was heated either in the microwave or on the bench for the time stated. Following this the excess solvent was removed under reduced pressure, and the product was collected *via* filtration. The desired product was not isolated.

Reaction number	**Amount of porphyrin**	**Amount of viologen**	**Amount of catalyst**	**Solvent used**	**Temperature**	**Time**
1	50 mg	25 mg	10 mg	DMF	60 °C	24 h
2	50 mg	25 mg	10 mg	DMF	100 °C	48 h
3	50 mg	50 mg	20 mg	DMF	90 °C	24 h
4	20 mg	20 mg	10 mg	DMF	100 °C	4 h MW
5	10 mg	10 mg	5 mg	DMF	100 °C	6 h MW

Zinc 5-[4-bromophenyl]-10,15,20-tri-(3,5-dimethoxyphenyl) porphyrin (50)

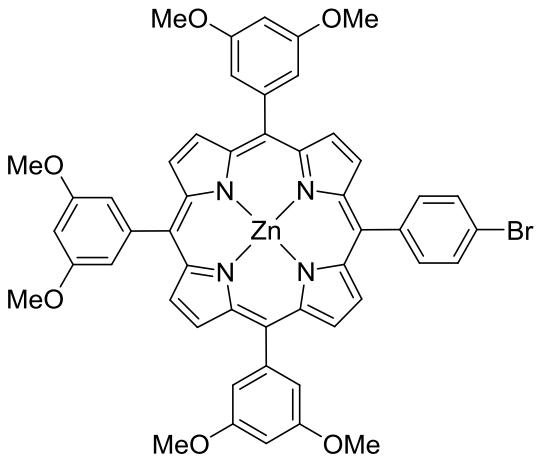

To a solution of 5-[4-bromophenyl]-10,15,20-tri-(3,5-dimethoxyphenyl) porphyrin (100 mg, 0.1144 mmol) in DMF was added zinc acetate (100 mg, 0.455 mmol). The solution was stirred at 60°C overnight. Following this, the excess solvent was removed under reduced pressure, and the residue was dissolved in dichloromethane and precipitated using methanol to give a purple solid after isolation *via* filtration (90 mg, 84% yield).

UV-Vis (CH_2Cl_2): λ_{max} (nm) 422, 552, 588 ε (422 nm) = 929722 M^{-1} cm^{-1}. ^{1}H-NMR ($CDCl_3$): δ 3.92 (18H, br s, 6 x OC*H*$_3$), 6.85 (3H, t, *p*Ph, J = 3.6 Hz), 7.36-7.38 (6H, m, *o*Ph), 7.87 (2H, d, *o*PhBr, J = 8.6 Hz), 8.07 (2H, d, *m*Ph, J = 8.0 Hz), 8.90-9.05 (8H, m, βH).^{13}C-NMR ($CDCl_3$): δ 55.7, 100.1, 113.8, 119.5, 121.0, 122.3, 129.8, 131.7, 132.1, 135.8, 141.9, 144.7,150.2, 158.8. MS (NSI): m/z 937 (100$[M+H]^+$) HRMS: *calcd. for* $C_{50}H_{40}BrN_4O_6Zn$: 935.1424 found 935.1417.

Zinc 5-[4-bromophenyl]-10,15,20-tri-(4-pyridyl) porphyrin (51)

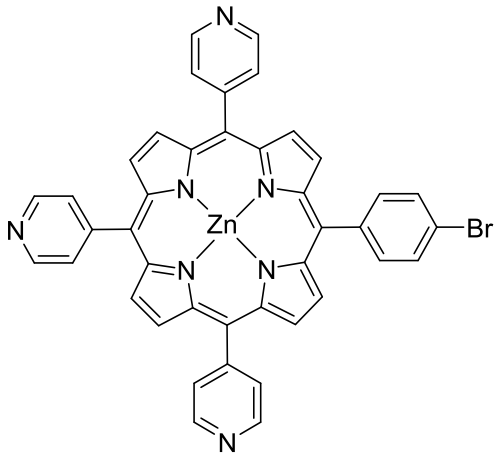

To a stirred solution of 5-[4-bromophenyl]-10,15,20-tri-(4-pyridyl) porphyrin (400 mg, 0.575 mmol) in DMF (300.0 mL) was added zinc acetate (504 mg, 0.229 mmol), and the solution was stirred at 60°C overnight. Following this, the excess solvent was removed under reduced pressure, and the product precipitated from water over DMF to give a purple solid after isolation *via* filtration (430 mg, 98% yield).

UV-Vis (DMF): λ_{max} (nm): 426, 558, 598, ε (426 nm) = 962563 M^{-1} cm^{-1}.^{1}H-NMR (C_2D_6SO): δ 7.96 (2H, d, *o*Ph, J = 8.0 Hz), 8.09 (2H, d, *m*Ph, J = 8.0 Hz), 8.17 (6H, d, *o*Py, J = 6.8 Hz), 8.76-8.83 (8H, m, βH), 8.96 (2H, d, *m*Py, J = 6.6 Hz). ^{13}C-NMR (C_2D_6SO): δ 118.5, 129.8, 130.1, 132.2, 132.8, 136.5, 148.5, 149.1, 149.9, 150.0, 162.8. MS (NSI): m/z 759 (100 $[M+H]^+$) HRMS: calcd. for $C_{41}H_{25}BrN_7Zn$: 758.0641 found 758.0641.

Zinc 5-[4-bromophenyl]-10,15,20-tri-(3-pyridyl) porphyrin (52)

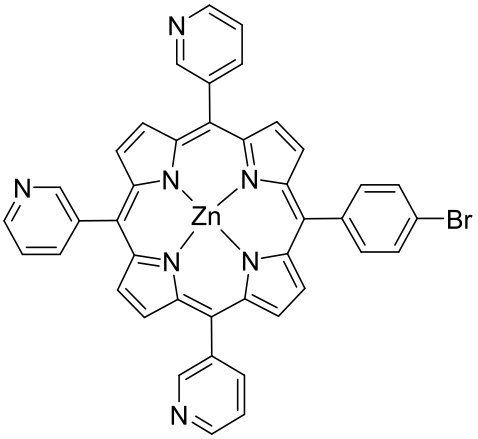

To a stirred solution of 5-[4-bromophenyl]-10,15,20-tri-(3-pyridyl) porphyrin (400 mg, 0.575 mmol) in DMF was added zinc acetate (400 mg, 2.18 mmol) in methanol (1.00 mL) and the solution heated at 60°C for 6 h. The excess solvent was removed under reduced pressure and the product precipitated from water over DMF to give a purple solid after isolation *via* filtration (406 mg, 93% yield).

UV-Vis (DMF): λ_{max} (nm): 426, 564, 600, ε (426 nm) = 454877 M^{-1} cm^{-1}. MS (NSI): m/z 759 (100$[M+H]^+$) HRMS: *calcd. for* $C_{41}H_{25}BrN_7Zn$: 758.0629 found 758.0641.

5-[4-Iodophenyl]-10,15,20-tri-(4-acetamido) porphyrin (53)

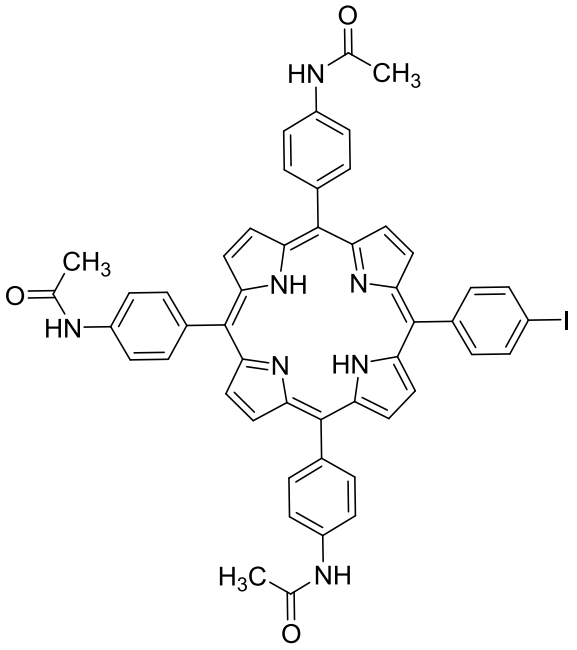

To a refluxing solution of 4-acetamidobenzaldehyde (5.507 g, 33.75 mmol) and 4-iodobenzaldehyde (2.611 g, 11.25 mmol) in propionic acid (250.0 mL) was added dropwise, *via* syringe, pyrrole (3.25 mL, 45.0 mmol). The solution was heated at reflux temperature for 3h. Following this, the solution was cooled and the excess solvent was removed under reduced pressure. The product was purified using a pre-column (silica) eluting with CH_2Cl_2:CH_3OH (90:10), and then further purified using a column (silica) eluting with CH_2Cl_2:CH_3OH (93:7), to give a purple solid (300 mg, 4 % yield).

Rf (CH_2Cl_2:CH_3OH (97:3) = 0.3056. UV-Vis (CH_2Cl_2): λ_{max} (nm): 420, 520, 560, 600, 655 ε (420 nm) = 507392 M^{-1} cm^{-1}.^{1}H-NMR ($CDCl_3$): δ 3.17 (9H, s, 3 x C*H*$_3$), 7.68 (2H, d, *o*PhI, J = 8.4 Hz), 7.76 (6H, d, *o*Ph, J = 8.0 Hz), 7.84 (2H, d, *m*PhI, J = 8.4 Hz), 7.94 (6H, d, *m*Ph, J = 8.0 Hz), 8.67 (8H, br s, βH).^{13}C-NMR ($CDCl_3$): δ 26.5, 96.8, 121.1, 122.8, 122.9, 137.8, 138.7, 138.9, 140.4, 141.2, 144.4, 173.5. MS (NSI): m/z 912 (100[M+H]$^+$) HRMS: calcd. for $C_{50}H_{39}O_3N_7I$: 912.2154 found 912.2154.

5-[4-Iodophenyl]-10,15,20-tri-(3,5-dimethoxyphenyl) porphyrin (54)

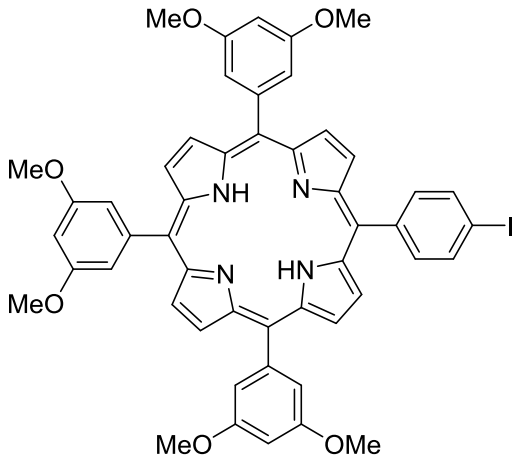

To a refluxing solution of 4-iodobenzaldeyde (2.617 g, 11.25 mmol) and 3,5-dimethoxybenzaldehyde (5.611 g, 33.75 mmol) in refluxing propionic acid (250.0 mL) was added dropwise, *via* syringe, pyrrole (3.10 mL, 45.0 mmol). The solution was heated at reflux temperature for 3 h. Following this, the reaction mixture was cooled to rt and then the excess solvent was removed under reduced pressure. The crude product was purified using a pre-column (silica) eluting with CH_2Cl_2:CH_3OH (98:2), and then further purified using column chromatography (silica) eluting with CH_2Cl_2: hexane (3:1). The excess solvent was removed under reduced pressure, and the residue dissolved in dichloromethane and precipitated from methanol to give a purple solid after isolation *via* filtration (620 mg, 6% yield).

Rf (CH_2Cl_2: hexane (3:1)) = 0.41.UV-Vis (CH_2Cl_2): λ_{max} (nm): 419, 514, 565, 645 ε (419 nm) = 944962 M^{-1} cm^{-1}.^{1}H-NMR ($CDCl_3$): δ 3.94-4.01 (18H, m, 6 x C*H*$_3$), 6.87-6.91 (3H, m, *p*PhOMe), 7.38-7.40 (6H, m, *o*PhOMe), 7.94 (2H, d, *o*PhI, J = 8.4 Hz), 8.09 (2H, d, *m*PhI, J = 8.2 Hz), 8.79-8.98 (8H, m, βH). ^{13}C-NMR ($CDCl_3$): δ 55.7, 94.2, 100.3, 113.9, 118.6, 120.1, 131.2, 136.0, 136.2, 141.8, 144.0, 159.0 (βC). MS (DEI): m/z 920 (100[M]) HRMS: calcd. for $C_{50}H_{41}IN_4O_6$: 920.2093 found 920.2017.

5-[4-Iodophenyl]-10,15,20-tri-(4-pyridyl) porphyrin (55)

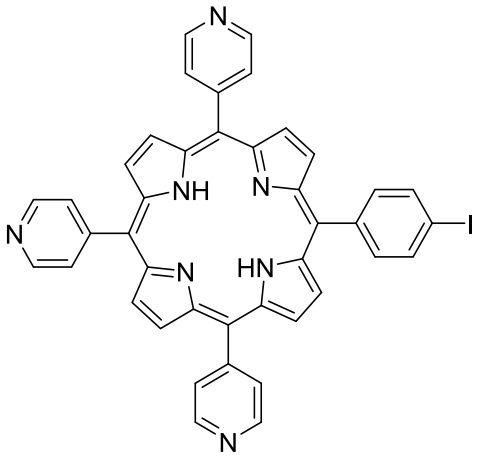

To a refluxing solution of 4-iodobenzaldeyde (2.617 g, 11.25 mmol) and 4-pyridinecarboxaldehyde (3.18 mL, 33.8 mmol) in propionic acid (250.0 mL) was added dropwise, *via* syringe, pyrrole (3.10 mL, 45.0 mmol). The solution was heated at reflux temperature for 3 h. Following this, the reaction mixture was cooled to rt and then the excess solvent was removed under reduced pressure. The crude product was purified using a pre-column (silica) eluting with CH_2Cl_2:CH_3OH (90:10) and then further purified using column chromatography (silica) eluting with CH_2Cl_2:CH_3OH (96:4). The excess solvent was removed under reduced pressure, and then the product was precipitated from methanol over dichloromethane to give a purple solid after isolation *via* filtration (600 mg, 7% yield).

Rf (CH_2Cl_2:CH_3OH (96:4) = 0.16. UV-Vis (CH_2Cl_2): λ_{max} (nm): 415, 515, 545, 590, 645, ε (415 nm) = 798747 M^{-1} cm^{-1}.^{1}H-NMR ($CDCl_3$): δ 7.91-7.96 (2H, m, *o*Ph), 8.10-8.14 (2H, m, *m*Ph), 8.14-8.19 (6H, m, *o*Py), 8.80-8.93 (8H, m, βH), 9.06 (6H, d, *m*Py, J = 8.0 Hz).^{13}C-NMR ($CDCl_3$): δ 94.7, 117.4, 117.7, 120.1, 129.4 (βC), 131.3, 136.2, 141.1, 148.5 (βC), 150.0. MS (EI^+): m/z 743 (100[M^+]) HRMS: calcd. for $C_{44}H_{26}IN_7$: 743.1290 found 743.1294.

Zinc 5-[4-iodophenyl]-10,15,20-tri-(4-acetamidophenyl) porphyrin (56)

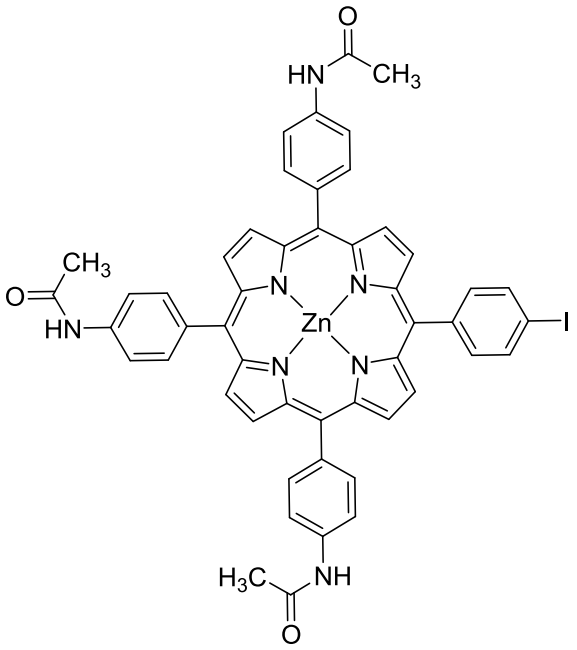

5-[4-iodophenyl]-10,15,20-tri-(4-acetamidophenyl) porphyrin (300 mg, 0.330 mmol) and zinc acetate (300 mg, 1.37 mmol) were dissolved in DMF (150.0 mL). The reaction was stirred at 60 °C overnight. Following this, the reaction mixture was cooled to rt and the excess solvent was removed under reduced pressure, and the product was precipitated from methanol over dichloromethane to give a bluey purple solid after isolation *via* filtration (289 mg, 90 % yield)

UV-Vis (CH_3OH): λ_{max} (nm): 425, 560, 600, ε (425 nm) = 585703 M^{-1} cm^{-1}.^{1}H-NMR (C_2D_6SO): δ 3.36 (9H, s, 3 x C*H*$_3$), 7.93 (2H, d, *o*PhI, J = 8.6 Hz), 7.98 (6H, d, *o*Ph, J =7.8 Hz), 8.06 (6H, d, *m*Ph, J = 8.0 Hz), 8.11 (2H, d, *m*PhI, J = 8.0 Hz), 8.73-8.81 (8H, m, βH).^{13}C-NMR (C_2D_6SO): δ 23.9, 24.8, 36.3, 94.9, 117.6, 119.1, 120.8, 120.9, 131.8, 132.2, 135.0, 135.9, 136.7, 137.8, 139.3, 142.9, 149.4, 150.0, 162.9, 169.2, 177.8. MS (NSI): m/z 975 (100[M+H]$^+$) HRMS: calcd. for $C_{50}H_{37}N_7O_3ZnI$: 974.1290 found 974.1289.

Zinc 5-[4-iodophenyl]-10,15,20-tri-(3,5-dimethoxyphenyl) porphyrin (57)

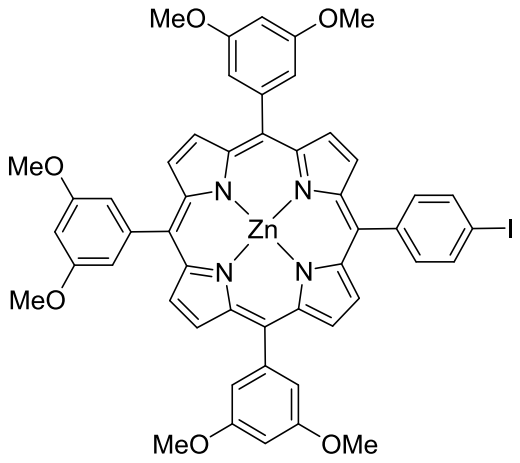

5-[4-iodophenyl]-10,15,20-tri-(3,5-dimethoxyphenyl) porphyrin (200 mg, 0.217 mmol) and zinc acetate (200 mg, 1.09 mmol) were dissolved in DMF (250.0 mL). The solution was stirred at 60 °C overnight. Following this, the reaction mixture was cooled to rt and the excess solvent was removed under reduced pressure. The residue was dissolved in methanol and precipitated from water to give a purple solid after isolation *via* filtration (201 mg, 94% yield).

UV-Vis (CH_2Cl_2): λ_{max} (nm): 419, 545, ε (419 nm) = 499057 M^{-1} cm^{-1}. ^{1}H-NMR (C_2D_6SO): δ 3.90 (18H, s, 6 x C*H*$_3$), 7.28 (6H, d, *o*PhOMe, J = 7.8 Hz), 7.92 (2H, d, *o*PhI, J = 7.8 Hz), 8.1 (2H, d, *m*PhI, J = 8.0 Hz), 8.71-8.86 (8H, m, βH).^{13}C-NMR (C_2D_6SO): δ 56.0, 94.9, 99.8, 114.1, 119.4, 120.6, 131.9, 132.2, 135.9, 136.6, 142.9, 145.2,158.9. MS (NSI): m/z 984 (100$[M+H]^+$) HRMS: calcd. for $C_{50}H_{40}IN_4O_6Zn$: 983.1280 found 983.1279.

Attempted synthesis of Porphyrin-viologen hybrid *via* Sonogashira coupling method (57b)

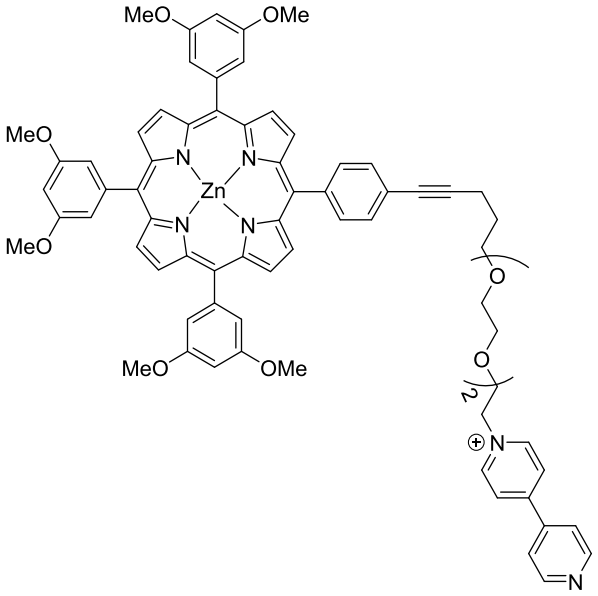

Zinc (II) 5,10,15-tris(3,5-dimethoxyphenyl)-20-(4-iodophenyl) porphyrin and 1-(3,6,9,12-tetraoxapentadec-14-yn-1-yl)-[4, 4'-bipyridin]-1-ium were dissolved in DCM (20.0 mL), then triethylamine (1.00 mL), palladium $(PPh_3)_4$ and copper iodide were added. The reaction mixture was heated either on the bench or in the microwave for the time given. The desired product was not isolated.

Reaction number	Porphyrin	Viologen	Catalyst	Solvent used	Temp	Time
1	40 mg	20 mg	$Pd(PPh_3)_2$ – 20 mg CuI – 20 mg	DCM/ TEA	40 °C	24 h
2	40 mg	20 mg	$Pd(PPh_3)_2$ – 20 mg CuI – 20 mg	DCM/ TEA	40 °C	48 h
3	40 mg	20 mg	$Pd(PPh_3)_2$ – 20 mg CuI – 20 mg	DCM/ TEA	40 °C	1 h MW
4	40 mg	20 mg	$Pd(PPh_3)_2$ – 20 mg CuI – 20 mg	DCM/ TEA	40 °C	2 h MW
5	40 mg	20 mg	$Pd(PPh_3)_2$ – 20 mg CuI – 20 mg	DCM/ TEA	60 °C	3 h MW

Zinc 5-[4-iodophenyl]-10,15,20-tri-(4-pyridyl) porphyrin (58)

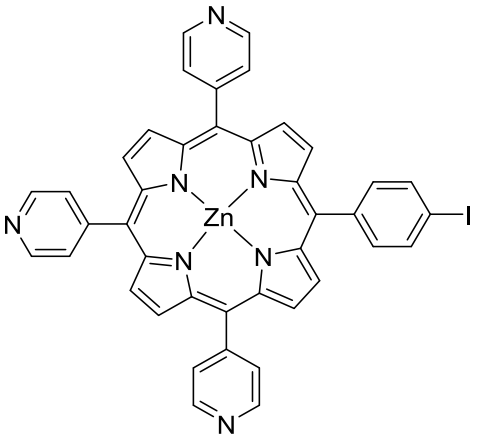

To a stirred solution of 5-[4-iodophenyl]-10,15,20-tri-(4-pyridyl) porphyrin (300 mg, 0.403 mmol) in DMF (200 mL) was added zinc acetate (300 mg, 1.64 mmol) in methanol. The solution was stirred at 60 °C for 48 h. The excess solvent was removed under reduced pressure, and the residue dissolved in dichloromethane and precipitated using methanol to give a purple solid after isolation *via* filtration (289 mg, 89% yield).

UV-Vis (THF): λ_{max} (nm): 425, 559 ε (425 nm) = 357366 M^{-1} cm^{-1}. ^{1}H-NMR (C_2D_6SO): 7.93 (2H, d, *o*PhI, J = 8.0 Hz), 8.13 (2H, d, *m*PhI, J = 8.0 Hz), 8.17 (6H, d, *o*Py, J = 6.4 Hz), 8.76-8.83 (8H, m, βH), 8.96 (6H, d, *m*Py, J = 6.4 Hz).^{13}C-NMR (C_2D_6SO): δ 118.4, 120.6, 129.8, 132.2, 135.9, 136.6, 148.5, 149.1, 149.8, 150.9, 162.8. MS (DEI): m/z 806 (100[M]) HRMS *calcd. for* $C_{41}H_{24}IN_7Zn$: 805.0431 found 805.0429.

5-[4-Carboxmethoxyphenyl]-10,15,20-tri-(4-pyridyl) porphyrin (59)

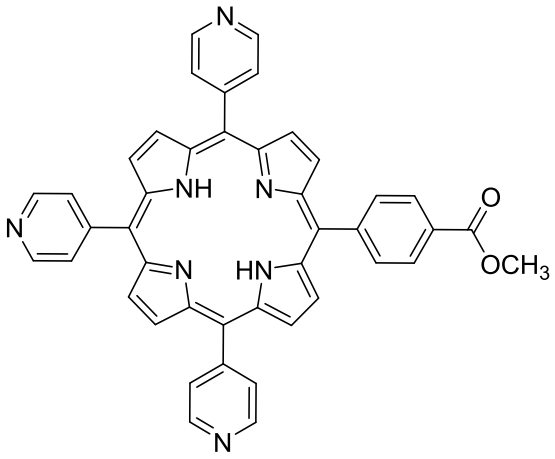

To a refluxing solution of methyl-4-formylbenzoate (3.693 g, 22.51 mmol) and pyridine-4-carboxaldehyde (6.40 mL, 67.5 mmol) in propionic acid (500.0 mL) was added dropwise, *via* syringe, pyrrole (5.54 mL, 90.0 mmol). The reaction was heated at reflux temperature for an hour. The solution was cooled, and following this, the excess solvent was removed under reduced pressure. The crude product was purified firstly using a pre-column (silica) eluting with CH_2Cl_2:CH_3OH (90:10). The product was further purified using column chromatography (silica) eluting with CH_2Cl_2:CH_3OH (95.5:4.5), and following this the excess solvent was removed under reduced pressure to give a purple solid after isolation *via* filtration (777 mg, 7 % yield).

Rf (silica (CH_2Cl_2:CH_3OH (95.5:4.5) = 0.35. UV-Vis (CH_2Cl_2): λ_{max} (nm) = 415, 515, 590, 645 ε (415 nm) = 860036 M^{-1} cm^{-1}.^{1}H-NMR ($CDCl_3$): δ 4.09-4.15 (3H, m, CH_3), 8.14-8.19 (6H, m, *o*Py), 8.27-8.31 (2H, m, *o*Ph), 8.43-8.48 (2H, m, *m*Ph), 8.80-8.91 (8H, m, βH), 9.02-9.08 (6H, m, *m*Py).^{13}C-NMR ($CDCl_3$): δ 52.6, 117.8, 120.2, 128.2, 129.4 (βC), 130.0, 134.6, 146.3, 148.5 (βC), 149.9, 167.3. MS (NSI): m/z 675 (100$[M+H]^+$) HRMS: calcd. for $C_{43}H_{30}N_7O_2$: 676.2447 found 676.2455.

5-[4-Carboxyphenyl]-10,15,20-tri-(4-pyridyl) porphyrin (60)

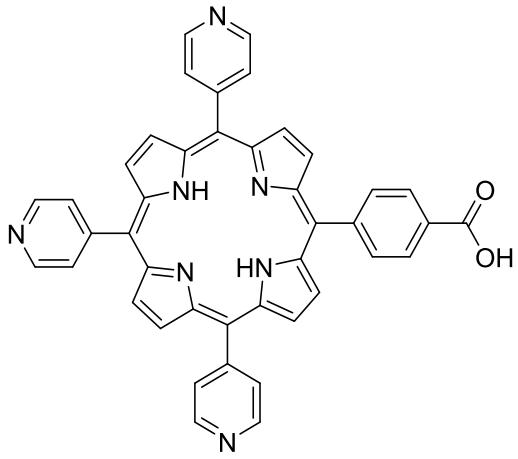

To a stirred solution of 5-[4-carboxmethoxyphenyl]-10,15,20-tri-(4-pyridyl) porphyrin (600 mg, 0.888 mmol, 1 equiv.) in DMF was added a 40 % solution of KOH (2.4 g, 0.043 mol, 50 equiv.) in water (15.0 mL). The reaction mixture was shielded from light and it was stirred at room temperature overnight. Following this, the excess solvent was removed under reduced pressure. The resultant solid was dissolved in dichloromethane and neutralised with 1 M HCl (5.00 mL). The solid was re dissolved in dichloromethane (50.0 mL) and extracted with water (2 x 50.0 mL). The excess solvent was removed under reduced pressure, and the product was precipitated from methanol over dichloromethane to give a purple solid after isolation *via* filtration (559 mg, 95% yield).

UV-Vis (CH_2Cl_2): λ_{max} (nm) = 415, 515, 550, 590, 645 ε (415 nm) = 715165 M^{-1} cm^{-1}. ^{1}H- NMR ($CDCl_3$) δ: −3.00 (2H, s, NH), 8.00 (2H, d, J = 8.0 Hz, *o*Ph), 8.02-8.05 (6H, m, 3,5Py), 8.18 (2H, d, J = 8.0 Hz, *m*Ph), 8.62 (8H, br s, βH), 8.74-8.80 (6H, m, 2,6Py).^{13}C-NMR ($CDCl_3$) δ 120.7, 121.1, 125.8, 131.6, 133.8, 138.1, 141.4, 147.1, 151.6, 154.9, 178.2. MS (NSI): m/z 660 (100[M-H]$^-$) HRMS: calcd. for $C_{42}H_{26}N_7O_2$: 661.22 found 660.2153

5-[4-(Succinimide-*N*-oxycarbonyl)phenyl]-10,15,20-tri-(4-pyridyl) porphyrin (61)

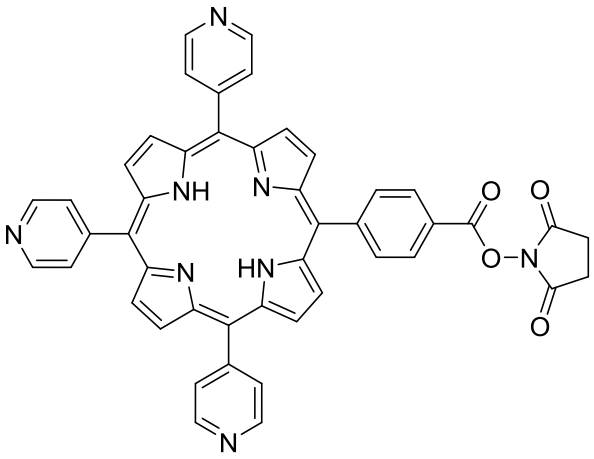

To a stirred solution of 5-[4-carboxyphenyl]-10,15,20-tri-(4-pyridyl) porphyrin (300 mg, 0.453 mmol) in dry pyridine (30.0 mL) was slowly added, *via* syringe, thionyl chloride (0.60 mL, 8.3 mmol). The reaction was stirred at 50 °C, protected from light and under inert atmosphere, for 30 mins. Following this, *N*-hydroxysuccinimide (1.20 g, 10.4 mmol) was added and the mixture kept under previous conditions for 3 h. Once the reaction had cooled the excess solvent was removed under reduced pressure and the residue was dissolved in dichloromethane. Subsequently, the residue was washed with sat. $NaHCO_3$ and then with water. The organic layer was then dried with magnesium sulphate and excess solvent removed under reduced pressure. The product was precipitated from hexane over dichloromethane to give a brick red solid after isolation *via* filtration (235 mg, 68% yield).

R_f (CH_2Cl_2:CH_3OH (94:6)) = 0.46. UV-Vis (CH_2Cl_2): λ_{max} (nm) 420, 515, 550, 590, 645 ε (420 nm) = 940258 M^{-1} cm^{-1}.^{1}H-NMR ($CDCl_3$): δ 3.03 (4H, br s, 2x C*H*$_2$), 8.13-8.22 (6H, m, *o*Py), 8.37 (2H, d, *o*Ph, J = 8.2 Hz), 8.57 (2H, d, *m*Ph, J = 8.8 Hz), 8.82-8.92 (8H, m, βH), 9.08 (6H, d, *m*Py, J = 8.0 Hz).^{13}C-NMR ($CDCl_3$): δ 25.6, 25.9, 117.8, 117.9, 119.2, 125.0, 127.4, 129.2, 129.4, 134.9, 148.5, 149.9, 162.1, 169.4. MS (NSI): m/z 757 (100[M+]) HRMS: calcd. for $C_{46}H_{31}O_4N_8$: 759.2453 found 759.2463.

5-[4-(Succinimide-*N*-oxycarbonyl)phenyl]-10,15,20-tri(*N*-methyl-4-pyridinium) porphyrin trichloride (62)

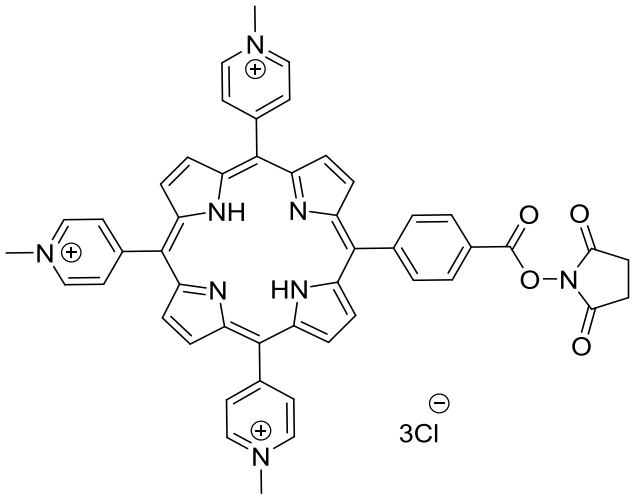

To a stirred solution of 5-[4-(succinimide-*N*-oxycarbonyl)phenyl]-10,15,20-tri-(4-pyridyl) porphyrin (200 mg, 0.264 mmol) in dry DMF (30.0 mL) was added, *via* syringe, methyl iodide (4.00 mL, 0.0643 mol). The reaction was heated at 40 °C overnight and then cooled. Once cooled, cool diethylether (100 mL) was added to the reaction and the mixture was filtered through cotton wool. Following this, the cotton was washed with water and then ammonium hexafluorophosphate was added and the mixture filtered. The filter cake was then dissolved in acetone and tetrabutylammoniumchloride was added, and the mixture subsequently filtered. The product was precipitated from diethyl ether over methanol to give a brick red solid after isolation *via* filtration (207 mg, 98% yield).

UV-Vis (H_2O): λ_{max} (nm) 424, 520, 564, 585, 640, ε (424 nm) = 801244 M^{-1} cm^{-1}.^{1}H-NMR (C_2D_6SO): δ 3.03 (4H, br s, 2 x C*H*$_2$), 4.73-4.76 (9H, m, 3 x C*H*$_3$), 8.03 (2H, d, *o*PhNHS, J = 8.0 Hz), 8.27 (2H, d, *m*PhNHS, J = 8.0 Hz), 8.94-9.04 (10H, m, 8*β*H + 2 *o*Py), 9.06-9.11 (4H, m, *o*Py), 9.46-9.52 (6H, m, *m*Py).^{13}C-NMR (C_2D_6SO): δ 14.0, 23.6, 48.4, 115.6, 116.1, 121.3, 125.2, 129.5, 132.0, 132.7, 135.7, 144.9, 147.9, 157.0, 162.6. MS (NSI): m/z 910 (100[M-3Cl]$^{3+}$) HRMS: calcd. for $C_{49}H_{39}N_8O_4$: 267.7700 found 267.7693.

Zinc 5-[4-(succinimide-*N*-oxycarbonyl)phenyl]-10,15,20-tri(N-methyl-4-pyridinium) porphyrin trichloride (63)

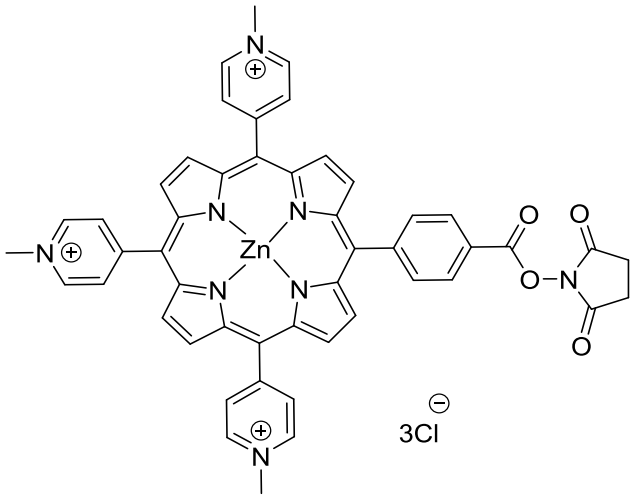

To a solution of 5-[4-(succinimide-*N*-oxycarbonyl)phenyl]-10,15,20-tri(N-methyl-4-pyridinium) porphyrin trichloride (50 mg, 5.49 $x10^{-5}$ mol) in methanol was added zinc acetate (50 mg, 2.73 x 10^{-4} mol). The solution was stirred at rt for an hour, and the reaction was monitored using TLC. The excess solvent was removed under reduced pressure and the residue dissolved in water and then ammonium hexafluorophosphate was added. The mixture was then filtered. The filter cake was dissolved in acetone and then tetrabutylammonium chloride was added. Following this, the mixture was filtered and then the product was precipitated from diethylether over methanol to give a purple solid after isolation *via* filtration (44 mg, 82% yield).

Rf (1:1:8 (water, sat. potassium nitrate: acetonitrile) = 0.61. UV-Vis (H_2O): λ_{max} (nm) 440, 565, 615, ε (440 nm) = 723691 cm^{-1} M^{-1}. MS (NSI): m/z 973 (100$[M]^{3+}$) HRMS calcd. for $C_{46}H_{36}N_7O_2Zn$: 260.7407 found 260.7402.

Palladium 5-[4-(succinimide-*N*-oxycarbonyl)phenyl]-10,15,20-tri(N-methyl-4-pyridinium) porphyrin trichloride (64)

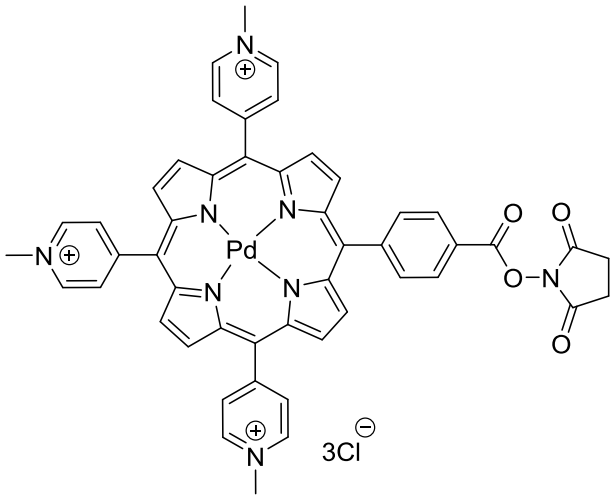

To a solution of 4,4',4''-(20-(4-(((2,5-dioxopyrrolidin-1-yl)oxy)carbonyl)phenyl)porphyrin-5,10,15-triyl)tris(1-methylpyridin-1-ium) chloride (90 mg, 9.88 $x10^{-5}$ mol) in 1-methylpyrrolidin-5-one (5mL) was added palladium (II) acetate (180 mg, 8.0178 x 10^{-4} mol) in methanol (3 mL). The solution was placed in a 10 mL microwave tube and degassed with argon for 5 mins. Following this, the reaction was heated in the microwave at 50 °C for an hour and then cooled to rt. Once cooled, diethyl ether (100 mL) was added to the solution and the mixture was filtered through celite. The excess solvent was removed under reduced pressure. The crude product was then dissolved in a 10% solution of ammoniumhexafluorophosphate in water and then filtered. The filter cake was dissolved in acetone and then precipitated using a 10% solution of tetrabutylammonium chloride in acetone. The product was precipitated from diethyl ether over methanol to give a purple solid after isolation *via* filtration (50 mg, 60% yield).

UV-Vis (water) λ_{max} (nm) = 420, 525, 560 ε (420 nm) = 298231 M^{-1} cm^{-1}.^{1}H-NMR (C_2D_6SO): δ 3.17 (4H, m, 2 x CH_2), 4.67-4.77 (9H, m, NCH_3), 8.42-8.51 (2H, m, Ph), 8.54-8.63 (2H, m, Ph), 8.90-9.19 (14H, m, 8βH + 6Py), 9.39-9.57 (6H, m, Py). MS (NSI): m/z 1014 (100[M-HCl_3]$^{2+}$) HRMS calcd. for $C_{49}H_{36}N_8O_4Pd$: 451.0951 found 451.0952.

***N*-Boc-2,2'-(ethylenedioxy)-diethylamine (65)**

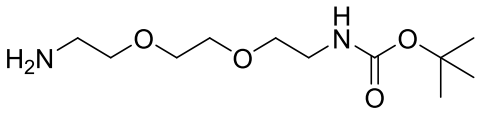

2,2'-(Ethane-1,2diylbis(oxy)diethanamine (12.00 g, 81 mmol) was dissolved in dry dichloromethane (20.0 mL) and the solution cooled to 0 °C under nitrogen. Di-tert-butyldicarbonate (2.62 g, 12.0 mmol) was dissolved in dry dichloromethane and added drop-wise to the solution, *via* syringe, over 30 mins and the reaction was then stirred at rt under nitrogen overnight. Following this, the excess solvent was removed under reduced pressure and the product residue was re-dissolved in water and washed thoroughly with dichloromethane and water to remove any by-products. The organic layer was dried with Na_2SO_4 and filtered, and subsequently the crude product was purified using column chromatography (silica) eluting with CH_2Cl_2: CH_3OH gradient 8-20%. The excess solvent was removed under reduced pressure to give a golden oil (1.43 g, 96 % yield).

^{1}H-NMR ($CDCl_3$): δ 1.25 (9H, s, C(C*H*$_3$)$_3$), 1.45 (2H, br s, N*H*$_2$), 2.69 (2H, t, CH_2-NH_2, J = 8.8 Hz), 3.07-3.17 (2H, m, C*H*$_2$NHBoc), 3.29-338 (4H, m, C*H*$_2$-C*H*$_2$), 3.40-3.47 (4H, s, 2 x O-C*H*$_2$).^{13}C-NMR ($CDCl_3$): δ 28.2 (C-(CH_3)$_3$), 40.2 (CH_2-NHBoc), 41.6 (CH_2-NH_2), 70.1, 73.3, 77.6 (C-(CH_3)$_3$), 78.9, 156.0 (C=O). MS (NSI): m/z 248 (100[M+H]$^+$) HRMS: calcd. for $C_{11}H_{25}N_2O_4$: 249.1807 found 249.1809.

***N*-(2-(2-*tert*-Butoxycarbonylaminoethoxy)ethoxy)ethyl)acryl amide (66)**

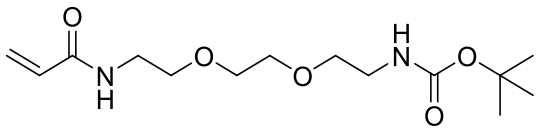

N-Boc-2,2'-(ethylenedioxy)-diethylamine (1.00 g, 4.03 mmol) and di-isopropylethylamine (1.40 mL) were dissolved in dry dichloromethane (10.0 mL) and the reaction mixture was placed under nitrogen. Acryloyl chloride (0.30 mL, 8.05 mmol) was added dropwise *via* syringe whilst the mixture was kept at 0 °C for an hour. Following this, the reaction was bought back to rt and stirred for 4 h. The crude reaction mixture was washed with aqueous 1 M citric acid (2 x 50.0 mL) and brine (2 x 50.0 mL) and then the organic layer was dried with sodium sulfate and filtered. The crude product was further purified using column chromatography (silica) eluting with CH_2Cl_2:CH_3OH gradient 5–8% methanol to give a near colourless oil (1.081 g, 88% yield).

^{1}H-NMR ($CDCl_3$): δ 1.43 (9H, s, C(C*H*$_3$)$_3$), 3.22-3.40 (2H, m, C*H*$_2$NHCOBoc), 3.46-3.72 (10H, m, CH_2PEG), 5.00 (1H, bs, N*H*CO), 5.64 (1H, dd, CH_2C*H*CO, J_{cis} = 10.8 Hz, J_{gem} = 1.6 Hz), 6.12 (1H, dd, CH_2C*H*CO, J_{trans} =14.0 Hz, J_{gem} = 2.0 Hz), 6.27 (1H, dd, CH_2C*H*CO, J_{trans} = 14.0 Hz, J_{gem} = 2.0 Hz).^{13}C-NMR ($CDCl_3$): δ 28.5, 39.3, 40.4, 69.8, 70.2, 70.3, 70.4, 77.5, 126.5, 130.9, 156.1. MS (NSI): m/z 303 (100[M+H]$^+$) HRMS: calcd. for $C_{14}H_{27}N_2O_5$: 303.1913 found 303.1914.

***N*-(2-(2-(2-Aminoethoxy)ethoxy)ethyl)acrylamide (67)**

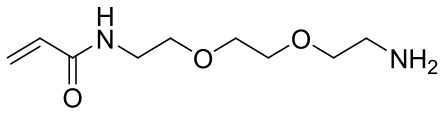

N-(2-(2-tert-Butoxycarbonylaminoethoxy)ethoxy)ethyl)acryl amide (1.07 g, 3.53 mmol) was dissolved in 4M HCl in dioxane (5.04 mL HCl in 14.96 mL of dioxane) and the mixture was stirred at rt for an hour. Following this, the excess solvent was removed under reduced pressure and the crude product was triturated with diethyl ether and the excess solvent was then removed under reduced pressure to give a yellow oil (0.697 g, 97% yield).

^{1}H-NMR (D_2O): δ 3.14-3.19 (2H, m, C*H*$_2$NH$_2$), 3.42-3.47 (2H, m, C*H*$_2$NHCOCH), 3.62-3.73 (10H, m, CH_2PEG), 5.70 (1H, dd, CH_2C*H*CO, J_{cis} = 10.0 Hz, J_{gem} =1.6 Hz), 6.12-6.28 (2H, m, CH_2C*H*CO + CH_2C*H*CO).^{13}C-NMR (D_2O): δ 39.1, 39.3, 66.6, 67.0, 69.6, 69.8, 127.6, 130.1, 168.9. MS (NSI): m/z 203 (100[M+H]$^+$) HRMS: calcd. for $C_9H_{19}O_3N_2$: 203.1387 found 203.1390.

5-[4-(2-(2-(2-Acrylamidoethoxy)ethoxy)ethyl]carboxyphenyl-10,15,20-tri-(4-pyridyl)porphyrin (68)

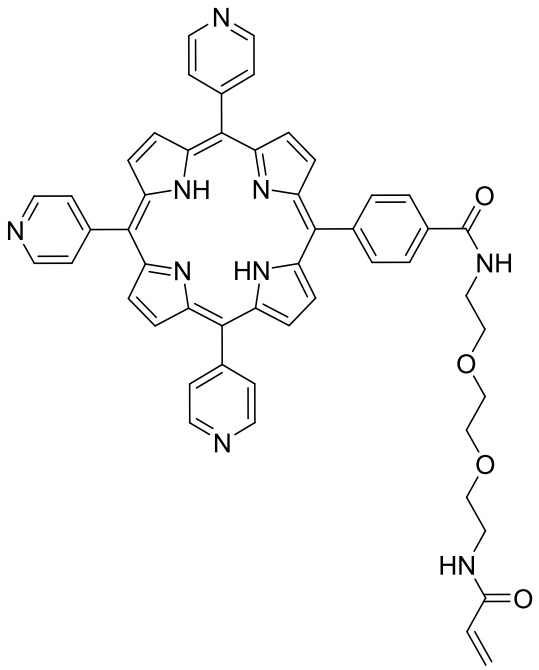

To a stirred solution of 5-[4-carboxyphenyl]-10,15,20-tri-(4-pyridyl) porphyrin (100 mg, 0.151 mmol, 1 equiv.), 1-ethyl-3-(3-dimethylaminopropyl)carbodiimide hydrochloride (EDCI·HCl) (44.0 mg, 0.230 mmol, 1.5 equiv.) and hydroxybenzotriazole (HOBt) (31.2 mg, 0.231 mmol 1.5 equiv.) in dry DMF (5.0 mL), was added, a solution of *N*-(2-(2-(2-aminoethoxy)ethoxy)ethyl)acrylamide (46.8 mg, 0.231 mmol, 1.5 equiv.) and 4-dimethylaminopyridine (DMAP) (31.2 mg, 0.255 mmol, 1.1 equiv.) in dry DMF (2.0 mL). The reaction mixture was stirred at rt under nitrogen for 24 h. At reaction completion (TLC: silica gel, dichloromethane/methanol 92:8), the solvent was removed under reduced pressure. The resulting dark solid was washed with water (3 x 50.0 mL) and diethyl ether (2 x 50.0mL). The crude product was purified using column chromatography (silica) eluted in CH_2Cl_2:CH_3OH (92:8). The product was obtained as a purple solid (53 mg, 42 % yield).

UV-Vis (H_2O): λ_{max} (nm) 415, 515,545, 590 and 645, ε (415 nm) = 798987 M^{-1} cm^{-1}. ^1H ($CDCl_3$) δ: 3.30-3.33 (2H, m, C*H*$_2$NH), 3.51 (2H, t, C*H*$_2$NHCOCH, J = 5.8 Hz), 3.57-3.73 (8H, m, CH_2 PEG), 5.56 (1H, dd, CH_2C*H*CO, J_{cis} = 10.4 Hz, J_{gem}= 1.6 Hz), 6.07(1H, dd, CH_2C*H*CO, J_{trans} = 17.1 Hz, J_{gem} = 1.6 Hz), 6.27 (1H, dd, CH_2C*H*CO, J_{trans} = 17.1 Hz, J_{cis} = 10.0 Hz), 8.22 (1H, t, CH_2N*H*, J= 5.0 Hz), 8.26-8.30 (6H, m, 2,6Py), 8.30-8.35 (4H,

m, o/mPh), 8.84-8.93 (8H, m, βH), 9.02-9.08 (6H, m, 3,5Py).^{13}C-NMR ($CDCl_3$) δ: 48.4, 69.6, 69.7, 70.2, 115.3, 116.0, 122.5, 125.7, 126.7, 132.7, 134.7, 143.6, 144.8, 157.1, 165.3, 166.7. MS (ESI): m/z 845 (100$[M+Na]^+$) HRMS: calcd. for $C_{51}H_{43}N_9O_4$: 845.34 found 868.3330.

5-[4-(2-(2-(2-Acrylamidoethoxy)ethoxy)ethyl]carboxyphenyl-10,15,20-tris(4-*N*-methylpyridyl)porphyrin trichloride (69)

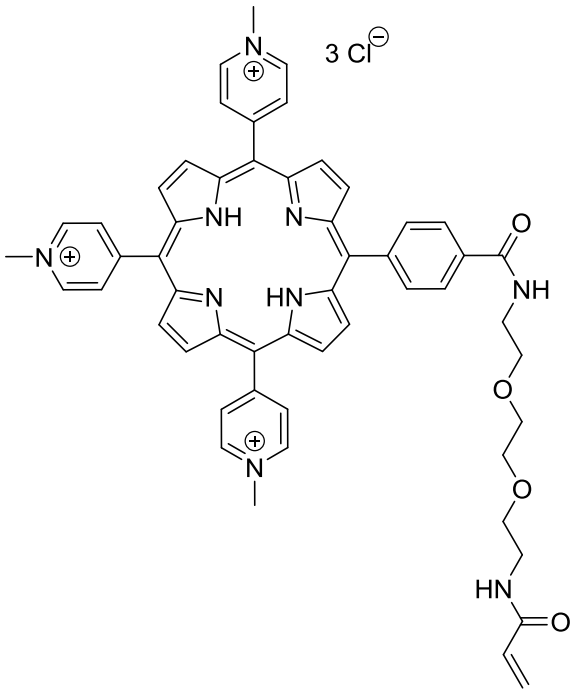

To a solution of 5-(4-(2-(2-(2-acrylamidoethoxy)ethoxy)ethyl)carboxyphenyl-10,15,20-tris(4-*N*-methylpyridinium)porphyrin (150 mg, 0.177 mmol, 1 equiv.) in DMF (50.0 mL) was added, *via* syringe, methyl iodide (1.50 mL, 0.0241 mol, 130 equiv.). The reaction mixture was shielded from light and stirred at 40 °C for 24 h. At reaction completion (TLC: silica gel, TLC: silica gel, sat. potassium nitrate/water/acetonitrile (1:1:8), diethyl ether (100.0 mL) was added and the resultant precipitate was filtered off through cotton. The solid was washed off the cotton, and then dissolved again in a 10% solution of ammonium hexafluorophosphate in water (100 mL). The resulting precipitate was filtered and the filter cake was dissolved in a 10% solution of tetrabutylammonium chloride in acetone (100 mL). The resulting precipitate was filtered, and the filter cake was dissolved in methanol (10.0 mL) and precipitated with diethyl ether (20.0 mL). The product was isolated via filtration to give the product as a chloride salt (131 mg, 75% yield).
UV-Vis (H_2O): λ_{max} (nm) 420, 520, 560, 585 and 645, ε (420 nm) = 224511 M^{-1} cm^{-1}.

^{1}H-NMR (C_2D_6SO) δ: -3.03 (2H, s, 2 x N*H*), 3.30-3.33 (2H, m, C*H*$_2$-NH), 3.52 (2H, t, C*H*$_2$-NH, J = 4.0 Hz), 3.57-3.74 (8H, m, CH_2PEG), 4.72-4.75 (9H, m, 3 x N-C*H*$_3$), 5.56 (1H, dd, CH_2C*H*CO, J_{cis} = 10.4 Hz, J_{gem} = 2.0 Hz), 6.07 (1H, dd, CH_2C*H*CO, J_{trans} = 17.1

Hz, J_{gem} = 1.6 Hz), 6.29 (1H, dd, CH_2CHCO, J_{trans} = 17.1 Hz, J_{cis} = 10.0 Hz), 8.30-8.27 (1H, m, CH_2NH), 8.33 (2H, d, oPh, J = 8.0 Hz), 8.39 (2H, d, mPh, J = 8.2 Hz), 8.98-9.06 (10H, m, 8βH + Py), 9.17 (4H, br s, Py), 9.50-9.53 (6H, m, 2,6Py).^{1}H-NMR (D_2O): δ: 2.96 (2H, t, J = 5.2 Hz, $CONHCH_2$), 3.17 (2H, t, J = 5.2 Hz, $CH_2NHCOCH$), 3.22-3.46 (8H, m, CH_2PEG), 4.69 (9H, s, 3 x N-CH_3), 5.18 (1H, d, CH_2CHCO, J = 10.0 Hz), 5.69 (1H, d, CH_2CHCO, J_{trans} = 16.6 Hz), 5.79 (1H, dd, CH_2CHCO, J_{trans} = 17.1 Hz, J_{cis} = 10.0 Hz), 6.74 (1H, d, J = 6.1 Hz, CH_2CHCO), 6.91 (1H, d, J = 6.9 Hz, CH_2CHCO), 8.39 (4H, d, J = 5.0 Hz, *o*/*m*Ph), 8.60 (6H, d, J = 6.2 Hz, 3,5Py), 9.27 (8H, d, J = 6.0 Hz, βH), 9.27 (6H, d, J = 6.2 Hz, 2,6Py).^{13}C-NMR (C_2D_6SO) δ: 48.4, 69.6, 70.2, 115.3, 116.0, 122.5, 132.3, 132.7, 134.6, 134.9, 143.6, 144.8, 157.1, 165.3,166.7. MS (ESI): m/z 995 (100[M-3Cl]$^{3+}$) HRMS: calcd. for $C_{54}H_{52}N_9O_4Cl_3$: 995.32; found 296.8042. HPLC: t_R : 8.40 min.

Palladium 5-[4-(2-(2-(2-acrylamidoethoxy)ethoxy)ethyl]carboxyphenyl-10,15,20-tris(4-*N*-methylpyridyl)porphyrin trichloride (70)

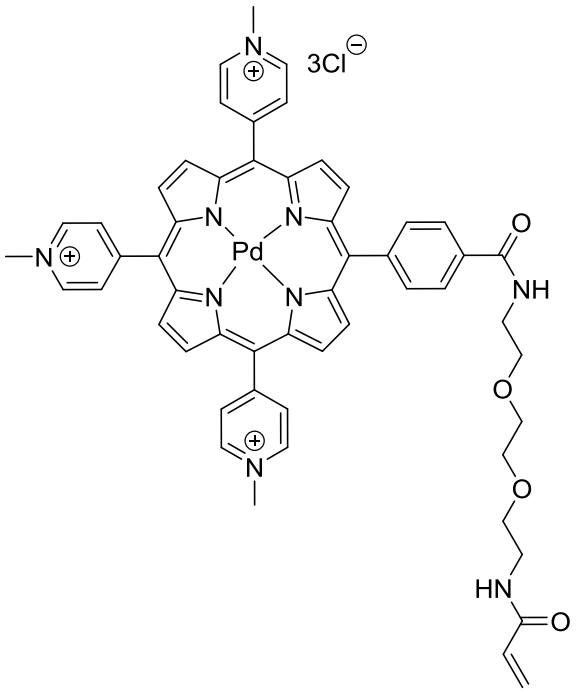

To a 35 mL microwave vessel was added 5-[4-(2-(2-(2-acrylamidoethoxy)ethoxy)ethyl]carboxyphenyl-10,15,20-tris(4-*N*-methylpyridinium) porphyrin trichloride (120.0 mg, 0.1200 mmol, 1 equiv.) and palladium acetate (180.0 mg, 0.8021 mmol, 6.660 equiv.) in a mixture of water/methanol (25.0 mL) (90:10). The mixture was heated at 100 °C for 2 h. At reaction completion, TLC: silica gel, sat. potassium nitrate/water/acetonitrile (1:1:8), the mixture was cooled and filtered through celite to remove any palladium impurities. A 10% solution of ammonium hexafluorophosphate in water was added (10.0 mL) and the resulting precipitate was filtered and redissolved in a 10% solution of tetrabutylammonium chloride in acetone (100.0 mL). The resulting precipitate was filtered to give the product as the chloride salt. The product was then dissolved in methanol (10 mL) and precipitated adding diethylether (20 mL) to give the product as a purple solid (87 mg, 65 % yield).

UV-Vis (H_2O): λ_{max} (nm) 420, 525 and 560, ε (420 nm) = 217732 M^{-1} cm^{-1}.^{1}H-NMR(C_2D_6SO) δ: 3.30-3.33 (2H, m, C*H*$_2$-NH), 3.44-3.76 (12H, m, CH_2PEG + C*H*$_2$-NH), 4.73 (9H, s, 3 x N-C*H*$_3$), 5.56 (1H, dd, CH_2C*H*CO, J_{cis} = 10.4 Hz, J_{gem} = 2.0 Hz), 6.07 (1H, dd, CH_2C*H*CO, J_{trans} = 17.1 Hz, J_{gem} = 1.6 Hz), 6.24-6.34 (1H, dd, CH_2C*H*CO, J_{trans}

= 17.1 Hz, J_{cis} = 10.0 Hz), 8.37 (4H, dd, o/mPh), 8.93-9.05 (10H, m, 8βH + 2 Py), 9.07-9.13 (4H, m, Py), 9.44-9.59 (6H, m, 2,6Py).^{13}C-NMR (C_2D_6SO) δ: 69.6, 70.2, 117.7, 123.8, 126.7, 132.4, 134.3, 140.2, 140.5, 142.0, 143.2, 144.7, 144.9, 156.6. HPLC: t_R: 8.52 minutes.

Copper 5-[4-(2-(2-(2-acrylamidoethoxy)ethoxy)ethyl]carboxyphenyl-10,15,20-tris(4-*N*-methylpyridyl)porphyrin trichloride (71)

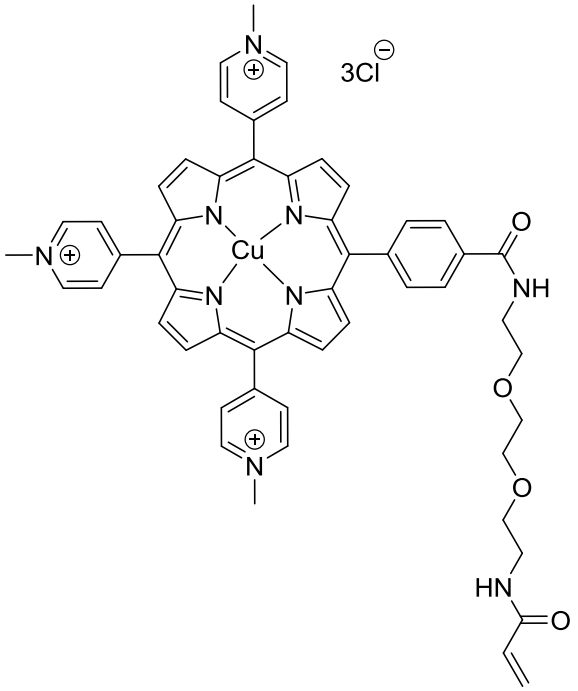

To a stirred solution of 5-[4-(2-(2-(2-acrylamidoethoxy)ethoxy)ethyl]carboxyphenyl-10,15,20-tris(4-*N*-methylpyridinium)porphyrin trichloride (50.0 mg, 0.0500 mmol, 1 equiv.) in water (8 mL) was added copper(II) sulphate pentahydrate (50.0 mg, 0.200 mmol, 4 equiv.). The reaction mixture was shielded from light and stirred at room temperature for 24 h. At reaction completion (TLC: silica gel, sat. potassium nitrate/water/acetonitrile (1:1:8), 10 mL of a 10% solution of ammonium hexafluorophosphate in water was added and the resulting precipitate was filtered and redissolved in a 10% solution of tetrabutylammonium chloride in acetone (100.0 mL). The resulting precipitate was filtered to give the product as the chloride salt. The product was dissolved in methanol (10.0 mL) and precipitated with diethyl ether (20.0 mL) to give the product as a purple solid (48.2 mg, 91 % yield).

UV-Vis (H_2O): λ_{max} (nm) 425, 550 and 575, ε (425 nm) = 213249 cm^{-1} M^{-1}. MS (ESI): m/z 997 (100$[M-3Cl]^{3+}$) HRMS: calcd. for $C_{54}H_{52}N_9O_4Cl_3Cu$: 1056.24; found 317.1088. HPLC: tR: 8.55 minutes.

Immobilisation of porphyrin and polyviologen on silica support

Method one

Poly(benzylviologen)dibromide (0.096g) was dissolved in distilled water (4.0 mL), to this solution was added ethanol (0.8 mL) and glacial acetic acid (0.5 mL). Following this tetraethoxyorthosilicate (TEOS) (3.998 g) was added. The mixture was stirred and then covered with parafilm with holes pierced in the top to allow solvent evaporation. Once solvent evaporation was complete the resulting solid was washed with water and ethanol then placed in the vaccum oven at 120 °C for 48 h to give a glassy solid. Analysis was carried out by SEM and showed a non-porous structure.

Method two

Poly(benzylviologen)dibromide (0.096g) was dissolved in distilled water (4 mL), to this solution was added methanol (0.8 mL) and glacial acetic acid (0.5 mL). Following this tetramethoxyorthosilicate (TMOS) (3.998 g) was added. The mixture was stirred and then covered with parafilm with holes pierced in the top to allow solvent evaporation. Once solvent evaporation was complete the resulting solid was washed with water and ethanol then placed in the vaccum oven at 120 °C for 48 h to give a glassy solid. Analysis was carried out by SEM and showed a non-porous structure.

Method three – Porphyrin entrapped

Poly(benzylviologen)dibromide (0.096g) and porphyrin (0.01g) were dissolved in distilled water (4 mL), to this solution was added ethanol (0.8 mL) and glacial acetic acid (0.5 mL). Following this tetraethoxyorthosilicate (TEOS) (3.998 g) was added. The mixture was stirred and then covered with parafilm with holes pierced in the top to allow solvent evaporation. Once solvent evaporation was complete the resulting solid was washed with water and ethanol then placed in the vaccum oven at 120 °C for 48 h to give a glassy solid. Analysis was carried out by SEM and showed a non-porous structure.

Polyacrylamide support

Entrapment method

A stock solution of 30% acrylamide and bisacrylamide was prepared by dissolving acrylamide (5.8 g) and bisacrylamide (0.2 g) in 20 mL of distilled water, the stock solution was sonicated until the two monomers were fully dissolved.

To prepare the control hydrogel the 30% acrylamide mixture (6.60 mL) and water (3.20 mL) were mixed in a 3.3 cm diameter mould. To this sodium dodecylsulphate (SDS) (0.10 mL) was added, followed by the addition of ammonium peroxydisulphate (APS) (0.10 mL) and tetramethylethylenediamine (TEMED) (0.05 mL). The solution was mixed and then left to polymerise for 15-20 minutes when a blank gel was formed. The gel was washed with water several times to remove any unreacted vinyl monomers.

To prepare the porphyrin-viologen hydrogel the 30% acrylamide mixture (6.60 mL) with the polyviologen dissolved in it, and THF/DMF/dioxane with the porphyrin dissolved (3.20 mL) were mixed in a 3.3 cm diameter mould. To this sodium dodecylsulphate (SDS) (0.10 mL) was added, followed by the addition of ammonium peroxydisulphate (APS) (0.10 mL) and tetramethylethylenediamine (TEMED) (0.05 mL). The solution was mixed and then left to polymerise for 15-20 minutes when a gel was formed. The gel was washed with water several times to remove any unreacted vinyl monomers, and also with the chosen solvent to remove any unreacted porphyrin.

Conjugation method with porphyrin bearing vinyl functionality

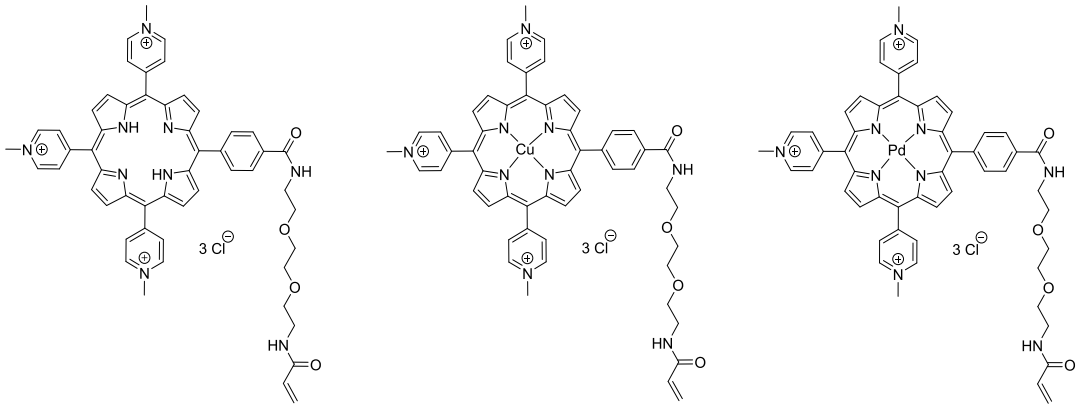

Gel preparation:

Three different gels for the metal free porphyrin were prepared to have increasing concentrations of porphyrins immobilised. The molarity of the gel was 3.3 mmol L^{-1}, which was kept the same during the synthesis of the gels with the different porphyrins containing metals. The palladium porphyrin gel contained 4.4 mg cm^{-3}, the copper porphyrin contained 4.1 mg cm^{-3} of porphyrin in the final gel and the metal free porphyrin contained 4.4 mg cm^{-3}.

In the polyacrylamidic support the final crosslinker ratio was 5% in all synthesized gels, and the final monomer concentration was 20% in all of the synthesized gels.

I used moulds with l = 3.3 cm, w = 3.3 cm and h = 1cm. Volume = 3.3 cm x 3.3cm x 1cm = 10.89 cm^3

Gels	**nMP mg cm^{-3}**	**CuP mg cm^{-3}**	**PdP mg cm^{-3}**
Porphyrins dissolved (mg)	4.0	4.1	4.4
H_2O*	3.2 ml	3.2 ml	3.2 ml
30% acrylamide mix (with 19:1 on acrylamide/bis ratio)	6.6 ml	6.6 ml	6.6 ml
10% SDS	100 µl	100 µl	100 µl
10% APS	100 µl	100 µl	100 µl
TEMED	2 drop (40 µl)	2 drop (40 µl)	2 drop (40 µl)

* the porphyrin is previously dissolved here

The 30% acrylamide mixture (6.60 mL) and water with the porphyrin dissolved (3.20 mL) were mixed in a 3.3 cm diameter mould. To this sodium dodecylsulphate (SDS) (0.10 mL) was added, followed by the addition of ammonium peroxydisulphate (APS) (0.10 mL) and tetramethylethylenediamine (TEMED) (0.05 mL). The solution was mixed and then left to polymerise for 15-20 minutes when a gel was formed. The gel was washed with water several times to remove any unreacted vinyl monomers.

General method for the synthesis of porphyrin hydrogels: Acrylamide (1.91 g, 26.9 mmol) and N',N'-methylene bis acrylamide (66.0 mg, 0.428 mmol) were dissolved in 6.60 mL of distilled water. To this solution was added 100 µL of a 10% solution of SDS (9.956 mg, 0.035 mmol) and one of compound **69**, **70**, **71** (4.00 mg, 4.40 mg and 4.10 mg respectively, 3.3 mmol) previously dissolved in 3.30 mL of distilled water was added. The mixture was gently stirred, and then 100 µL of a 10% solution of APS and 20 µL of TEMED were subsequently added and the solution transferred into a mould (l = 3.3 cm, w = 3.3 cm, h= 1 cm) and left for 15-20 min~~s~~ to polymerise in the dark. The gel was then removed from the mould and washed with distilled water then kept moist in a dust-free chamber.

Biology experimental

The biological evaluation was carried out as part of a collaboration with Prof. John Greenman at the University of the West of England and Dr Cinzia Spagnul at the University of Hull.

Antibacterial activity of hydrogels

E. coli strain DH5a contains the plasmid pGLITE, a derivative of pBBR1MCS-2 containing the lux CDABE operon of Photorhabdus luminescense was maintained from frozen stock on nutrient agar (Oxoid Ltd, Basingstoke, UK) and were grown as broth cultures using Reinforced Clostridial Medium (RCM; Oxoid Ltd Basingstoke, UK) with addition of kanamycin (10 mg L^{-1}) to selectively maintain the lux plasmids.

For experiments on photodynamic killing, microbial cells were obtained by inoculation of test species in 10 mL volumes of appropriate liquid medium and incubated in a shaking incubator (model S 150, Stuart shakers, UK) at 37° C for 4 to 6 hours to obtain mid exponential phase cultures. A total of 100 µL of bacterial suspension was appropriately diluted in 2 mL PBS (pH = 6.0) to obtain approximately 10^6 colony-forming units (cfu) mL^{-1}.

Standard method (with porphyrin immobilised in the hydrogel)

The photoantimicrobial hydrogels were cut into four squares and equilibrated with PBS (pH = 6.0) for 30 minutes. Then the media was discarded, the gel was washed with PBS of the same pH and placed into the diluted bacterial suspension in borosilicate glass tubes (12 by 75 mm; Fisher Scientific, Loughborough, UK) using the same tube for both light irradiation and measurement of bioluminescence light output. The samples were irradiated with a white light at a fluence rate of 14.5 mW cm^2 for 20 or 25 minutes (total light dose was either 17.4 or 21.8 J cm^2).

The illumination was performed using a fiber optic cable (F = 1 cm) and lamp (Fiber Illuminator, OSL1-EC, ThorLabsInc, Ely, Cambridgeshire) with a 150 W halogen lamp. Luminescence light output was measured by quickly inserting the tube into a FB12 luminometer (Berthold Detection Systems, Germany) to quantify the light output as relative light units (RLU). A borosilicate tube was similarly treated, but not exposed to light and used as a reference for the dark toxicity under the same experimental conditions. The blank hydrogel not containing porphyrin was tested following the same protocol. A control experiment on an *E. coli* suspension irradiated and in the dark indicated that light doses alone up to 21.8 J cm^{-2} cause no evident bacterial damage. All experiments were conducted in duplicate.

References

1 J. A. Al-Tawfiq and P. A. Tambyah, *J. Infect. Public Health*, 2014, **7**, 339–344.
2 World Health Organization, Antimicrobial resistance: global report on surveillance, 2014, 1-257
3 S. E. Cosgrove, *Clin. Infect. Dis.*, 2006, **42**, S82–S89.
4 The Comptroller and Auditor general, Reducing Healthcare Associated Infections in Hospitals in England, HC560 session, 2008-2009.
5 S. Perni, P. Prokopovich, I. P. Parkin, M. Wilson and J. Pratten, *J. Mater. Chem.*, 2010, **20**, 8668-8673.
6 C. W. Dunnill, Z. Ansari, A. Kafizas, S. Perni, D. J. Morgan, M. Wilson and I. P. Parkin, *J. Mater. Chem.*, 2011, **21**, 11854-11861.
7 M. Wainwright, T. Maisch, S. Nonell, K. Plaetzer, A. Almeida, G. P. Tegos, M. Hamblin, *Lancet Infect Dis*, 2017, **17**, 49–55.
8 G. Gottlieb, *Bull. R. Coll. Surg. Engl.*, 2016, **98**, 45–45.
9 H. C. Gram, *Immunologia*, 1992, 11(4), 140-150
10 J. B. Kaper, J. P. Nataro and H. L. T. Mobley, *Nat. Rev. Microbiol.*, 2004, **2**, 123–140.
11 S. J. Dancer, *J. Hosp. Infect.*, 2009, **73**, 378–385.
12 K. Page, M. Wilson and I. P. Parkin, *J. Mater. Chem.*, 2009, **19**, 3819-3831.
13 B. Allegranzi, S. B. Nejad, C. Combescure, W. Graafmans, H. Attar, L. Donaldson and D. Pittet, *The Lancet*, 2011, **377**, 228–241.
14 A. V. Emeline, V. N. Kuznetsov, V. K. Rybchuk and N. Serpone, *Int. J. Photoenergy*, 2008, **2008**, 1–19.
15 S. Perni, J. Pratten, M. Wilson, C. Piccirillo, I. P. Parkin and P. Prokopovich, *J. Biomater. Appl.*, 2011, **25**, 387–400.
16 G. Cheng, H. Xue, Z. Zhang, S. Chen and S. Jiang, *Angew. Chem.*, 2008, **120**, 8963–8966.
17 C. Piccirillo, S. Perni, J. Gil-Thomas, P. Prokopovich, M. Wilson, J. Pratten and I. P. Parkin, *J. Mater. Chem.*, 2009, **19**, 6167-6171.
18 V. Decraene, J. Pratten and M. Wilson, *Appl. Environ. Microbiol.*, 2006, **72**, 4436–4439.
19 S. Sato, *Chem. Phys. Lett.*, 1986, **123**, 126–128.
20 S. Livraghi, M. C. Paganini, E. Giamello, A. Selloni, C. Di Valentin and G. Pacchioni, *J. Am. Chem. Soc.*, 2006, **128**, 15666–15671.
21 J. C. Yu, W. Ho, J. Yu, H. Yip, P. K. Wong and J. Zhao, *Environ. Sci. Technol.*, 2005, **39**, 1175–1179.
22 M. Pelaez, N. T. Nolan, S. C. Pillai, M. K. Seery, P. Falaras, A. G. Kontos, P. S. M. Dunlop, J. W. J. Hamilton, J. A. Byrne, K. O'Shea, M. H. Entezari and D. D. Dionysiou, *Appl. Catal. B Environ.*, 2012, **125**, 331–349.
23 A. Thomas, W. Flavell, A. Mallick, A. Kumarasinghe, D. Tsoutsou, N. Khan, C. Chatwin, S. Rayner, G. Smith, R. Stockbauer, S. Warren, T. Johal, S. Patel, D. Holland, A. Taleb and F. Wiame, *Phys. Rev. B*, 2007, **75**, 035105
24 S. M. Gupta and M. Tripathi, *Chin. Sci. Bull.*, 2011, **56**, 1639–1657..
25 J. Buha, I. Djerdj, M. Antonietti and M. Niederberger, *Chem. Mater.*, 2007, **19**, 3499–3505
26 T. Rajh, J. Nedeljkovic, X. Chen, O. Poluektov and M.G. Thurnaur, *J. Phys. Chem.*, 1999, **103**, 3515–3519.
27 M. S. Baptista and M. Wainwright, *Braz. J. Med. Biol. Res.*, 2011, **44**, 1–10.
28 R. F. Donnelly, P. A. McCarron and M. M. Tunney, *Microbiol. Res.*, 2008, **163**, 1–12.
29 L. Ryskova, V. Buchta and R. Slezak, *Cent. Eur. J. Biol.*, 2010, **5**, 400–406.
30 A. Almeida, A. Cunha, M. A. F. Faustino, M. G. P. M. S. Neves and A. C. Tome in Photodynamic Inactivation of Microbial Pathogens: Medical and Environmental

Applications, Ed. M. R. Hamblin and G. Jori, RSC publishing, Cambridge, 1st edn, 2011, vol. 11, ch. 5, pp. 83–160.
31 M. Wainwright, *J. Antimicrob. Chemother.*, 2012, **67**, 787–788.
32 C. Spagnul, L. C. Turner and R. W. Boyle, *J. Photochem. Photobiol. B*, 2015, **150**, 11-30.
33 M. Wainwright, *Int. J. Antimicrob. Agents*, 2014, **44**, 26–29.
34 C. M. Cassidy, M. M. Tunney, P. A. McCarron and R. F. Donnelly, *J. Photochem. Photobiol. B*, 2009, **95**, 71–80.
35 M. Wainwright, *J. Antimicrob. Chemother.*, 1998, **42**, 13–28.
36 T. Maisch, S. Hackbarth, J. Regensburger, A. Felgenträger, W. Bäumler, M. Landthaler and B. Röder, *JDDG J. Dtsch. Dermatol. Ges.*, 2011, **9**, 360–366.
37 F. Harris, L. K. Chatfield and D. A. Phoenix, *Curr. Drug Targets*, 2005, **6**, 615–627.
38 M. C. DeRosa and R. J. Crutchley, *Coord. Chem. Rev.*, 2002, **233**, 351–371.
39 S. Banfi, E. Caruso, L. Buccafurni, V. Battini, S. Zazzaron, P. Barbieri and V. Orlandi, *J. Photochem. Photobiol. B*, 2006, **85**, 28–38.
40 J. P. M. L. Rolim, M. A. S. de-Melo, S. F. Guedes, F. B. Albuquerque-Filho, J. R. de Souza, N. A. P. Nogueira, I. C. J. Zanin and L. K. A. Rodrigues, *J. Photochem. Photobiol. B*, 2012, **106**, 40–46.
41 N. Komerik, H. Nakanishi, A. J. MacRobert, B. Henderson, P. Speight and M. Wilson, *Antimicrob. Agents Chemother.*, 2003, **47**, 932–940.
42 C. F. Lee, C. J. Lee, C.-T. Chen and C.-T. Huang, *J. Photochem. Photobiol. B*, 2004, **75**, 21–25.
43 M. Wainwright, *Photodiagnosis Photodyn. Ther.*, 2005, **2**, 263–272.
44 M. Wainwright, *Chem Soc Rev*, 1996, **25**, 351–359.
45 T. Maisch, *Lasers Med. Sci.*, 2007, **22**, 83–91.
46 A. Minnock, D.I. Vernon, J.Schofield, J. Griffiths, J.Howard Parish, S. B. Brown, 1994, *Antimicrobial agents and chemotherapy*, **32**, 159–164.
47 M. Merchat, G. Bertoilini, P. Giacomini, A. Villanneva, G. Jori, *J. Photochem. Photobiol. B*, 1996, **32**, 153–157.
48 M. Wainwright, *Photosensitisers in Biomedicine*, John Wiley & Sons, Ltd, Chichester, UK, 2009.
49 G. Jori and O. Coppellotti, *Anti-Infective Agents in Medicinal Chemistry*, 2007, **6**, 119–131.
50 P. Rothemund, *J. Am. Chem. Soc.*, 1936, **58**, 625–627.
51 J. S. Lindsey, I. C. Schreiman, H. C. Hsu, P. C. Kearney and A. M. Marguerettaz, *J. Org. Chem.*, 1987, **52**, 827–836.
52 A. D. Adler, F. R. Longo, J. D. Finarelli, J. Goldmacher, J. Assour and L. Korsakoff, *J. Org. Chem.*, 1967, **32**, 476–476.
53 G. P. Arsenault, E. Bullock and S. F. MacDonald, *J. Am. Chem. Soc.*, 1960, **82**, 4384–4389.
54 C. M. B. Carvalho, E. Alves, L. Costa, J. P. C. Tomé, M. A. F. Faustino, M. G. P. M. S. Neves, A. C. Tomé, J. A. S. Cavaleiro, A. Almeida, A. Cunha, Z. Lin and J. Rocha, *ACS Nano*, 2010, **4**, 7133–7140.
55 M. Kuruppuarachchi, H. Savoie, A. Lowry, C. Alonso and R. W. Boyle, *Mol. Pharm.*, 2011, **8**, 920–931.
56 E. Alves, J. M. M. Rodrigues, M. A. F. Faustino, M. G. P. M. S. Neves, J. A. S. Cavaleiro, Z. Lin, Â. Cunha, M. H. Nadais, J. P. C. Tomé and A. Almeida, *Dyes Pigments*, 2014, **110**, 80–88.
57 M. Magaraggia, G. Jori, M. Soncin, C. L. Schofield and D. A. Russell, *Photochem. Photobiol. Sci.*, 2013, **12**, 2170-2176.
58 C. Ringot, V. Sol, M. Barrière, N. Saad, P. Bressollier, R. Granet, P. Couleaud, C. Frochot and P. Krausz, *Biomacromolecules*, 2011, **12**, 1716–1723.

59 E. Feese, H. Sadeghifar, H. S. Gracz, D. S. Argyropoulos and R. A. Ghiladi, *Biomacromolecules*, 2011, **12**, 3528–3539.
60 K. Sakakibara, F. Nakatsubo, A. D. French and T. Rosenau, *Chem. Commun.*, 2012, **48**, 7672-7674.
61 V. S. Gaware, M. Håkerud, K. Leósson, S. Jónsdóttir, A. Høgset, K. Berg and M. Másson, *J. Med. Chem.*, 2013, **56**, 807–819.
62 R. Lucas, R. Granet, V. Sol, C. Le Morvan, C. Policar, E. Rivière and P. Krausz, *E-Polym.*, 2007, **7**, 1031–1038.
63 H. Jiang, W. Su, J. Hazel, J. T. Grant, V. V. Tsukruk, T. M. Cooper and T. J. Bunning, *Thin Solid Films*, 2000, **372**, 85–93.
64 C. Ringot, V. Sol, R. Granet and P. Krausz, *Mater. Lett.*, 2009, **63**, 1889–1891.
65 M. Krouit, R. Granet, P. Branland, B. Verneuil and P. Krausz, *Bioorg. Med. Chem. Lett.*, 2006, **16**, 1651–1655.
66 M. Krouit, R. Granet and P. Krausz, *Bioorg. Med. Chem.*, 2008, **16**, 10091–10097.
67 M. Krouit, R. Granet and P. Krausz, *Eur. Polym. J.*, 2009, **45**, 1250–1259
68 B. L. Carpenter, E. Feese, H. Sadeghifar, D. S. Argyropoulos and R. A. Ghiladi, *Photochem. Photobiol.*, 2012, **88**, 527–536.
69 J. P. Mbakidi, K. Herke, S. Alvès, V. Chaleix, R. Granet, P. Krausz, S. Leroy-Lhez, T.-S. Ouk and V. Sol, *Carbohydr. Polym.*, 2013, **91**, 333–338.
70 R. Bonnett, M. A. Krysteva, I. G. Lalov and S. V. Artarsky, *Water Res.*, 2006, **40**, 1269–1275.
71 R. Bonnett, *Chem Soc Rev*, 1995, **24**, 19–33.
72 S. M. Ribeiro, A. C. Serra and A. M. d'A. Rocha Gonsalves, *Tetrahedron*, 2007, **63**, 7885–7891.
73 V. V. Vasil'ev and S. M. Borisov, *Sens. Actuators B Chem.*, 2002, **82**, 272–276.
74 J. Kopecek, *J. Polym. Sci. Part Polym. Chem.*, 2009, **47**, 5929–5946.
75 R. M. Unruh, J. R. Roberts, S. P. Nichols, S. Gamsey, N. A. Wisniewski and M. J. McShane, *J. Diabetes Sci. Technol.*, 2015, **9**, 985-992
76 M. Mukherjee and A. R. Ray, *J. Mol. Catal. Chem.*, 2007, **266**, 207–214.
77 F. Giuntini, F. Dumoulin, R. Daly, V. Ahsen, E. M. Scanlan, A. S. P. Lavado, J. W. Aylott, G. A. Rosser, A. Beeby and R. W. Boyle, *Nanoscale*, 2012, **4**, 2034-2045
78 C. Xing, Q. Xu, H. Tang, L. Liu and S. Wang, *J. Am. Chem. Soc.*, 2009, **131**, 13117–13124.
79 M. G. Alvarez, M. L. Gómez, S. J. Mora, M. E. Milanesio and E. N. Durantini, *Bioorg. Med. Chem.*, 2012, **20**, 4032–4039.
80 B. Gao, L. Fang, J. Men and Q. Lei, *Mater. Chem. Phys.*, 2012, **134**, 1049–1058.
81 A. G. Griesbeck and A. Bartoschek, *Chem. Commun.*, 2002, 1594–1595.
82 A. G. Griesbeck and T. T. El-Idreesy, *Photochem. Photobiol. Sci.*, 2005, **4**, 205-209.
83 J. Johnson Inbaraj, M. V. Vinodu, R. Gandhidasan, R. Murugesan and M. Padmanabhan, *J. Appl. Polym. Sci.*, 2003, **89**, 3925–3930.
84 R. Rychtarikova, S. Sabata, J. Hetflejs and G. Kuncova, *J. Sol-Gel Sci. Technol.*, 2012, **61**, 119–125.
85 J. Mosinger, K. Lang, P. Kubát, J. Sýkora, M. Hof, L. Plíštil and B. Mosinger, *J. Fluoresc.*, 2009, **19**, 705–713.
86 S. Noimark, C. W. Dunnill and I. P. Parkin, *Adv. Drug Deliv. Rev.*, 2013, **65**, 570–580.
87 A. Mills, R. H. Davies and D. Worsley, *Chem. Soc. Rev.*, 1993, **22**, 417–425.
88 Z. X. Lu, L. Zhou, Z. L. Zhang, W. L. Shi, Z. X. Xie, H. Y. Xie, D. W. Pang and P. Shen, *Langmuir*, 2003, **19**, 8765–8768.
89 K. Page, R. G. Palgrave, I. P. Parkin, M. Wilson, S. L. P. Savin and A. V. Chadwick, *J. Mater. Chem.*, 2007, **17**, 95–104.
90 C. W. Dunnill, K. Page, Z. A. Aiken, S. Noimark, G. Hyett, A. Kafizas, J. Pratten, M. Wilson and I. P. Parkin, *J. Photochem. Photobiol. Chem.*, 2011, **220**, 113–123.

91 H. C. Pappas, S. Phan, S. Yoon, L. E. Edens, X. Meng, K. S. Schanze, D. G. Whitten and D. J. Keller, *ACS Appl. Mater. Interfaces*, 2015, **7**, 27632–27638.
92 Z. Shi, K. G. Neoh and E. T. Kang, *Biomaterials*, 2005, **26**, 501–508.
93 C. L Bird and A. T Kuhn, *Chem. Soc. Rev.*, 1981, **10**, 49–82.
94 A. Mills and S-K. Lee, Sensor for oxidising agents, US Patent number 8,114,673 B2, 2012, 1–8
95 L. Michaelis and E. S. Hill, *J. Gen. Physiol.*, 1933, **16**, 859–73
96 M. C. Grenier, R. W. Davis, K. L. Wilson-Henjum, J. E. LaDow, J. W. Black, K. L. Caran, K. Seifert and K. P. C. Minbiole, *Bioorg. Med. Chem. Lett.*, 2012, **22**, 4055–4058.
97 M. Krompiec, I. Grudzka, M. Filapek, Ł. Skórka, S. Krompiec, M. Łapkowski, M. Kania and W. Danikiewicz, *Electrochimica Acta*, 2011, **56**, 8108–8114.
98 L. Roberts, R. Lines, S. Reddy and J. Hay, *Sens. Actuators B Chem.*, 2011, **152**, 63–67
99 R. J. Young and P. A. Lovell, *Introduction to polymers*, CRC press Taylor & Francis, Boca Raton, 2011.
100 P. K. Bhowmik, H. Han, J. J. Cebe, R. A. Burchett and A. M. Sarker, *J. Polym. Sci. Part Polym. Chem.*, 2002, **40**, 659–674.
101 A. Harriman and M. C. Richoux, *J. Chem. Soc. Faraday Trans. 2 Mol. Chem. Phys.*, 1980, **76**, 1618–1626.
102 A. Harriman, G. Porter and M.C. Richoux, *J. Chem. Soc. Faraday Trans. 2 Mol. Chem. Phys.*, 1981, **77**, 1175–1187.
103 I. Okura, *Photosensitization of Porphyrins and Phthalocyanines*, Gordon and Breach Science Publishers, Tokyo, 2000.
104 P. A. Christensen, W. Erbs and A. Harriman, *J. Chem. Soc. Faraday Trans. 2 Mol. Chem. Phys.*, 1985, **81**, 575–580.
105 A. El-Faham and F. Albericio, *Chem. Rev.*, 2011, **111**, 6557–6602
106 A. Suzuki, *Journal of Organometallic chemistry*, 1999, **576**, 147–168.
107 N. Miyaura and A. Suzuki, *Chem. Rev.*, 1995, **95**, 2457–2483.
108 R. Chinchilla and C. Nájera, *Chem. Soc. Rev.*, 2011, **40**, 5084.
109 H. Doucet and J. C. Hierso, *Angew. Chem. Int. Ed.*, 2007, **46**, 834–871.
110 R. Chinchilla and C. Nájera, *Chem. Rev.*, 2007, **107**, 874–922.
111 K. Sonogashira, Y. tohda and N. Hagihara, *Tetrahedron lett.*, 1975, **50**, 4467–4470.
112 H. C. Kolb, M. G. Finn and K. B. Sharpless, *Angewandte chemie*, 2001, **40**, 2004-2021.
113 F. Dumoulin and V. Ahsen, *J. Porphyr. Phthalocyanines*, 2011, **15**, 481–504.
114 J. E. Moses and A. D. Moorhouse, *Chem. Soc. Rev.*, 2007, **36**, 1249-1262.
115 J. F. Lutz, *Angew. Chem. Int. Ed.*, 2007, **46**, 1018–1025.
116 H. C. Kolb and K. B. Sharpless, *Drug Discov. Today*, 2003, **8**, 1128–1137..
117 B. Helms, J. L. Mynar, C. J. Hawker and J. M. J. Fréchet, *J. Am. Chem. Soc.*, 2004, **126**, 15020–15021
118 R. Fielden and L. A. Summers, *Experientia*, 1974, **30**, 843–844.
119 R. M. Elofson, R. L. Edsberg, *Can. J. Chem*, 1957, 646–650.
120 J.T. Stevens and D. D. Sumner, in Handbook of Pesticide Toxicology, ed. W. J. Hayes and E. R. Laws,, Academic Press, San Diego, 1991, ch. 20, pp. 1317-1391.
121 A. Calderbank, *Adv. Pest Control Res.*, 1968, **8**, 127-235.
122 J. H. Ross and R. I. Krieger, *J. Agric. Food Chem.*, 1980, **28**, 1026–1031.
123 M. S. Simon and P. T. Moore, *J. Polym. Sci. Polym. Chem. Ed.*, 1975, **13**, 1–16.
124 Z. Shi, K. G. Neoh and E. T. Kang, *Biomaterials*, 2005, **26**, 501–508.
125 M. S. Simon and P. T. Moore, *J. Polym. Sci. Polym. Chem. Ed.*, 1975, **13**, 1–16.
126 A. Mills, *Chem. Soc. Rev.*, 2005, **34**, 1003-1011.

127 J. D. Batteas, A. Harriman, Y. Kanda, N. Mataga and A. K. Nowak, *J. Am. Chem. Soc.*, 1990, **112**, 126–133..
128 H. Hosono, T. Tani and I. Uemura, *Chem Commun*, 1996, 1893–1894.
129 S. Aono, N. Kaji and I. Okura, *J. Chem. Soc. Chem. Commun.*, 1986, 170–171.
130 Y. Amao and I. Okura, *J. Mol. Catal. B Enzym.*, 2002, **17**, 9–21..
131 S. Noda, H. Hosono, I. Okura, Y. Yamamoto and Y. Inoue, *J. Chem. Soc. Faraday Trans.*, 1990, **86**, 811–814
132 R. N. Vrtis, C. P. Rao, S. Warner and S. J. Lippard, *J. Am. Chem. Soc.*, 1988, **110**, 2669–2670.
133 T. Yui, Y. Kobayashi, Y. Yamada, K. Yano, Y. Fukushima, T. Torimoto and K. Takagi, *ACS Appl. Mater. Interfaces*, 2011, **3**, 931–935.
134 M. T. Barton, N. M. Rowley, P. R. Ashton, C. J. Jones, N. Spencer, M. S. Tolley and L. J. Yellowlees, *New J. Chem.*, 2000, **24**, 555–560.
135 Y. Amao, T. Hiraishi, I. Okura, *J. Mol. Catal. A*, 1997, **126**, 13–20.
136 A. Harriman, G. Porter and M. C. Richoux, *J. Chem. Soc. Faraday Trans. 2 Mol. Chem. Phys.*, 1981, **77**, 833–844.
137 A. Harriman, *Inorganica chimica Acta*, 1984, **88**, 213–213.
138 S. Konno, T. Fujimura, Y. Otani, T. Shimada, H. Inoue and S. Takagi, *J. Phys. Chem. C*, 2014, **118**, 20504–20510.
139 Y. Nosaka, A. Kuwabara and H. Miyama, *J. Phys. Chem.*, 1986, **90**, 1465–1470..
140 M. Pelaez, N. T. Nolan, S. C. Pillai, M. K. Seery, P. Falaras, A. G. Kontos, P. S. M. Dunlop, J. W. J. Hamilton, J. A. Byrne, K. O'Shea, M. H. Entezari and D. D. Dionysiou, *Appl. Catal. B Environ.*, 2012, **125**, 331–349.
141 A. Fujishima, T. N. Rao and D. A. Tryk, *J. Photochem. Photobiol. C Photochem. Rev.*, 2000, **1**, 1–21.
142 S. Livraghi, M. C. Paganini, E. Giamello, A. Selloni, C. Di Valentin and G. Pacchioni, *J. Am. Chem. Soc.*, 2006, **128**, 15666–15671.
143 C. Tahtaoui, I. Parrot, P. Klotz, F. Guillier, J.-L. Galzi, M. Hibert and B. Ilien, *J. Med. Chem.*, 2004, **47**, 4300–4315.
144 E. Dyer and H. Scott, *J. Am. Chem. Soc.*, 1957, **79**, 672–675.
145 M. J. Adeogun, J. N. Hay, *Polymer int.*, 1996, **41**, 123–134.
146 K. Nikitin and D. Fitzmaurice, *J. Am. Chem. Soc.*, 2005, **127**, 8067–8076.
147 Z. M. Wang and M. Shen, *J. Org. Chem.*, 1998, **63**, 1414–1418.
148 W. Chen, X.-D. Yang, Y. Li, L.-J. Yang, X. Q. Wang, G. L. Zhang and H. B. Zhang, *Org. Biomol. Chem.*, 2011, **9**, 4250-4255.
149 C. W. Dunnill, Z. Ansari, A. Kafizas, S. Perni, D. J. Morgan, M. Wilson and I. P. Parkin, *J. Mater. Chem.*, 2011, **21**, 11854-11861.
150 T. Peng, D. Zhao, K. Dai, W. Shi and K. Hirao, *J. Phys. Chem. B*, 2005, **109**, 4947–4952.
151 K. M. Katubi, PhD thesis, University of Hull, 2015.
152 *National bureau of standards*, 1969, **25**, 82..
153 V. Rocher, J. Manerova, M. Kinnear, D. J. Evans and M. G. Francesconi, *Dalton Trans*, 2014, **43**, 2948–2952.
154 Z. Sharrett, S. Gamsey, P. Levine, D. Cunningham-Bryant, B. Vilozny, A. Schiller, R. A. Wessling and B. Singaram, *Tetrahedron Lett.*, 2008, **49**, 300–304.
155 Luke A. Roberts, MEng thesis, University of Surrey, 2010.
156 Paul M.S Monk and Neil M. Hodgkinson, *Charge-Transf. Complexes Viologens Eff. Complexation Rate Electron Transf. Methylviologen*, 1997, **43**, 245–255.
157 L. R. Milgrom, *The Colours of Life An introduction to the chemistry of porphyrins and related compounds*, Oxford University Press, Oxford, 1997.
158 D. M. Wallace, S. Leung, M.O. Senge and K. Smith *J. Org. Chem.*, 1993, **58 (25)**, 7245-7257.

159 B. Littler, M. Miller, C. Hsiung Hun, R. W. Wagner, D. F. O'Shea, P. D. Boyle and J. S. Lindsey, *J. Org. Chem.*, 1999, **64**, 1391–1396.
160 B. J. Littler, Y. Ciringh and J. S. Lindsey, *J. Org. Chem.*, 1999, **64**, 2864–2872.
161 F. Bryden and R. W. Boyle, in *Advances in Inorganic Chemistry*, ed. R. van Eldik and C. D. Hubbard, Elsevier, Burlington, 2016, vol. 68, ch. 4, pp. 141–221.
162 Y. Zhang and J. F. Lovell, *Theranostics*, 2012, **2**, 905–915.
163 C. O. Kappe, *Angew. Chem. Int. Ed.*, 2004, **43**, 6250–6284.
164 F. Langa, P. de la Cruz, A. de la Hoz, A. Díaz-Ortiz and E. Díez-Barra, *Contemp. Org. Synth.*, 1997, **4**, 373–386.
165 P. Lidström, J. Tierney, B. Wathey and J. Westman, *Tetrahedron*, 2001, **57**, 9225–9283.
166 H. M. Marques and K. L. Brown, *Coord. Chem. Rev.*, 2002, **225**, 123–158.
167 L. B. Josefsen and R. W. Boyle, *Met.-Based Drugs*, 2008, **2008**, 1–23.
168 D. Praseuth, A. Gaudemer, J.-B. Verlhac, I. Kraljic, I. Sissoeff and E. Guille, *Photochem. Photobiol.*, 1986, **44**, 717–724.
169 L. B. Josefsen and R. W. Boyle, *Theranostics*, 2012, **2**, 916–966.
170 F. Giuntini, V. M. Chauhan, J. W. Aylott, G. A. Rosser, A. Athanasiadis, A. Beeby, A. J. MacRobert, R. A. Brown and R. W. Boyle, *Photochem. Photobiol. Sci.*, 2014, **13**, 1039-1051
171 J. D. Moseley and C. O. Kappe, *Green Chem.*, 2011, **13**, 794-806.
172 M. L. Dean, J. R. Schmink, N. E. Leadbeater and C. Brückner, *Dalton Trans.*, 2008, 1341-1345.
173 B. F. O. Nascimento, M. Pineiro, A. M. d'A. Rocha Gonsalves, M. Ramos Silva, A. Matos Beja and J. A. Paixão, *J. Porphyr. Phthalocyanines*, 2007, **11**, 77–84.
174 H. Ali and J. E. van Lier, *Chem. Rev.*, 1999, **99**, 2379–2450.
175 T. E. O. Screen, K. B. Lawton, G. S. Wilson, N. Dolney, R. Ispasoiu, T. Goodson III, S. J. Martin, D. D. C. Bradley and H. L. Anderson, *J. Mater. Chem.*, 2001, **11**, 312–320
176 T. E. O. Screen, I. M. Blake, L. H. Rees, W. Clegg, S. J. Borwick and H. L. Anderson, *J. Chem. Soc. [Perkin 1]*, 2002, 320–329.
177 D. Gryko and J. S. Lindsey, *J. Org. Chem.*, 2000, **65**, 2249–2252.
178 C. Luo, D. M Guldi, H. Imahari, K. Tamaki and Y. Sakata, *J. Am. Chem. Soc.*, 2000, **122**, 6535–6551.
179 S. V. Bhosale, C. Chong, C. Forsyth, S. J. Langford and C. P. Woodward, *Tetrahedron*, 2008, **64**, 8394–8401..
180 L. Yu, K. Muthukumaran, P. Sreedharan and J. S. Lindsey, *Methods and intermediates for the synthesis of dipyrrin-substituted porphyrinic macrocycles*, US Pat., 7 332 599, 2008.
181 J. W. Buchler and J. R. Simon, *Eur. J. Inorg. Chem.*, 2000, **66,** 2615–2622.
182 P. M. R. Paulo and S. M. B. Costa, *J. Photochem. Photobiol. Chem.*, 2012, **234**, 66–74.
183 M. E. El-Khouly, O. Ito, P. M. Smith and F. D'Souza, *J. Photochem. Photobiol. C Photochem. Rev.*, 2004, **5**, 79–104.
184 O. B. Locos, C. C. Heindl, A. Corral, M. O. Senge and E. M. Scanlan, *Eur. J. Org. Chem.*, 2010, **2010**, 1026–1028.
185 F. Bryden, A. Maruani, H. Savoie, V. Chudasama, M. E. B. Smith, S. Caddick and R. W. Boyle, *Bioconjug. Chem.*, 2014, **25**, 611–617.
186 F. Bryden, H. Savoie, E. V. Rosca and R. W. Boyle, *Dalton Trans*, 2015, **44**, 4925–4932.
187 F. Giuntini, F. Bryden, R. Daly, E. M. Scanlan and R. W. Boyle, *Org. Biomol. Chem.*, 2014, **12**, 1203-1206
188 F. Bryden and R. W. Boyle, *Synlett*, 2013, **24**, 1978–1982.

189 N. K. Devaraj, R. A. Decreau, W. Ebina, J. P. Collman and C. E. Chidsey, *J. Phys. Chem. B*, 2006, **110**, 15955–15962.
190 C. Maeda, S. Yamaguchi, C. Ikeda, H. Shinokubo and A. Osuka, *Org. Lett.*, 2008, **10**, 549–552.
191 L. Sun, H. Chen, Z. Zhang, Q. Yang, H. Tong, A. Xu and C. Wang, *J. Inorg. Biochem.*, 2012, **108**, 47–52.
192 A. G. Hyslop, M. A. Kellett, P. M. Iovine and M. J. Therien, *J. Am. Chem. Soc.*, 1998, **120**, 12676–12677.
193 B. Vaz, R. Alvarez, M. Nieto, A. I. Paniello and A. R. de Lera, *Tetrahedron Lett.*, 2001, **42**, 7409–7412.
194 B. Shi and R. W. Boyle, *J. Chem. Soc., Perkin Trans. 1*, 2002, 1397–1400.
195 S. Fukuzumi, *J. Porphyr. Phthalocyanines*, 2000, **4**, 398–400.
196 S. Fukuzumi, *Org. Biomol. Chem.*, 2003, **1**, 609–620.
197 R. F. Pasternack, P. R. Huber, P. Boyd, G. Engasser, L. Francesconi, E. Gibbs, P. Fasella, G. Cerio Venturo and L. deC Hinds, *J. Am. Chem. Soc.*, 1972, **94**, 4511–4517.
198 R. Hudson, M. Carcenac, K. Smith, L. Madden, O. J. Clarke, A. Pèlegrin, J. Greenman and R. W. Boyle, *Br. J. Cancer*, 2005, **92**, 1442–1449.
199 F. Giuntini, C. M. A. Alonso and R. W. Boyle, *Photochem. Photobiol. Sci.*, 2011, **10**, 759-791.
200 K. A. Carrado and R. E. Winans, *Chem. Mater.*, 1990, **2**, 328–335.
201 T. N. Demidova and M. R. Hamblin, *Appl. Environ. Microbiol.*, 2005, **71**, 6918–6925.
202 Y. Ishikawa, A. Yamashita and T. Uno, *Chem. Pharm. Bull. (Tokyo)*, 2001, **49**, 287–293
203 J. P. C. Tomé, M. G. P. M. S. Neves, A. C. Tomé, J. A. S. Cavaleiro, M. Soncin, M. Magaraggia, S. Ferro and G. Jori, *J. Med. Chem.*, 2004, **47**, 6649–6652.
204 D. B. Papkovsky and T. C. O'Riordan, *J. Fluoresc.*, 2005, **15**, 569–584.
205 A. Favre, J. Grugier, A. Brans, B. Joris and J. Marchand-Brynaert, *Tetrahedron*, 2012, **68**, 10818–10826..
206 C. Spagnul, J. Greenman, M. Wainwright, Z. Kamil and R. W. Boyle, *J. Mater. Chem. B*, 2016, **4**, 1499–1509.
207 P. M. Antoni, A. Naik, I. Albert, R. Rubbiani, S. Gupta, P. Ruiz-Sanchez, P. Munikorn, J. M. Mateos, V. Luginbuehl, P. Thamyongkit, U. Ziegler, G. Gasser, G. Jeschke and B. Spingler, *Chem. - Eur. J.*, 2015, **21**, 1179–1183.
208 J. Scott, J. M. E. Quirke, H. J. Vreman, D. K. Stevenson and K. R. Downum, *J. Photochem. Photobiol. B*, 1990, **7**, 149–157.
209 D. Gao, H. Xu, M. A. Philbert and R. Kopelman, *Angew. Chem.*, 2007, **119**, 2274–2277.
210 D. Gao, H. Xu, M. A. Philbert and R. Kopelman, *Nano Lett.*, 2008, **8**, 3320–3324.
211 L. B. Josefsen, J. W. Aylott, A. Beeby, P. Warburton, J. P. Boyle, C. Peers and R. W. Boyle, *Photochem. Photobiol. Sci.*, 2010, **9**, 801.
212 A. K. Poulsen, A. M. Scharff-Poulsen and L. F. Olsen, *Anal. Biochem.*, 2007, **366**, 29–36.
213 J. Kopeček, *Biomaterials*, 2007, **28**, 5185–5192.
214 A. S. Hoffman, *Adv. Drug Deliv. Rev.*, 2012, **64**, 18–23.
215 J. K. Oh, R. Drumright, D. J. Siegwart and K. Matyjaszewski, *Prog. Polym. Sci.*, 2008, **33**, 448–477.
216 N. A. Peppas, J. Z. Hilt, A. Khademhosseini and R. Langer, *Adv. Mater.*, 2006, **18**, 1345–1360.
217 O. Wichterle, D. Lim, *Nature*, 1960, **158**, 117–118.
218 J. F. Lovell, A. Roxin, K. K. Ng, Q. Qi, J. D. McMullen, R. S. DaCosta and G. Zheng, *Biomacromolecules*, 2011, **12**, 3115–3118.

219 C. Brady, S. E. J. Bell, C. Parsons, S. P. Gorman, D. S. Jones and C. P. McCoy, *J. Phys. Chem. B*, 2007, **111**, 527–534..
220 C. Parsons, C. P. McCoy, S. P. Gorman, D. S. Jones, S. E. J. Bell, C. Brady and S. M. McGlinchey, *Biomaterials*, 2009, **30**, 597–602.
221 Y. Guo, S. Rogelj and P. Zhang, *Nanotechnology*, 2010, **21**, 065102.
222 A. K. Benabbou, C. Guillard, S. Pigeot-Rémy, C. Cantau, T. Pigot, P. Lejeune, Z. Derriche and S. Lacombe, *J. Photochem. Photobiol. Chem.*, 2011, **219**, 101–108.
223 S. M. Ribeiro, A. C. Serra and A. M. d'A. Rocha Gonsalves, *J. Mol. Catal. Chem.*, 2010, **326**, 121–127.
224 S. Artarsky, S. Dimitrova, R. Bonnett and M. Krysteva, *Sci. World J.*, 2006, **6**, 374–382.
225 J. Mosinger and B. Mosinger, *Experientia*, 1995, **51**, 106–109.
226 M. J. Adeogun and J. N. Hay, *Chem. Mater.*, 2000, **12**, 767–775.
227 C. Spagnul, L. C. Turner, F. Giuntini, J. Greenman and R. W. Boyle, *J. Mater. Chem. B*, 2017 DOI: 10.1039/C6TB03198F.
228 B. Wilson, M.-J. Fernández, A. Lorente and K. B. Grant, *Org. Biomol. Chem.*, 2008, **6**, 4026-4035.
229 J. A. González-Delgado, P. M. Castro, A. Machado, F. Araújo, F. Rodrigues, B. Korsak, M. Ferreira, J. P. C. Tomé and B. Sarmento, *Int. J. Pharm.*, 2016, **510**, 221–231.
230 M. O. Senge and M. Zawadzka, *Acta. Crystallogr. Sect. C Struct. Chem.*, 2014, **70**, 1143–1146.
231 R. Aston, K. Sewell, T. Klein, G. Lawrie and L. Grøndahl, *Eur. Polym. J.*, 2016, **82**, 1–15..
232 S. Kimel, B. J. Tromberg, W. G. Roberts and M. W. Berns, *Photochem. Photobiol.*, 1989, **50**, 175–183.
233 X. Wang and O. S. Wolfbeis, *Chem Soc Rev*, 2014, **43**, 3666–3761.
234 I. Banerjee, D. Mondal, J. Martin and R. S. Kane, *Langmuir*, 2010, **26**, 17369–17374.
235 J. Mosinger, O. Jirsak, P. Kubat, K. Lang and B. Mosinger, *J. Mater. Chem.*, 2007, **17**, 164-166.
236 P. Henke, H. Kozak, A. Artemenko, P. Kubát, J. Forstová and J. Mosinger, *ACS Appl. Mater. Interfaces*, 2014, **6**, 13007–13014.
237 S. Jesenská, L. Plíštil, P. Kubát, K. Lang, L. Brožová, Š. Popelka, L. Szatmáry and J. Mosinger, *J. Biomed. Mater. Res. A*, 2011, **99**, 676–683.
238 A. Memmi, R. Granet, M. Aouni, A. Bakhrouf and P. Krausz, *E-Polym.*, 2012, **12**, 467–478.
239M. D. Funes, D. A. Caminos, M. G. Alvarez, F. Fungo, L. A. Otero and E. N. Durantini, *Environ. Sci. Technol.*, 2009, **43**, 902–908.
240 Y. Wang, Y. Liu, G. Li and J. Hao, *Langmuir*, 2014, **30**, 6419–6426.
241 G. Jori, C. Fabris, M. Soncin, S. Ferro, O. Coppellotti, D. Dei, L. Fantetti, G. Chiti and G. Roncucci, *Lasers Surg. Med.*, 2006, **38**, 468–481.
242 A. Parveen, G. Smith, V. Salisbury, S. M. Nelson, *FEMS Microbiology Letters*, 2001, **199**, 115–118.
243 D. B. G. Williams and M. Lawton, *J. Org. Chem.*, 2010, **75**, 8351–8354..
244 C. Tahtaoui, I. Parrot, P. Klotz, F. Guillier, J.-L. Galzi, M. Hibert and B. Ilien, *J. Med. Chem.*, 2004, **47**, 4300–4315.
245 E. Dryer and S. Harvey, *J. Am. Chem. Soc.*, 1957, **79**, 672–675.